THEME C

Estimation of the probability of failure of a gravity dam for the sliding failure mode

FORMULATORS:

Ignacio Escuder Bueno
Civil Engineer, Ph.D.; UPV Professor; eDams Group

Luis Altarejos García
Civil Engineer, Ph.D.; Consultant; UPV Assistant Professor; eDams Group

Armando Serrano Lombillo
Civil Engineer; UPV Researcher; eDams Group

Polytechnic University of Valencia (UPV)
Camino de Vera s/n
46022 Valencia, Spain

Contact person:

Luis Altarejos García
eDams Group
Polytechnic University of Valencia (UPV)
ETSICCP, Edificio 4E – Camino de Vera s/n
46022 Valencia, Spain
luis.ag@hma.upv.es
Tl. +34 605 256 951

INDEX

1.- FOREWORD

All civil engineering structures, and particularly dams and reservoirs, should meet the highest requirements of safety and economy. Large dams provide extraordinary benefits to society, but, at the same time, dams impose high potential risks over population and properties downstream. In this context, and in the field of dam engineering, risk-based analysis techniques are being developed, offering not only a complementary view to the classical approach to dam safety, but also an entire new tool that can help robust management of dam safety, including some useful criteria to rationalize dam investments and a better understanding of the risk posed by dams.

Risk analysis methodologies need risk quantification. For an initial state of the dam-reservoir system, and for a certain failure mode, this risk quantification requires the estimation of both the probability of the loading scenarios and the conditional probability of the associated response of the dam-reservoir system, together with the estimation of the consequences.

In dam engineering, the main loading scenarios are those of hydrological and seismic nature. Hydrology and seismic engineering are well established sciences with a wide and solid body of knowledge which is constantly in development, as the estimation of the probability of floods and earthquakes has been on the focus of researchers and engineers for a long time. The estimation of the conditional probability of the response of a system for a certain loading scenario can be done with the help of reliability theory, which is based on a powerful mathematical framework that has been used successfully on the field of structural analysis. The estimation of consequences (in terms of loss of lives and impacts on economy), for a certain response of the dam-reservoir system (partial or total failure for a given loading scenario), represents a much more recent landmark in dam safety engineering. However, the development of this issue during the last decades of the past century has been remarkable.

Following the distinction between the three components of risk aforementioned, the problem proposed herein deals with the second of them: conditional probability of the response of a dam-reservoir system for a certain loading scenario. The conditional probability can be assessed by means of three different methods, namely historical references, probability elicitation, and reliability analysis. Probability estimation of the response of complex systems such as dams is an issue subjected to much controversy and discussion by dam engineering community.

Reliability techniques have been used in structural analysis while its application to other civil engineering fields, such as dam engineering, has been scarce, due to a variety of reasons such as the prototype character of each dam, uncertainties associated with the foundation, presence of water flow, and others. The complexity of the dam-reservoir behaviour, with several phenomena of different nature interacting simultaneously, has been tackled by following strong simplifications in the models of analysis together with the adoption of large safety margins on loads and resistances. On the other hand, the development of advanced numerical models (finite element and finite difference based methods) and the growing calculation power of computers, allow the use of complex mathematical models in the analysis of dam safety problems.

2.- AIM OF THE THEME

The objective is to obtain relationships between water levels, factors of safety and probabilities of failure for a gravity dam. This can be done using behaviour models for the dam-foundation system together with reliability techniques that allow for uncertainties in the parameters, using random variables.

For the purpose of comparison and evaluation of advances in this field, the dam proposed is taken from the Theme 2 of the 1999 ICOLD Benchmark.

The proposed exercise aims at analysing the dam with a 2D model. The model should be chosen by participants and it can be a limit equilibrium model or a deformable body model. The factor of safety against sliding is then calculated for several water levels.

Following this step, participants should estimate the probability of failure for the sliding failure mode using at least one Level 2 reliability method and a Level 3 Monte Carlo simulation method. On the Appendix, some useful information on reliability techniques and how they can be applied to this problem can be found.

The charts provided by different teams will be compared and analysed by formulators.

3.- FORMULATION OF THE THEME

3.1.- DATA

3.1.1.- GEOMETRY OF THE DAM

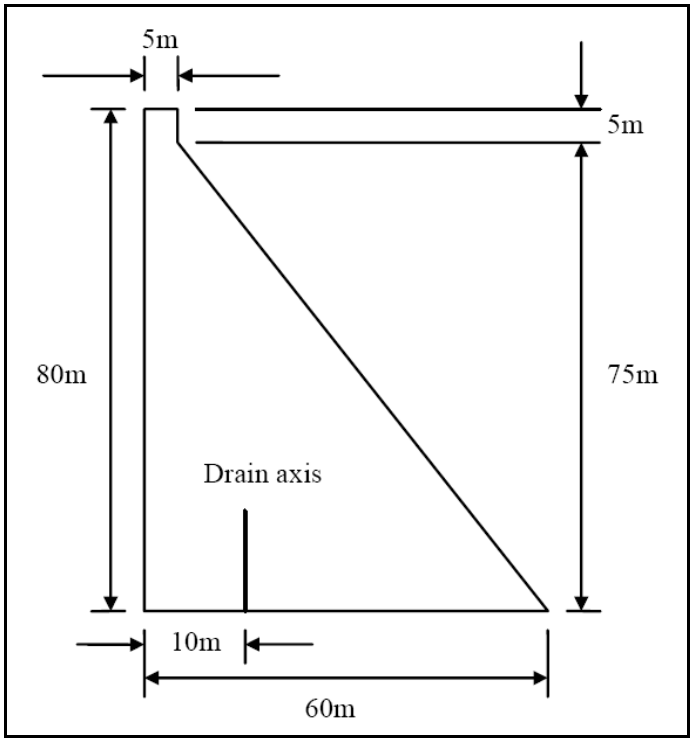

Figure 1: Dam geometry

The full geometry including the foundation is shown in the next figure. The foundation has a rectangular shape with height of 80 m and a total length of 300 m (120 m upstream, 60 m under de dam, 120 m downstream).

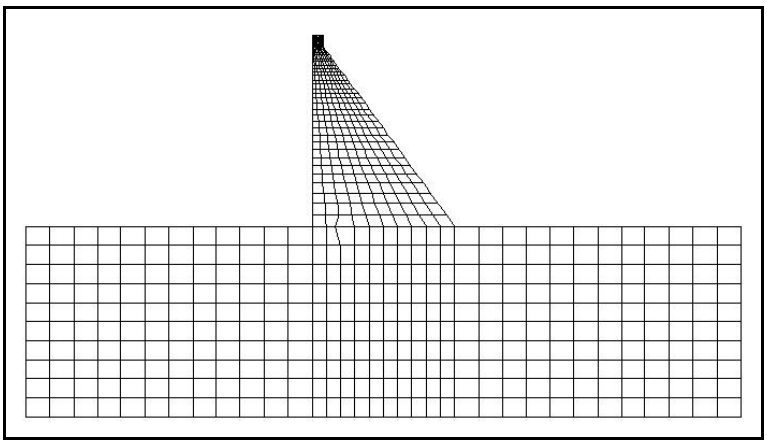

Figure 2: Dam and foundation geometry

3.1.2.- MATERIAL PROPERTIES

Data on material properties for dam and foundation are given in Table 1.

Table 1.- Data for dam and foundation materials

Material parameters	Dam	Foundation
Young's modulus (MPa)	24000	41000
Poisson`s ratio	0.15	0.10
Mass density (kg/m^3)	2400	2700
Compressive strength (MPa)	24	40
Tensile strength (MPa)	1.5	2.6
Strain at peak compressive strength	0.0022	0.0025
Strain at end of compressive softening curve	0.10	0.15
Fracture energy (N/m)	150	200

Data for material properties for dam-foundation interface are given in Table 2.

Table 2.- Data for dam-foundation interface

Parameter	Value
Shear stiffness (MPa/mm)	20
Tensile strength (MPa)	0.0
Friction angle (º)	See Table 3
Cohesion (MPa)	See Table 3
Dilatancy angle (º)	0
Softening modulus (MPa/mm)	-0.7

Friction angle and cohesion at the dam-foundation interface are considered as random variables. Available data in the form of fifteen pairs of values are given in Table 3.

Table 3.- Data for friction and cohesion at the interface

Sample	Friction angle (º)	Cohesion (MPa)
1	45	0.5
2	37	0.3
3	46	0.3
4	45	0.7
5	49	0.8
6	53	0.2
7	54	0.6
8	45	0.0
9	49	0.1
10	60	0.2
11	63	0.2
12	62	0.4
13	60	0.7
14	56	0.1
15	62	0.4

3.1.3.- LOADING

The considered loadings are self-weight, hydraulic pressure acting on the upstream face of the dam and uplift acting on the base of the dam. Development of a crack at the interface should be addressed by participants and uplift pressure should be evaluated accordingly.

Two cases of drain effectiveness are considered, with discrete probabilities associated:

- Case A: Drains effective (probability of 0.90)
- Case B: Drains not effective (probability of 0.10)

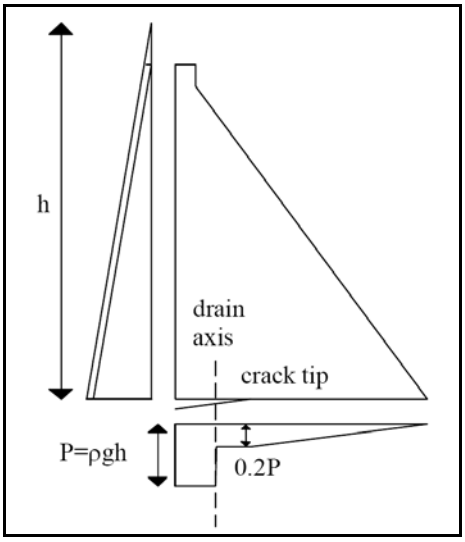

Case A. Drains effective

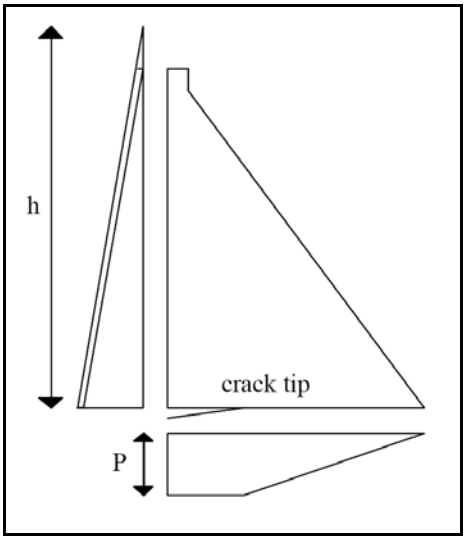

Case B. Drains ineffective

3.2.- PROBLEM

3.2.1.- PART 1

Participants should generate at least one model of behaviour for the dam and calculate the factor of safety against sliding for the 5 water levels given in Table 4.

Table 4. Results of Part 1

Water Level (in m over dam-foundation contact plane)	Factor of Safety (for sliding failure mode)
75	-
78	-
80	-
82	-
85	-

3.2.2.- PART 2

Estimate the probability of failure using Level 2 reliability methods. At least results with the First Order Second Moment (FOSM) Taylor's series approximation should be provided.

Table 5. Results of Part 2

Water Level (in m over dam-foundation contact plane)	Probability of failure (for Level 2 FOSM Taylor Method)	Probability of failure (for other Level 2 Method)
75	-	-
78	-	-
80	-	-
82	-	-
85	-	-

3.2.3.- PART 3

Estimate the probability of failure using the Level 3 reliability method Monte Carlo simulation.

Table 6. Results of Part 3

Water Level (in m over dam-foundation contact plane)	Probability of failure (for Level 3 Monte Carlo simulation)
75	-
78	-
80	-
82	-
85	-

APPENDIX

ASSESSMENT OF THE SLIDING FAILURE PROBABILITY OF A CONCRETE GRAVITY DAM

www.ipresas.upv.es

ASSESSMENT OF THE SLIDING FAILURE PROBABILITY OF A CONCRETE GRAVITY DAM

2nd INTERNATIONAL WEEK ON RISK ANALYSIS AS APPLIED TO DAM SAFETY AND DAM SECURITY

26-29th FEBRUARY 2008

UNIVERSIDAD POLITECNICA DE VALENCIA

iPresas
INSTITUTO DE INGENIERÍA DEL AGUA Y MEDIO AMBIENTE
UPV, ETSICCP, Edificio 4E – Camino de Vera s/n

Luis Altarejos García
luis.ag@hma.upv.es

CONTENTS

1.- INTRODUCTION.

The objective is to show different methods of analysis to estimate the conditional probability of failure by sliding along the dam-foundation contact on a concrete gravity dam. These methods can be classified as Level 1, Level 2 and Level 3 methods.

If our project variables $(X_1,X_2,...,X_n)$ are considered as random variables, it is possible to define the strength function $r(x_1,x_2,...,x_n)$ and the load function $s(x_1, x_2,...,x_n)$ and write the limit state equation as follows:

$$g^*(x_1, x_2,..., x_n) = g(x_1, x_2,..., x_n) - 1 = \frac{r(x_1, x_2,..., x_n)}{s(x_1, x_2,..., x_n)} - 1 = 0 \qquad \text{(Eq. 1)}$$

According to this, the failure domain in the n-dimensional space is defined as all the possible values $(x_1,x_2,...,x_n)$ that verify the condition:

$$g^*(x_1, x_2,..., x_n) \le 0 \qquad \text{(Eq. 2)}$$

and the safety domain is defined as all possible values $(x_1,x_2,...,x_n)$ that verify the condition:

$$g^*(x_1, x_2,..., x_n) > 0 \qquad \text{(Eq. 3)}$$

According to the concept of the probability density function, the probability of a single n-dimensional point $(x_1,x_2,...,x_n)$ to be in the failure domain defined by $g^*(x_1,x_2,...,x_n)$, is calculated as the integral over the failure domain of the joint probability density function of all random variables:

$$P_f\left[g^*(x_1, x_2,..., x_n) \le 0\right] = \int_{g^*(x_1,x_2,...,x_n)\le 0} f_{X_1,X_2,...,X_n}(x_1, x_2,..., x_n)\,dx_1 dx_2 ... dx_n \qquad \text{(Eq. 4)}$$

As long as the joint probability density function and the integration domain are defined with precision, and the integral can be calculated, Equation (4) provides a value for probability that is mathematically exact.

The methods for failure probability estimation can be grouped in different levels (Mínguez [1]):

> **Level 1**: Method of safety factors. Does not provide probability of failure. Uncertainty is measured by arbitrary factors.
>
> **Level 2**: Second Moment Methods. The probability of failure can be obtained under some assumptions. Only the first two moments (mean and standard deviation) of the joint probability density function $f_{X1,X2,...,Xn}(x_1,x_2,...,x_n)$ are used. Eventually, also the failure domain $g^*(x_1,x_2,...,x_n)$ is approximated.
>
> **Level 3**: Exact Methods. These methods provide the probability of failure, as they work with all the information of the joint probability density function. Integration is carried out by means of specific methods.

Table 1. Levels of reliability analysis.

LEVEL	Method of calculation	Probability distributions	Limit state equations	Treatment of uncertainty	Output
Level 1	Code calibration with level 2 or level 3 methods	Not used	Linear	Arbitrary factors	Coefficients
Level 2	Second order algebra	Normal distributions only	Linear or aprox. Linear	Can be included as normal distribution	Probability of failure
Level 3	Transformations	Equivalent normal distributions	Linear or aprox. Linear	Can be included	Probability of failure
	Numerical integration and simulation	Any distribution	Any form	Random variables	

2.- CASE STUDY.

Dam geometry is depicted in Figure 1 and in Table 2.

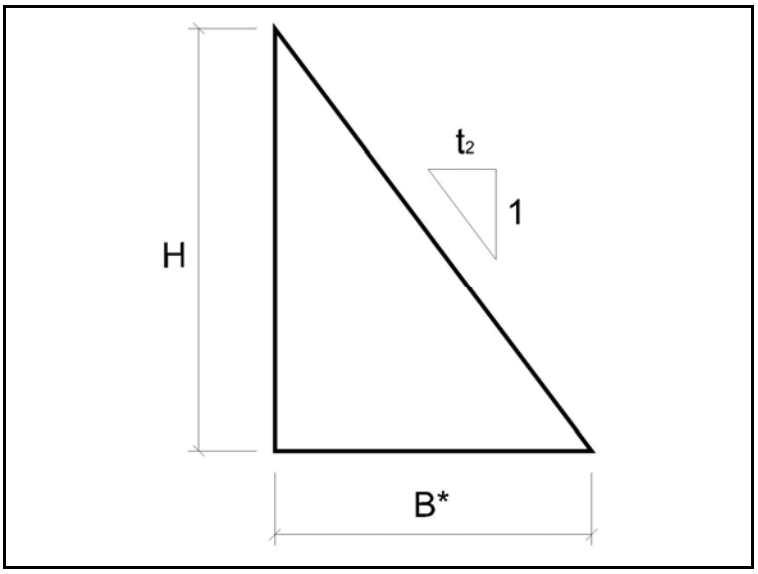

Figure 1. Dam geometry.

Table 2. Dam geometry.

Geometry	Values
Height (m)	100
Base width (m)	75
Upstream slope	Vertical
Downstream slope (H:V)	0.75

Properties of concrete and rock materials are given in Table 3.

Table 3. Concrete and rock properties.

Material properties	Concrete	Rock
Mass density (kg/m^3)	2300	2600
Compressive strength (Pa)	200×10^5	300×10^5
Tensile strength (Pa)	20×10^5	25×10^5

Properties of the dam-foundation contact are given in Table 4.

Table 4. Properties of the dam-foundation contact.

Material properties	Values
Peak Cohesion (Pa)	5×10^5
Residual Cohesion (Pa)	0
Peak Friction Angle (º)	45
Residual Friction Angle (º)	35
Tensile strength (Pa)	4×10^5

Data of water pressures are given in Table 5.

Table 5. Data of water pressures.

Data of water pressures	Values
Density of water, ρw (kg/m^3)	1000
Water level upstream, h (m)	90
Water level downstream (m)	0
Drainage system efficiency	0

Gravity acceleration is taken as g = 10 m/s^2.

3.- MATHEMATICAL MODEL OF ANALYSIS.

Sliding stability can be analysed by means of a simple two-dimensional limit equilibrium model.

Hydrostatic load, S (N/m), is the driving force and can be evaluated by (5).

$$S = \frac{1}{2}\rho_w g h^2 \qquad \text{(Eq. 5)}$$

Shear strength, R(N/m) is calculated with (6).

$$R = (N - U)tg\varphi + B \times c \qquad \text{(Eq. 6)}$$

N (N/m) is the sum of vertical forces acting on the dam-foundation contact surface.
U (N/m) is the uplift.
B (m^2/m) is the area in compression in the dam-foundation contact.
φ (º) is the friction angle in the contact.
c (Pa) is the cohesion in the contact.

4.- LEVEL 1 METHODS. GLOBAL SAFETY FACTOR

4.1.- THEORETICAL BASIS.

This is the classical approach in structural safety assessment. All the variables of a certain problem (geometry, material properties, loads,...) form a vector $(X_1,X_2,...,X_n)$ in a n-dimensional space, and if we define a strength function $r(x_1,x_2,...,x_n)$ and a loading function $s(x_1,x_2,...,x_n)$, it is possible to derive a function $g(x_1,x_2,...,x_n)$ as:

$$g(x_1, x_2,..., x_n) = \frac{r(x_1, x_2,..., x_n)}{s(x_1, x_2,..., x_n)} \qquad \text{(Eq. 7)}$$

Any point $(x_1,x_2,...,x_n)$ in the n-dimensional space is in the safety domain if:

$$g(x_1, x_2,..., x_n) > 1 \qquad \text{(Eq. 8)}$$

On the other hand, it is in the failure domain if:

$$g(x_1, x_2,..., x_n) \leq 1 \qquad \text{(Eq. 9)}$$

The frontier between these two domains, or limit state region, is defined by the n-dimensional hyper surface defined by:

$$g(x_1, x_2,..., x_n) = 1 \qquad \text{(Eq. 10)}$$

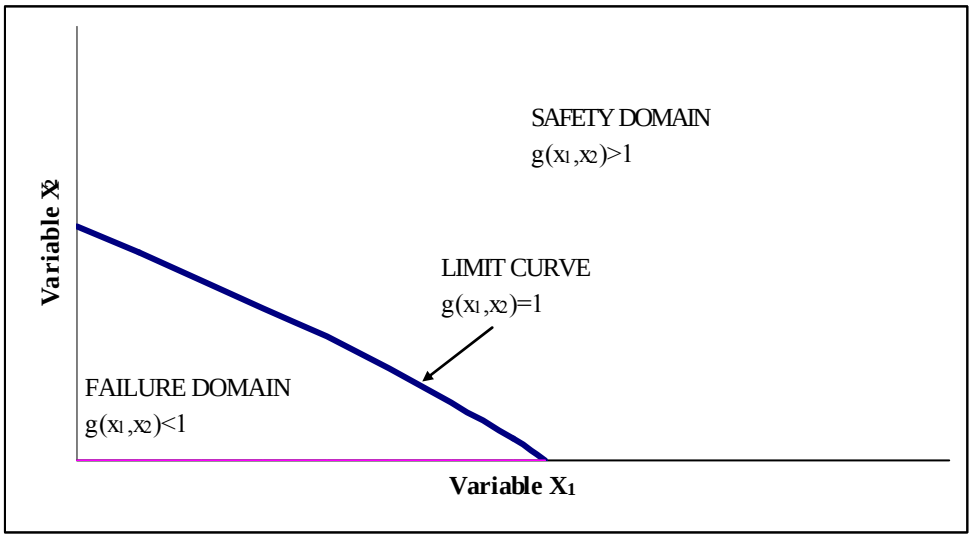

Figure 2: Safety and failure domains and limit state in a two-dimensional case.

The global safety factor, F (F>1), is defined as:

$$g(x_1, x_2,..., x_n) - F > 0 \qquad \text{(Eq. 11)}$$

Or, in the most common expression:

$$\frac{r(x_1, x_2, ..., x_n)}{s(x_1, x_2, ..., x_n)} > F \qquad \text{(Eq. 12)}$$

This method is used in common practice with constant values for the variables (X_1,X_2,..., X_n), so-called representative values.

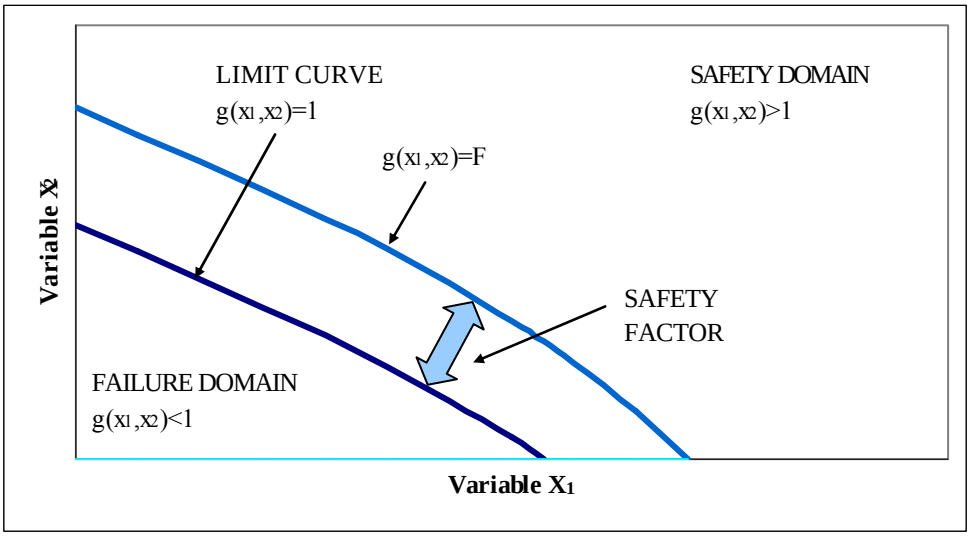

Figure 3. Safety margin expressed in terms of safety factor.

4.2.- APPLICATION TO THE CASE STUDY.

Evaluating the forces acting on the dam:

$$S = \frac{1}{2} 1000 \times 10 \times 90^2 = 4.05 \times 10^7 \text{ (N/m)} \qquad \text{(Eq. 13)}$$

$$R = ((0.5 \times 75 \times 100 \times 2300 \times 10) - ((0.5 \times 75 \times 90 \times 1000 \times 10) tg45 + (75 \times 5 \times 10^5))) = 9.00 \times 10^7 \text{ (N/m)} \qquad \text{(Eq. 14)}$$

And the global safety factor obtained is:

$$FS = \frac{R}{S} = \frac{9.00 \times 10^7}{4.05 \times 10^7} = 2.22 \qquad \text{(Eq. 15)}$$

5.- LEVEL 1 METHODS. PARTIAL SAFETY FACTORS

5.1.- THEORETICAL BASIS.

In this methodology different safety factors are associated with different variables. This method is common practice in the reinforced concrete and steel structures analysis.

Two groups of coefficients are defined, a group γ_i (γ_i <1) associated with strength variables, R_i, and a group λ_j (λ_j > 1) associated to loadings, S_j, so (Eq. 12) can be re-written as:

$$\sum_i \gamma_i R_i > \sum_j \lambda_j S_j \qquad \text{(Eq. 16)}$$

This methodology allows "weighting" of the different variables depending upon the uncertainties associated to the representative values adopted. Coefficients associated to strength variables decrease their values with respect to their representative ones and coefficients associated to loading variables increase their values with respect to their representative values.

5.2.- APPLICATION TO THE CASE STUDY.

It is possible to evaluate the sliding safety of a gravity dam with partial safety factors, as the Spanish recommendations for dam calculation state (Technical Guide nº2 Criteria for dam project).

Partial safety factors are assigned to shear strengths (friction and cohesion in the dam-foundation contact) The values for these factors are different depending upon the kind of evaluation being carried out: normal, abnormal or extreme. They also vary depending on the dam classification.

In this case assumption of an abnormal situation is reasonable, as the drainage system is supposed to be ineffective. Dam classification according to Spanish standards is A.

Friction strength, R_1, cohesion strength, R_2, and loading, S_1, can be calculated:

$$R_1 = (A \cdot \rho_c g - U) tg\phi = (3750 \times 2300 \times 10 - 3.375 \times 10^7) tg45 = 5.25 \times 10^7 \text{ N/m} \qquad \text{(Eq. 17)}$$

$$R_2 = B \cdot c = 75 \times 5.00 \times 10^5 = 3.75 \times 10^7 \text{ N/m} \qquad \text{(Eq. 18)}$$

$$S_1 = 0.5 \cdot \rho_w g \cdot h^2 = 0.5 \times 1000 \times 10 \times 90^2 = 4.05\text{e}7 \text{ N/m} \qquad \text{(Eq. 19)}$$

and equation (16) can be written as:

$$\gamma_1 R_1 + \gamma_2 R_2 > \lambda_1 S_1 \qquad \text{(Eq. 20)}$$

According to Spanish recommendations, partial safety factors for abnormal situation and A category dam are:

Friction, γ_1 = 1/1.2 = 0.833
Cohesion, γ_2 = 1/4 = 0.25

Cohesion decrease is larger than friction decrease. Recommendations do not assign any loading increase, so λ = 1. Substituting in (20) the sliding safety can be checked::

$$0.833 \times 5.25 \times 10^7 + 0.25 \times 3.75 \times 10^7 = 5.31 \times 10^7 > 1 \times 4.05 \times 10^7 \qquad \text{(Eq. 21)}$$

6.- LEVEL 2 METHODS. THEORETICAL BASIS.

Level 2 methods make a linear (first order) approximation of the function $g^*(x_1,x_2,...,x_n)$. In addition, only the first two moments (second moment) of the joint probability density function distribution are considered, so these methods are called FOSM Methods (First Order Second Moment).

The typical output of these methods is the reliability index, β, which is defined as the number of standard deviations between the expected value of the function $g^*(x_1,x_2,...,x_n)$ and the limit state value defined as $g^*(x_1,x_2,...,x_n)=0$. This value gives us a relative measure of reliability (distance between the most probable value and the failure domain, in the sense that the larger the value of β, the safer the structure will be, but it does not tells us anything about the probability of failure by itself.

$$\beta = \frac{E[g^*] - (g^*)_{fallo}}{\sigma_{g^*}} = \frac{E[g^*] - 0}{\sigma_{g^*}} = \frac{E[g^*]}{\sigma_{g^*}} \qquad \text{(Eq. 22)}$$

As $X_1,X_2,...,X_n$ are random variables, $g^*(x_1,x_2,...,x_n)$ is a random variable with a certain probability distribution, usually unknown. To get an estimate of the probability of failure, and hypothesis on the shape of this distribution is to be done. With the shape of the probability distribution and its first two moments, both the reliability index and the probability of failure can be obtained.

There are different techniques to deal with the problem:

- Taylor's Series Method
- Rosenblueth's Point Estimate Method
- Hasofer & Lind Method

7.- LEVEL 2 METHODS. FOSM – TAYLOR'S SERIES.

7.1.- THEORETICAL BASIS.

The function $g^*(x_1,x_2,...,x_n)$ must be linear to obtain the first two moments of the probability distribution of $g^*(x_1,x_2,...,x_n)$ from the first two moments of the probability distributions of the random variables $X_1,X_2,...,X_n$:

$$g^*(x_1, x_2, ..., x_n) = a_0 + a_1x_1 + a_2x_2 + ... + a_nx_n \qquad \text{(Eq. 23)}$$

The first moment of the probability distribution of g*, assuming that the random variables are correlated can be calculated as:

$$E[g^*] = g^*(E[X_1], E[X_2], ..., E[X_n]) + \frac{1}{2}\sum\left(\frac{\partial^2 g^*}{\partial X_i \partial X_j}\rho_{X_iX_j}\sigma_{X_i}\sigma_{X_j}\right) \qquad \text{(Eq. 24)}$$

where σ_{Xi} is the standard deviation of the random variable X_i and ρ_{XiXj} is the correlation coefficient between random variables X_i y X_j.

Being a first order approximation, second order derivatives can be ignored, so the final expression is the same for correlated and independent random variables:

$$E[g^*] = g^*(E[X_1], E[X_2], ..., E[X_n]) \quad \text{(Eq. 25)}$$

So the expected value of g* is obtained evaluating the function in the n-dimensional point corresponding to the expected values of the random variables. The variance of the probability distribution of g*, assuming correlated random variables, is calculated as:

$$Var[g^*] = \sum_i \left(\left(\frac{\partial g^*}{\partial X_i} \right)^2 \sigma_{X_i}^2 \right) + 2 \sum_{i \neq j} \left(\frac{\partial g^*}{\partial X_i} \frac{\partial g^*}{\partial X_j} \rho_{X_i X_j} \sigma_{X_i} \sigma_{X_j} \right) \quad \text{(Eq. 26)}$$

where σ^2_{Xi} is the variance of the random variable X_i.

If the random variables are independent, equation (26) can be written as:

$$Var[g^*] = \sum_i \left(\left(\frac{\partial g^*}{\partial X_i} \right)^2 \sigma_{X_i}^2 \right) \quad \text{(Eq. 27)}$$

First order derivatives can be obtained straightforward if g* is a linear function. If it is not, first order derivatives are approximated by the first order elements of the Taylor's series expansion of g* about the expected values. The partial derivatives are calculated numerically using a very small increment (positive and negative) centred on the expected value. Following the USACE practice, a large increment of one standard deviation will be used, in order to capture some of the behaviour of the nonlinear functions.

$$\frac{\partial g^*}{\partial X_i} \approx \frac{g^*(E[X_i] + \sigma_{X_i}) - g^*(E[X_i] - \sigma_{X_i})}{(X_i + \sigma_{X_i}) - (X_i - \sigma_{X_i})} = \frac{g^*(E[X_i] + \sigma_{X_i}) - g^*(E[X_i] - \sigma_{X_i})}{2\sigma_{X_i}} \quad \text{(Eq. 28)}$$

And the square of the first order derivative can be estimated by:

$$\left(\frac{\partial g^*}{\partial X_i} \right)^2 \approx \frac{1}{\sigma_{X_i}^2} \left(\frac{g^*(E[X_i] + \sigma_{X_i}) - g^*(E[X_i] - \sigma_{X_i})}{2} \right)^2 \quad \text{(Eq. 29)}$$

Substituting (29) in (27):

$$Var[g^*] = \sum_i \left(\left(\frac{g^*(E[X_i] + \sigma_{X_i}) - g^*(E[X_i] - \sigma_{X_i})}{2} \right)^2 \right) \quad \text{(Eq. 30)}$$

With this method a number of 2n+1 evaluations of the performance function g* is needed, being n the number of random variables considered.

7.2.- APPLICATION TO THE CASE STUDY.

In this example only two variables are considered as random variables: friction angle and cohesion along the dam-foundation contact. All the other variables are considered as constant variables with their respective constant values. Friction angle is supposed to be defined by a normal probability function, with mean of 45º and standard deviation of 6.75º. Cohesion is normally distributed with mean of 5.00×10^5 N/m^2 and standard deviation of 1.25×10^5 N/m^2. Both variables are independent.

The performance function g is defined as:*

$$g^* = \frac{r}{s} - 1 \qquad \text{(Eq. 31)}$$

Where r is the shear strength function and s is the loading function. According to the values of the case study:

$$r = (A\cdot\rho_c g - U)tg\phi + B\cdot c = (3750\times2300\times10 - 3.375\times10^7)tg\phi + 75\times c$$
$$r = 5.25\times10^7\times tg\phi + 75\times c \qquad \text{(Eq. 32)}$$

And the loading function:

$$s = 0.5\cdot\rho_w g\cdot h^2 = 0.5\times1000\times10\times90^2 = 4.05\times10^7 \text{ N/m} \qquad \text{(Eq. 33)}$$

So the performance function can be written as:

$$g^*(\varphi,c) = \frac{5.25\times10^7\times tg\phi + 75\times c}{4.05\times10^7} - 1 \qquad \text{(Eq. 34)}$$

The $tg\varphi$ introduces a non linearity in the function. First moment of g, according to (25), is:*

$$E[g^*] = \frac{5.25\times10^7\times tg45 + 75\times5.00\times10^5}{4.05\times10^7} - 1 = 1.222222 \qquad \text{(Eq. 35)}$$

And 4 more evaluations of g are needed:*

$$g^*(45+6.75, 5.00e5) = \frac{5.25\times10^7\times tg51.75 + 75\times5.00\times10^5}{4.05e7} - 1 = 1.570270$$
$$g^*(45-6.75, 5.00e5) = \frac{5.25\times10^7\times tg38.25 + 75\times5.00\times10^5}{4.05e7} - 1 = 0.947844$$
$$g^*(45, 5.00e5+1.25e5) = \frac{5.25\times10^7\times tg45 + 75\times6.25\times10^5}{4.05e7} - 1 = 1.453704$$
$$g^*(45, 5.00e5-1.25e5) = \frac{5.25\times10^7\times tg45 + 75\times3.75\times10^5}{4.05e7} - 1 = 0.990741 \qquad \text{(Eq. 36)}$$

And applying (30):

$$\mathrm{Var}[g^*] = \left(\frac{1.570270 - 0.947844}{2}\right)^2 + \left(\frac{1.453704 - 0.990741}{2}\right)^2 \qquad \text{(Eq. 37)}$$
$$\mathrm{Var}[g^*] = 0.096854 + 0.053584 = 0.150438$$

Once the first two moments are known, the reliability index can be calculated using equation (22):

$$\beta = \frac{E[g^*] - (g^*)_{fallo}}{\sigma_{g^*}} = \frac{E[g^*] - 0}{\sigma_{g^*}} = \frac{E[g^*]}{\sigma_{g^*}} = \frac{1.222222}{\sqrt{0.150437}} = 3.151174 \qquad \text{(Eq. 38)}$$

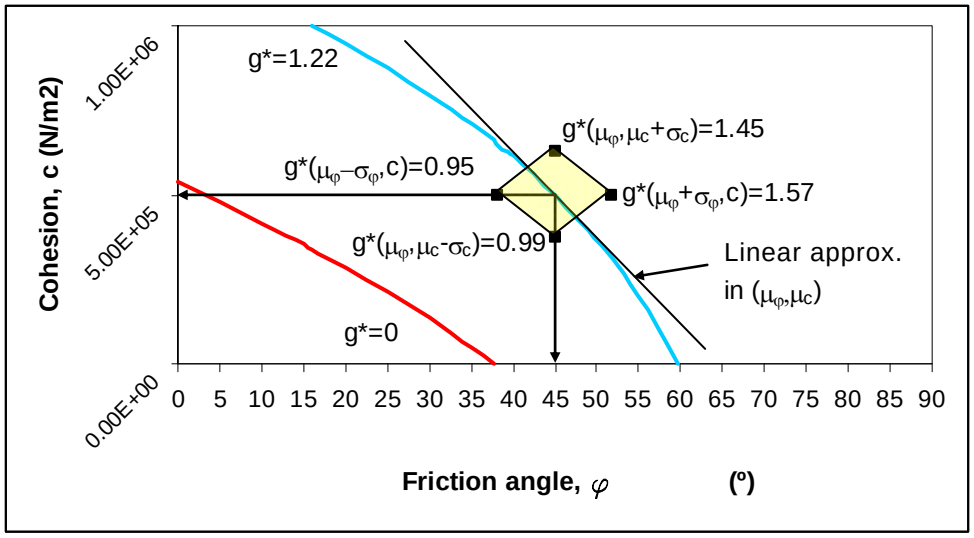

Figure 4: Taylor's series method.

Contribution of each random variable to overall variance is:

Contribution of φ: (0.096854/0.150438)→ 64.38%
Contribution of c: (0.053584/0.150438)→ 35.62%

To obtain a probability of failure, we have to make an assumption on how the performance function g is distributed. If the hypothesis is that g* is normally distributed, then:*

$$g^* \sim N(\mu_{g^*}; \sigma^2_{g^*}) \sim N(1.222222;\ 0.150438)$$

and the probability of failure $P_f[g^* \le 0]$ can be calculated:

$$P_f[g^* \le 0] = F_N(0) = \Phi\left(\frac{0 - \mu_{g^*}}{\sigma_{g^*}}\right) = \Phi(-\beta) = \Phi(-3.151174) = 0.000813 \qquad \text{(Eq. 39)}$$

Note that this is a CONDITIONAL probability for a certain water level upstream and certain drainage system efficiency.

8.- LEVEL 2 METHODS. POINT ESTIMATE METHOD.

8.1.- THEORETICAL BASIS.

The point estimated method determine the first two moments of the performance function g* by the discretization of the probability distributions of the random variables $X_1,X_2,...,X_n$. This discretization is made in a few points for each random variable (two or three points), where mass probability is concentrated in such a fashion that the sum of the probabilities assigned to each point is 1 for each random variable (Rosenblueth [2] y Harr [3]). In the more general approximation, the method determines the third moment of the distributions, which allows analysis with skewed (asymmetrical) distributions. Random variables can be independent or correlated.

With this method there is no need to evaluate partial derivatives of the performance function g*. A disadvantage of the method is that the performance function has to be evaluated 2^n times, being *n* the number of random variables. If *n* is large, the method requires a considerable computational effort, above all if g* evaluation is not straightforward.

The method concentrates the mass probability of the random variable X_i in two points, x_{i+} y x_{i-}, each of them with a mass probability of P_{i+} and P_{i-}. Points are centred about the mean value, μ_{Xi}, at a distance of d_{i+} and d_{i-} times the standard deviationσ_{Xi} , respectively.

$$\begin{aligned} P_{i+} + P_{i-} &= 1 \\ x_{i+} &= \mu_{X_i} + d_{i+} \cdot \sigma_{X_i} \\ x_{i-} &= \mu_{X_i} + d_{i-} \cdot \sigma_{X_i} \end{aligned} \qquad \text{(Eq. 40)}$$

Coefficients d_{i+} y d_{i-} are determined using the skew coefficient, γ_i, of the random variable X_i:

$$\begin{aligned} d_{i+} &= \frac{\gamma_i}{2} + \sqrt{1 + \left(\frac{\gamma_i}{2}\right)^2} \\ d_{i-} &= d_{i+} - \gamma_i \end{aligned} \qquad \text{(Eq. 41)}$$

Probabilities are assigned to each point according to:

$$\begin{aligned} P_{i+} &= \frac{d_{i-}}{d_{i+} + d_{i-}} \\ P_{i-} &= 1 - P_{i+} \end{aligned} \qquad \text{(Eq. 42)}$$

In figures 5 and 6 the discretization of a random variable is shown. A number of 2^n values of discrete probabilities should be obtained by combination of the point probabilities of each random variable with the other random variable's probabilities. These probabilities are $P_{(\delta 1,\delta 2,\ldots,\delta n)}$, where δ_i is the sign (+ ó -).

Values of these probabilities are calculated as:

$$P_{(\delta 1,\delta 2,\ldots,\delta n)} = \prod_{i=1}^{n} P_{i,\delta i} + \sum_{i=1}^{n-1}\left(\sum_{j=i+1}^{n} \delta_i \delta_j a_{ij}\right) \qquad \text{(Eq. 43)}$$

Where the coefficients a_{ij} are calculated as:

$$a_{ij} = \frac{\frac{\rho_{ij}}{2^n}}{\sqrt{\prod_{i=1}^{n}\left(1+\left(\frac{\gamma_i}{2}\right)^2\right)}} \qquad \text{(Eq. 44)}$$

Being ρ_{ij} the correlation coefficient between random variables X_i y X_j.

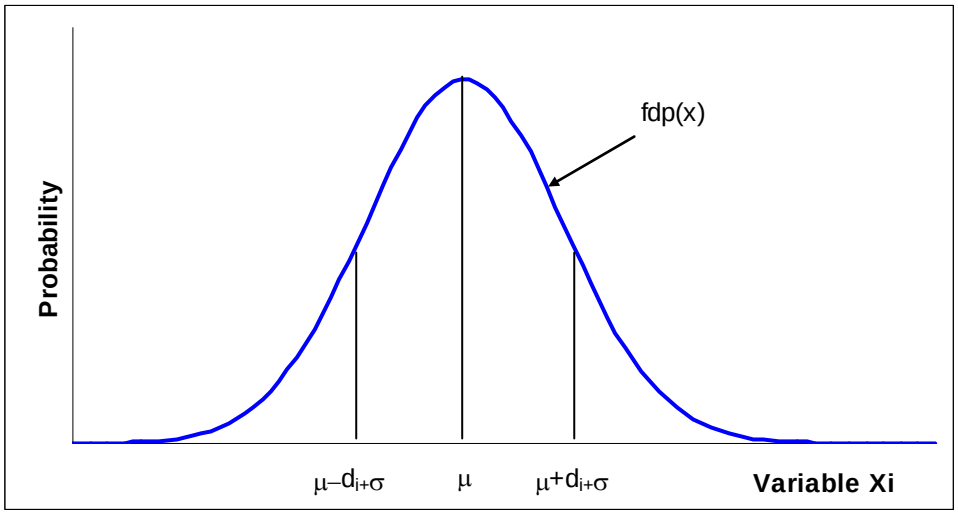

Figure 5: Probability density function of a random variable X_i.

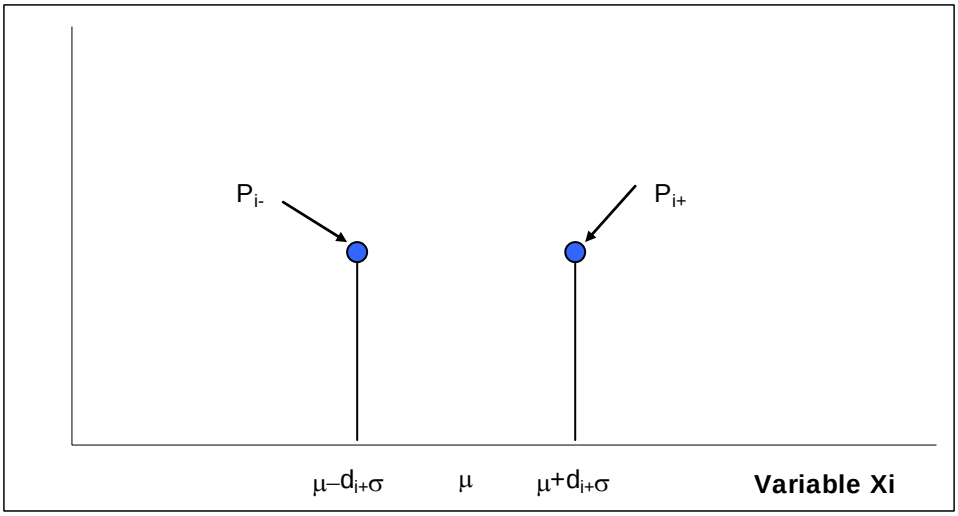

Figure 6: Point Estimate Method discretization of probability of a random variable.

The performance function g* has to be evaluated 2^n times, corresponding to the 2^n possible combinations of discrete probability points $P_{(\delta 1,\delta 2,\ldots,\delta n)}$, obtaining $g^*_{(\delta 1,\delta 2,\ldots,\delta n)}$. Once this is accomplished, the moment of *m* order of the probability distribution of g* is determined by:

$$E\left[g^{*m}\right] \approx \sum P_{(\delta 1,\delta 2,\ldots,\delta n)} g^{*m}_{(\delta 1,\delta 2,\ldots,\delta n)} \qquad \text{(Eq. 45)}$$

So for the first moment:

$$E[g^*] = \sum P_{(\delta 1,\delta 2,...,\delta n)} g^*_{(\delta 1,\delta 2,...,\delta n)} \quad \text{(Eq. 46)}$$

And for the second moment:

$$E[g^{*2}] = \sum P_{(\delta 1,\delta 2,...,\delta n)} g^{*2}_{(\delta 1,\delta 2,...,\delta n)} \quad \text{(Eq. 47)}$$

The variance of g* can be calculated:

$$Var[g^*] = E[(g^* - \mu_{g^*})^2] = E[g^{*2}] - \mu^2_{g^*} \quad \text{(Eq. 48)}$$

So it is possible to determine the mean and the variance of the probability distribution of g* but the shape of the distribution is not known. If what we want is a probability of failure, again a hypothesis of how g* is distributed is to be done.

The method loses precision with the increasing nonlinearity of g* and if moments over the second are to be obtained. It does not provide a measure of the contribution of each random variable to the overall variance, so it is not an adequate method to filter the most relevant random variables.

8.2.- APPLICATION TO THE CASE STUDY.

First step is to make the discretization of probability distributions of the random variables. Variables φ and c are normally distributed (symmetrical), so $\gamma_\varphi = \gamma_c = 0$ (null skewness). Applying (41) we can obtain $d_{\varphi+} = d_{\varphi-} = 1$ and $d_{c+} = d_{c-} = 1$, and the points where mass probabilities will concentrate are, using (40):

$$\begin{aligned}
\phi_+ &= \mu_\phi + \sigma_\phi = 45 + 6.75 = 51.75 \\
\phi_- &= \mu_\phi - \sigma_\phi = 45 - 6.75 = 38.25 \\
c_+ &= \mu_c + \sigma_c = 5.00 \times 10^5 + 1.25 \times 10^5 = 6.25 \times 10^5 \\
c_- &= \mu_c - \sigma_c = 5.00 \times 10^5 - 1.25 \times 10^5 = 3.75 \times 10^5
\end{aligned} \quad \text{(Eq. 49)}$$

And mass probability values for each random variable are, using (42):

$$\begin{aligned}
P_{\varphi+} &= \frac{d_{\varphi-}}{d_{\varphi+} + d_{\varphi-}} = \frac{1}{1+1} = 0.5 \\
P_{\varphi-} &= 1 - P_{\varphi+} = 1 - 0.5 = 0.5 \\
P_{c+} &= \frac{d_{c-}}{d_{c+} + d_{c-}} = \frac{1}{1+1} = 0.5 \\
P_{c-} &= 1 - P_{c+} = 1 - 0.5 = 0.5
\end{aligned} \quad \text{(Eq. 50)}$$

As friction and cohesion are supposed to be independent variables, correlation coefficient is null ($\rho_{\varphi c} = 0$), and applying (44), $a_{\varphi c} = 0$.

So the calculation of the $2^n = 2^2 = 4$ probabilities given in (43) are as follows:

$$\begin{aligned} P_{(\varphi+,c+)} &= P_{\varphi+} \cdot P_{c+} = 0.5 \times 0.5 = 0.25 \\ P_{(\varphi+,c-)} &= P_{\varphi+} \cdot P_{c-} = 0.5 \times 0.5 = 0.25 \\ P_{(\varphi-,c+)} &= P_{\varphi-} \cdot P_{c+} = 0.5 \times 0.5 = 0.25 \\ P_{(\varphi-,c-)} &= P_{\varphi-} \cdot P_{c-} = 0.5 \times 0.5 = 0.25 \end{aligned} \qquad \text{(Eq. 51)}$$

The evaluation of the performance function g in the $2^n = 2^2 = 4$ points where probabilities have been calculated leads to:*

$$\begin{aligned} g^*(\phi_+, c_+) &= g^*\left(51.75, 6.25\times10^5\right) = \frac{5.25\times10^7 \times tg51.75 + 75\times6.25\times10^5}{4.05\times10^7} - 1 = 1.801751 \\ g^*(\phi_+, c_-) &= g^*\left(51.75, 3.75\times10^5\right) = \frac{5.25\times10^7 \times tg51.75 + 75\times3.75\times10^5}{4.05\times10^7} - 1 = 1.338788 \\ g^*(\phi_-, c_+) &= g^*\left(38.25, 6.25\times10^5\right) = \frac{5.25\times10^7 \times tg38.25 + 75\times6.25\times10^5}{4.05\times10^7} - 1 = 1.179325 \\ g^*(\phi_-, c_-) &= g^*\left(38.25, 3.75\times10^5\right) = \frac{5.25\times10^7 \times tg38.25 + 75\times3.75\times10^5}{4.05\times10^7} - 1 = 0.716362 \end{aligned} \qquad \text{(Eq. 52)}$$

So the first moment can be determined with equation (46):

$$\begin{aligned} E[g^*] &= 0.25\times1.801751 + 0.25\times1.338788 + 0.25\times1.179325 + 0.25\times0.716362 \\ E[g^*] &= 1.259057 \end{aligned} \qquad \text{(Eq. 53)}$$

And the second moment with equation (47):

$$\begin{aligned} E\left[g^{*2}\right] &= 0.25\times1.801751^2 + 0.25\times1.338788^2 + 0.25\times1.179325^2 + 0.25\times0.716362^2 \\ E\left[g^{*2}\right] &= 1.735661 \end{aligned} \qquad \text{(Eq. 54)}$$

And the variance of g is calculated with equation (48):*

$$Var[g^*] = E\left[g^{*2}\right] - \mu_{g^*}^2 = 1.735661 - 1.259057^2 = 0.150437 \qquad \text{(Eq. 55)}$$

To obtain a probability of failure, we have to make an assumption on how the performance function g is distributed. If the hypothesis is that g* is normally distributed, then:*

$$g^* \sim N(\mu_{g^*}; \sigma^2_{g^*}) \sim N(1.259057;\ 0.150437)$$

and the probability of failure $P_f[g^* \le 0]$ can be calculated:

$$P_f\left[g^* \le 0\right] = F_N(0) = \Phi\left(\frac{0 - \mu_{g^*}}{\sigma_{g^*}}\right) = \Phi\left(\frac{-1.259057}{\sqrt{0.150437}}\right) = \Phi(-3.246142) = 0.000585 \qquad \text{(Eq. 56)}$$

Note that the probability value obtained with PEM is slightly less than the value estimated with Taylor's series and that variance is the same in both cases.

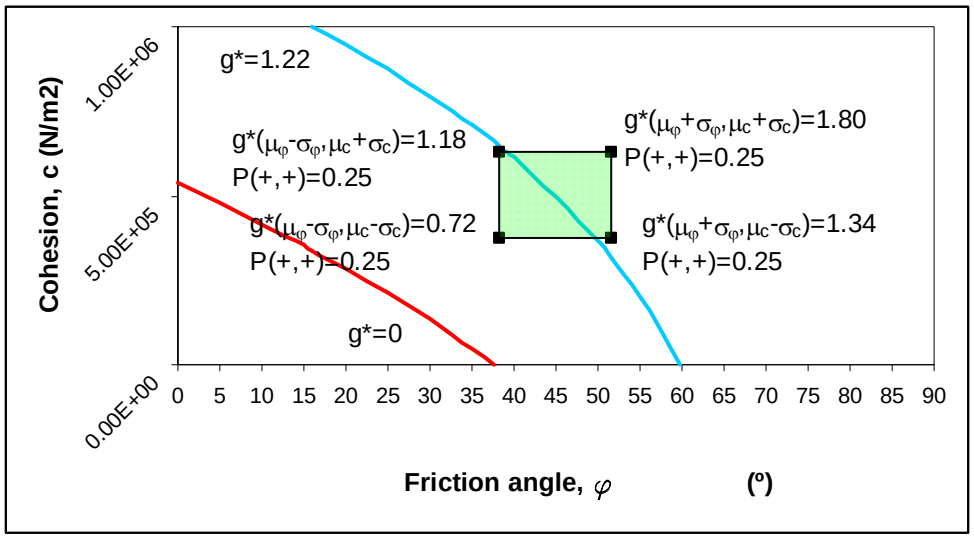

Figure 7: Point Estimate Method.

9.- LEVEL 2 METHODS. HASOFER-LIND.

9.1.- THEORETICAL BASIS.

One of the problems of the Taylor's series method and Point Estimate Method is the lack of invariance of the reliability indexes obtained, as their value depend upon the formulation of the performance function g*. To avoid this, Hasofer and Lind [4] developed an invariant definition of the reliability index.

Let **X** be the vector of the random variables $(X_1,X_2,...,X_n)$, normally distributed, $\boldsymbol{\mu_X}$ the vector of the mean values, $\boldsymbol{\sigma_X}$ the variance-covariance matrix and g^*_X the performance function, supposed to be linear. The reliability index proposed by Hasofer and Lind is defined by:

$$\beta = \underset{x}{Min}\sqrt{(x-\mu_X)^T \sigma_X^{-1}(x-\mu_X)} \qquad \text{(Eq. 57)}$$

Subject to:

$$g^*_X(x) = 0 \qquad \text{(Eq. 58)}$$

The point of the n-dimensional space that verifies the condition is the "design-point", which lies on the limit state region between the safety and the failure domains. Of all of the possible point lying on the limit state region, the design-point is the most likely. That is to say that of all possible points on the limit state region, at the design point, the joint probability density function $f_{X1,X2,..,Xn}$ of all the random variables reaches the highest value.

If random variables are independent, then the variance-covariance matrix is a diagonal matrix, where values lying on the diagonal are the variances of the random values, so the problem defined by (57) y (58) can be re-written as:

$$\beta = \underset{x_i}{Min}\sqrt{\sum_{i=1}^{n}\left(\frac{x_i-\mu_{X_i}}{\sigma_{X_i}}\right)^2} \qquad \text{(Eq. 59)}$$

Subject to:

$$g_X^*(x_1, x_2, ..., x_n) = 0 \qquad \text{(Eq. 60)}$$

To apply this method is a common practice to transform normal correlated random variables (X_1,X_2,...,X_n) in standard normal uncorrelated random variables with null mean and standard deviation being unity (Z_1,Z_2,...,Z_n). To keep the metric in both spaces an orthogonal transformation should be done. The first step is to transform initial normal correlated random variables in normal uncorrelated random variables (U_1,U_2,...,U_n). This is accomplished by a transformation matrix **B**:

$$\mathbf{U} = \mathbf{BX} \qquad \text{(Eq. 61)}$$

As the variance-covariance matrix is symmetric and defined positive, it can be expressed as:

$$\boldsymbol{\sigma}_X = \mathbf{L}\mathbf{L}^T \qquad \text{(Eq. 62)}$$

Where **L** is a triangular matrix which can be obtained from $\boldsymbol{\sigma}_X$. The transformation matrix is determined as:

$$\mathbf{B} = \mathbf{L}^{-1} \qquad \text{(Eq. 63)}$$

It can be proved that $\boldsymbol{\sigma}_U = \mathbf{I}$ (Mínguez [1]).

Variable standardization is done by:

$$Z = U - \mu_U = B(X - \mu_X) \qquad \text{(Eq. 64)}$$

In the transformed space, the formulation of the problem is as follows:

$$\beta = \underset{z}{Min} \sqrt{z^T z} \qquad \text{(Eq. 65)}$$

Subject to:

$$g_Z^*(z) = 0 \qquad \text{(Eq. 66)}$$

In the transformed space β is the minimum distance between the origin of coordinates and the failure domain. Vector along which the distance β is defined in the transformed space has the director cosines determined by:

$$\alpha = \frac{\dfrac{\partial g_Z^*}{\partial z}}{\sqrt{\dfrac{\partial g_Z^*}{\partial z}^T \dfrac{\partial g_Z^*}{\partial z}}} \qquad \text{(Eq. 67)}$$

This director cosines represent the sensitivity of the performance function g_z* to changes in the values of the variable z_i.

To solve the minimization problem different algorithms may be used (Newton, gradient, etc.).

As in previous methods, probability is derived from the reliability index making an assumption on how the performance function is distributed. If random variables are normally distributed and the performance function is linear, then it is normally distributed too.

9.2.- APPLICATION TO THE CASE STUDY.

The calculation of the reliability index with the Hasofer-Lind method is expressed by:

$$\beta = \underset{(\phi,c)}{Min} \sqrt{\left(\frac{\phi-\mu_\phi}{\sigma_\phi}\right)^2 + \left(\frac{c-\mu_c}{\sigma_c}\right)^2} = \underset{(\phi,c)}{Min} \sqrt{\left(\frac{\phi-45}{6.75}\right)^2 + \left(\frac{c-5.00e5}{1.25e5}\right)^2} \qquad \text{(Eq. 68)}$$

Subject to:

$$g^*(\varphi,c) = \frac{5.25e7 \times tg\varphi + 75 \times c}{4.05e7} - 1 = 0 \qquad \text{(Eq. 69)}$$

The numerical problem can be solved with different algorithms, as Newton's or gradient method. In this particular case the tool "Solver" implemented in the commercial spreadsheet Excel© has been used to solve the problem.

Initial values are $\varphi = c = 0$. Reliability index obtained is $\beta = 3.656443$, for values at the design point of $\varphi = 28.8987^o$ and $c = 1.54e5$ N/m^2.

Assuming that g is normally distributed, sliding probability of failure is determined:*

$$P_f[g^* \le 0] = F_N(0) = \Phi(-3.656443) = 0.000128 \qquad \text{(Eq. 70)}$$

This value of probability is less than the values provided by previous methods, and it is a more accurate one..

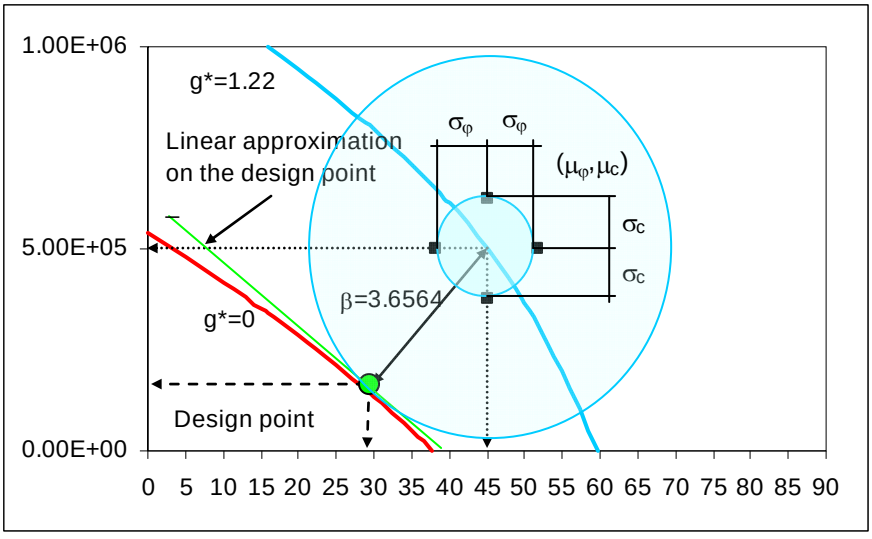

Figure 8: Hasofer-Lind method.

10.- LEVEL 3 METHODS. SIMULATION.

10.1.- THEORETICAL BASIS.

Level 3 methods provide a more accurate evaluation of the probability of failure, as they consider all the information of the probability density function and not only the first two moments. The formulation of the problem is that of equation (4).

To evaluate the integral we can resort to two groups of methods.

In the first group we can find methods based on the transformation of the random variables in a fashion similar to FOSM methods. FORM (First Order Reliability Methods) y SORM (Second Order Reliability Methods) are methods of this kind.

In the second group we can find methods that try to calculate directly the integral defined by equation (4). We have on one side the numerical methods of integration (Simpson, Gauss-Laguerre, Gauss-Hermite, etc.) and on the other side the simulation methods (Monte Carlo Methods).

With the simulation methods we generate N sets of values for the random variables according to their probability distributions and possible correlations:

$$\hat{x}(i) = \left(\hat{x}_1, \hat{x}_2, ..., \hat{x}_n \right)_{(i)} ; \mathbf{i = 1,..., N} \qquad \text{(Eq. 71)}$$

Generation of these values is accomplished by statistical techniques as the inverse transform method, the composition method, the acceptance-rejection method, and others (Rubinstein [5]).

The performance function is evaluated for each one of these sets of values, and the number of failures, m, (when g*≤0) is calculated. The probability of failure can be then estimated by:

$$P_{fallo} \approx \frac{m\left(g^*\left(\hat{x}_1, \hat{x}_2, ..., \hat{x}_n \right) \le 0 \right)}{N} = \hat{P}_f \qquad \text{(Eq. 72)}$$

This method of simulation is the normal Monte Carlo method ("Hit or Miss Monte Carlo Method"). These simulation methods are deemed "exact methods" in the sense that they provide the exact value of the probability of failure when $N \to \infty$. For lower values of N, what we get is an approximation of the value of the integral (4). The estimator of the probability of failure shows a mean and a variance given by:

$$E\left[\hat{P}_f \right] = P_f$$
$$\sigma^2_{\hat{P}_f} = \frac{1}{N} P_f \left(1 - P_f\right) \qquad \text{(Eq. 73)}$$

The accuracy of the estimation is measured by inverse of the standard deviation of the estimator, which is proportional to $N^{0.5}$. So we can double the precision in the approximation of the value of the probability of failure by multiplying by four the number of experiments (USACE [6]).

Probabilities of failure in civil engineering in general and in dam engineering in particular are very low, being of an order of 1 out of 10000 and less. So to capture this order of magnitude with simulation, a large number of experiments are needed, as each experiment is a Bernouilli process, with an individual probability of failure equal to the sought probability of failure.

From the early days of the development of the method, researchers have explored techniques with the aim of increasing the efficiency of the method (obtain low variances with less experiments). Between these techniques to reduce the variance we can find the "importance sampling" (Clark [7]), the "correlated sampling" (Cochran [8]), and the "stratified sampling", being one of its variants the "Latin Hypercube Sampling" (Iman et al. [9, 10], McKay et al [11] y Startzman el al [12]).

Latin hypercube divides the probability distribution in different intervals equally distributed along the Y axis, corresponding to the cumulative probability. During the sampling process an identical number of experiments are generated on each of the intervals, so all the probability distribution space is swept, even those areas of very low probability that would not have been sampled unless a very large number of experiments had been done.

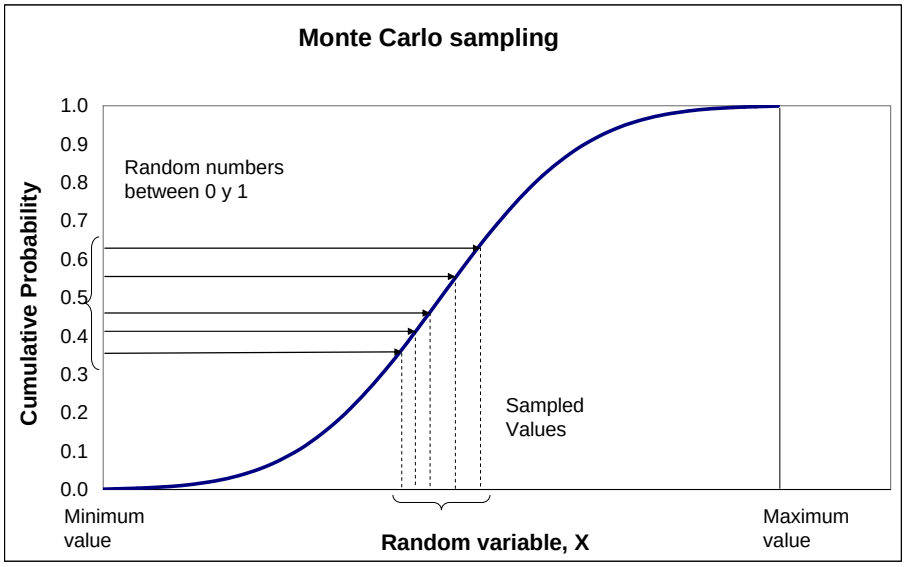

Figure 9: Monte Carlo sampling.

So it is very useful to estimate the order of magnitude of the probability of failure previously to the programming of a Monte Carlo to optimize the simulation.

It is a common practice to use Monte Carlo techniques to make inferences of the probability distribution of the performance function and of the probability distribution of the safety factor, which are closely related.

The N evaluations of the performance function form a sample of a random variable, so it is possible to make estimations on important parameters (mean, standard deviation, skewness, etc.) that help to understand how the performance function is distributed in terms of probability.

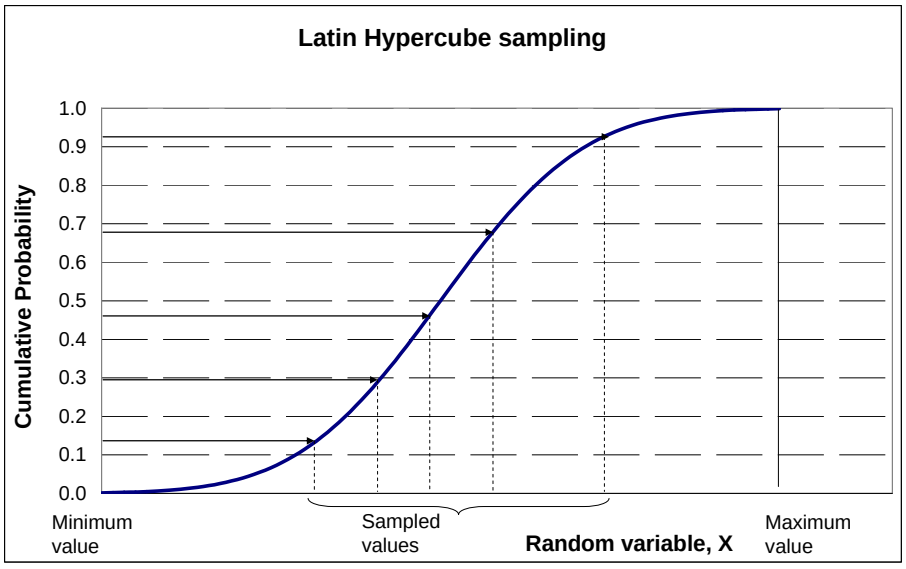

Figure 10: Latin Hypercube sampling.

Once the probability distribution function F_{g*}, of the performance function is derived, the probability of failure can be determined straightforward by:

$$P_f = P[g^* \le 0] = F_{g^*}(0) \qquad \text{(Eq. 74)}$$

An apparent advantage of this procedure is that, once F_{g*} is known, which can be done with a relative low number of experiments, N, the whole probability domain is fully determined, so probability estimations can be done at any level, even in the tails of the distributions. The problem that immediately arises is that the estimation made on the probability distribution function can be (and it usually is) inaccurate in the tails of the distribution, which are the key areas to estimate the probability of failure

10.2.- APPLICATION TO THE CASE STUDY

The failure domain g=0 is defined by equation (75):*

$$g^*(\phi, c) = a_0 + a_1 \times tg\phi + a2 \times c = -1 + 1.30 tg\phi + 1.85 \times 10^6 \times c = 0 \qquad \text{(Eq. 75)}$$

We consider two random variables: friction angle and cohesion, being both normally distributed.

By Monte Carlo techniques different sets of experiments are generated. The number of experiments differs for each set: N =100, 1000, 10000, 100000 y 1000000. The sampling is done using two techniques: Monte Carlo sampling and Latin Hypercube sampling.

Each pair of sampled values will be used to evaluate the performance function, g, and so determination of the number of "failures", m, where $g^* \le 0$ will be calculated. Probability of failure, Pf, is estimated using equation (72). The variance of the probability obtained is calculated using equation (73).*

Calculations had been carried out with the commercial tool @RISK® implemented in an Excel® spreadsheet. Results are given in Tables 6 and 7.

Table 6. Estimation of the probability of failure with Monte Carlo sampling

Simulations with Monte Carlo sampling					*Direct Integration Method*
Number of experiments, N	*Number of misses, m*	*Probability of failure, Pf = m/N*	*Variance*	*Standard deviation*	*Exact probability of failure, Pf*
1000	*0*	*0*	*0*	*0*	1.11×10^{-4}
10000	*1*	1.00×10^{-4}	1.00×10^{-8}	1.00×10^{-4}	1.11×10^{-4}
100000	*18*	1.80×10^{-4}	1.80×10^{-9}	4.24×10^{-5}	1.11×10^{-4}
1000000	*135*	1.35×10^{-4}	1.35×10^{-10}	1.16×10^{-5}	1.11×10^{-4}

Table 7. Estimation of the probability of failure with Latin Hypercube sampling

Simulations with Latin Hypercube					*Direct Integration Method*
Number of experiments, N	*Number of misses, m*	*Probability of failure, Pf = m/N*	*Variance*	*Standard deviation*	*Exact probability of failure, Pf*
1000	*0*	*0*	*0*	*0*	1.11×10^{-4}
10000	*2*	2.00×10^{-4}	2.00×10^{-8}	1.41×10^{4}	1.11×10^{-4}
100000	*10*	1.00×10^{-4}	1.00×10^{-9}	3.16×10^{-5}	1.11×10^{-4}
1000000	*116*	1.16×10^{-4}	1.16×10^{-10}	1.08×10^{-5}	1.11×10^{-4}

It should be noted that the method provides accurate results for a number of experiments of the same order of magnitude or larger that the probability of failure Latin Hypercube shows slightly better results for the same number of experiments. In Figure 11 is shown graphically the calculation of the probability of failure with Monte Carlo sampling for N=10000.

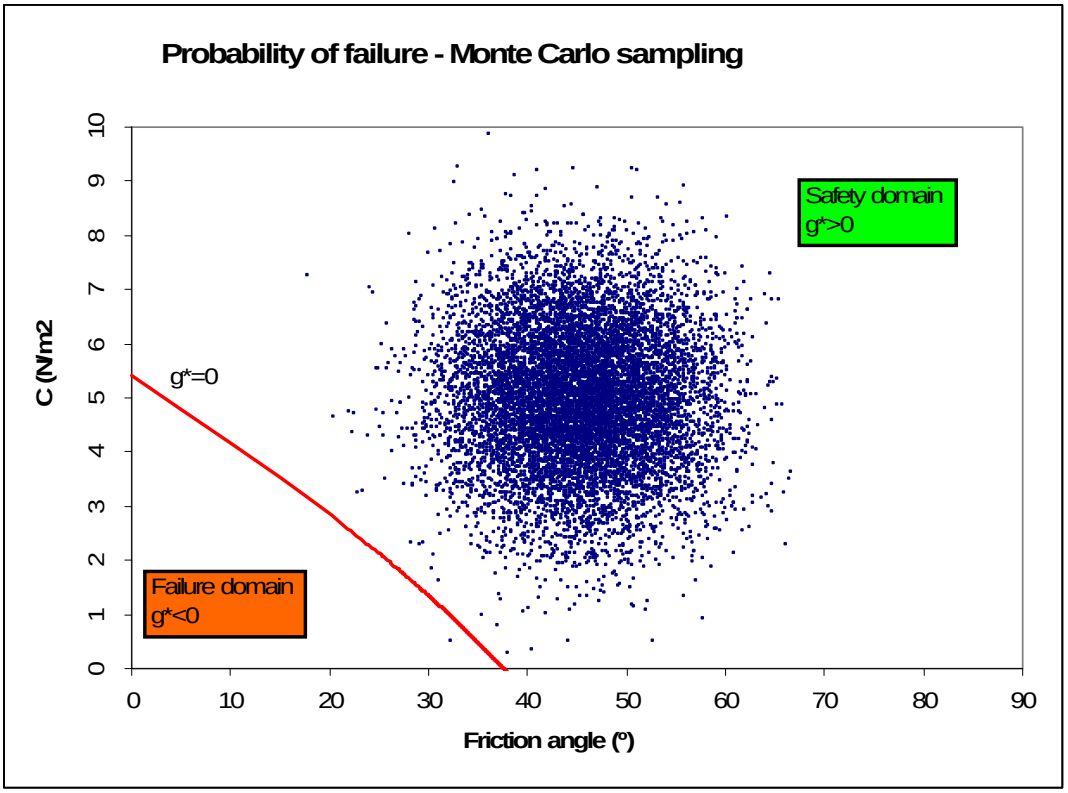

Figure 11: Probability of failure with Monte Carlo sampling.

We can try to adjust a probability distribution to the N values of g sampled. Table 8 shows the estimators for the mean, variance, standard deviation and skewness, for the sampled values using Monte Carlo sampling.*

Table 8. Estimators for parameters of g*. Monte Carlo sampling

Estimators for parameters of g. Monte Carlo sampling*				
Number of experiments, N	*Mean*	*Variance*	*Standard deviation*	*Skewness*
1000	*1.278071*	*0.170130*	*0.412469*	*0.500776*
10000	*1.268753*	*0.170377*	*0.412768*	*0.590840*
100000	*1.260465*	*0.163442*	*0.404279*	*0.482087*
1000000	*1.260573*	*0.162467*	*0.403072*	*0.474239*

Results for values sampled using Latin Hypercube techniques are given in Table 9.

Table 9. Estimators for parameters of g*. Latin Hypercube sampling

Estimators for parameters of g. Latin Hypercube sampling*				
Number of experiments, N	*Mean*	*Variance*	*Standard deviation*	*Skewness*
1000	*1.260921*	*0.160528*	*0.400660*	*0.372136*
10000	*1.261030*	*0.163296*	*0.404099*	*0.465118*
100000	*1.261040*	*0.163101*	*0.403858*	*0.479242*
1000000	*1.261041*	*0.162702*	*0.403364*	*0.483939*

It should be noted that faster convergence is obtained with Latin Hypercube.

Adjustment for two probability distribution functions has been done for the case of N=10000 experiments with both sampling methods (Monte Carlo and Latin Hypercube). This adjustment has been carried out with @RISK®. Chi-square good-of-fitness test has been carried out as well.

Two distributions have been tested: normal and lognormal. Lognormal distribution has been considered as results show certain skewness while normal distribution is symmetric.

The performance function g, defined by equation (75) can adopt both positive and negative values.*

Normal distribution is defined in the whole domain ($-\infty < g^* < +\infty$) while Lognormal distribution is defined in the positive interval ($0 \le g^* < +\infty$). This is the reason why in the process of adjustment it is necessary to consider an offset, s, so the adjustment is done for a transformed function G, defined as:*

$$G^* = g^* + s \quad ; 0 \le G^* < \infty \qquad \text{(Eq. 76)}$$

Chi-square goodness-of-fit test is based in the estimation of::

$$\chi^2 = \sum_{i=1}^{k} \frac{(n_i - E_i)}{E_i} \qquad \text{(Eq. 77)}$$

where:

k = number of intervals in which is divided the domain of g (74 in this case)*
n_i = number of sampled values lying in the i interval.
E_i = expected value of the number of values corresponding to the i interval.

The better the fit between a certain probability distribution and the sampled values, the less is the value of χ^2.

One the adjustment is made, the probability of failure can be estimated with equation (74).

Results for adjustments and probabilities of failure with Monte Carlo sampling are given in Table 10. In Figures 12 and 13 the adjustment is shown graphically. The Lognormal distribution shows a better fit to sampled values.

Table 10. Fit of probability distributions to g*. Monte Carlo sampling

Values of g evaluated with Monte Carlo sampling*					
Number of experiments, N =10000					*Probability of failure P (g*≤0)*
Distribution	*Mean*	*Variance*	*Offset*	*Test χ^2*	
Normal	*1.268753*	*0.170377*	*0*	*268.5*	*1.06×10^{-3}*
Lognormal	*2.728899*	*0.168983*	*-1.460194*	*84.5*	*2.07×10^{-5}*

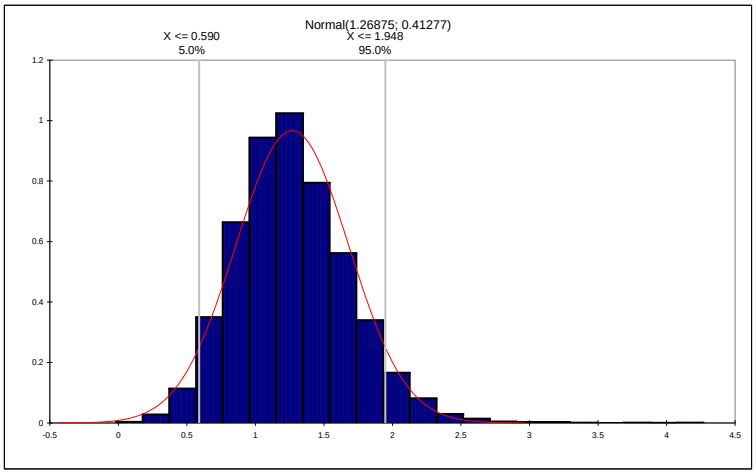

Figure 12: Fit of a normal distribution to the performance function, g*.

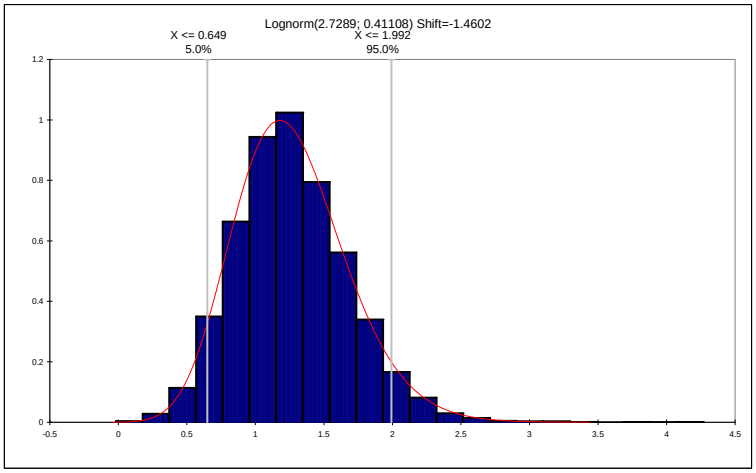

Figure 13: Fit of a lognormal distribution to the performance function, g*.

If comparison is made between the probability of failure provided by simulation for N=10000 experiments (1.41×10^{-4}) and the probability of failure estimated adjusting a normal distribution to the sampled values of g (1.06×10^{-3}) it is shown that there is an overestimation of the probability of failure. On the other hand, the probability of failure obtained adjusting a Lognormal distribution (2.07×10^{-5}) is underestimated. This illustrates the strong difficulties that come from fitting distributions to data, if the sought information is in the tails of the distributions.*

Results for adjustments and probabilities of failure with Latin Hypercube sampling are given in Table 11. In Figures 14 and 15 the adjustment is shown graphically. The Lognormal distribution shows again a better fit to sampled values.

Table 11. Fit of probability distributions to g*. Latin Hypercube sampling.

Values of g evaluated with Latin Hypercube sampling*					
Number of experiments, N =10000					*Probability of failure P (g*≤0)*
Distribution	*Mean*	*Variance*	*Offset*	*Test χ^2*	
Normal	*1.261030*	*0.163296*	*0*	*264.8*	*9.02×10^{-4}*
Lognormal	*3.047930*	*0.162627*	*-1.786922*	*87.1*	*3.34×10^{-5}*

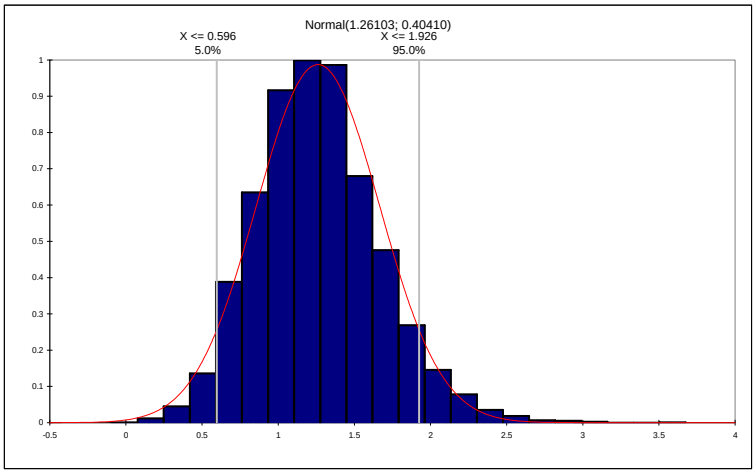

Figure 14: Fit of a normal distribution to the performance function, g*.

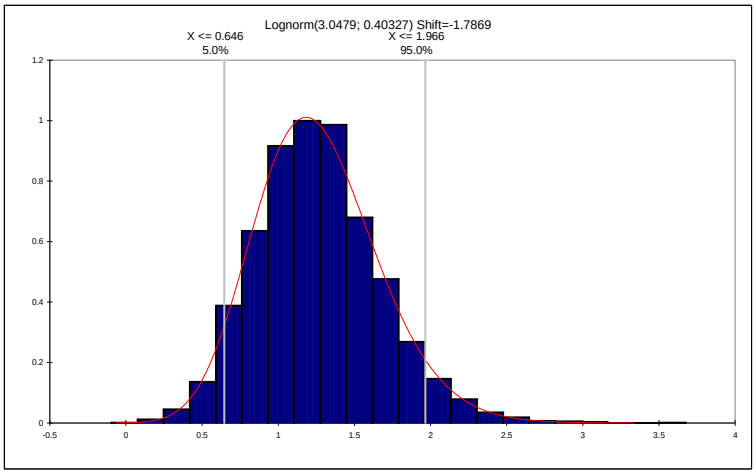

Figure 15: Fit of a lognormal distribution to the performance function, g*.

If comparison is made between the probability of failure provided by simulation for N=10000 experiments (1.41×10^{-4}) and the probability of failure estimated adjusting a normal distribution to the sampled values of g (9.02×10^{-4}) it is shown that there is an overestimation of the probability of failure. On the other hand, the probability of failure obtained adjusting a Lognormal distribution (3.34×10^{-5}) is underestimated*

11.- REFERENCES.

[1] MÍNGUEZ, R. (2003)
Seguridad, fiabilidad y análisis de sensibilidad en obras de ingeniería civil mediate technical de optimization poor decomposition. Applications.
Testis Doctoral. Universidad de Catbrier.

[2] ROSENBLUETH, E. (1975)
Point estimates for probability moments.
Proceedings of the National Academy of Science, USA, 72 (10)

[3] HARR, M.E. (1987)
Reliability-based design in civil engineering.
John Wiley and Sons, New York, USA.

[4] HASOFER, A.M.; LIND, N.C. (1974)
Exact and invariant second moment code format.
Journal of Engineering Mechanics. 100, EM1, 111-121

[5] RUBINSTEIN, R.Y. (1981)
Simulation and the Monte Carlo Method.
John Wiley & Sons.

[6] US ARMY CORPS OF ENGINEERS (1999)
ETL 1110-2-556. Appendix A: An overview of probabilistic analysis for geotechnical engineering problems.
Washington, DC.

[7] CLARK, E. (1961)
Importance sampling in Monte Carlo Analyses.
Operations Research, 9 – 603-6

[8] COCHRAN, W.S. (1966)
Sampling techniques.
2nd ed. Wiley, New York

[9] IMAN, R.L.; DAVENPORT, J.M.; ZEIGLER, D.K. (1980)
Latin Hypercube Sampling
Technical Report SAND79-1473.
Sandia Laboratories. Albuquerque

[10] IMAN, R.L.; CONOVER, W.J. (1980)
Risk Methodology for geologic disposal of radioactive waste: a distribution-free approach to inducing correlations among input variables for simulation studies.
Technical Report NUREG CR 0390.
Sandia Laboratories. Albuquerque

[11] McKAY, M.D.; CONOVER, W.J.; BECKMAN, R.J. (1979)
A comparison of three methods for selecting values of input variables in the analysis of output from a computer code.
Technometrics 211, 239-245

[12] STARTZMAN, R.A.; WATTENBARGER, R.A. (1985)
An improved computation procedure for risk analysis problems with unusual probability functions
SPE Hydrocarbon Economics and Evaluation Symposium Proceedings. Dallas

XI ICOLD BENCHMARK WORKSHOP ON NUMERICAL ANALYSIS OF DAMS

Valencia, October 20-21, 2011

THEME C

SLIDING FAILURE PROBABILITY ESTIMATION OF A CONCRETE GRAVITY DAM

Faggiani, Giorgia[1]

Frigerio, Antonella[1]

Masarati, Piero[1]

Meghella, Massimo[1]

CONTACT

Meghella Massimo, RSE S.p.A., Environment and Sustainable Development Department, Via R.Rubattino 54, 20134 Milan, Italy, Ph. +39 02 3992 5731, massimo.meghella@rse-web.it.

Summary

The aim of Theme C is to promote a probabilistic approach in dam safety assessment, based on structural reliability methods.

In this paper the sliding failure probability of a concrete dam , under different reservoir level conditions was estimated. Different methods were applied: FOSM and Hasofer-Lind, as Level 2 methods; Montecarlo, as Level 3 method. The formers are approximated techniques, while the Level 3 methods are deemed to be exact if the number of samples tends to infinity. For each loading scenario the safety factor was computed as well.

Several limit-state functions to define the sliding stability (ratio of the driving hydrostatic force and the shear strength) were considered, assuming the friction angle (or its tangent) and the cohesion along the dam-foundation interface as uncertain parameters, under both the hypotheses of effective and ineffective drainage system.

All methods provided quite similar results, in terms of failure probability and reliability index, when uncertain parameters are modeled with the Normal distribution. Level 3 methods, such as Montecarlo, capable to model the uncertain parameters with different distributions types (having in particular the possibility to exclude unrealistic or negative values, such as, e.g., the Lognormal), provide failure probabilities generally lower and ideally more accurate than Level 2 methods.

[1] RSE S.p.A., Environment and Sustainable Development Department, Milan, Italy.

1. Geometry and material properties

The 2D block geometry of the concrete gravity dam under examination is depicted in Figure 1. According to Theme C requirements (*Escuder et al* [1]), (*Hartford & Baecher* [2]), a limit equilibrium model, assuming the block as undeformable, was adopted to evaluate the sliding failure of the gravity dam. The mass density of the concrete is 2400 kg/m^3 and the experimental values for modeling the uncertain parameters (cohesion and friction angle along the potential sliding surface) are summarized in Table 1.

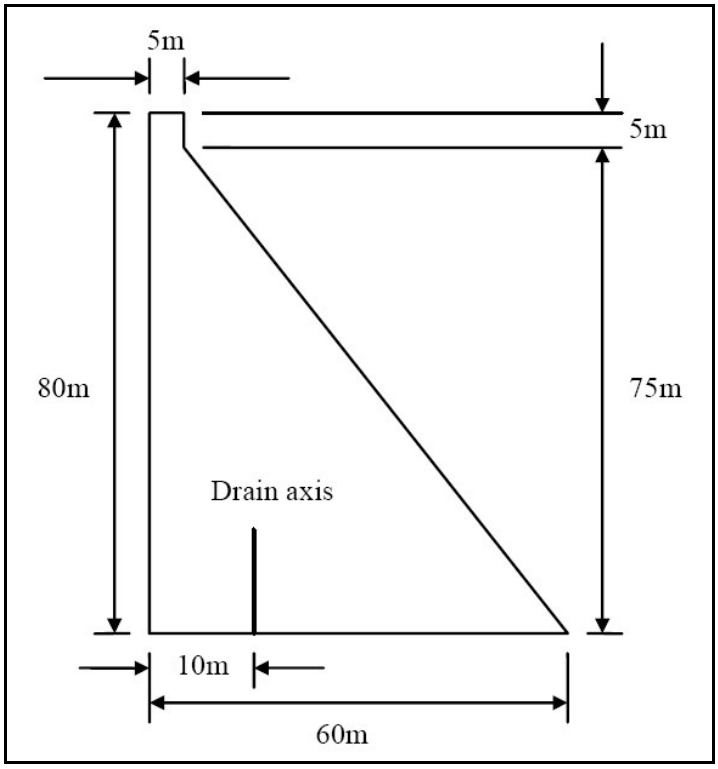

Figure 1: Geometric vertical section of the provided gravity dam

Table 1: Angle of friction and cohesion random data

SAMPLE	ANGLE OF FRICTION φ (°)	COHESION c (MPa)
1	45	0.5
2	37	0.3
3	46	0.3
4	45	0.7
5	49	0.8
6	53	0.2
7	54	0.6
8	45	0.0
9	49	0.1
10	60	0.2
11	63	0.2
12	62	0.4
13	60	0.7
14	56	0.1
15	62	0.4

3. Model definition

3.1. Loadings

The proposed exercise takes into account the following loadings, acting on the 2D rigid model:

1. dead weight
2. hydraulic pressure
3. uplift pressure acting over the dam base

The hydraulic pressure was accounted considering five different water levels (Table 2) that represent possible operating or limit conditions, as well as overtopping.

The uplift pressure (Figure 2) was evaluated considering the following assumptions:

1. Case A: Drainage system effective (probability = 0.90)
2. Case B: Drainage system ineffective (probability = 0.10)

For each water level, and for both effective and ineffective drain, the crack length (Table 2) was determined according to the rotational limit equilibrium. The cross section of the dam was idealized as a beam with variable section, in which the normal compressive stress varies linearly, and no tensile stress is allowed at the sliding surface. The evolution of the horizontal crack was simulated by reducing accordingly the effective area at the interface dam-foundation that provides resistance to overturning moment.

The pressure distributions along the sliding surface vary according to Figure 2 (Case A: left; Case B: right).

Table 2: Water levels and crack lengths according to drain conditions

WATER LEVEL (in m over dam-foundation contact plane)	CRACK LENGTH (in m) for an effective drain (Case A)	CRACK LENGTH (in m) for an ineffective drain (Case B)
75	0.0	0.0
78	0.0	18.1
80	0.0	40.1
82	3.7	60.0
85	12.0	60.0

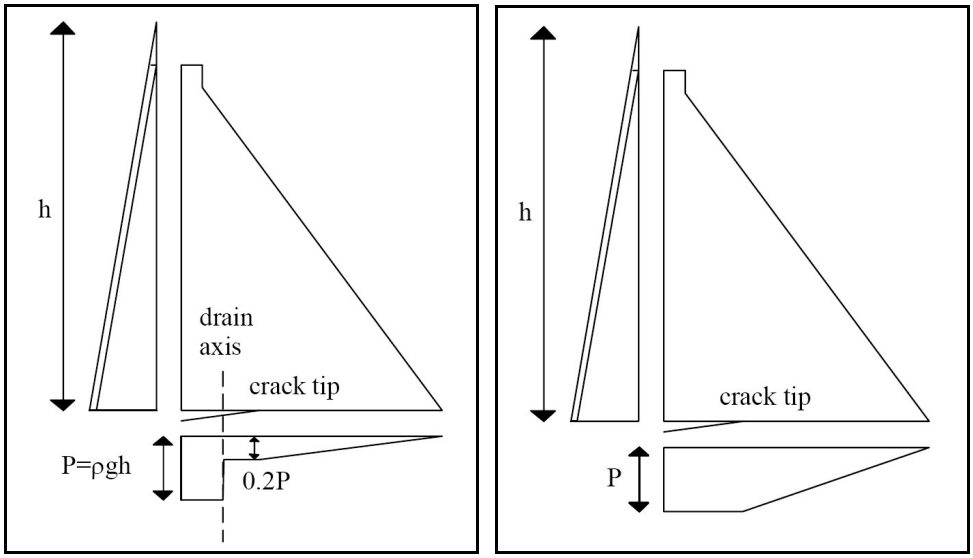

Figure 2: Uplift pressure variation along the dam base in case of an effective (left) and an ineffective (right) drain

3.2. Limit state functions

The limit state function, g* - expressed as a function of the random independent variables, friction angle, φ and cohesion, *c* - is obtained by balancing the shear strength, *R* along the sliding surface and the driving hydrostatic force, *S* :

$$g^*(\varphi, c) = \frac{R(\varphi, c)}{S} - 1 = 0 \qquad (1)$$

Any point (φ ,*c*) in the 2-dimensional space is in the *safety* or *failure* domain, depending on whether the function is positive or negative (Figure 3).

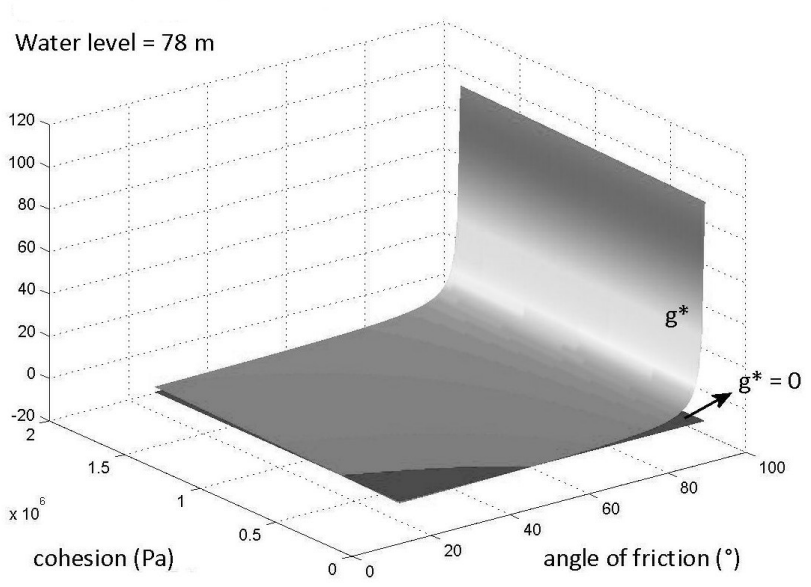

Figure 3: Example of 3D surface relevant to a non-linear limit state function

The resistance force *R* can be expressed as:

$$R = (N - U)\,\mathrm{tg}\,\varphi + B\,c \tag{2}$$

being:

N, the dead weight in N/m (*fixed*)
U, the uplift in N/m (*fixed*)
B, the contact area in m^2/m (*fixed*)
φ, the angle of friction along the contact surface in degrees (*random*)
c, the cohesion along the contact surface in Pa (*random*)

The driving hydrostatic force does not depend on the random variables and can be expressed as:

$$S = \frac{1}{2}\rho_w\, g h^2 \tag{3}$$

being:

ρ_w the water density in kg/m^3 (*fixed*)
g the gravity acceleration in m/s^2 (*fixed*)
h the water level in m (*fixed*)

The limit state functions, defined on the basis of the considered water levels and depending on the drainage system effectiveness, are summarized in Table 3 and Table 4.

Table 3: g* functions (Case A: effective drain)

Water level [m]	**g* function - (Case A: effective drain)**
75	$\frac{46940850 \cdot \mathrm{tg}\varphi + 60 \cdot c}{27590625} - 1 = 0$
78	$\frac{46499400 \cdot \mathrm{tg}\varphi + 60 \cdot c}{29842020} - 1 = 0$
80	$\frac{46205100 \cdot \mathrm{tg}\varphi + 60 \cdot c}{31392000} - 1 = 0$
82	$\frac{45910800 \cdot \mathrm{tg}\varphi + 60 \cdot c}{32961600} - 1 = 0$
85	$\frac{45302580 \cdot \mathrm{tg}\varphi + 60 \cdot c}{35316000} - 1 = 0$

Table 4: g* functions (Case B: ineffective drain)

Water level [m]	**g* function - (Case B: ineffective drain)**
75	$\frac{35904600 \cdot \mathrm{tg}\varphi + 60 \cdot c}{27590625} - 1 = 0$
78	$\frac{28096821 \cdot \mathrm{tg}\varphi + 60 \cdot c}{29842020} - 1 = 0$
80	$\frac{18697860 \cdot \mathrm{tg}\varphi + 60 \cdot c}{31392000} - 1 = 0$
82	$\frac{9711900 \cdot \mathrm{tg}\varphi + 60 \cdot c}{32961600} - 1 = 0$
85	$\frac{7946100 \cdot \mathrm{tg}\varphi + 60 \cdot c}{35316000} - 1 = 0$

3.3. Reliability methods and probability density functions

Estimations of sliding failure probability P_f were computed by means of different methods grouped into three levels according to the classification proposed by *Mínguez* [3]:

1. **Level 1**: the global safety factor according to the classical approach used in structural safety assessment.
2. **Level 2**: they includes the First Order Second Moment (FOSM) methods, which make a linear approximation of the limit state function and consider the first two moments of the

joint probability density function distribution only. In the present work the *FOSM Taylor method* and the *Hasofer-Lind method* were used.

3. **Level 3**: They provide a more accurate evaluation of the probability of failure, as they consider all the information of the probability density function and not only the first two moments. In the present work *Montecarlo simulations* method was used.

In the following sections few hints of each adopted method are provided (*Altarejos García* [4]).

3.3.1. Safety factor approach

The global safety factors Fs are obtained from (4), assigning the mean value of both friction angle (μ_φ = 37°) and cohesion (μ_c = 0.367 MPa):

$$F_S = \frac{R\left(\mu_\varphi, \mu_C\right)}{S} = \frac{(N-U)\,tg\mu_\varphi + B\mu_C}{\frac{1}{2}\rho_w g h^2} \tag{4}$$

3.3.2. FOSM methods

The FOSM Taylor method and the Hasofer-Lind method can deal with normally distributed random variables only and make a linear approximation of the limit state function.

The typical output of these methods is the *reliability index*, β, which is defined as the number of standard deviations between the expected value of the function g*(φ, c) and the limit state value defined as g*(φ, c)=0. The reliability index β gives a relative measure of safety: the higher β, the safer the structure. The probability of failure, P_f can be evaluated through the following equation:

$$P_f\left[g^*(\varphi, c) \le 0\right] = \Phi\left(-\beta\right) \tag{5}$$

where Φ denotes the Cumulative Density Function (CDF) of the standard Normal Distribution, computed as the integral of the Probability Density Function (PDF).

With the FOSM Taylor method, the reliability index β can be calculated as follows:

$$\beta = \frac{E[g^*]}{\sigma_{g^*}} = \frac{g^*(\mu_\varphi, \mu_c)}{\sigma_{g^*}} \tag{6}$$

being E[g*] and $\sigma^2_{g^*}$ respectively the first and second moment of the probability distribution of the limit state function. The first moment E[g*] is computed introducing the means μ of the random values into the limit state function, while the second moment is given by:

$$\sigma_{g^*}{}^2 = \mathrm{Var}[g^*] = \left(\frac{g^*(\mu_\varphi + \sigma_\varphi) - g^*(\mu_\varphi - \sigma_\varphi)}{2}\right)^2 + \left(\frac{g^*(\mu_c + \sigma_c) - g^*(\mu_c - \sigma_c)}{2}\right)^2 \qquad (7)$$

being Var[g*] the variance of the probability distribution g*, and σ the standard deviations of the random values.

With the Hasofer-Lind method, with random variables statistically independent, as in this case, the reliability index β is calculated as follows:

$$\beta = \min_{(\varphi,c)} \sqrt{\left(\frac{\varphi - \mu_\varphi}{\sigma_\varphi}\right)^2 + \left(\frac{c - \mu_c}{\sigma_c}\right)^2} \qquad \text{subjected to } g^*(\varphi, c) = 0 \qquad (8)$$

The point (φ, *c*) that minimizes the reliability index equation (8) was computed with Microsoft Excel optimization *Solver*.

3.3.3. Montecarlo simulations

The MATLAB Statistic Toolbox [5] was used to perform the Montecarlo simulations.

The Probability Density Functions (PDF) to properly model the random variables φ and c were selected by fitting experimental data with the best Cumulative Density Functions (CDF) available in the Statistic Toolbox.

The Normal Distribution provides the best fit for the friction angle, while Rayleigh and Lognormal Distributions for the cohesion (Figure 4). The latters, in particular, prevent the random variables to assume unrealistic or non-physical values (e.g. < 0). Table 5 summarizes the three combinations of probability distributions adopted in this study for the Montecarlo simulations.

Table 5: Distributions for Montecarlo simulations

CASE	FRICTION ANGLE DISTRIBUTION	COHESION DISTRIBUTION
1	Normal	Normal
2	Normal	Rayleigh
3	Normal	Lognormal

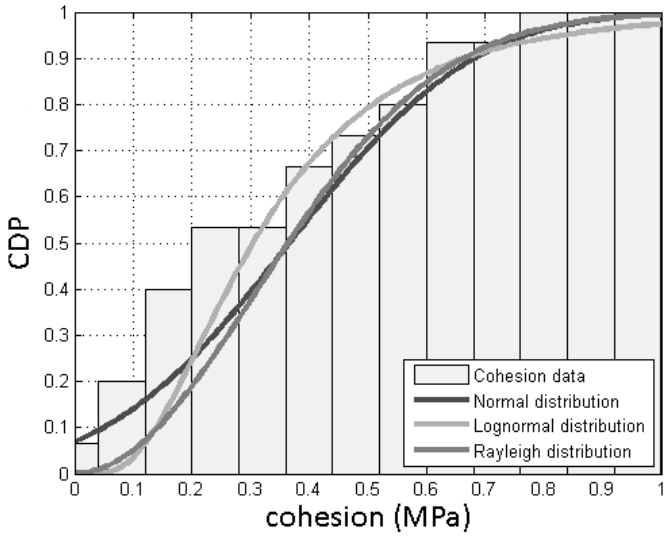

Figure 4: Distributions fitting the Cumulative Density Function of provided cohesion data

Since Montecarlo method becomes more and more accurate as the number of samples increases, one million of simulations have been found to be the optimum to provide stable and accurate solutions.

The Normal Probability Density Function is given by:

$$PDF_{ND} = \frac{1}{\sqrt{2\pi\sigma_{x_i}^2}} e^{-\left(\frac{(x_i-\mu_{x_i})^2}{2\sigma_{x_i}^2}\right)} \tag{9}$$

where μ_{Xi} and σ_{Xi} represent the mean and the standard deviation of φ and c respectively, obtained from the experimental data of Table 1.

The Rayleigh Probability Density Function for the cohesion is given by:

$$PDF_{RD} = \frac{c}{b^2} e^{-\left(\frac{c^2}{2b^2}\right)} \quad \text{with } c \geq 0 \tag{10}$$

where b = 309300 Pa, identified through the fitting process (Figure 4).

The Lognormal Probability Density Function requires first the computation of parameters λ and ζ of the cohesion, starting from its mean μ_c and variance Var[c]:

$$\lambda = \ln(\mu_c) - \frac{1}{2}\zeta^2 \tag{11}$$

$$\zeta^2 = \ln\left(1 + \frac{\mathrm{Var}[c]}{\mu_c^2}\right) \tag{12}$$

The PDF of the Lognormal Distribution is defined as (Figure 5):

$$\mathrm{PDF}_{LN} = \frac{1}{c\sqrt{2\pi\sigma^2}} e^{-\left(\frac{(\ln(c)-\mu)^2}{2\sigma^2}\right)} \tag{13}$$

The probability of failure P_f can be then estimated by

$$P_f = \frac{m\left(g^*(\varphi, c) \le 0\right)}{N} \tag{14}$$

where *m* is the number of failures (when $g^*(\varphi, c) \le 0$) and *N* is the number of trials (one million in this case):

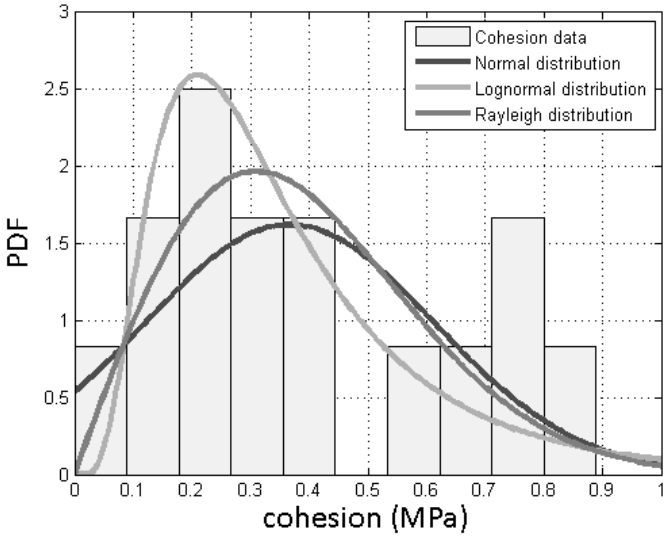

Figure 5: Probability Density Functions fitting the provided cohesion data

3.4. Event tree for failure probability calculation

According to the formulators requirements, for each water level the following conditions must be considered:

1. Case A: effective drain probability = 0.90
2. Case B: ineffective drain probability = 0.10

It means that P_f can be calculated with the following equation:

$$P_f = 0.9 \cdot P_{f,CaseA} + 0.1 \cdot P_{f,CaseB} \tag{15}$$

resulting from the event tree of Figure 6.

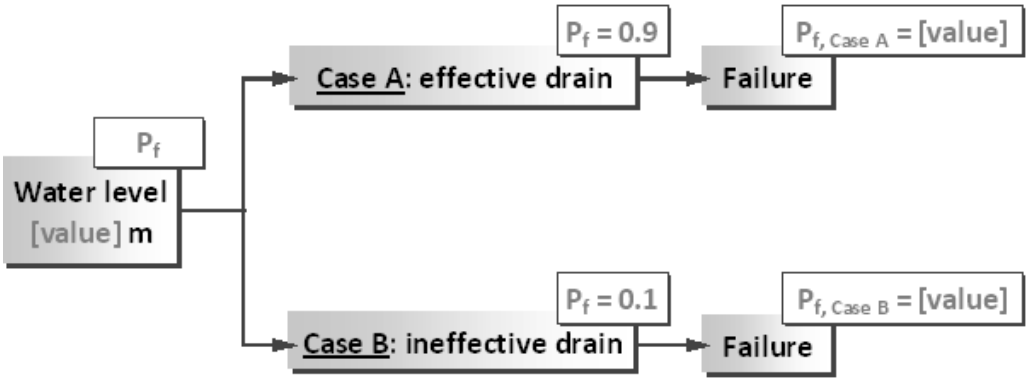

Figure 6: Event tree for P_f calculation

4. Results

Results in terms of sliding failure probability (except for Level 1 method for which the global safety factors are provided) are summarized in Tables 6 to 11.

Table 6: Level 1– Global Safety Factor (variables: φ, c)

Water level (m)	Global Safety Factor
75	2.95
78	2.68
80	2.50
82	2.33
85	2.15

Table 7: Level 2– FOSM Taylor and Hasofer-Lind (variables: φ, c)

Water level (m)	**P_f (FOSM Taylor)**	**P_f (Hasofer-Lind)**
75	1.06E-02	3.95E-03
78	1.72E-02	9.03E-03
80	3.19E-02	2.32E-02
82	6.20E-02	5.27E-02
85	7.96E-02	6.85E-02

Table 8: Level 3– Montecarlo Simulations (variables: φ, c)

Water level (m)	**P_f**		
	Friction angle: Normal **Cohesion:** Normal	**Friction angle:** Normal **Cohesion:** Rayleigh	**Friction angle:** Normal **Cohesion:** Lognormal
75	3.48E-03	1.12E-04	7.95E-05
78	8.08E-03	1.08E-03	9.85E-04
80	2.14E-02	1.05E-02	1.27E-02
82	5.02E-02	4.34E-02	5.41E-02
85	6.58E-02	5.84E-02	6.84E-02

It can be noticed the Level II methods provide quite different results, in particular for lower water levels. That is possibly due, apart the different level of approximation of the two methods, to the fact that the limit state functions are non-linear at the design point (Figure 3).

In order to understand such discrepancies, we additionally considered tanφ as random variable, instead of φ (Table 9 to 11). In this way the limit state functions become linear (Figure 8) and the Level II methods converge to the same results (Table 10).

With Level 3 methods, the solution still depend on g* function (non-linear or linear, Figure 9) but also it strongly depends on the type of distribution model chosen to model the random variables (Table 8).

As it can be seen in Figure 7, if trials include negative values for cohesion, as it may happen with the Normal Distribution, the number of samples falling in the failure domain grows significantly. That justifies the fact that Rayleigh and Lognormal distributions provide closer results, being their difference mainly due to the possibility of the Rayleigh Distribution to impose a threshold to the highest values.

When Normal Distribution are used for both φ and c, Level II and III results can be directly compared, highlighting in particular that Hasofer-Lind method provides more accurate results than FOSM Taylor.

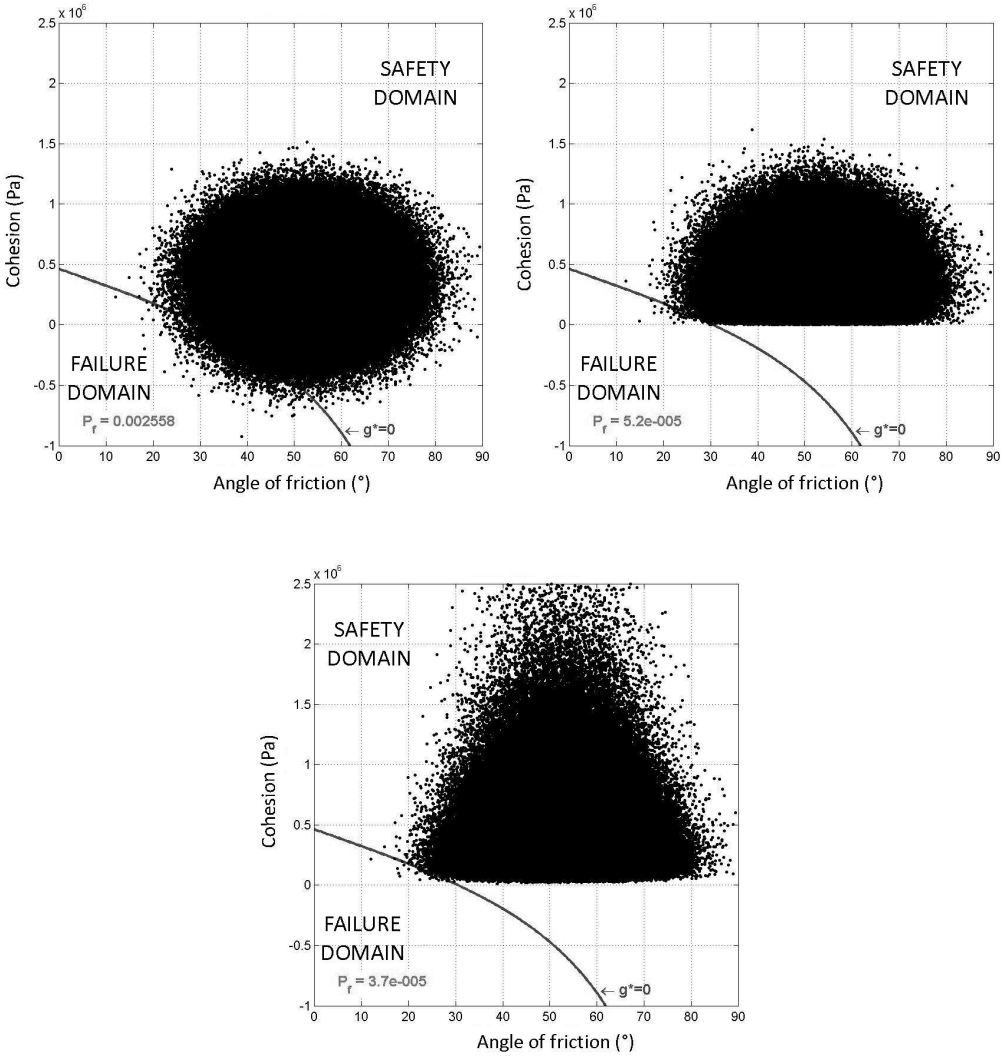

Figure 7: Sampling from Normal, Rayleigh and Lognormal Distributions drawn in the plane (φ, *c*) in case of effective drain and 75 m of water level

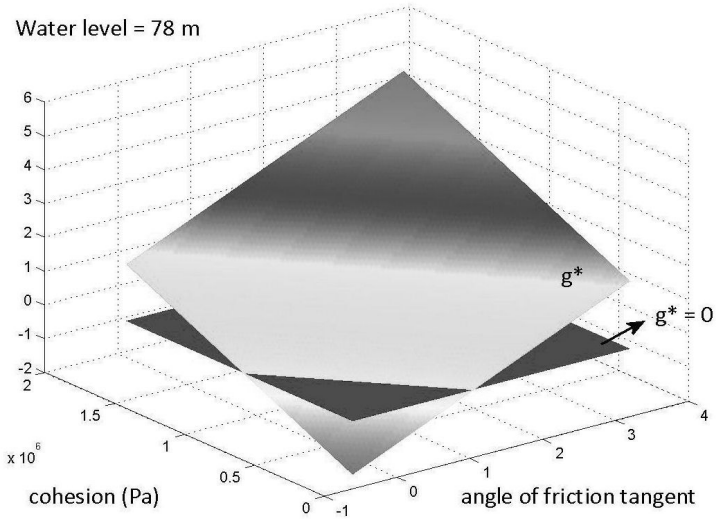

Figure 8: linear limit state function

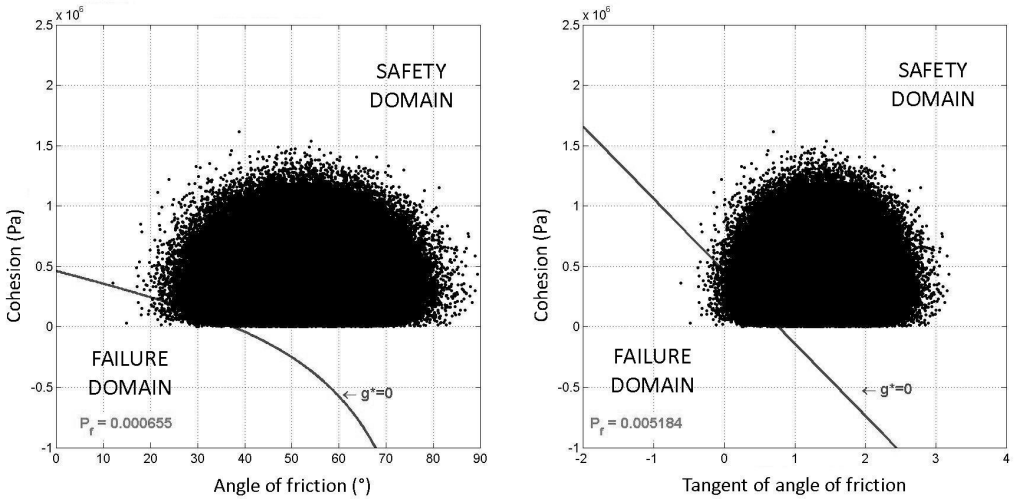

Figure 9: Failure/safety domains for a non-linear (left) and a linear (right) g* function in case of an ineffective drain and 75 m of water level

Table 9: Level 1– Global Safety Factor (variables: tanφ, c)

Water level (m)	Global Safety Factor
75	3.06
78	2.78
80	2.59
82	2.42
85	2.23

Table 10: Level 2– FOSM Taylor and Hasofer-Lind (variables: tanφ, c)

Water level (m)	P_f (FOSM Taylor)	P_f (Hasofer-Lind)
75	7.67E-03	7.67E-03
78	1.30E-02	1.30E-02
80	2.63E-02	2.63E-02
82	5.60E-02	5.60E-02
85	7.27E-02	7.27E-02

Table 11: Level 3 methods – Montecarlo Simulations (variables: tanφ, c)

Water level (m)	P_f		
	Friction angle: Normal **Cohesion:** Normal	**Friction angle:** Normal **Cohesion:** Rayleigh	**Friction angle:** Normal **Cohesion:** Lognormal
75	7.65E-03	2.69E-03	3.07E-03
78	1.30E-02	4.96E-03	5.65E-03
80	2.63E-02	1.41E-02	1.67E-02
82	5.59E-02	4.80E-02	5.99E-02
85	7.26E-02	6.51E-02	7.65E-02

5. Conclusions

In this paper reliability methods were applied to evaluate the sliding failure probability to be compared with the global safety factors of a concrete gravity dam, for different reservoir levels and considering different assumptions on the effectiveness of the drainage system.

Results have highlighted the importance to properly select the distribution type to model the random variables. Tails effects (low probability values) can strongly affect the results. For such reason the experimental fitting process must be particularly accurate. Also, when possible, it may be convenient to transform random variables in order to obtain linear, or almost linear, limit state functions. That reduces the approximation level in the analyses and, for this particular case, it should be more appropriate, as usually shear tests on concrete samples provide directly tanφ, instead of φ.

Level III methods, as Montecarlo simulations, allow to model random variables with different type of distributions, so that tail effects can be better investigated and results are definitely more accurate, provided that the trial number is sufficiently high.

Of course, in case of more complex models with more random variables, Montecarlo simulations may become impracticable due to the high number of simulations to perform, and reliability methods, such Level II methods, can provide good estimations of P_f.

References

[1] Escuder Bueno, I., Altarejos García, L., Serrano Lombillo, A. (2011). Theme C formulation. Estimation of the probability of failure of a gravity dam for the sliding failure mode. 11th ICOLD Benchmark Workshop on Numerical Analysis of Dams, Valencia, Spain.

[2] Haertford, D.N.D., Baecher, G.B. (2004). Risk and uncertainty in dam safety. Thomas Telford Books

[3] Mínguez, R. (2003). Seguridad, fiabilidad y análisis de sensibilidad en obras de ingeniería civil mediate technical de optimization poor decomposition. Applications. Testis Doctoral. Universidad de Catbrier.

[4] Altarejos García, L. (2008). Assessment of the sliding failure probability of a concrete gravity dam. 2nd International Week on Risk Analysis as applied to Dam Safety and Dam Security. UPV, Valencia, Spain.

[5] MATLAB Statistic Toolbox User's Guide, Release R2011b, The MathWorks

XI ICOLD BENCHMARK WORKSHOP ON NUMERICAL ANALYSIS OF DAMS
Valencia, October 20-21, 2011
THEME C

Analysis of the sliding failure probability of a gravity dam profile based on limit equilibrium method

Popovici, Adrian*
Ilinca, Cornel**

* Prof. PhD, Hydraulic Structures Department, Technical University of Civil Engineering Bucharest-020396; 124, Lacul Tei Bd., Email: popovici@utcb.ro
** Ass.Prof., PhD, Hydraulic Structures Department, Technical University of Civil Engineering, Bucharest, Email: cornel@utcb.ro

Summary

The limit equilibrium method was chosen to evaluate safety factor against sliding of the gravity dam cross profile for several water levels. The crack on dam-foundation interface starting from dam's upstream edge is considered to develop in the contact area subject to bending tensile stresses (σ_v) from load combinations consisting of dead weight + hydrostatic load + uplift load..

Initially, the safety factors against sliding mode of the profile for five reservoir water levels are computed as averages of the safety coefficient values obtained for f and c pairs given by formulator (deterministic method with global safety factor).

The probabilities of failure for the sliding mode of the profile for five reservoir water levels are computed using Level 2 methods (FOSM – Taylor's series, Point estimate method and Hasofer-Lind method) and Level 3 method (Monte Carlo simulation). In order to compute failure probabilities the safety coefficient functions were considered to be normally distributed.

A specialized computer program in the frame of MATHCAD computer code was written to perform these analysis...

A comparative analysis, using SAP 2000 program, by linear elastic finite element method (FEM) for unitary system dam-foundation was carried out for two reservoir water depths to compare the crack lengths versus values obtained by limit equilibrium method.

A general remark is that the crack lengths and the probabilities of failure are very sensitive with the method used for their evaluation.

1. Introduction

Traditionally, in the design of the gravity dam cross sections are checked the followings two conditions:

- sliding stability along the dam-foundation interface or along a weak plane surface in the dam foundation;
- safety to overturning around downstream edge of the profile.

Usually, the sliding stability is condition leading to the profile size [1], [2].

The common procedure recommended by regulations for gravity dam cross section design consists of limit equilibrium method. Once the dam's profile is determined the behavior of the unitary dam-foundation system may be checked and improved using other refined methods especially based on finite element procedure (FEM). Generally, the limit equilibrium method leads to conservative values of the dam's profile safety factors against sliding or overturning, but it has the advantage of the simplicity.

It may points out the behavior of the dam-foundation unitary system is a complex task. Intensive investigations concerning gravity dam failure based on fracture mechanics and nonlinear finite element procedure carried out in the last decades have contributed to understand this complex task [3]. However, reliable computation results of this analysis need in situ data very difficult to obtain. Local factors as foundation rock heterogeneousness and discontinuity (faults, breccias, cracks), irregularities of the dam-foundation interface, large variability of the mechanical characteristics (friction coefficient and especially cohesion – on the dam-foundation contact) can have significant influence on results.

For the above mentioned reasons, the limit equilibrium method was chosen in the present paper as base to evaluate the probability of failure of a gravity dam for the sliding failure mode [4]. The safety factors and the failure probabilities against sliding for the dam's cross profile given by formulator are computed using a specialized computer program in the frame of MATHCAD computer code.

Appearance and extension of the crack on the dam-foundation interface starting from dam's upstream edge is accepted in the area where the vertical normal stresses from load combinations are bending tensile ones. The vertical normal stress diagram on the contact is a linear one, computed according to strength of materials (eccentric compression). The working (active) area on the dam-foundation interface to load combinations after crack's development is considered only the compressed area. The size on upstream-downstream direction of the working area is calculated be successive iterations.

The cracks extension computed as above mentioned are compared for two reservoir water level with equivalent analyses finite element method (FEM) using SAP2000 computer code.

2. Method of analysis

The sliding stability of the dam's profile given by formulator (fig.1) is determined by two-dimensional limit equilibrium method.

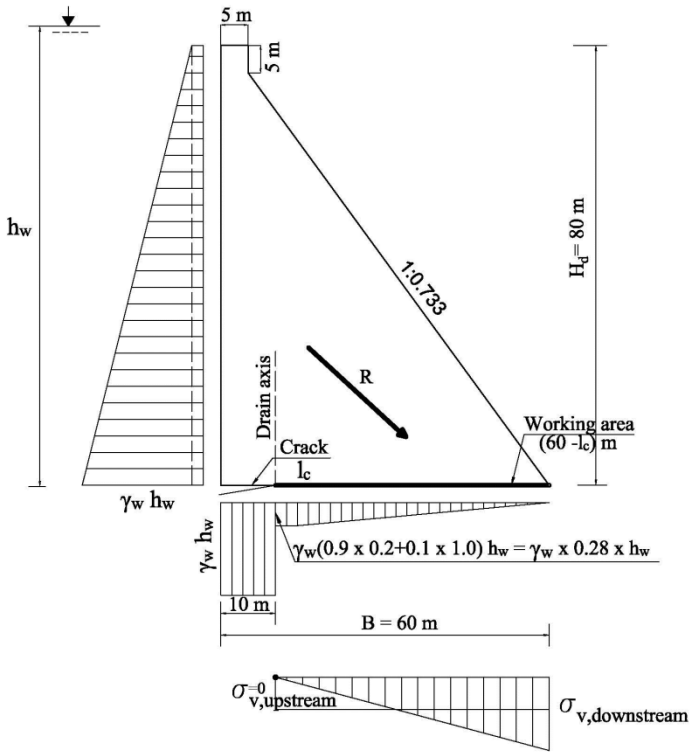

Fig.1. Loads acting in dam's profile and working area exemplification after crack development

The load combinations consist of: dam's dead weight, hydrostatic load for five reservoir water level given by formulator and uplift load corresponding to each reservoir water level.

The parameters taken into account for analysis are presented in Table 1

Table 1

Parameter	Value
Mass gravity of the dam body (kN/m^3)	24
Compressive strength of the dam body (kPa)	24000
Tensile strength of the dam body (kPa)	1500
Compressive strength of the foundation rock (kPa)	40000
Tensile strength of the foundation rock (kPa)	2600
Tensile strength on the dam-foundation interface (kPa)	0.0
Cohesion on the dam-foundation interface **c** (kPa)	See Table 2
Friction angle on the dam-foundation interface φ (^{0})	See Table 2

The friction angle and cohesion on the dam-foundation interface are considered as random variables and available data in the form of fifteen pairs of values are given in Table 2.

Table 2

Sample	Friction angle (^{0})	Cohesion (kPa)
1	45	500
2	37	300
3	46	300
4	45	700
5	49	800
6	53	200
7	54	600
8	45	0
9	49	100
10	60	200
11	63	200
12	62	400
13	60	700
14	56	100
15	62	400

The uplift load is calculated as weighted average of two cases of drain effectiveness with discrete probabilities associated, as follows (fig. 1):

• drains effective with 90% probability corresponding to 0.2 $\gamma_w h_w$ at drain axis if $l_c \leq 10$ m and at drain axis and downstream crack limit if $l_c > 10$ m;

• drains not effective with 10% probability corresponding to $\gamma_w h_w$ at drain axis if $l_c \leq 10$ m and at drain axis and downstream crack limit if $l_c > 10$ m;

(γ_w - water mass gravity, h_w – reservoir water depth given by formulator, respectively 75,78,80, 82 and 85 m, l_c – crack length starting from dam's upstream edge).

Consequently the uplift pressure *(p_u)* at drain axis if $l_c \leq 10$ m and at drain axis and downstream crack limit if $l_c > 10$ m results:

$$p_u = (0.9 \times 0.2 + 0.1 \times 1.0)\ \gamma_w \cdot h_w = 0.28\ \gamma_w \cdot h_w \qquad (1)$$

Uplift pressure at the dam's downstream edge is zero in all the cases.

The global sliding safety factor (FS) is calculated with much known relations:

$$FS = \frac{\left[G - S(l_c)\right]\tan\varphi + B(l_c) \cdot c}{H} \qquad (2)$$

where G is dam's profile weight (kN/m), $S(l_c)$ – uplift load depending of crack development, (kN/m) φ - friction angle in the interface, $B(l_c)$ (m) – working area on dam-foundation interface depending of crack development, c – cohesion in the interface (kN/m^2), H – hydrostatic load acting on dam upstream face (kN/m).

The vertical normal stresses on the dam-foundation interface are calculated with eccentric compression relation:

$$\sigma_{v,\,downstream\ \ edge}^{upstream\ \ edge} = \frac{\sum V}{\Omega(l_c)} \pm \frac{\sum M}{W(l_c)} \qquad (3)$$

where $\sum V$ is summation of all vertical loads (dam weight, upstream load etc), $\Omega(l_c)$ – working (active) area depending of crack length, $\sum M$ - summation of moments of all loads versus gravity center of the working area, $W(l_c)$ - strength modulus.

The length of the crack on interface developed from dam's upstream edge corresponds with interface area where the vertical normal stresses calculated with relation (3) are tensile stresses. The cracked area becomes non-active one and the calculus is repeated with the remaining active (working) area. In about three iterations is reached the real crack length and corresponding working area $B(l_c)$ (see fig. 1):

$$B(lc)\cdot 1 = (B - lc)\cdot 1 \qquad (4)$$

The data set for friction angle *(φ)* and cohesion *(c)* given by formulator were considered as sample from population statistics. Statistic analysis of data set has pointed out the difference between standard deviations assuming the data as sample (number of values N≤30) or as population statistics (N>30) is less than 3.5%.

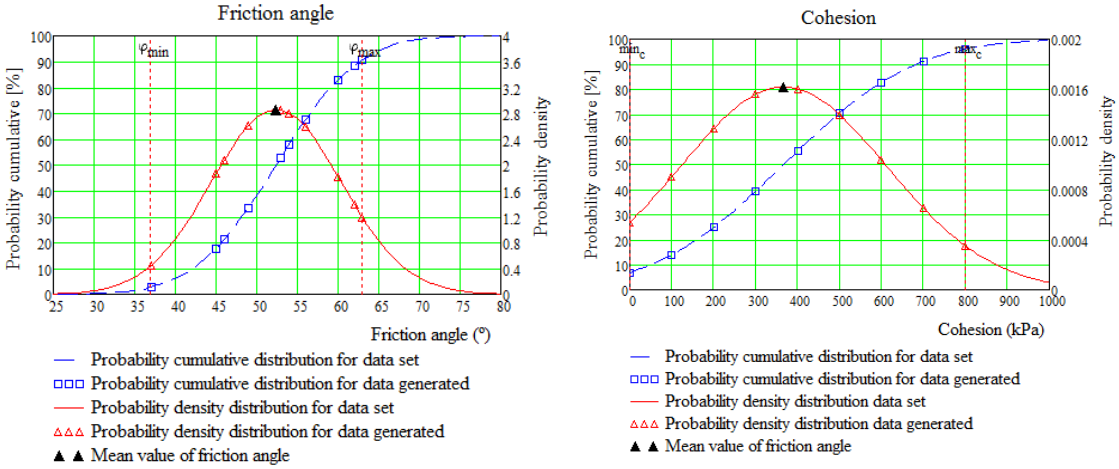

Fig.2 The probability distribution for friction angle (φ) and cohesion (c) on dam – foundation interface

The distribution of *(φ)* and *(c)* are very close of a normal distribution (fig.2). For physical reasons the variations of the friction angle on dam-foundation interface was limited between 25^0 and 80^0. The variation domain of the cohesion on interface was also limited between 0 and 800 kPa (negative cohesion isn't physically possible).

In order to compute probabilities of failure for the sliding mode using Level 2 method (FOSM Taylor's series, Point estimate method and Hasofer – Lind method) the safety factor functions were considered to be normally distributed.

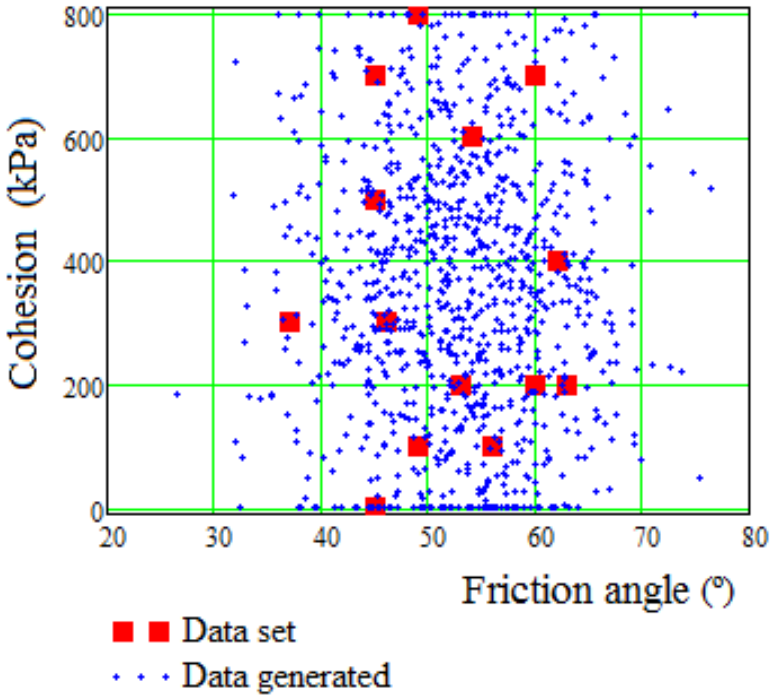

Fig.3 Exemplification with φ and c data set and data generated by Monte Carlo simulation.

The evaluation of the safety factor in Monte Carlo method, a set of values corresponding to *(φ)* and *(c)* in the restricted domain due to physical characteristics was generated randomly following a normal distribution (fig. 3). Probability of failure is given by ratio between the numbers of unfavorable values versus the total number of values computed for the safety coefficient. The total number of evaluation of the safety coefficient was 10^7.

3. Results of analysis

In the Table 3 are presented some results concerning crack's lengths (l_c), vertical normal stresses (σ_v) at the interface working area B(l_c) and safety factors against sliding using limit equilibrium method.

Table 3

Water level (in m over dam-foundation contact plane)	Crack's length m	σ_v at the interface working area (kPa)		Factor of safety
		Upstream edge	Downstream edge	(for sliding failure mode)
75	0	249	1296	3.031
78	0	80	1448	2.779
80	1.517	0	1556	2.610
82	6.369	0	1684	2.419
85	14.367	0	1934	2.137

The contours of the global safety factors to sliding failure mode function of ϕ and c for 75 m and 85 m reservoir water depths are illustrated in figure 4.

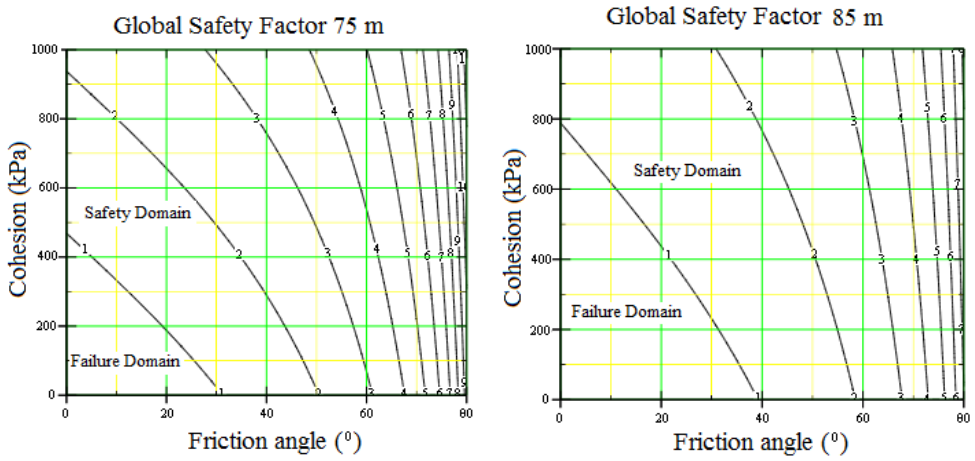

Fig.4 Contours of the global safety factors to sliding failure mode for 75 m and 85 m reservoir water depths

The failure probabilities against sliding of the gravity dam cross profile using Level 2 reliability methods are presented in the Table 4.

Table 4

Water level (in m over dam-foundation contact plane)	Probability of failure (%)		
	FOSM Taylor Method	Point Estimate Method	Hasofer-Lind Method
75	1.035	0.706	0.120
78	1.386	0.960	0.267
80	1.695	1.183	0.435
82	2.123	1.482	0.679
85	3.226	2.266	1.317

Normal distributions of the data concerning safety factors against sliding failure mode computed with Level 2 reliability method for 75 m and 85 m are illustrated in figures 5, 6 and 7.

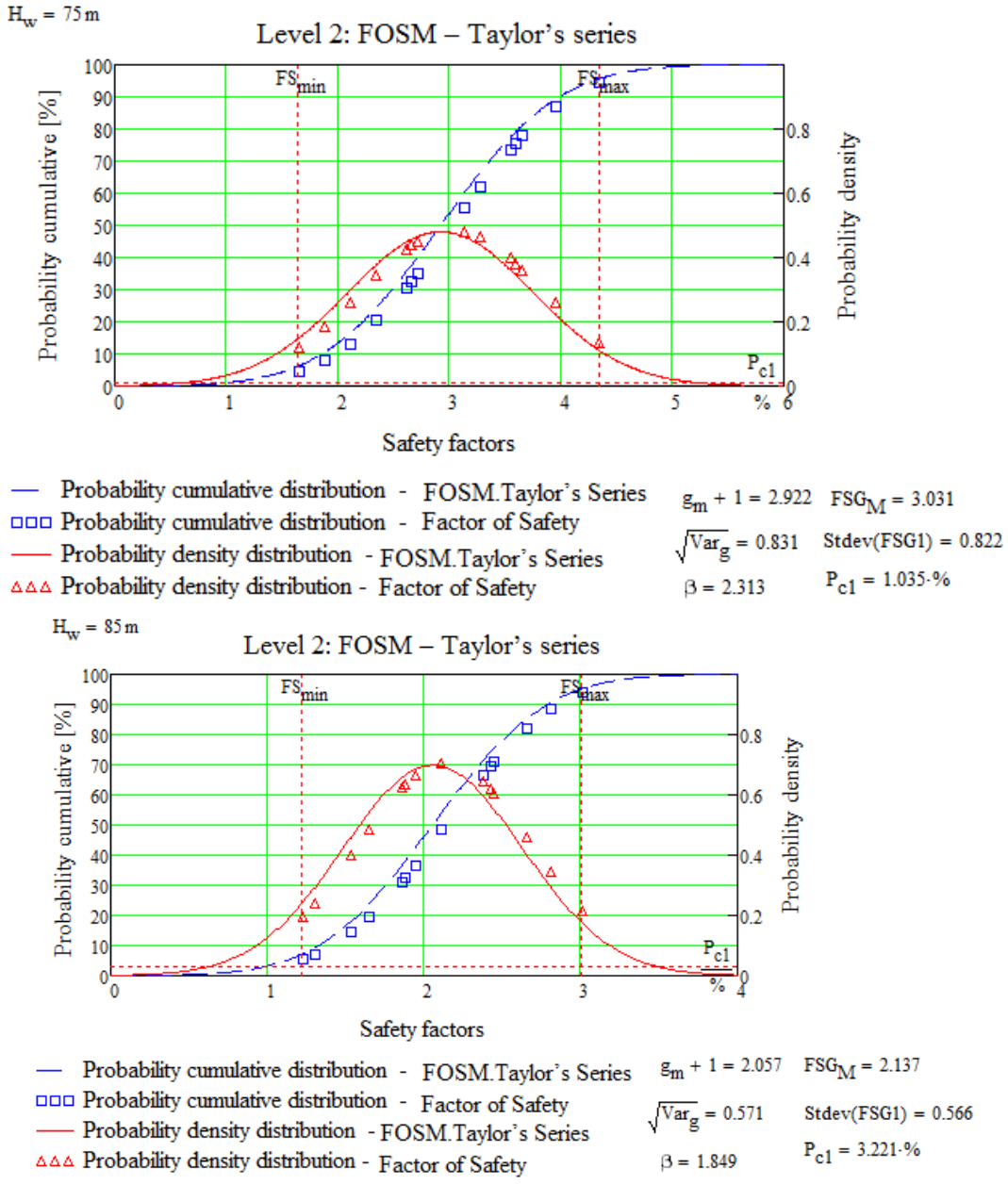

Fig. 5 Normal distributions of the data concerning safety factors against sliding computed by FOSM Taylor's series for 75 m and 85 m reservoir water depths.

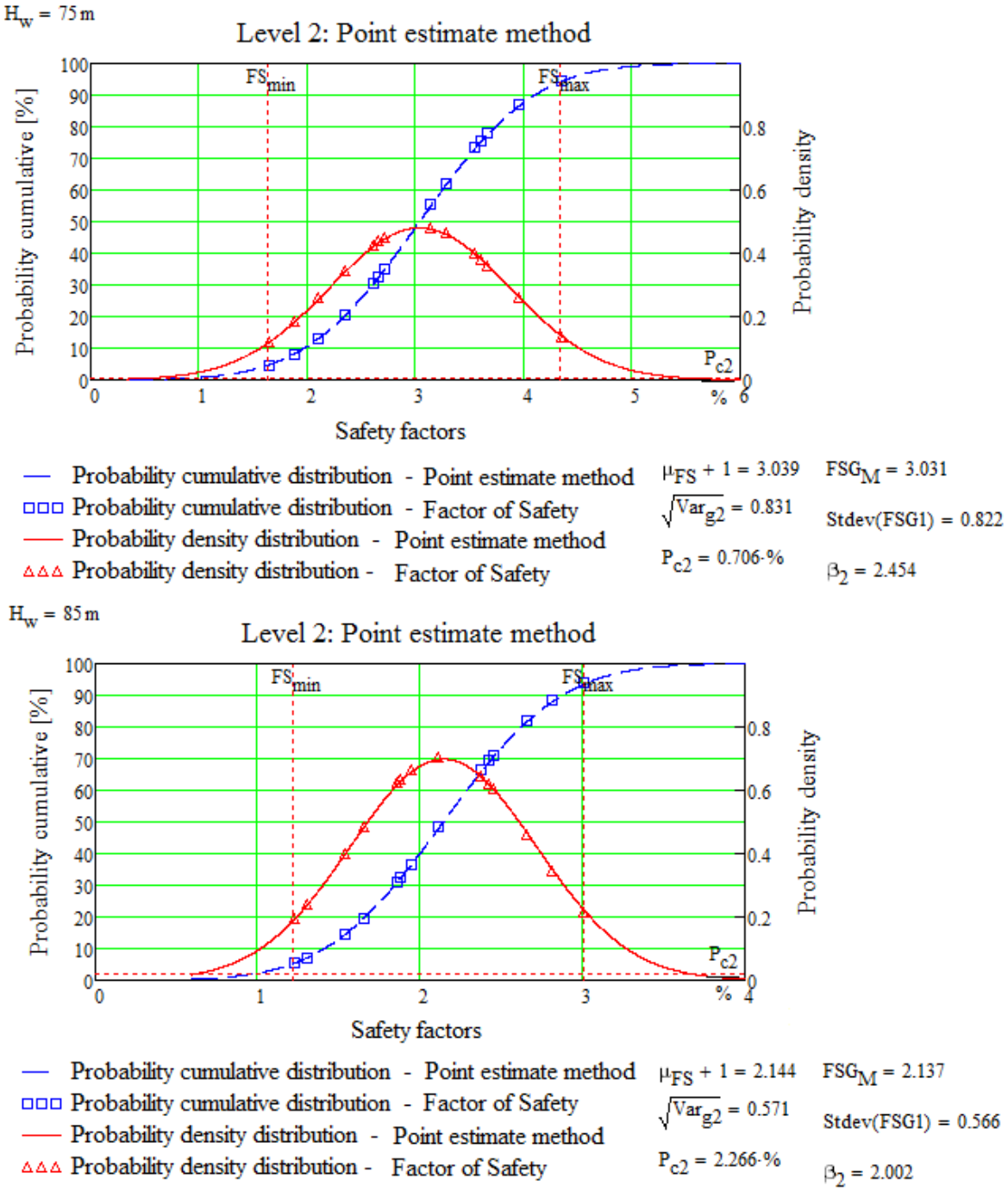

Fig. 6 Normal distributions of the data concerning safety factors against sliding computed by point estimate method for 75 m and 85 m reservoir water depths.

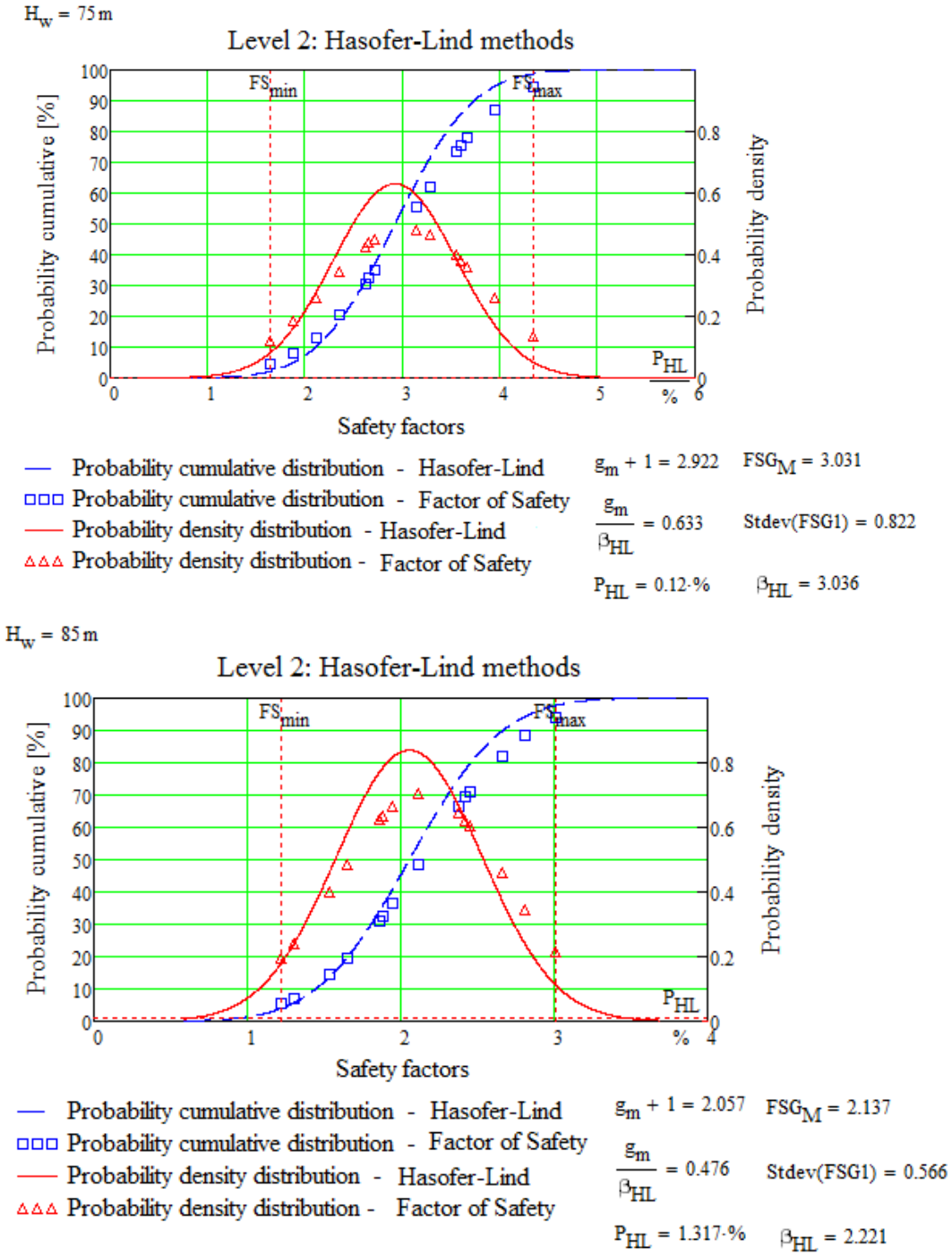

Fig. 7 Normal distributions of the data concerning safety factors against sliding computed by Hasofer – Lind method for 75 m and 85 m reservoir water depths.

The failure probabilities against sliding of the gravity dam cross profile using Level 3 reliability method – Monte Carlo simulation are presented in the Table 5

Table 5

Water level (in m over dam-foundation contact)	Probability of failure by Monte Carlo simulation (%)
75	0.039
78	0.093
80	0.163
82	0.283
85	0.681

4. Comparative analysis by finite element procedure

In order to evaluate the degree of approximation of values for crack lengths (l_c) calculated on the basis of the limit equilibrium method a comparative analysis by finite element procedure (FEM) was performed.

The finite element mesh of the unitary dam-foundation system is illustrated in the figure 8. The same two-dimensional PLANE element with incompatible modes included from SAP2000 element library was used for both, dam body and foundation area. This element is a quadrilateral with 4 (3) nodes having two translation degrees in each node. The mesh consisted from 1912 nodes, 1810 finite element, and 4382 degree of freedom total (fig. 8).

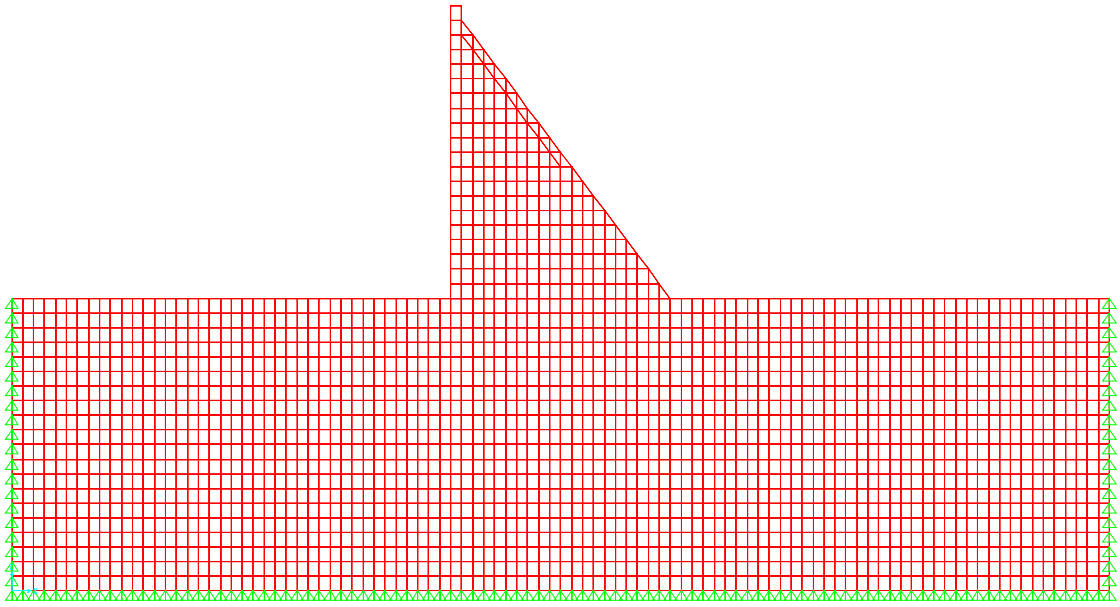

Fig.8 Finite element mesh of the dam-foundation system

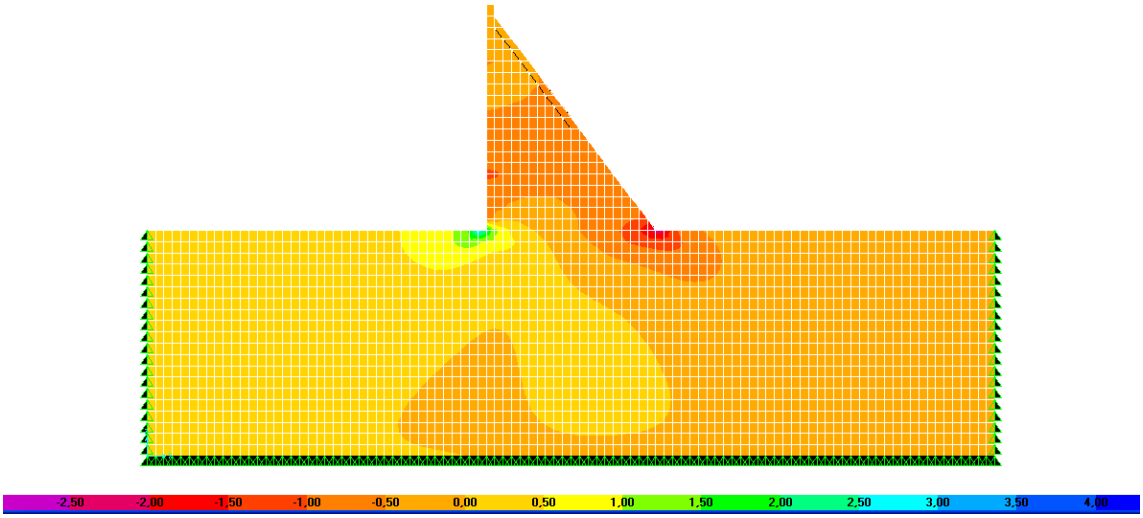

Fig.9 Contours of the vertical normal stresses (σ_v) for dead weight + hydrostatic load (h_w = 85 m) + uplift pressure load combination.

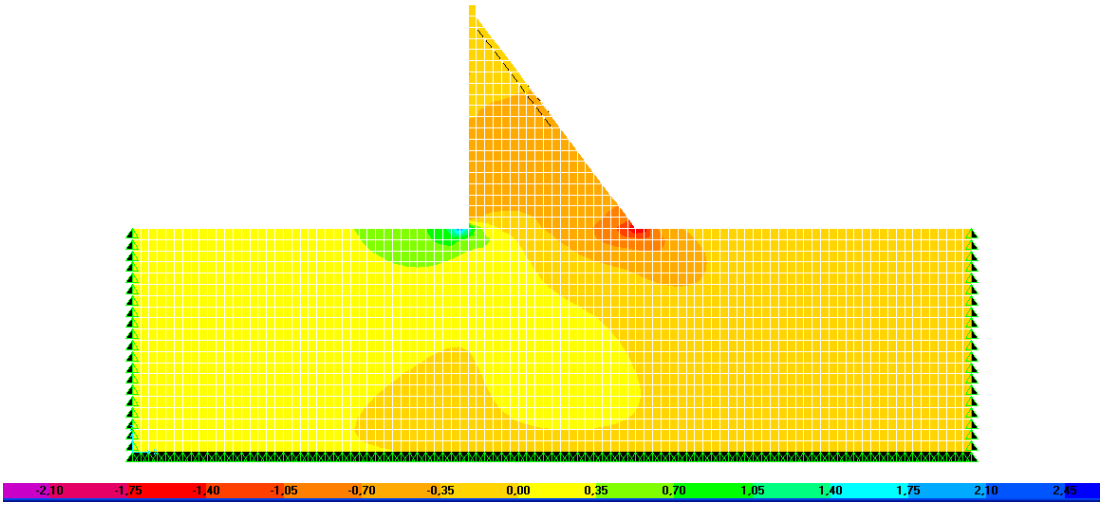

Fig.10. Contours of the vertical normal stresses (σ_v) for dead weight + hydrostatic load (h_w = 82 m) + uplift pressure load combination

The translations of nodes placed on lateral and inferior edges of the foundation were blocked on both directions. The analysis was performed in the strain plane hypothesis and linear elastic behavior of both, dam concrete and foundation rock. In the Table 6 are presented the material characteristics taken into account in this analysis.

Table 6

Material parameters	Dam	Foundation
Young modulus (MPa)	24000	41000
Poisson ratio	0.15	0.10
Mass gravity (kN/m^3)	24	0.

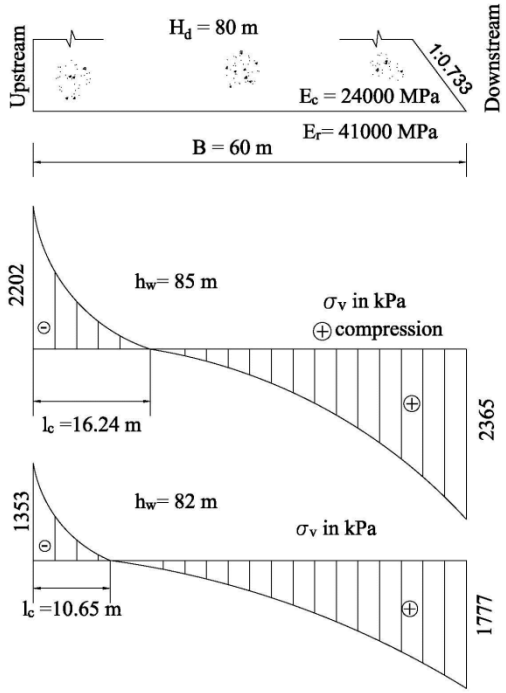

Fig.11 Vertical normal stresses diagrams (σ_v) on dam-foundation interface for load combinations of dead weight + hydrostatic load (85 m and 82 m reservoir water depths) + uplift pressure load.

The analysis was performed for two levels in the reservoir, corresponding to 85 m and, respectively 82 m water depths. The load combinations consisted of dead weight, hydrostatic load on upstream dam face and uplift load considered as weighted average of two cases of drain effectiveness given by formulator (see formula 1).

The hypothesis accepted in the limit equilibrium method, namely the crack on the dam-foundation interface is corresponding to area where the vertical normal stresses (σ_v) are tension was assumed also in the finite element analysis.

The contours of the vertical normal stresses (σ_v) for the load combinations mentioned above with water depth of 85 m are illustrated in figure 9 and, respectively with water depth of 82 m are illustrated in fig 10.

In figure 11 are selected σ_v on dam foundation interface corresponding to figures 9 and 10. It can be seen the lengths of cracks are 16.24 m for 85 m reservoir water depth and, respectively 10.65 m for 82 m reservoir water depth.

A compared between results obtained by limit equilibrium method and linear elastic FEM is presented in the Table 7.

Table 7

Water level (in m over dam-foundation contact plane)	Crack length (m)		Increase rate in FEM %
	Limit equilibrium method	Linear elastic FEM	
85	14.367	16.24	13 %
82	6.369	10.65	67 %

It seems that crack's lengths developed on dam-foundation interface starting from dam's upstream edge are very sensitive with methods used for their evaluation.

5. **Concluding remarks**

Based on results of analysis, the followings concluding remarks may be pointed out:

• The evaluations of the failure probabilities to sliding failure mode of the gravity dam profile were based on limit equilibrium method, a simple method known as conservative one. However, the lengths of cracks on dam-foundation interface starting from dam upstream edge computed by linear elastic FEM have resulted longer with 11…67% versus those computed in equivalent conditions by limit equilibrium method.

• In all cases the failure probabilities computed by Monte Carlo simulation were smaller versus those computed by Level 2 reliability methods. The highest values for failure probabilities have resulted in FOSM Taylor method.

• The analysis have shown that both, crack length on dam-foundation interface and failure probabilities to sliding failure mode of the gravity dam profile are very sensitive with methods used for their evaluation.

References

[1] Popovici, A., Popescu, C. (1992). Dams for water storage vol. 1 (in Romanian). Editura Tehnica, Bucuresti, pp. 257-281.

[2] Bureau of Reclamation (1976) Design of Gravity Dams. A Water Resources Technical Publication, Denver – Colorado pp. 30-34.

[3] USCOLD (1999) Proceedings Fifth Benchmark Workshop on Numerical Analysis of Dams Theme A2 Imminent flood for a concrete gravity dam. Denver -Colorado pp. 147-228.

[4] Bueno, I.E., Garcia, L.A., Lombillo, A.S. (2011) Estimation of the probability of failure of a gravity dam for the sliding failure mode Theme C 11-th Benchmark Workshop on Numerical Analysis of Dams, Valencia.

XI ICOLD BENCHMARK WORKSHOP ON NUMERICAL ANALYSIS OF DAMS

Valencia, October 20-21, 2011

THEME C

Gravity dam probability of sliding failure with overtopping and conditional drainage

Bachir Touileb

CONTACT
Bachir Touileb, Sogreah Consultants, ARTELIA Group, Dams and Hydraulics Department, Water and Environment Sector, 6 rue de Lorraine, Echirolles, France. Phone: +33 (0) 4 76 33 42 66, E-mail: Bachir.Touileb@artelia.com.

Summary
Risk assessment of dams (DRA) is nowadays very well accepted especially for the assessment of existing dams. The last decade corresponds indeed to an important widespread of DRA worldwide. Either qualitative or quantitative, these methods reframed the notions of probability of loading, and consequently the probability of failure.

The actual ICOLD Benchmark Workshop is aimed to provide a comprehensive review of most of the relevant existing methods that are qualified for providing an evaluation of the probability of failure of a given dam.

The actual paper provides three different methods for the stability assessment of the proposed 80m high gravity dam: (1:) Deterministic approach (Level-1), (2:) Taylor's series approximation limited to the FOSM or First Order Second Moment (Level-2), and finally (3:) Monte-Carlo method (Level-3).

While Level-1 method do provide a factor of safety only, both Level-2 and Level-3 methods do provide the probability of failure. Comparison of the results provided by means of the latter two methods, and causes of the discrepancy are discussed.

1. Objectives
The objective is to obtain relationships between water levels, factors of safety and probabilities of failure for a gravity dam. This can be done using behavior models for the dam-foundation system together with reliability techniques that allow for uncertainties in the parameters, using random variables.

For the purpose of comparison and evaluation of advances in this field, the dam proposed is taken from the Theme 2 of the 1999 ICOLD Benchmark.

The proposed exercise aims at analyzing the dam with a 2D model. The model should be chosen by participants and it can be a limit equilibrium model or a deformable body model. The factor of safety against sliding is then calculated for several water levels.

Following this step, participants should estimate the probability of failure for the sliding failure mode using at least one Level 2 reliability method and a Level 3 Monte Carlo simulation method. On the Appendix, some useful information on reliability techniques and how they can be applied to this problem can be found.

2. Dam Description

2.1 Geometry

The gravity dam that is considered for the actual benchmark is an 80m high concrete dam. Its geometry is shown hereafter:

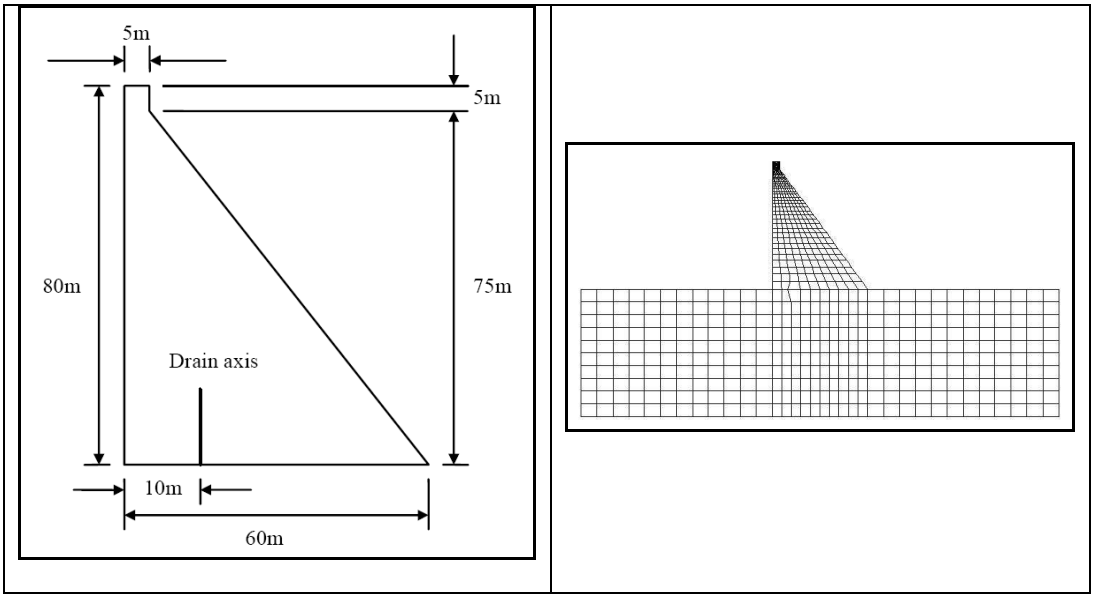

Figure 1 Dam geometry

2.2 Foundation

The full geometry including the foundation is shown in the next figure. The foundation has a rectangular shape with height of 80 m and a total length of 300 m (120 m upstream, 60 m under de dam, 120 m downstream).

2.3 Material properties

Data on material properties for dam and foundation are given in Table 1.

Table 1 Data for dam and foundation materials

Material parameters	**Dam**	**Foundation**
Young's modulus (MPa)	24000	41000
Poisson`s ratio	0.15	0.10
Mass density (kg/m3)	2400	2700
Compressive strength (MPa)	24	40
Tensile strength (MPa)	1.5	2.6
Strain at peak compressive strength	0.0022	0.0025
Strain at end of compressive softening curve	0.10	0.15
Fracture energy (N/m)	150	200

Data for material properties for dam-foundation interface are given in Table 2.

Table 2 Data for dam-foundation interface

Parameter	**Value**
Shear stiffness (MPa/mm)	20
Tensile strength (MPa)	0.0
Friction angle (º)	See Table 3
Cohesion (MPa)	See Table 3
Dilatancy angle (º)	0
Softening modulus (MPa/mm)	-0.7

Friction angle and cohesion at the dam-foundation interface are considered as random variables. Available data in the form of fifteen pairs of values are given in Table 3.

Table 3 Data for friction and cohesion at the interface

Sample	Friction angle (º)	Cohesion (MPa)	Sample	Friction angle (º)	Cohesion (MPa)
1	45	0.5	**9**	49	0.1
2	37	0.3	**10**	60	0.2
3	46	0.3	**11**	63	0.2
4	45	0.7	**12**	62	0.4
5	49	0.8	**13**	60	0.7
6	53	0.2	**14**	56	0.1
7	54	0.6	**15**	62	0.4
8	45	0.0			

3. Water Levels

The stability of the dam is to be determined for five (5) different water levels (Table 4). Three (3) of them do not cause crest overtopping; that is 75m, 78m and 80m. However, water levels 82m and 85m do cause an overtopping corresponding respectively to 2m and 5m.

It is known from dam safety experience that gravity dams, even though not designed for such high water levels, are able to withstand overtopping with water depth varying from moderate (about 1m) to few meters. An overtopping with a water depth of 5m constitutes a very important loading for a gravity dam that was not designed for such a loading case.

Table 4 Considered water levels

Water Level (m)	**75**	**78**	**80**	**82**	**85**
Overtopping ?	No	No	No	Yes	Yes

4. Drainage Conditions

The considered loadings are self-weight, hydraulic pressure acting on the upstream face of the dam and uplift acting on the base of the dam. Development of a crack at the interface is to be taken into account and uplift pressure should be evaluated accordingly.

Two cases of drain effectiveness are considered, with discrete probabilities associated:

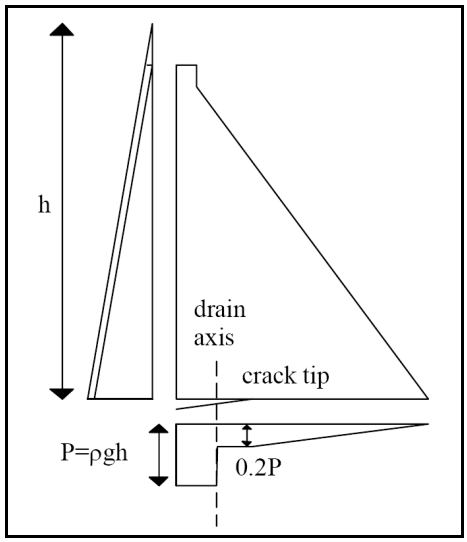

Case A. Drains effective

Associated probability of occurrence:

P_A = 0.90

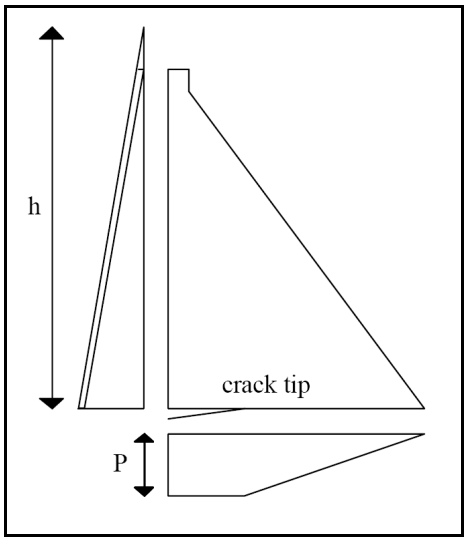

Case B. Drains ineffective

Associated probability of occurrence:

P_B = 0.10

Figure 2 Proposed uplift pressure profiles alternatives

5. Software

Calculation of the factor of safety was achieved by means of CADAM software that was developed in Ecole Polytechnique de Montreal. The software allows for the computation of the factor of safety under various usual conditions such different water levels and failure modes (mainly: sliding and overturning).

Overtopping loading conditions are implemented, by taking into account the forces due the presence of water above the crest and on the downstream slope of the dam. Uplift pressures are adjusted accordingly.

It allows also for the evaluation of the probability of failure under the framework of the Monte-Carlo method. Various parameters can be presented on a probabilistic form using a uniform, a normal, or a lognormal distribution. For instance, cohesion and friction angle are considered independent. The maximum number of samples that are randomly issued is limited to 250,000. For a given parameter, the required data are the minimum, mean and maximum values, the standard deviation, and probability distribution type. The difference between the maximum and the minimum is limited to 5 times the standard deviation. The software does not check if the source data follows the distribution that is chosen by the user.

6. Deterministic traditional approach

6.1 Actual status in practice

Based on the majority of dam safety and dam design guidelines, the dam stability assessment is based on the comparison between a calculated factor of safety and a required factor of safety. The dam is said stable under a given loading condition and a given failure whenever the calculated factor of safety is below the required one. The latter is usually steadily decreased in order to take into account the less frequent character of transient loadings, as well as any other loadings of low probability of occurrence.

In general, all modern dam safety and dam design guidelines, that are in accordance with ICOLD bulletins and current State of the Art, provide similar and comparable dam stability requirements.

6.2 Strength parameters

In the case of a limit equilibrium or friction factor stability assessment, the main parameters that are required in order to conduct the analysis are the cohesion (c) and the friction (⍰) along the dam-foundation interface.

In the case of the actual dam, 15 (c, ϕ) values are provided such as shown in Table 3. It is recalled that the origin of these data is not discussed within the formulation of the problem. Data #8 with a cohesion of zero is found quiet particular since it is usually corresponding to a purely frictional material.

All the 15 data are plotted hereafter considering a Mohr-Coulomb failure mode. Moreover, the lower bound (i.e. Line 20) and the upper bound (i.e. Line 21) corresponding to the interval of confidence based on a normal distribution for either c and ϕ, are shown in bolt red lines.

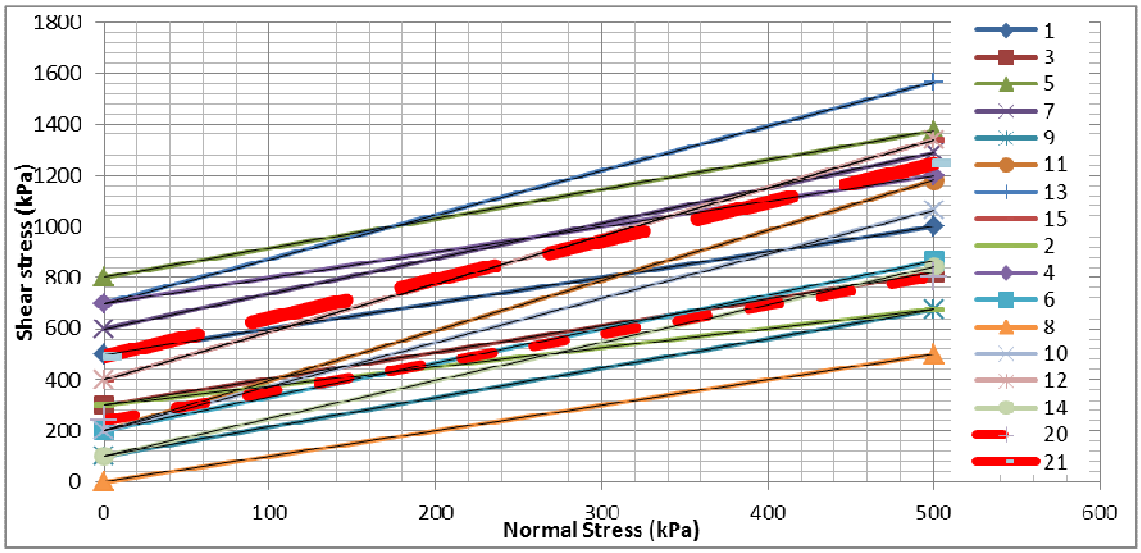

Figure 3 Mohr-Coulomb strength parameters at dam-foundation interface

6.3 Choice of strength parameters

In the case of a limit equilibrium or friction factor stability assessment, the main data are limited to a single set of strength parameter (c,ϕ).

Due to the very important scatter in the provided data set, a decision is to be made regarding the selection of data that are to be used for the stability analysis.

For the actual work, it was decided to consider three (3) different strength parameters datasets and two (2) drainage conditions.

6.4 Results

The selected parameters and the results are provided in the following Tables.

Table 5 Results of Part 1. Deterministic Approach. Lower bound (ϕ =48,36° ; c =241,73 kPa)

Water Level (m)	Factor of Safety (No Drainage)	Factor of Safety (Drainage)
75	1,99	2,59
78	1,40	2,16
80	0,82	2,04
82	0,33	1,94
85	0,26	1,78

Table 6 Results of Part 1. Deterministic Approach. Upper bound (ϕ=56,44° ; c =491,61 kPa)

Water Level (m)	Factor of Safety (No Drainage)	Factor of Safety (Drainage)
75	3,03	3,83
78	2,11	3,17
80	1,21	3,00
82	0,45	2,85
85	0,35	2,62

Table 7 Results of Part 1. Deterministic Approach. Average (ϕ =52,40° ; c =366,67 kPa)

Water Level (m)	Factor of Safety (No Drainage)	Factor of Safety (Drainage)
75	2,49	3,18
78	1,74	2,93
80	1,01	2,77
82	0,39	2,64
85	0,30	2,18

6.5 Discussion

The results presented in the Tables attest and recall the tremendous increase of stability corresponding to the contribution of an efficient drainage system. The important scatter that is noticed regarding the data is totally overridden by the condition of the drainage system.

7. Taylos's Series Approximation Approach

7.1 Actual status of this method in practice

This method is not widely used in the professional practice for the moment.

7.2 Main aspects of the FOSM method

The details of the method are comprehensively developed by the Formulator of the actual Theme (see provided Appendix of Theme C). The main aspects are recalled hereafter for completeness purposes.

The performance function is stated by the Formulator as:

$$g^*(c,\phi) = r/s - 1$$

Where r is the resistance and s the strength.

Noting that (r/s) represents the factor of safety (Fs), one can restate the latter as follows:

$$g^*(c,\phi) = Fs - 1$$

The performance $g^*(c, \phi)$ is evaluated based on the chosen dataset (c,□). That is the first moment:

$$g_1^*(c, \phi)$$

It is evaluated as well based on the limits of possible datasets. That is based on four (4) different strength parameters such as follows:

$$g_{21}^*(c , \phi + \sigma_\phi),\ g_{22}^*(c , \phi - \sigma_\phi),\ g_{23}^*(c + \sigma_c , \phi) \text{ and } g_{24}^*(c - \sigma_c , \phi)$$

The second moment is calculated as follows:

$$Var[g^*] = \sigma_{g^*} = [(g_{21}^* - g_{22}^*)/2]^2 + [(g_{23}^* - g_{24}^*)/2]^2$$

The reliability index is then calculated such as follows:

$$\beta = (E[g^*] - g^*_{failure}) / \sigma_{g^*} = (E[g^*] - 0) / \sigma_{g^*} = (E[g^*]) / \sigma_{g^*}$$

In order to end up with a probability of failure, an assumption is to be made regarding the distribution of g*. One can suggest a normal distribution since the average (μg* or E[g*]) of g*, as well as the standard deviation (Var[g*] = σg*) of g* are known:

$$g^* \approx \mathcal{N}(\mu_g^* , \sigma_{g^*}^2)$$

Finally the probability of failure $P_f(g^* \leq 0)$ is calculated as follows:

$$P_f(g^* \leq 0) = F_N(0) = \Phi[(0 - \mu_g^*) / \sigma_{g^*}] = \Phi[-\beta]$$

7.3 Results

Derived results are displayed in the following Table.

Table 8 Results of Part 2. FOSM Probability of failure.

Water Level (m)	Probability of failure
75	0,009275148
78	0,016510281
80	0,060090653
82	0,1129972
85	0,12443765

7.4 Discussion

It is found that the probability of failure in the case of the highest water levels is directly linked to the probability of occurrence of an efficient drainage system. This is in the vicinity of 0,10 such as shown in the Table above.

8. Monte-Carlo Method

8.1 Actual status of this method in practice

This method is gaining a large acceptation and a tremendous popularity. Its main advantage relates to the unavoidable existence of a scatter that is encountered when strength parameters are to be defined.

While deterministic methods require a single strength parameters dataset, Monte-Carlo method allows for the consideration of large range of datasets that are still within the engineering limits and the brackets that are usually proposed by the expert.

8.2 Randomly processed datasets

Strength parameters datasets that are considered while running a dam stability software featuring the Monte-Carlo are randomly processed by means of a special engine. Due to this inherent random nature, it is worthwhile recalling that different runs using the same frozen data will provide different results: that is different probabilities of failure. The difference between these calculated values are essentially small.

8.3 Datasets statistical distributions

Monte-Carlo simulation requires a probabilistic distribution for each probabilistically varying parameter. In the actual case, both Mohr-Coulomb strength parameters, cohesion and friction angle, c and □, should be linked to a chosen distribution.

A statistical analysis of the provided data shows that both parameters fall fairly well into the widely used normal distribution. For instance, a Henry diagram can be used for such a demonstration, together with considering the cumulative probability of occurence.

Such a hypothesis was considered for all three analysis levels: the determination of confidence intervals in order to define a lower bound and an upper bound in the case of the deterministic approach (Level 1), for the Taylor's method (Level 2), and finally for the Monte-Carlo simulation (Level 3).

8.4 Results

Strength parameters datasets that are considered while running a stability software featuring the

Table 9 Results of Part 3. Monte-Carlo Probability of failure.

Water Level (m)	Probability of failure
75	0
78	0,000006

80	0,040654
82	0,100001
85	0,100002

8.5 Discussion

It is found that the probability of failure in the case of the highest water levels is directly linked to the probability of occurrence of an efficient drainage system. This is in the vicinity of 0,10 such as shown in the Table above.

9. Taylor's series FSOM Versus Monte-Carlo Method

9.1 Results comparison

Both Taylor's series approximation limited to the FOSM or First Order Second Moment (Level-2), and Monte-Carlo method do provide a probability of failure.

Probabilities of failure provided by the use of Taylor's FOSM are found to be systematically higher than those provided by means of the Monte-Carlo method.

Table 10 Probability of failure: Taylor's FOSM versus Monte-Carlo Method

	Probability of failure	**Probability of failure**
	Level 2	**Level 3**
	FOSM Taylor Method	**Monte Carlo simulation**
Water Level (m)		
75	0,009275148	0
78	0,016510281	0,000006
80	0,060090653	0,040654
82	0,1129972	0,100001
85	0,12443765	0,100002

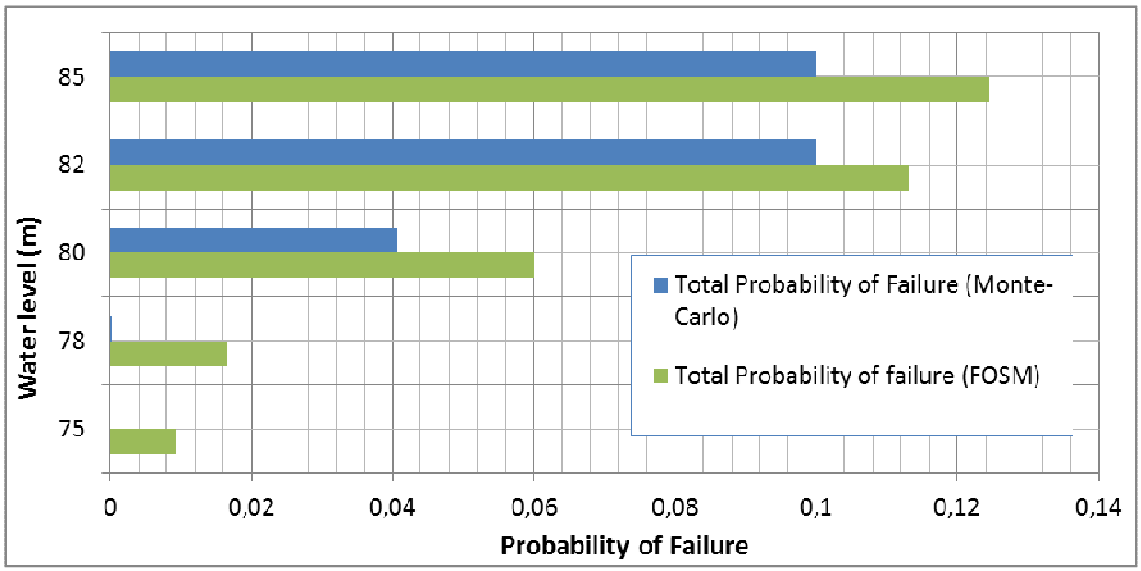

Figure 4 Probability of failure comparison. Taylor's FOSM versus Monte-Carlo Method

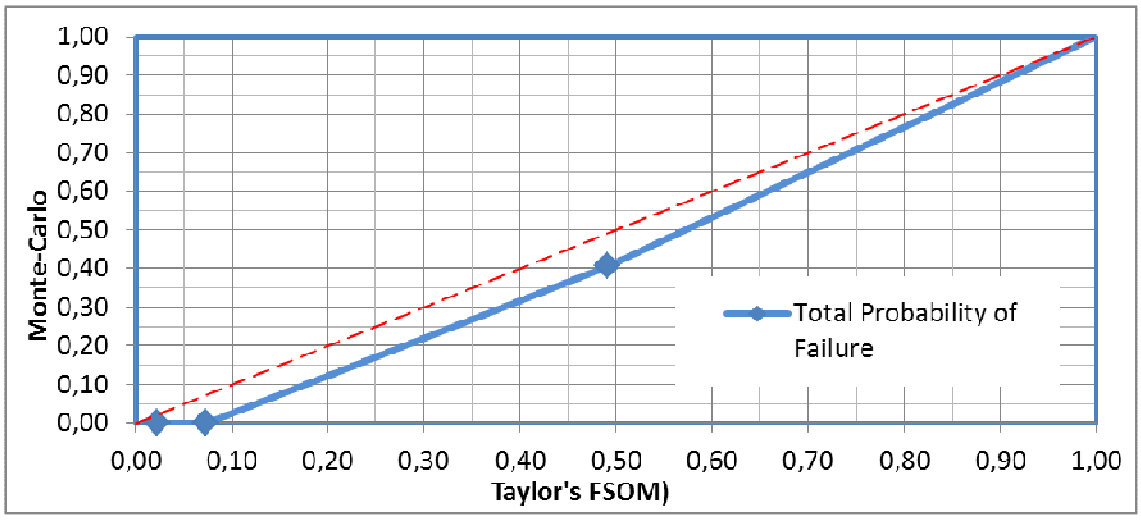

Figure 5 Probability of failure comparison. Taylor's FOSM versus Monte-Carlo Method

9.2 Discussion

Taylor's series approximation FOSM and Monte-Carlo methods lead practically to very similar results.

Result N°.1: For overtopping water levels, the probability of failure is practically equal to the probability of having an efficient drainage system. That is about 10% in the actual case.

Result N°.2: Probabilities of failure provided by means of the Taylor's series approximation FOSM are systematically, but only slightly, higher that those provided by means of the Monte-Carlo method.

9.3 Main conclusion

The main conclusion that can be derived from this comparison can be stated as follows:

Result N°.3: Taylor's FOSM, although requiring much less complex computations compared to the Monte-Carlo simulation, do provide results that are very fairly close to the later. The question is then naturally raised about the relevance of the Monte-Carlo simulation, at least for the actual case.

10. Results Synthesis

10.1 Overall results comparison

In general, it is quite difficult to compare deterministic and probabilistic methods since attached frameworks are very different. The following picture is an attempt to capture the entire process showing factors of safety as well as probabilities of failure.

Since the probability of failure contains already the probabilities associated with the efficiency of the drainage system, it was found appropriate to show the factor of safety in each drainage case.

From the picture below, one can realize that the water level corresponding to 82m represents a particular value either for probabilistic or deterministic methods. It is an inflexion point. All curves display a trend change above that particular water level. Such a water level corresponds to an overtopping water thickness of 2m above the crest.

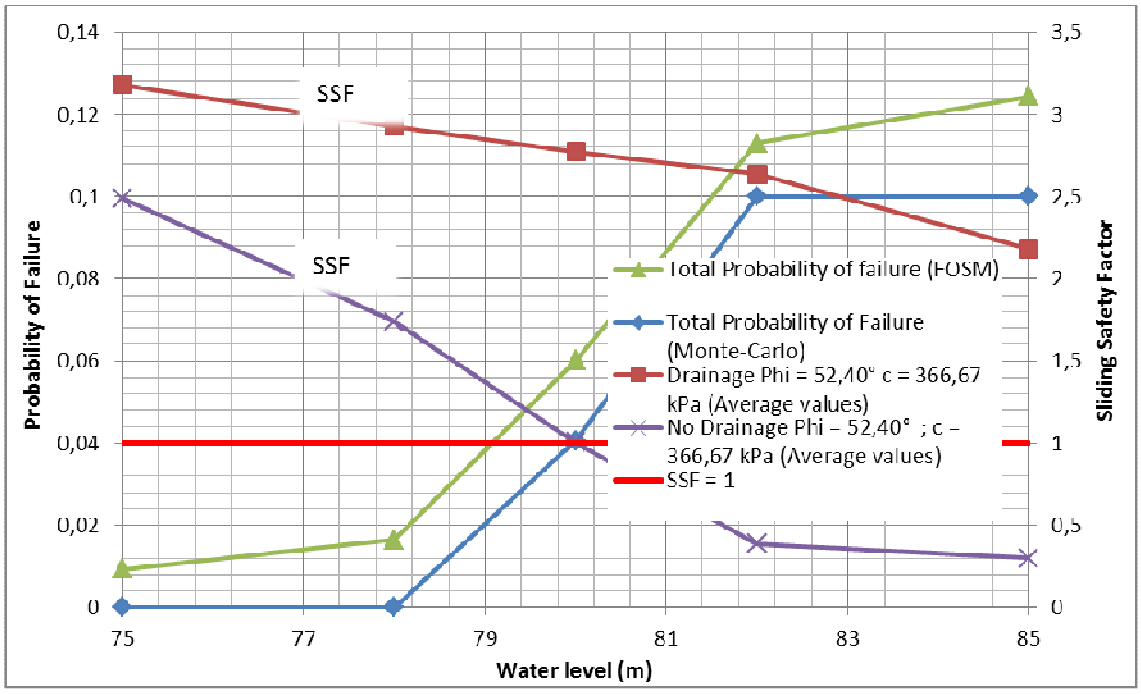

Figure 6 Probability of failure comparison. Taylor's FOSM versus Monte-Carlo Method

11. Consequences for Safety Assessment of Existing Dams

11.1 Critical water level - Definition

The notion of “Critical water level” is found to be increasingly used by a large number of National ICOLD Chapters worldwide. It corresponds to the water level that bring the structure to its limit of stability; that is consequently with a factor of safety of 1,0.

Such a particular water level is called “Cote de danger” in the case of the French ICOLD chapter (CFBR: Comité Français des Barrages et Réservoirs). It is widely used such as in the French dam safety guidelines for concrete dams, and the 2007 French Dam Safety Bill, and more specifically in the Bill of June 12th, 2008 dealing with the Dam Risk Assessment issues.

11.2 Critical water level from the deterministic approach

Based on the considered strength parameters, the critical water level seems to correspond to a low or moderate overtopping, at least in the case of no drainage. That is about 80,5m to 81m. In the case of an efficient drainage, with a ratio of about 80%, factors of safety higher than 1,0 are found.

It is recalled that such a value reflects the practice when in absence of comprehensive data and further detailed calculations, the critical water level is usually considered as about 1m above the crest elevation.

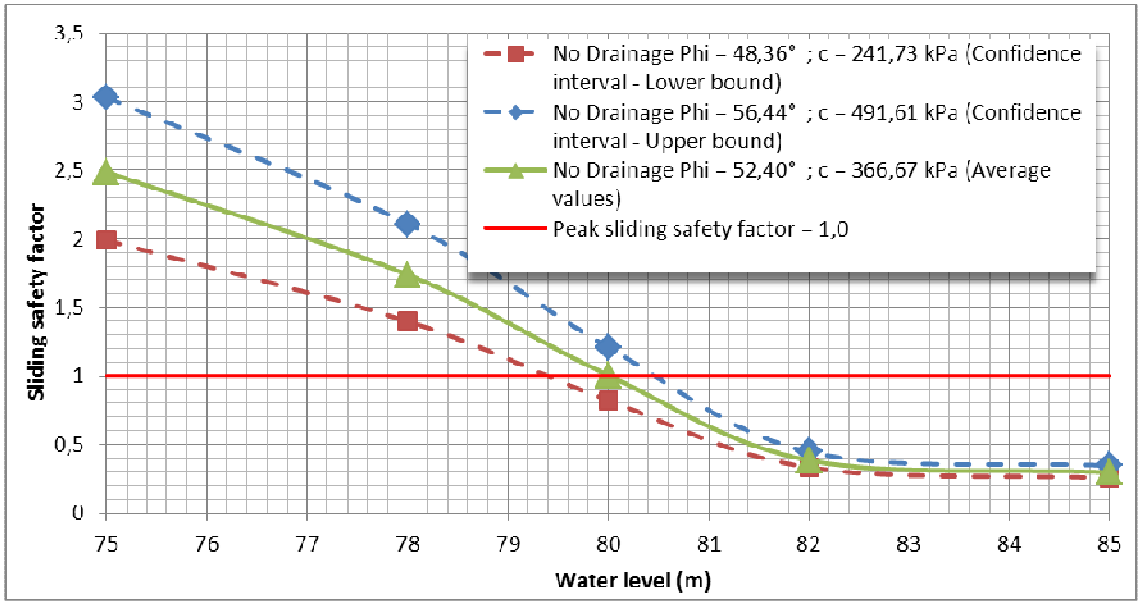

Figure 7 Factor of safety. No drainage.

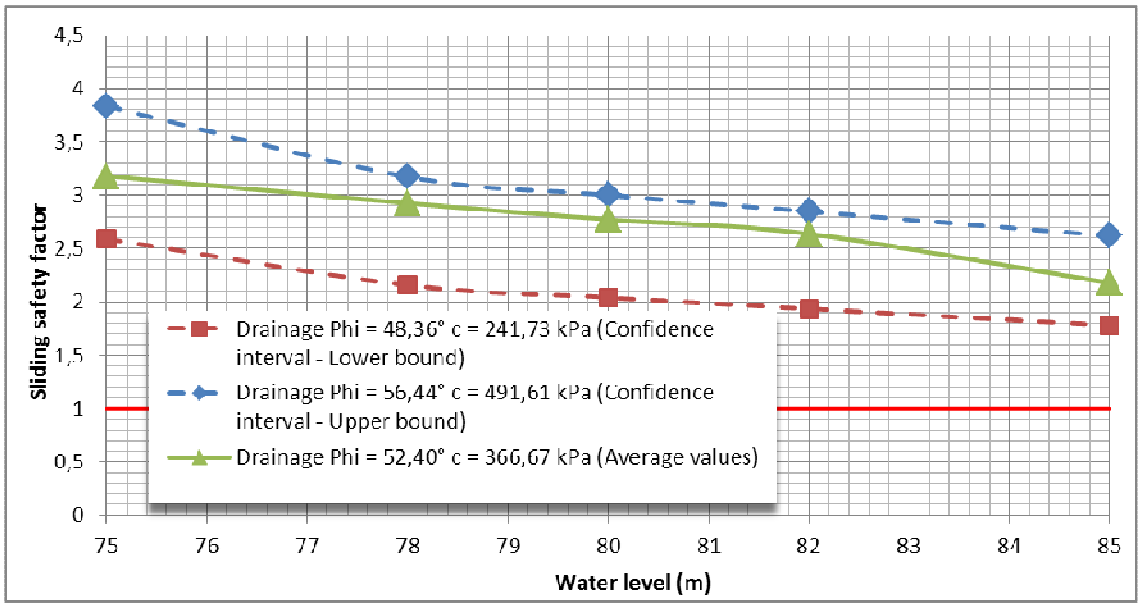

Figure 8 Factor of safety. With drainage.

11.3 Critical water level from the probabilistic approach

Calculated probabilities of failure by means of Monte-Carlo simulation would suggest that the critical water level is in the vicinity of 82m. This corresponds to an overtopping with a water depth of about 2m.

12. Consequences for Dam risk assessment

"Risk analysis methodologies need risk quantification. For an initial state of the dam-reservoir system, and for a certain failure mode, this risk quantification requires the estimation of both the probability of the loading scenarios and the conditional probability of the associated response of the dam-reservoir system, together with the estimation of the consequences" (ESCUDER et al. 2011).

12.1 Maximum probability of failure

Each water level is normally linked to a given probability of occurrence P(Hw). In this case, the probability of failure associated to a given water level corresponds to the probability of occurrence of the given water level ($P(H_w)$) times the probability of failure under that particular water level $P_f(H_w)$:

$$P_f = P(H_w) \times P_f(H_w)$$

Since the occurrence of very high water levels is usually very low, one can suspect that the probability of failure corresponding to each water level will display a peak, that is then followed by a steady decrease.

12.2 Implementation

The five (5) different water levels provided in the actual Benchmark are stated deterministically, with no attached probability. When undertaking a dam safety assessment, the different water levels could turn to be attached to various probabilities of occurrence.

For instance, one can suggest that highest water level (85m) could be attached to the PMF (Probable Maximum Flood), and that the lowest water level could be considered as the normal water level with a relatively high probability of occurrence.

The following Table was built based on the fact that several existing gravity dams were designed for an inflow design flood (IDF) that is below the 1,000 years return period flood. It is noticed worldwide that the existing spillway capacity of old dams is hardly sufficient for accommodating large floods, knowing that the hydrologic hazard is dramatically increasing in the case of a large number of dams worldwide; especially those with low to average reservoir capacity.

Table 11 Overall probability of failure the probability of occurrence of water levels

Water Level (m)	**75**	**78**	**80**	**82**	**85**
Water depth above normal water level (m)	0	+3	+5	+7	+10
Crest Overtopping ?	No	No	No	Yes	Yes
Water depth above crest (m)	-	-	-	+2	+5
Type of water level	Normal water level	Maximum water	Limit of overtopping	Accidental N°.1	Accidental N°.2
Possible associated hydrologic event	-	-	-	10,000[1]	PMF[2]
Possible associated probability of occurrence P(Hw)	10^{-1}	10^{-2}	10^{-3}	10^{-4}	10^{-6}
Probability of failure based on Monte-Carlo method Pf(Hw)	0	0,000006	0,040654	0,10000	0,10000
Overall probability of failure Pf including the probability of occurrence of water levels	0	$6x10^{-8}$	$4,07x10^{-5}$	$1,0x10^{-5}$	$1,0x10^{-7}$

Note 1 : This is the 10,000 years return period flood.

Note 2 : PMF standing for the Probable Maximum Flood.

Table 12 Maximum overall probability

Water Level (m)	**81**	**81**
Water depth above normal water level (m)		
Crest Overtopping ?	Yes	Yes
Water depth above crest (m)	1	1
Type of water level	Accidental N°.1	Accidental N°.2
Possible associated hydrologic event	-	-
Possible associated probability of occurrence P(Hw)	$3{,}16x10^{-4}$	$5{,}00x10^{-4}$
Return Period (Years)	$3{,}162x10^{3}$	$2{,}000x10^{3}$
Probability of failure based on Monte-Carlo method Pf(Hw)	0,1	0,1
Overall probability of failure Pf including the probability of occurrence of water levels	$3{,}16x10^{-5}$	$5{,}00x10^{-5}$
Associated Figure below	Figure 10	Figure 11
Case #	Case 1	Case 2

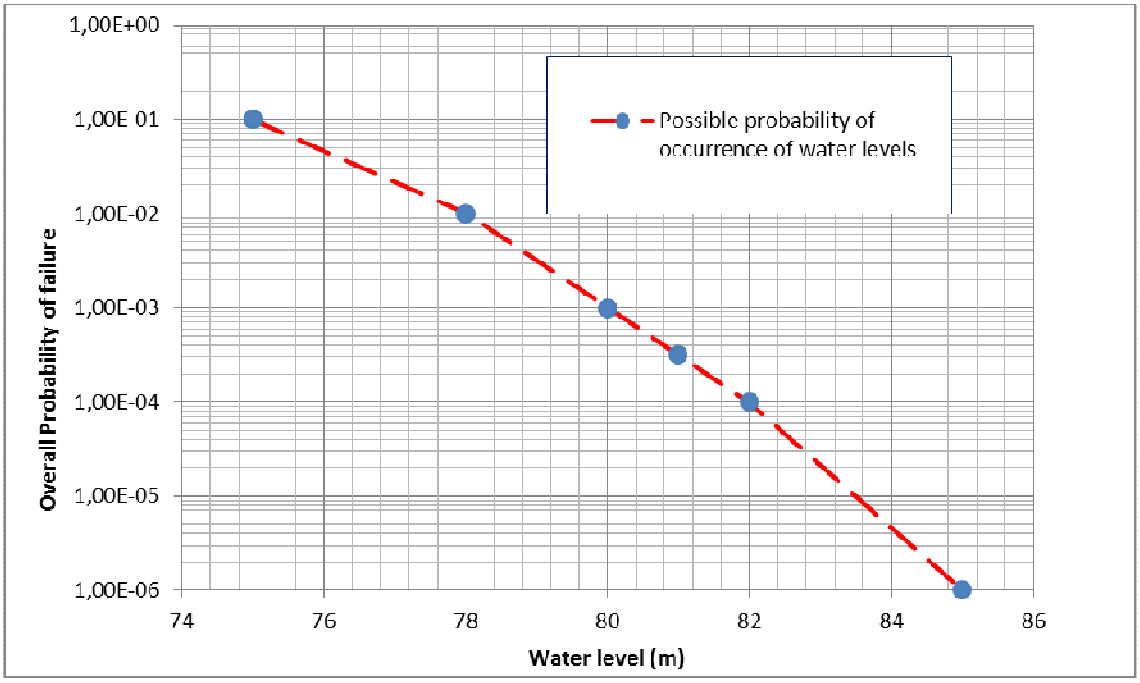

Figure 9 Probability of occurrence of water levels

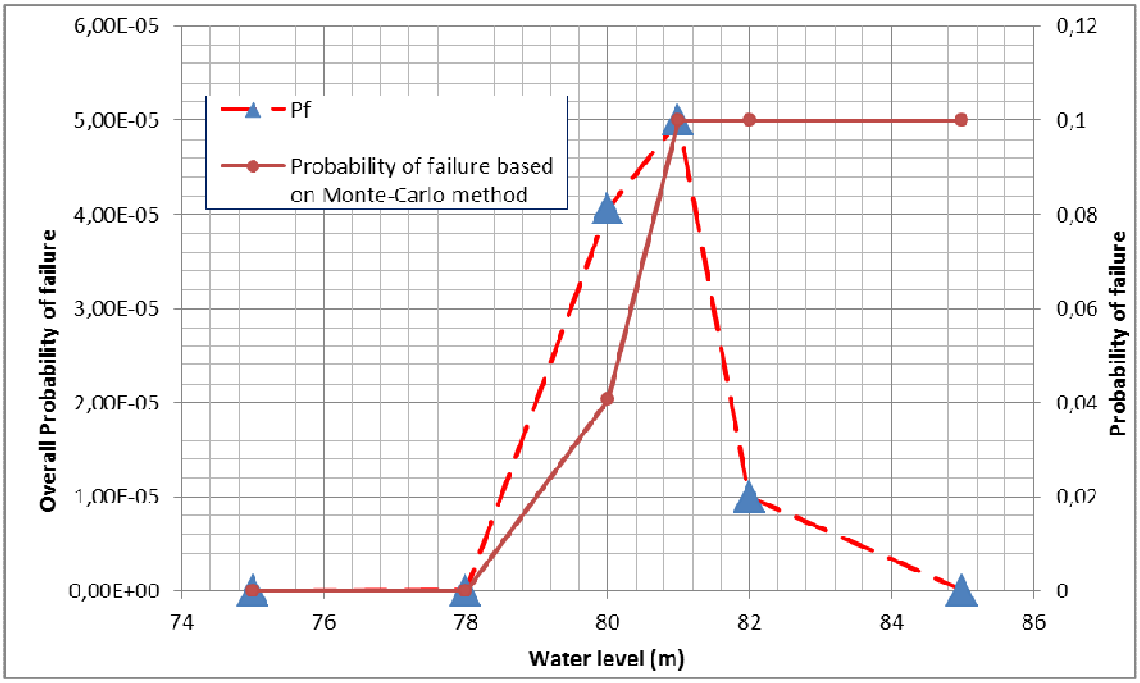

Figure 10 Probability of failure Pf including the probability of occurrence of water levels

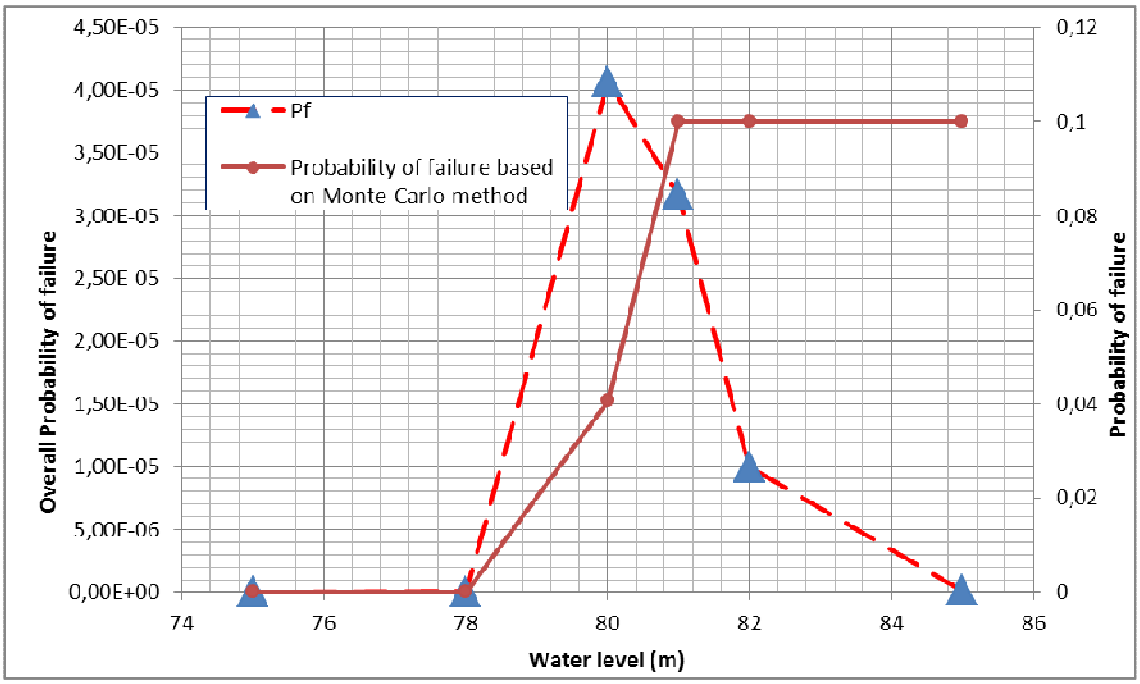

Figure 11 Probability of failure Pf including the probability of occurrence of water levels)

12.3 Discussion

Such as announced above, the maximum overall probability of failure Pf including the probability of occurrence of the different water levels do reach a peak in the neighborhood of a water level located between the crest elevation (i.e. 80m) and 1m above the crest the crest (i.e. 81m).

The peak is found to move from 80m to 81m water levels depending upon the probability of occurrence of the 81m water level.

Result N°.4: Based on the actual dam stability analysis, but also in the case of other dams, it is found that the critical water level could be set equal to the crest elevation plus 1m. Such a result confirms the widely used "rule of thumb" particularly in absence of more comprehensive analysis.

The maximum probability of failure should be between $4{,}07 \times 10^{-5}$ and $5{,}00 \times 10^{-5}$. This is within the values that are usually computed for gravity dams. The total probability of failure according to the sliding mode, together with taking into account the entire Author's reservoir water management sample, would be in the vicinity of $8{,}3 \times 10^{-5}$.

4. Conclusion

The actual analysis consisted on the use of three different methods for the stability assessment of the proposed 80m high gravity dam: (1:) Deterministic approach (Level-1), (2:) Taylor's series approximation limited to the FOSM or First Order Second Moment (Level-2), and finally (3:) Monte-Carlo method (Level-3).

Although various important results deserve to be highlighted, it is found that the main result is related to the fact that the relatively simple Taylor's series approximation - limited to the FOSM or First Order Second Moment (Level-2) -, is able to provide results that are fairly well comparable to

the much more complex Monte-Carlo simulation. The former is found to provide probabilities of failure that are only few percent below the later.

As an extension of the required results, the paper tackles and discusses the engineering meaning of the deterministic critical water level versus probabilistic critical water level. That is the water level leading the structure to the limits of its stability. When the water level is attached to corresponding probability of occurrence, one can find that the overall probability of failure for each water level reaches a maximum for a given water level. Such results are of first importance in the framework of a Dam Risk Assessment.

ACKNOWLDGEMENTS

The author of this contribution would like to thank the formulators of this Theme, Dr. ESCUDER, Dr. ALTAREJOS and Dr. SERRANO.

REFERENCES

[1] ESCUDER, I.B., ALTAREJOS, L.G., SERRANO, A.L. (2011). Theme C – Estimation of the probability of failure of a gravity dam for the sliding failure mode. Valencia, Spain. 2011

[2] ROYET, P., PEYRAS, L. 2006. Recommandations pour la justification de la stabilité des barrages poids, propositions de recommandations. Comité français des barrages et réservoirs, Le Bourget du Lac, 62 p, 2006 (to be reviewed in 2012).

XI ICOLD BENCHMARK WORKSHOP ON NUMERICAL ANALYSIS OF DAMS

Valencia, October 20-21, 2011

THEME C – ESTIMATION OF THE PROBABILITY OF FAILURE OF A GRAVITY DAM FOR THE SLIDING FAILURE MODE

Krounis, Alexandra[1]

Johansson, Fredrik[2]

CONTACT

Alexandra Krounis, Royal Institute of Technology, Division of Soil- and Rock Mechanics, Brinellvägen 23, 100 44 Stockholm, Sweden, +46 8 7908060, alexandra.krounis@byv.kth.se

Summary

Safety assessment of concrete dams is traditionally based on deterministic methods where factors of safety are used. In recent years there has been a discussion considering the use of reliability based methods in dam engineering. With these methods, the safety of the dam is assessed using the calculated probability of failure. The objective of Theme C is to obtain relationships between factors of safety and probabilities of failure for a given 2D dam. The factors of safety for the dam are calculated using the commonly used and accepted limit equilibrium method. The probabilities of failure are calculated using three different reliability based techniques with different stages of accuracy, namely the Taylor series method, the Hasofer Lind reliability index and Monte Carlo simulations. When deterministic methods are used, separate safety factors are calculated for each load case while in the structural reliability analyses the dam is considered as a system consisting of several load cases with different probabilities of occurring.

[1] PhD student, Division of Soli and Rock Mechanics, Royal Institute of Technology, Stockholm, Sweden

[2] PhD, Division of Soli and Rock Mechanics, Royal Institute of Technology, Stockholm, Sweden

1. Introduction

The objective of Theme C is to obtain relationships between factors of safety and probabilities of failure for different water levels for a given 2D dam model. Only failure due to sliding at the concrete-rock interface is considered. Considerations regarding displacements are excluded.

2. Deterministic methods

There are several techniques in order to calculate the factor of safety against sliding for a concrete dam. The most popular and accepted method is the limit equilibrium approach that will be used in this paper. In the limit equilibrium approach, the dam is considered to be a rigid body that is allowed to slide along critical surfaces such as the base, lift joints or weakness planes in the foundation. The safety is assessed by evaluating the force balance of the dam.

2.1 Criteria for sliding safety assessment

In the Swedish guidelines for dam safety, *SwedEnergy [1]*, the safety factor against sliding is based on the ratio between ΣH, the sum of the horizontal forces, and ΣV, the sum of the vertical forces. According to a comparison conducted by *Ruggeri et al. [2]*, this type of criteria is only used in two of the fourteen investigated countries. The criterion most commonly used is the ratio between the driving forces and the available shear strength of the studied sliding surface.

The available shear strength of the sliding surface is in general represented by a Mohr- Coulomb failure envelope. In its modern form, it is expressed according to equation 1.

$$\tau_{\mathrm{f}} = c + \sigma'_{\mathrm{N}} \tan \phi \tag{1}$$

Where τ_{f} is the shear stress at failure along the theoretical failure plane, c is the cohesion of the plane, σ_{N}' is the effective normal stress acting on the failure plane and ϕ is the friction angle of the failure plane. The factor of safety can then be calculated according to equation 2.

$$FS = \frac{c + \sigma'_{\mathrm{N}} \tan \phi}{\tau} \tag{2}$$

Where τ is the applied shear stress. This relationship holds locally, for each point of the potential sliding surface. When the global safety of the dam is assessed, the applied normal and shear stresses are integrated over the potential sliding plane, assuming that ultimate capacity is achieved at each point of the sliding surface. The global safety factor is then expressed as

$$FS = \frac{T_{\mathrm{f}}}{T} = \frac{c \cdot A + N \tan \phi}{T} \tag{3}$$

where T_{f} is the maximum resisting shear load, T is the applied shear load, N is the resultant of the forces normal to the assumed sliding plane including the effects of uplift and A is the contact area. As mentioned in *Ruggeri et al. [2]*, a fully ductile behaviour has to be assumed for equation 3 to be valid. However, the experimentally observed behaviour of a bonded sliding surface between concrete and rock is not ductile. Tests conducted on concrete/shotcrete-rock cores by *Saiang et al. [3], Lo et al. [4]* and *Seidel & Haberfield [5]* among others show that a semi-brittle response is a more correct description of the observed behaviour. This leads to a model uncertainty related to the cohesive part of equation 3.

Another uncertainty related to the cohesive part of equation 3 is in defining the magnitude of the cohesion for a bonded or partially bonded concrete-rock interface. The strength parameters of the interface between the dam and the rock foundation are commonly based on a limited number of tests. However, the cohesion of the concrete-rock interface can vary over the surface. As a result, there exists an uncertainty whether or not the test results are representative for the entire surface.

The common way of dealing with the above mentioned uncertainties in deterministic design is to apply larger safety factors when both cohesion and friction are used. In this paper, the factor of safety will be calculated according to equation 3, including the cohesive part.

3 Structural reliability analysis

3.1 Component reliability

Structural reliability analysis (SRA) is concerned with finding the reliability, *R,* or the probability of failure, P_f, of a feature, structure or system. When SRA is used, the reliability index, β, is the most commonly used measure of the structural safety. The reliability index is related to the probability of failure, P_f, as shown by equation 4.

$$P_f = \Phi(-\beta) \tag{4}$$

Where Φ is the cumulative standard normal distribution function. The probability of failure is given by

$$P_f = p(G(X) < 0) \tag{5}$$

where G(X) is the limit state function.

As mentioned by *Dalsgaard Sörensen [6],* structural reliability methods are classified according to level, moment and order. Level refers to the extent of information about the structural reliability problem that is provided and used.

In level I methods, the uncertain parameters are modeled with a characteristic value. Examples of such methods are codes based on the partial safety factor concept. Reliability methods which use the mean values and standard deviations, supplemented by the coefficients of correlation, to model the uncertain parameters are classified as level II methods. In level III methods, the uncertain parameters are modeled by their joint distribution functions. The probability of failure is estimated as a measure of the reliability in level II and level III methods. In level four methods the risk is used as a measure of reliability since consequences (cost) are also taken into account.

Moment refers to the order of statistical moments applied to represent an uncertain variable and its probability distribution. Order refers to the order of the polynomial applied for local approximation of the limit-state surface. In first order reliability methods, the limit state function is linearized and the reliability is estimated using level II or III methods. In second order reliability methods, a quadratic approximation to the failure function is determined and the probability of failure for the quadratic surface is estimated.

In this paper, the probability of failure of the dam due to sliding is calculated using three different reliability methods: the Taylor series method; the Hasofer-Lind method and Monte Carlo simulations. A short explanation of each method is provided bellow. For a more thorough coverage the reader is directed to textbooks in the subject such as *Thoft-Christensen & Baker [7].*

3.1.1 Taylor´s Series method of reliability analysis

The Taylor´s series method is a first order, second moment, FOSM, method based on Taylor´s series expansion of the performance function about some point. It uses only second moment statistics, mean and standard deviation, of the random variables. Since it is a first order method, only the first order, linear terms of the Taylor series expansion are used.

In order to perform an analysis using Taylor´s series method, a limit state function has to be defined. The limit state function, g*, for the analyses conducted in this paper is defined as

$$g^* = \frac{R}{S} - 1 \tag{6}$$

where *R* is the shear resistance of the concrete-rock interface and *S* is the sum of the driving forces. The expected value of the function, retaining only first-order terms, is the function of the expected values:

$$E[g^*] = g^*(E[X_1], [X_2], \dots [X_\mathrm{n}]) \tag{7}$$

The variance of the probability distribution of g*, assuming correlated random variables, is calculated as

$$Var[g^*] = \sum_i \left(\frac{\partial g^*}{\partial X_\mathrm{i}}\right)^2 \sigma_{\mathrm{X_i}}^2 + 2 \sum_{i \neq j} \frac{\partial g^*}{\partial X_i} \frac{\partial g^*}{\partial X_\mathrm{j}} \rho_{\mathrm{X_i X_j}} \sigma_i \sigma_\mathrm{j} \tag{8}$$

where σ^2_{Xi} is the variance of the random variable $\mathrm{X_i}$. If the random variables are independent equation 8 can be written as

$$Var[g^*] = \sum_i \left(\frac{\partial g^*}{\partial X_\mathrm{i}}\right)^2 \sigma_{X_\mathrm{i}}^2 \tag{9}$$

First order derivates can be obtained straightforward if g* is a linear function. If it is not, the variance term can be expressed using finite difference approximations of the derivates. The derivates are then calculated numerically using a very small increment (positive and negative) centred on the expected value. However, in these analyses the *USACE [8]* practise will be followed, meaning that a large increment of one standard deviation will be used, see equation 10. This is done in order to capture some of the behaviour of the nonlinear functions.

$$Var\,[g^*] = \sum_\mathrm{i} \left(\frac{g\big(E[X_\mathrm{i}] + \sigma_{\mathrm{X_i}}\big) - g\big(E[X_\mathrm{i}] - \sigma_{\mathrm{X_i}}\big)}{2}\right)^2 \tag{10}$$

Having the expected value and variance of the performance function and assuming that the function is normally distributed, the reliability index can be calculated according to equation 11.

$$\beta = \frac{E[g^*]}{\sqrt{Var[g^*]}} \tag{11}$$

3.1.2 Hasofer-Lind reliability index

A problem with Taylor´s series method is its lack of failure function invariance (the reliability index based on the linearized safety margin becomes dependent on the mathematical formulation of the safety margin). This introduces an error of unknown magnitude to the analyses. The degree of error depends on the degree of nonlinearity in the performance function and the coefficient of variation of the random variables. A more general definition of the reliability index that does not exhibit the invariance problem was proposed by *Hasofer & Lind [9]*. In their method, the limit state function is evaluated at a point known as the “design point” instead of the mean or the expected values. The design point is a point on the failure surface g*=0 that is generally not known a priori. In the general case, an iterative solution must be used to find the design point.

Consider a limit state function g(X_1, X_2,...,X_n) where the random variables X_i are all uncorrelated. The first step in defining Hasofer and Lind´s reliability index is to rewrite the limit state function in terms of the standard form of the variables which are defined by

$$U_{\mathrm{i}} = \frac{X_{\mathrm{i}} - \mu_{\mathrm{X_i}}}{\sigma_{\mathrm{X_i}}} \tag{12}$$

The failure surface in the new u-space is then given by

$$g^*(\mu_{\mathrm{X_1}} + \sigma_{\mathrm{X_1}}, \mu_{\mathrm{X_2}} + \sigma_{\mathrm{X_2}}, \dots, \mu_{\mathrm{X_n}} + \sigma_{\mathrm{X_n}} = g_{\mathrm{u}}^*(\boldsymbol{u}) = 0 \tag{13}$$

The Hasofer-Lind reliability index β is defined as the shortest distance from the origin O in the u-space to the failure surface, $g_u^*(\boldsymbol{u})=0$ and expressed according to equation 14. The Hasofer- Lind reliability index will coincide with the reliability index β as defined by equation 11 when the failure surface is linear.

$$\beta = \min_{g_{\mathrm{u}}(u)=0} \sqrt{\sum_{\mathrm{i}=1}^{\mathrm{n}} u_{\mathrm{i}}^2} \tag{14}$$

The calculation of the Hasofer-Lind reliability index as defined by equation 14 can be undertaken in a number of different ways. In this paper, the statistical software COMREL, *RCP Consult [10]*, was used in order to solve the problem presented in theme C.

3.1.3 Monte Carlo simulation

Monte Carlo simulation (MCS) is a numerical level III method that provides a more accurate evaluation of the probability of failure compared to level II methods. It includes all the information of the probability density function and not only the first two moments.

The following summary is based on the books of *Baecher & Christian [11]* and *Ang & Tang [12]* but many other authors present similar material. A MCS starts with the generation of a random value for each uncertain variable. Calculations are performed in order to yield a solution for that set of values. This gives one sample to the process. Each new sample results from repetition of the numerical process and may be considered a sample of a true solution analogous to an observed sample from a physical experiment. Once a large number of runs have been completed, it is possible to study the output statistically and to obtain values of means, variances, probabilities of various percentiles, and other statistical parameters. The probability of failure for each failure mode is calculated according to equation 15.

$$P_f = p[G \leq 0] = \frac{n}{N} \tag{15}$$

Where G is the limit state equation, *n* are the number of times G is below zero and *N* is the total number of Monte Carlo realizations. The accuracy of the solution obtained through MCS will improve with the sample size and may be measured by the coefficient of variation (c.o.v) of the solution.

$$Cov(\bar{P}) = \sqrt{\frac{1-\bar{P}}{n\bar{P}}} \tag{16}$$

Where $\bar{P}$ is the sample mean. Using equation 16, the error in percent of a Monte Carlo solution with a given sample size *n* can be evaluated

$$error(in\ \%) = 200\sqrt{\frac{1-\bar{P}}{n\bar{P}}} \tag{17}$$

The problem presented in theme C was solved using *MATLAB [13]*.

3.2 System Reliability

For a structure with several elements, or for one with several failure modes, the reliability has to be considered for the entire system. There are two fundamental types of systems, namely series systems and parallel systems. A system is a series system when the total system fails as soon as one component of the system fails. If failure in a single component doesn't result in failure of the total system, then the system is a parallel system.

The probability of failure for an ideal series system can be expressed according to equation 18.

$$P_{\mathrm{f}} = P(F_{\mathrm{s}}) = P(\cup F_{\mathrm{i}}) = P(\cup \{G_{\mathrm{i}}(x) \leq 0\}) = P(\{\min G_{\mathrm{i}}(x) \leq 0\}) \tag{18}$$

The system reliability may be approximated by reliability bounds, but in this paper the system reliability is approximated by integration of the bivariate normal density function. An approximation of the safety index of a series system of two components is then given by:

$$\beta_{\mathrm{sys}} = -\Phi^{-1}(\mathrm{P_f}) \approx -\Phi^{-1}(1 - \Phi_2(\beta_1, \beta_2; \rho_{12})) \tag{19}$$

where β_1 and β_2 are the reliability indices of limit state 1 and 2, respectively, ρ_{12} is the correlation of coefficient between the elements or failure modes and Φ_2 is the bivariate normal distribution function defined by

$$\Phi_2(\mathrm{x_1}, \mathrm{x_2}; \rho_{12}) = \int_{-\infty}^{\mathrm{x_2}} \int_{-\infty}^{\mathrm{x_1}} \varphi_2(\mathrm{t_1}, \mathrm{t_2}; \rho_{12}) \mathrm{dt_1 dt_2} \tag{20}$$

where ϕ_2 is the bivariate normal density function with zero mean given by

$$\varphi_2(t_1, t_2; \rho_{12}) = \frac{1}{2\pi\sqrt{1-\rho^2}} \exp\left(-\frac{1}{2(1-{\rho_{12}}^2)}(t_1^2 + t_1^2 - 2\rho_{12} t_1 t_2)\right) \tag{21}$$

The coefficient of linear correlation, ρ, describes the dependency that can occur among failure modes or elements of a system due to the same loads, building material etc and is for any pair of i-j modes, given by

$$\rho_{\mathrm{ij}} = \frac{Cov[g_{\mathrm{i}}, g_{\mathrm{j}}]}{\sigma_{g_{\mathrm{i}}} \sigma_{g_{\mathrm{j}}}} \tag{22}$$

in which Cov is the covariance of variables g_i and g_j and σ_{gi} and σ_{gi} are their standard deviations. The coefficient of correlation, ρ_{ij}, can also be calculated by means of the sensitivity factors, α, of the failure modes i and j according to equation 23.

$$\rho_{\mathrm{ij}} = \sum_{\mathrm{k=1}}^{\mathrm{m}} \alpha_{\mathrm{ik}} \alpha_{\mathrm{jk}}\ , \mathrm{i} \neq \mathrm{j} \tag{23}$$

4. Input

4.1 Geometry

The geometry of the dam is presented in Figure 1.

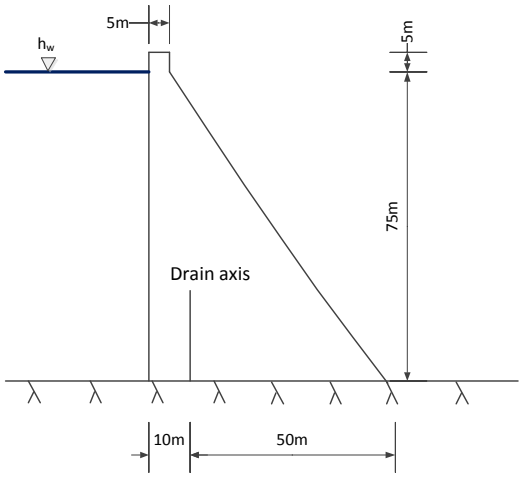

Figure 1: Illustration of the concrete dam

4.2 Variables

In a deterministic analysis, all variables are considered deterministic which means that they are represented by a single value since the value of each variable is considered to be known. However, in a reliability analysis, two types of variables can be included, deterministic variables and random variables. Random variables are variables described by statistical distributions which represent the uncertainties of the variable, e.g. natural randomness and statistical uncertainty. In order to simplify the analyses, only two random variables were considered in the performed reliability analyses; cohesion, *c*, and friction, tan *ø*, of the concrete-rock interface. All other variables were assumed deterministic variables.

4.2.1 Resistance variables

Regression of the available observations was used in order to define the statistical distribution and the moments for cohesion and friction. The friction was found to be normally distributed. An assumption of normality for the cohesion variable would imply a significant probability of negative values due to the large coefficient of variation. Therefore, a lognormal distribution was used. The correlation between the variables is equal to -0.26. Assuming uncorrelated variables when a negative correlation exists between two variables is a conservative assumption and simplifies the analyses. Therefore, the correlation between friction and cohesion will not be accounted for in this paper. The resistance parameters used in the analyses are presented in Table 1.

Table 1: Resistance parameters

			Deterministic analysis	**Reliability analysis**		
Resistance variables	**Unit**	**Notation**	**Value**	**Distribution**	**Expected value**	**Standard deviation**
Cohesion	MPa	*c*	0.37	Lognormal	0.48	0.40
Friction	Deg.	tan *ø*	1.36	Normal	1.36	0.39
Unit weight concrete	kN/m^3	γ_c	24	Constant	24	
Volume	m^3	V_c	2463	Constant	2463	

4.2.2 Load variables

Besides the self weight of the dam, the horizontal water load acting on the upstream face of the dam and the uplift pressure acting on the base of the dam were included in the analyses. The model considers the uplift distribution according to drain location and drain effectiveness as proposed in theme C. The hydrostatic and uplift loads for each load case are presented in Table 2.

Table 2: Hydrostatic and uplift loads

Load Case	Water level over foundation [m]	Drains	Hydrostatic load [kN]	Uplift load [kN]
1	75	Effective Ineffective	28125	8250 22500
2	78	Effective Ineffective	30420	8580 25335*
3	80	Effective Ineffective	32000	8800 27511*
4	82	Effective Ineffective	33620	9020 29426*
5	85	Effective Ineffective	36125	10705* 31961*

*Adjusted uplift pressure due to tension crack

4.3 Limit State

In order to perform the analyses, a limit state has to be defined for the actual failure mode. The failure mode studied in this study is sliding in the interface between concrete and foundation. In order for the results to be comparative with those from the deterministic analyses, sliding occurs if the load parallel to the sliding plane exceeds the shear resistance, T, of the plane. Also, the Mohr-Coulomb failure criterion is used to define the shear strength of the interface. The limit state function used in the Taylor series analyses is expressed according to equation 24.

$$g^*(\tan\phi, c) = \frac{R}{S} - 1 = \frac{c \cdot A + N \cdot \tan\phi}{T} - 1 \tag{24}$$

The limit state function used in the Hasofer-Lind analyses and Monte Carlo simulations is defined by

$$G(\tan\phi, c) = c \cdot A + N \cdot \tan\phi - T \tag{25}$$

4.4 System

In this paper, the dam is treated as one structural member with two components with probability of occurring according to Figure 2. Since failure of the dam will occur if either failure mode occurs, the system will be treated as a series system.

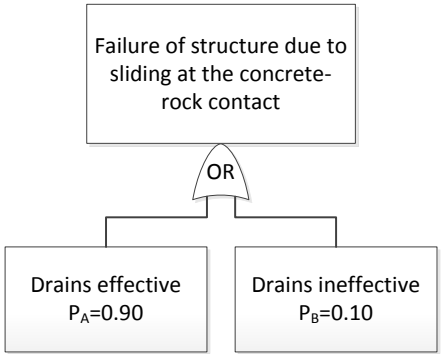

Figure 2: Reliability of the system in theme C

5. Results

5.1 Deterministic analyses

The results from the deterministic analyses are presented in Table 3.

Table 3: Results from deterministic analyses

Load Case	Water level over foundation [m]	Drains	Factor of safety
1	75	Effective	3.25
		Ineffective	2.56
2	78	Effective	2.99
		Ineffective	2.24
3	80	Effective	2.83
		Ineffective	2.04
4	82	Effective	2.69
		Ineffective	1.86
5	85	Effective	2.44
		Ineffective	1.64

5.2 Reliability analyses

5.2.1 Component reliability

For each of load case, the conditional probability of failure and the coefficient of correlation between failure modes were calculated using the three different methods described above. The results are shown in Table 4-6.

Table 4: Results from analyses using Taylor series method

Load Case	Water level over foundation, H_w [m]	Drains	Conditional probability of failure, P_{fc}	Reliability index, β	Coefficient of correlation between failure modes
1	75	Effective	8.63e-3	2.381	0.987
		Ineffective	2.67e-2	1.931	
2	78	Effective	1.11e-2	2.286	0.980
		Ineffective	4.35e-2	1.711	
3	80	Effective	1.32e-2	2.220	0.974
		Ineffective	6.19e-2	1.539	
4	82	Effective	1.57e-2	2.153	0.967
		Ineffective	8.55e-2	1.369	
5	85	Effective	2.24e-2	2.007	0.961
		Ineffective	1.33e-1	1.114	

Table 5: Results from analyses using Hasofer-Lind reliability index

Load Case	Water level over foundation, H_w [m]	Drains	Conditional probability of failure, P_{fc}	Reliability index, β	Coefficient of correlation between failure modes
1	75	Effective	2.60e-3	2.794	0.990
		Ineffective	6.71e-3	2.473	
2	78	Effective	3.68e-3	2.680	0.990
		Ineffective	1.31e-2	2.224	
3	80	Effective	4.64e-3	2.601	0.983
		Ineffective	2.16e-2	2.022	
4	82	Effective	5.86e-3	2.520	0.985
		Ineffective	3.52e-2	1.809	
5	85	Effective	9.11e-3	2.361	0.975
		Ineffective	7.08e-2	1.470	

Table 6: Results from analyses using Monte Carlo Simulations

Load Case	Water level over foundation, H_w [m]	Drains	Conditional probability of failure, P_{fc}	Reliability index, β	Coefficient of correlation between failure modes
1	75	Effective Ineffective	5.83e-4 0.0011	3.247 3.066	0.988
2	78	Effective Ineffective	8.55e-4 0.0022	3.136 2.855	0.981
3	80	Effective Ineffective	0.0011 3.60e-3	3.057 2.688	0.974
4	82	Effective Ineffective	0.0014 0.0062	2.983 2.500	0.967
5	85	Effective Ineffective	0.0023 0.0141	2.837 2.193	0.960

system reliability, the conditional probability of failure was multiplied with the probability of occurrence of the case, according to equation 26.

$$P_{\mathrm{f}} = P(E_1 \cap E_2) = P(E_1)P(E_2) \tag{26}$$

Where E_1 is the event of conditional failure and E_2 is the event of the drains being effective or ineffective.

5.2.2 System reliability

The safety index for the entire system (drains effective – drains ineffective) was calculated for each water level. The results are presented in Table 7.

Table 7: Results from analyses using Monte Carlo Simulations

	Taylor series method		Hasofer-Lind Reliability index		Monte Carlo simulations	
Water level over foundation, H_w [m]	**Conditional probability of failure, P_f**	**Reliability index, β**	**Conditional probability of failure, P_f**	**Reliability index, β**	**Conditional probability of failure, P_f**	**Reliability index, β**
75	7.79e-3	2.42	2.34e-3	2.83	5.25e-4	3.28
78	1.03e-2	2.32	3.33e-3	2.71	7.79e-4	3.16
80	1.27e-2	2.24	4.41e-3	2.62	0.0010	3.08
82	1.58e-2	2.15	5.89e-3	2.52	0.0014	2.98
85	2.33e-2	1.99	1.06e-2	2.31	0.0026	2.80

In order to obtain the probability of failure, $P_{f,}$ for each load case for use in the evaluation of the

6. Discussion

The methods available for SRA are in varying stages of accuracy. Of the three reliability approaches used in this paper, the Taylor series method is considered the most inaccurate while Monte Carlo simulations provide the most accurate estimations of the probability of failure. It can be seen in Table 7 that the Taylor series method underestimates the safety of the dam for all load cases compared with the Monte Carlo simulations.

When the sliding stability of concrete dams is evaluated using SRA a lot of uncertainties of unknown magnitude arise. Most of them are related to the shear strength of the concrete- rock interface. It is not accurate to assume that a bonded interface loses its load-bearing capacity completely after “failure”. As mentioned earlier, tests performed by several researchers indicate that a semi-brittle behaviour is closer to reality. However, it is unclear how this affects the global sliding stability of the dam. Another difficulty that arises is to define the cohesion of a bonded or partly bonded interface, since it has a spatial variation and the number of tests is in general limited. In order for a SRA to be reliable, all related uncertainties have to be identified, quantified and included in the analysis.

In this study, the correlation between the cohesion and friction angle was not accounted for. This limitation was chosen in order to simplify the calculations. However, it is likely that including the observed negative correlation between the shear strength would increase the reliability of the structure.

The correlation between the components of the system was calculated and included in the analyses. As can be seen in Tables 4 to 6, the failure modes of the system in theme C are strongly correlated. This increases the reliability of the system.

Although it is important to recognize the limitations and uncertainties related to SRA, it should also be recognized that many of these limitations are shared with traditional, deterministic methods.

7. Conclusion

SRA is not widely used in dam engineering at this time. Further research is needed in order to define and quantify the uncertainties related with SRA. However, practical dam safety decisions should be made using the best available information so reliability based analyses can be used as a support to traditional deterministic approaches when necessary.

Acknowledgements

The research presented was carried out as a part of “Swedish Hydropower Centre – SVC”. SVC has been established by the Swedish Energy Agency, Elforsk and Svenska Kraftnät together with Luleå University of Technology, The Royal Institute of Technology, Chalmers University of Technology and Uppsala University. www.svc.nu

References

[1] SwedEnergy. (2008). Kraftföretagens riktlinjer för dammsäkerhet. (Swedish Hydropower companies guidelines for dam safety). In Swedish
[2] Ruggeri et al. (2004). Sliding Stability of Existing Gravity Dams – Final Report. ICOLD European Club http://cnpgb.inag.pt/IcoldClub/documents/Sliding_safety_FinalReport.pdf
[3] Saiang, D., Malmgren, L., & Nordlund, E. (2005). Laboratory Tests on Shotcrete-rock joints in direct shear, tension and compression. Rock Mechancis and Rock Engingeering 38(4) pp. 275-297
[4] Lo, K.Y., Ogawa, T., Lukajic B. & Dupak, D. (1991). Measurements of strength parameters of concrete rock contact at the dam-foundation interface. Geo-technical Testing Journal. 14(4) pp. 383-394
[5] Seidel, J.P. & Haberfield, C.M. (2002). Laboratory testing of concrete-rock joints in constant normal stiffness direct shear. Geotechnical Testing Journal 25(4)
[6] Dalsggard Sørenssen, J. (2004). Notes in structural reliability theory and risk analysis, Aalborg University, Denmark
[7] Thoft-Christensen, P. & Baker, M.J. (1982). Structural Reliability and Theory and its Applications. Berlin, Heidelberg, New York: Springer-Verlag
[8] U.S. Army Corps of Engineers (1999). ETL 1110-2-556 Risk-based analysis in geotechnical engineering for support of planning studies, Washington, DC
[9] Hasofer, A.M. and Lind, N.C. (1974). An exact and invariant second-moment code format. Journal of the Engineering Mechanics Division. 100 pp.111-121
[10] RCP Consult (2003). STRUREL, A Structural Reliability Analysis Program-System, COMREL & SYSREL: USERS MANUAL. RCP GmbH Barer, München, Germany
[11] Baecher, G.B. & Christian, J.T. (2003). Reliability and Statistics in Geotechnical Engineering
[12] Ang, A.H-S. & Tang, W.H. (2007). Probability concepts in engineering – emphasis on applications to civil and environmental engineering. Hoboken:John Wiley & Sons, Inc
[13] MATLAB, version 7.1, The Mathworks, Inc., Natick, MA, 2010

XI ICOLD BENCHMARK WORKSHOP ON NUMERICAL ANALYSIS OF DAMS

Valencia, October 20-21, 2011

THEME C

Estimation of the probability of failure of a gravity dam for the sliding failure mode

Shcherba, Dmitry[1]

CONTACT

Dmitry Shcherba, JSC "VEDENEEV VNIIG" (Hydraulic engineering research institute), Department of Static and Seismic Stability Analyses of Concrete Structures 195220, Saint-Petersburg, Russia, 21 Gzhatskaya st., Tel.: +78124939318, e-mail address: scherbaDV@vniig.ru

Summary

An analysis of dam-foundation system with reliability-based technique is presented. Four cases of uplift pressure are considered. Safety factors for several water levels are calculated. Probabilities of failure using several methods of second and third levels of reliability theory re obtained. Third level method involves simulations which were performed with usual Monte-Carlo technique and its variation – Latin Hypercube. Several distributions of random variables are considered.

[1] JSC "VEDENEEV VNIIG", Department of Static and Seismic Stability Analyses of Concrete Structures, engineer

1. Introduction

Estimation of safety and reliability of hydraulic structures, and particularly dams, is one of the most topical technical problems in dam engineering. There are a lot of methods for reliability analysis, which provide quite powerful and practically suitable instruments for engineering decision-making. One faced to the problem of reliability analysis have to deal with probability of failure, which is a conditional probability for certain loading conditions. The methods of probability of failure estimation are usually grouped in three levels. The solution presented herein was provided for certain failure mode (sliding of dam along the dam-foundation contact) and carried out using methods of all three levels.

2. Model formulation and considerations

The geometry of the dam is shown in figure 1.

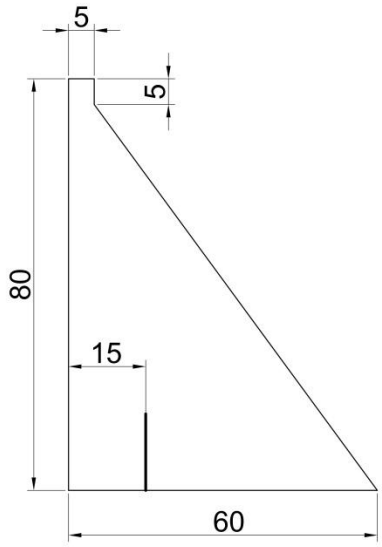

Figure 1: Dam geometry (m)

The assumed material properties are given in table 1.

Table 1.- Data for dam and foundation materials

Material parameters	**Dam**	**Foundation**
Young's modulus (MPa)	24000	41000
Poisson`s ratio	0.15	0.10
Mass density (kg/m^3)	2400	2700
Compressive strength (MPa)	24	40
Tensile strength (MPa)	1.5	2.6
Strain at peak compressive strength	0.0022	0.0025
Strain at end of compressive softening curve	0.10	0.15
Fracture energy (N/m)	150	200

Two-dimensional limit-equilibrium model was used to analyze the stability of dam. Model is simple, well-known and well-behaved, that allows focusing on estimation of probability of failure.

The model based on relationships between driving force and shear strength. Evaluation of them can be carried out using equation (1) and (2):

$$S = \frac{1}{2}\rho_W g h^2, \qquad (1)$$

where ρ_w is the density of water, g – gravity acceleration (taken as 10 m/s^2) and h is water level.

$$R = (N - U)tg\varphi + B \times c, \quad (2)$$

where N is the sum of vertical forces acting on the dam-foundation contact surface, U is the uplift, B is the area of the dam-foundation contact surface, φ is the friction angle in the contact, and c is the cohesion in the contact.

The uplift pressure depends on both water level and groundwater proof (grout curtain and drain). Presence of crack along the dam-foundation contact also influences the uplift. The four cases considered herein are shown in the figure 2.

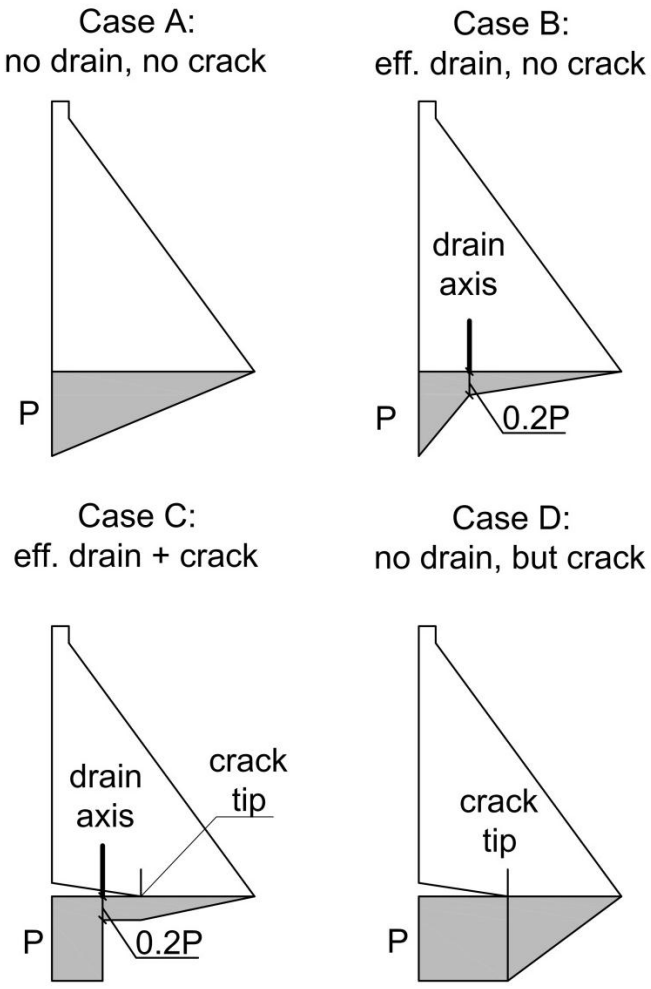

Figure 2: Four cases of uplift pressure

The distance between crack tip and upstream face (i.e. crack length) were estimated by finite element method.

3. Crack length estimating

Estimating of the crack length is very complicated problem itself. Even if can suggest the direction of the crack propagation (like in the case of the dam-foundation contact crack), the fracture properties of the interface between concrete and foundation often still obscure. Traditionally estimating of crack length is based on linear or non-linear elastic fracture mechanics or any of the so-called "traction-separation" models. On of such traction-separation models, provided by *Alfano and Criesfield* [2], were used during this research.

This model is implemented in release of ANSYS program as “Cohesive zone model” (CZM) and is to be used with contact elements. The model states relationships between contact pressure in the “process zone” near crack tip and crack opening (or gap between sides of the crack), like shown in figure 3.

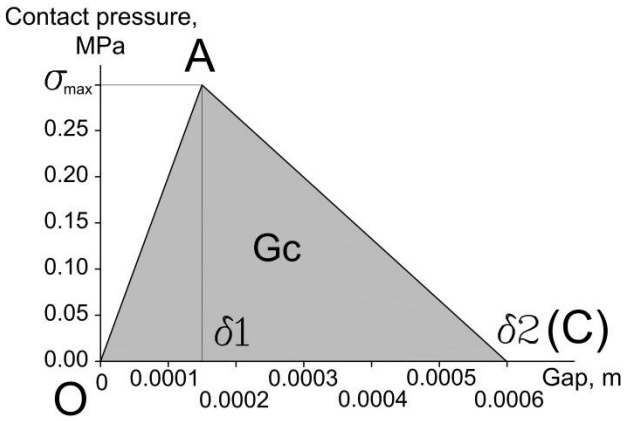

Figure 3: Bilinear cohesive zone material model

Model shows linear elastic loading (*OA*) followed by linear softening (*AC*). The maximum normal contact stress is achieved at point *A*. A process called debonding begins at point *A* and is completed at point *C* when the normal contact stress reaches zero value. Any further separation occurs without any normal contact stress. The area under the curve *OAC* is the energy released due to debonding which is usually called the critical fracture energy. This considerations were provided for so called “Mode I debonding”, in the sense that separation occurs in the direction normal to the interface. The same considerations should be applied to taking into account tangential direction, and similar parameters should be set (but, in general, with other values).

Hereby, there are four parameters in the model: G_c, σ_{max}, G_τ, τ_{max}. Values of these parameters are to be discussed, because, as were mentioned earlier, the properties of the interface itself are unknown. Taking into account that this is not the subject of this paper, for the sake of simplicity these parameters were taken for granted from *Alfano et al.* [3]. In that paper these values were provided for the benchmark considered herein: $G_c = 90\ J \cdot m^{-2}$, $\sigma_{max} = 0.3$ MPa, $G_\tau = 350\ J \cdot m^{-2}$, $\tau_{max} = 0.7$ MPa.

The modified finite element mesh is shown in figure 4.

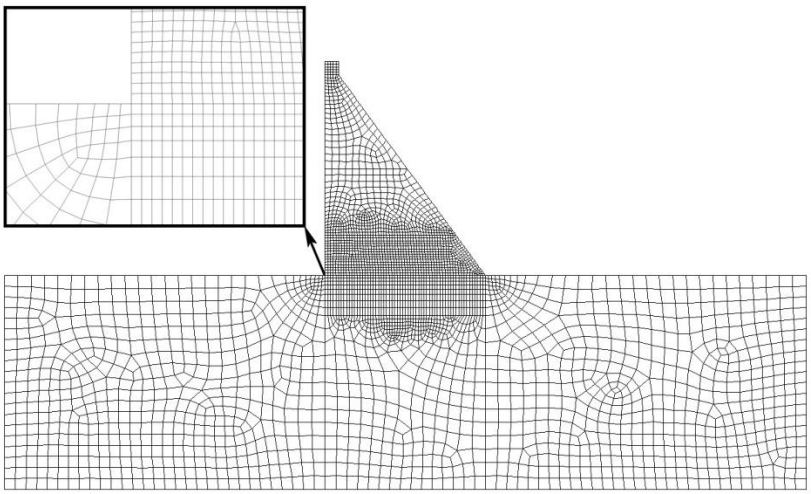

Figure 4: Finite element mesh

Crack opening diagram for water level of 85 m is shown in figure 5.

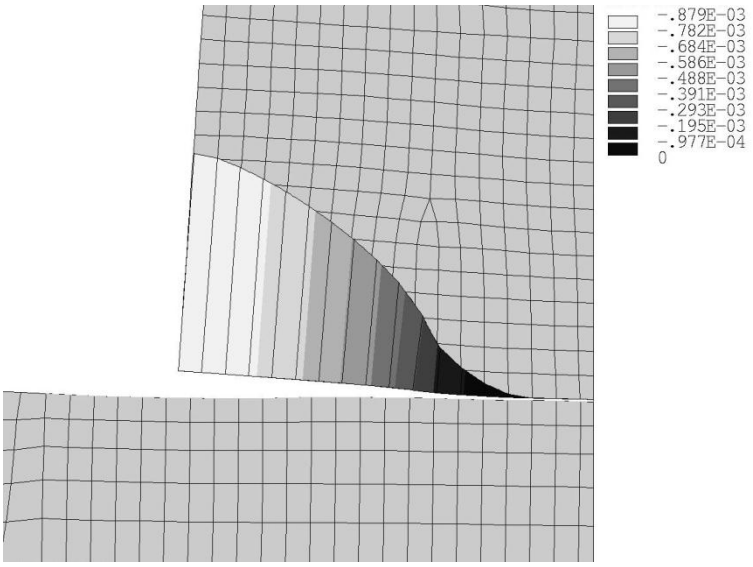

Figure 5: Diagram of crack opening (water level = 85 m)

The series of analyses resulted in values of crack length for several water levels and for two cases of drain effectiveness. These values are shown in table 2.

Table 2: Crack length versus water level

Water level, m	100 % eff. of drain	0 % eff. of drain
75	5	7
78	11	12
80	12	13
82	13	15
85	15	18

In fact, these values are quite approximate, but they are suitable in this particular analysis.

4. Interpretation of samples

In accordance with provided data, two of the design variables considered as random: friction angle and cohesion at the dam-foundation interface. Available information consists of 15 pairs of values, shown in table 3.

Table 3.- Data for friction and cohesion at the interface

Sample	Friction angle (º)	Cohesion (MPa)	Sample	Friction angle (º)	Cohesion (MPa)
1	45	0.5	9	49	0.1
2	37	0.3	10	60	0.2
3	46	0.3	11	63	0.2
4	45	0.7	12	62	0.4
5	49	0.8	13	60	0.7
6	53	0.2	14	56	0.1
7	54	0.6	15	62	0.4
8	45	0.0			

Analyzing this data with simple statistical tools, it is possible to obtain the most important statistics – sample mean and sample variance.

$$\bar{X} = \frac{\sum_{i=1}^{N} X_i}{N} \tag{3}$$

$$\bar{\sigma}^2 = \frac{\sum_{i=1}^{N} (X_i - \bar{X})}{N - 1} \tag{4}$$

Results are shown in table 4.

Table 4.- The most important sample estimates

Water level, m	φ,°	C, MPa
$\bar{X}$	52.40	0.367
$\bar{\sigma}^2$	63.83	0.061
$\bar{\sigma}$	7.99	0.246

These values are used through the paper. They are especially important in second level methods, where they are used for calculation of first two moments of probability distribution of the performance function.

For execution of third level methods it is needed to obtain (or suggest) how the performance function is distributed. For this purpose histograms are plotted (figure 6 and 7).

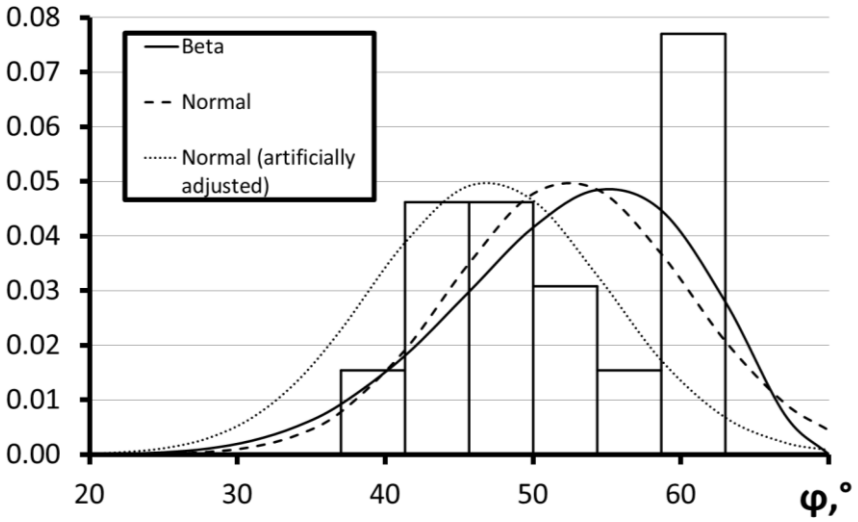

Figure 6: histogram and adjusting curves for friction angle

It is shown in [4] that good choise of adjustment function for friction angle is beta distribution because it can be limited, and values of friction angle a located within range. The range of 10 to 70 degrees was chosen.

And cohesion can be adjusted by lognormal distribution which is defined in the positive interval ($0 \leq g^* < +\infty$).

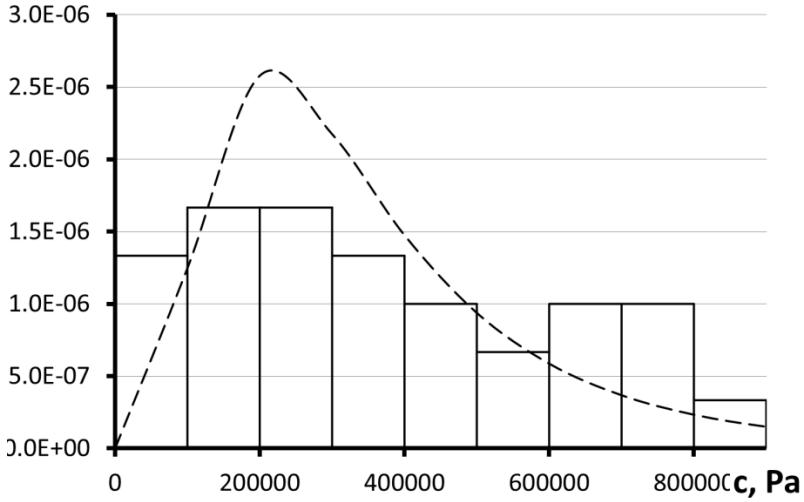

Figure 7: Histogram and adjusting curves for cohesion

The location of sampling points in (φ,c) axis is shown in figure 8.

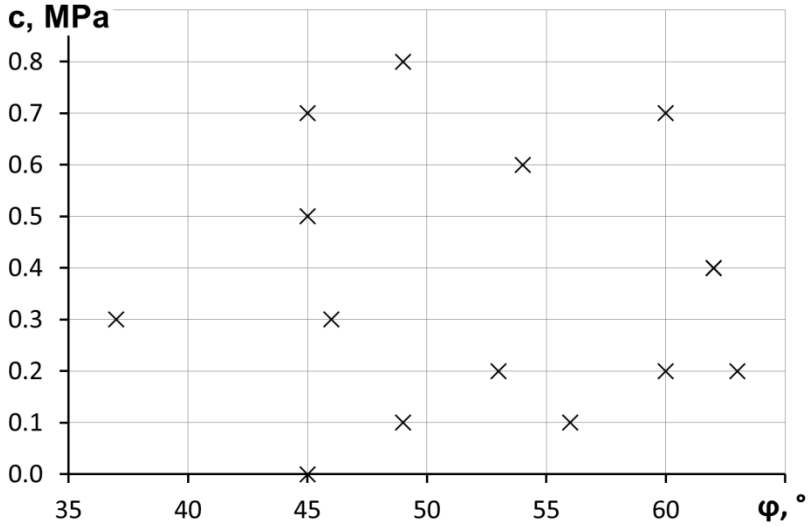

Figure 8: Sampling points in (φ,c) axis

It is suggested that there is no correlation between this variables, although in article of *R. Jimenez-Rodriguez [4]* wrote, that there is slight negative correlation.

4. Probability of failure estimating

As were mentioned, three groups of reliability analyses methods usually are sorted out also called “levels”. Methods of first level are concerned with safety factors evaluation. Methods of second level are often called “second moment” methods, because they use only first two moments of the joint probability density function. Methods of third level provide the most accurate probability of failure, but it concerned with numerical integration and simulations, which can be difficult for complex problems.

The analysis of probability appears for systems that contain uncertainties. In current model uncertainty was provided by considering two parameters as random variables - friction angle and cohesion at the dam-foundation interface.

Methods of theory of reliability based on consideration that the structure mustn’t reach the limit state – state, which not allow operating the structure normally.

For implementation of reliability methods mechanical model is needed. If there are n variables forming a vector (X_1,X_2,…,X_n) in n-dimensional space, it is possible to derive mechanical model as a function of strength r(x_1,x_2,…,x_n) and loading s(x_1,x_2,…,x_n) function:

$$g(x_1, x_2, \dots, x_n) = \frac{r(x_1, x_2, \dots, x_n)}{s(x_1, x_2, \dots, x_n)} \quad (3)$$

Then limit state equation can be written as follows:

$$g^*(x_1, x_2, \dots, x_n) = g(x_1, x_2, \dots, x_n) - 1 = \frac{r(x_1, x_2, \dots, x_n)}{s(x_1, x_2, \dots, x_n)} - 1 \quad (4)$$

It defines limit-state region as an n-dimensional hyper surface, which divides n-dimensional space into failure domain and safety domain.

The failure domain in the n-dimensional space is defined as:

$$g^*(x_1, x_2, \dots, x_n) \leq 0 \quad (5)$$

So, one can find out if the function g*(x_1,x_2,…,x_n) of certain variable values (also called representative values) is located in failure domain, or calculate the probability of failure as integral over the failure domain of the joint probability function of all random variables:

$$P_f[g^*(x_1, x_2, \dots, x_n) \leq 0] = \int_{g^*(x_1, x_2, \dots, x_n) \leq 0} f_{X_1, X_2, \dots, X_n}(x_1, x_2, \dots, x_n)\, dx_1 dx_2 \dots dx_n \quad (6)$$

4.1. Methods of first level. Global safety factor

Safety factors are widely used in common practice of structural safety assessment.

Taking into account eq.(1),(2) and (3) one can write the expression for mechanical model of current problem.

$$g(c, \varphi) - 1 = \frac{r(c, \varphi)}{s(c, \varphi)} - 1 = \frac{(N - U)tg\varphi + B \times c}{S} - 1 \quad (7)$$

It is possible to write limit state equation:

$$g^*(c, \varphi) = g(c, \varphi) - 1 = \frac{r(c, \varphi)}{s(c, \varphi)} - 1 = \frac{(N - U)tg\varphi + B \times c}{S} - 1 \quad (8)$$

This equation could be transformed:

$$\varphi = \operatorname{atan}\left(\frac{S + B \times c}{(N - U)}\right) \quad (9)$$

As the considered case is simple and we have only two design variable, we can represent limit state region as a curve and plot it graphically in the (φ,c) plot. Four curves for different cases, stated In section 2 of this paper, but for certain water level (85 m) are shown in figure 9.

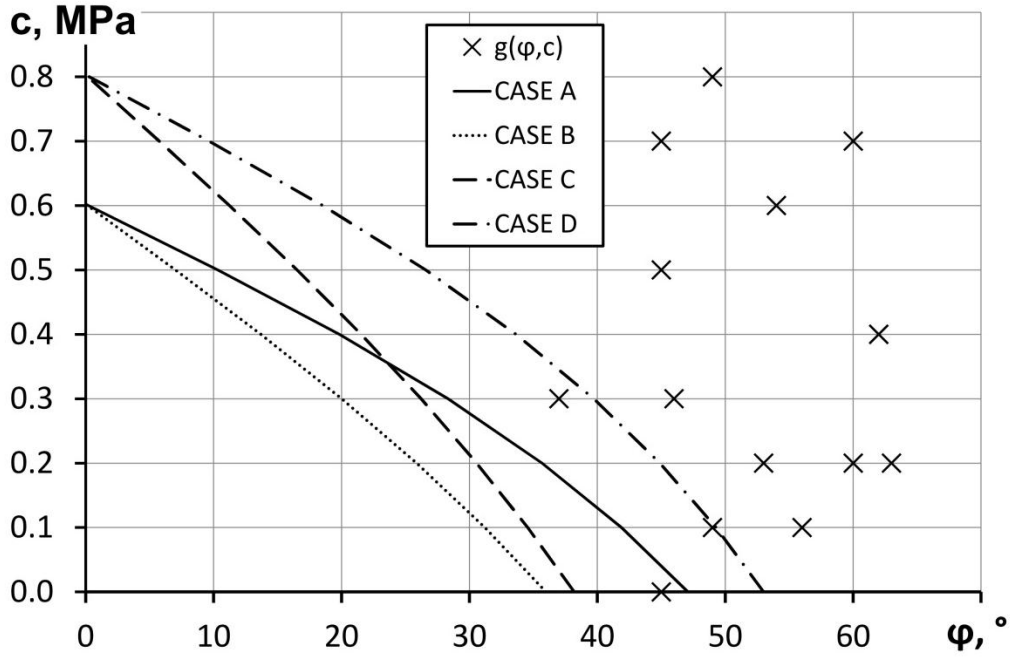

Figure 9: Limit-stated curves for different cases of uplift (water level = 85 m)

Values of safety factors were obtained for four cases, results are shown in table 4:

Table 5: Global safety factors for four cases

Water level, m	CASE A	CASE B	CASE C	CASE D
75	1.53	2.03	1.85	1.27
78	1.39	1.86	1.69	1.14
80	1.30	1.76	1.60	1.06
82	1.22	1.67	1.51	0.99
85	1.11	1.55	1.39	0.89

The main shortcoming of this method is that limit values of safety factors stated in regulatory rules (or codes) are often chosen with being based on experience. Result of this is a situation that nobody knows indeed if the structure is safe or not, and if it is safe, if the value of safety margin is unreasonably excessive or not.

4.2. Methods of second level. Firs Order Second Moment

The name of these methods caused by the fact that the function $g^*(x_1,x_2,\ldots,x_n)$ is approximated linearly and only first two moments of the joint probability density function are considered. At the output of analysis the reliability index, β, is usually obtained. Its meaning (distance between the most probable value and the failure domain) gives us a relative measure of reliability, but it doesn't tell us anything about the probability of failure by itself.

As $(X_1,X_2,\ldots,X_n)$ are random variables, $g^*(x_1,x_2,\ldots,x_n)$ is a random variable with certain distribution, usually unknown. For probability of failure estimation one should suggest the shape of this distribution.

Hereinafter values of reliability index and probability of failure are given, computed using three different methods.

4.2.1. Taylor's series method

Method based on expansion of performance function into Taylor's series about the expected value. Then only linear elements are taking into account during calculation of first two moments of the probability distribution of performance function [1].

Table 6: Values of reliability index and probability of failure for Taylor's series method

Water level, m	CASE A		CASE B		CASE C		CASE D	
	β	Φ(-β)	β	Φ(-β)	β	Φ(-β)	β	Φ(-β)
75	2.013	0.022074	2.420	0.007754	2.357	0.009221	1.902	0.028555
78	1.866	0.031003	2.320	0.010173	2.151	0.015729	1.635	0.051027
80	1.764	0.038862	2.250	0.012210	2.059	0.019765	1.496	0.067289
82	1.658	0.048650	2.179	0.014666	1.964	0.024793	1.332	0.091425
85	1.492	0.067854	2.068	0.019322	1.808	0.035301	1.075	0.141208

4.2.2. Point estimate method

The point estimate method determine the first two moments of the performance function g* by the discretization of the probability distributions of the random variables (X_1,X_2,…,X_n). This discretization is made in a few points for each random variable (two or three points), where mass probability is concentrated in such a fashion that the sum of the probabilities assigned to each point is 1 for each random variable (*Rosenblueth [5]*). In the more general approximation, the method determines the third moment of the distributions, which allows analysis with skewed (asymmetrical) distributions. Random variables can be independent or correlated.

Table 7: Values of reliability index and probability of failure for point estimate method

Water level, m	CASE A		CASE B		CASE C		CASE D	
	β	Φ(-β)	β	Φ(-β)	β	Φ(-β)	β	Φ(-β)
75	2.139	0.016212	2.566	0.005140	2.504	0.006133	2.032	0.021070
78	1.991	0.023237	2.466	0.006840	2.394	0.008334	1.863	0.031256
80	1.888	0.029531	2.396	0.008290	2.317	0.010242	1.744	0.040596
82	1.781	0.037488	2.324	0.010057	2.238	0.012597	1.620	0.052598
85	1.613	0.053404	2.213	0.013455	2.115	0.017195	1.425	0.077015

4.2.3. Hasofer-Lind method

In [7] it is shown that reliability indexes obtained with first two approaches is not invariant to form of the performance function. So, Hasofer and Lind developed another reliability index, which is invariant.

Table 8: Values of reliability index and probability of failure for Hasofer-Lind method

Water level, m	CASE A		CASE B		CASE C		CASE D	
	β	Φ(-β)	β	Φ(-β)	β	Φ(-β)	β	Φ(-β)
75	2.230	0.012870	2.905	0.001835	2.767	0.002826	2.088	0.018402
78	2.104	0.017675	2.711	0.003349	2.567	0.005124	1.884	0.029768
80	2.052	0.020079	2.577	0.004986	2.451	0.007119	1.744	0.040581
82	2.027	0.021313	2.458	0.006989	2.351	0.009354	1.600	0.054779
85	2.042	0.020586	2.318	0.010214	2.223	0.013112	1.378	0.084140

4.3. Methods of third level. Simulation

Monte-Carlo method is described in details in wide scope of literature (for example, [7]). Another method is Latin Hypercube method [6], which is similar to Monte-Carlo, but the sampling is stratified.

Results for Monte-Carlo sampling with consideration that both variables are normally distributed are shown in figure 10.

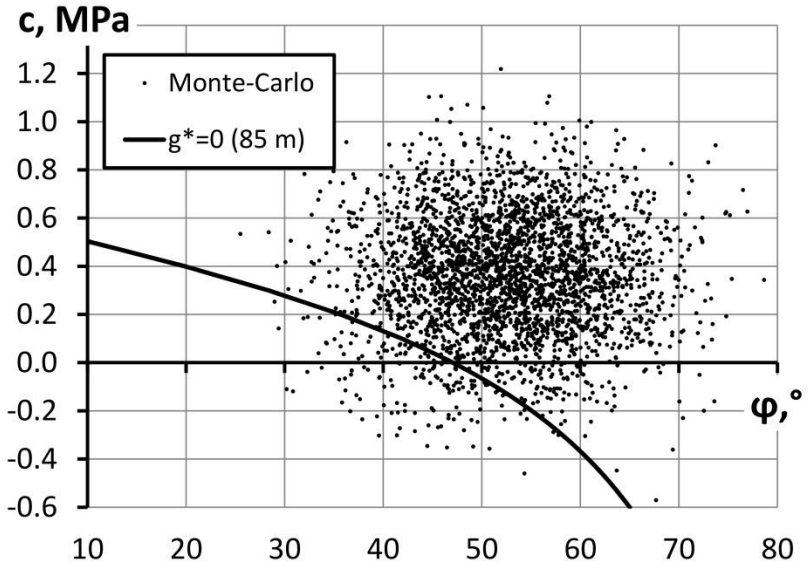

Figure 10: Monte-Carlo sampling. Both variables are normally distributed

One can see that for large number of samples the cohesion value is negative which is physically incorrect. So it is better to consider cohesion to be lognormally distributed.

Figure 11 shows sampling for normally distributed friction angle and lognormally distributed cohesion.

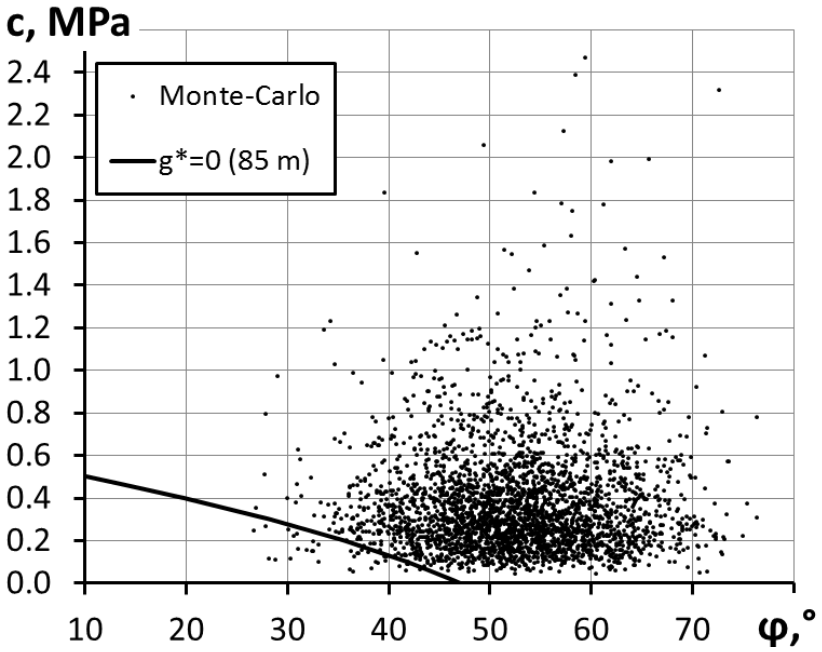

Figure 11: Monte-Carlo sampling. Normally distributed friction angle and lognormally distributed cohesion

Another way is to consider that friction angle is distributed according to beta distribution (figure 12).

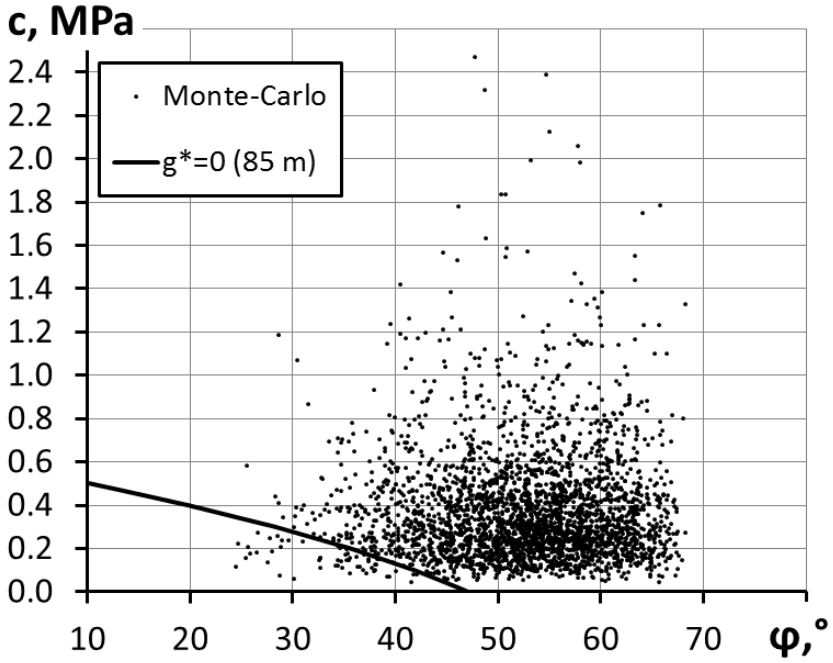

Figure 12: Monte-Carlo sampling. Beta distributed friction angle and lognormally distributed cohesion

Obtained probabilities of failure for all three cases illustrated above are provided in tables 9, 10 and 11, respectively ("WL" in caption means water level, MC-Monte-Carlo, LHS – Latin Hypercube).

Simulation was done for number of samples =1000000.

Table 9: Results of simulation for NORMAL-NORMAL case

WL, m	CASE A		CASE B		CASE C		CASE D	
	MC	LHS	MC	LHS	MC	LHS	MC	LHS
75	0.011798	0.011681	0.001016	0.001005	0.002725	0.002755	0.023271	0.023170
78	0.018289	0.018333	0.001742	0.001745	0.004209	0.004182	0.040213	0.040116
80	0.024435	0.024370	0.002476	0.002483	0.005645	0.005537	0.056895	0.056832
82	0.032467	0.032376	0.003467	0.003486	0.007460	0.007273	0.079062	0.079152
85	0.049093	0.049167	0.005841	0.005714	0.011140	0.011088	0.125456	0.126011

Table 10: Results of simulation for NORMAL-LOGNORMAL case

WL, m	CASE A		CASE B		CASE C		CASE D	
	MC	LHS	MC	LHS	MC	LHS	MC	LHS
75	0.000454	0.000469	0.000046	0.000041	0.000038	0.000038	0.004666	0.004709
78	0.001516	0.001538	0.000132	0.000111	0.000118	0.000103	0.013894	0.013823
80	0.003140	0.003188	0.000238	0.000222	0.000231	0.000227	0.026478	0.026397
82	0.006302	0.006300	0.000444	0.000449	0.000438	0.000455	0.046934	0.047094
85	0.015626	0.015595	0.001095	0.001133	0.001173	0.001196	0.099223	0.099393

Table 10: Results of simulation for BETA-LOGNORMAL case

Water level, m	CASE A		CASE B		CASE C		CASE D	
	MC	LHS	MC	LHS	MC	LHS	MC	LHS
75	0.001019	0.001030	0.000101	0.000110	0.000082	0.000089	0.007723	0.007684
78	0.002879	0.002907	0.000293	0.000285	0.000251	0.000257	0.019243	0.019280
80	0.005444	0.005377	0.000604	0.000535	0.000503	0.000500	0.033174	0.033041
82	0.009698	0.009631	0.001108	0.001041	0.000921	0.001008	0.054138	0.053940
85	0.021000	0.020870	0.002558	0.002447	0.002214	0.002386	0.102778	0.103354

4. Conclusions

The safety assessment of dams is an urgent question to discuss. The modern probability-based approach for this is reliability estimation.

Method of safety factor (level I) is a convenient tool for practical engineers, but it doesn't tell us anything about probability of failure. It should be noted that presence of drain influence the uplift and, then, can highly impact the factor of safety.

Methods of FOSM (level II) are good alternative to estimation of safety factor, because they are not concerned with complex computations and, on the other hand, provide us the probability of failure.

Method of simulation is a powerful tool to obtain the probability of failure with high precision, but large number of samples is needed, which may be concerned with high computational effort if the performance function is complex and there are several variables distributed in accordance with different laws (not only Gaussian). But modern computers (and their power increasing is going on) allow us to solve problems of large dimensionality in reasonable time period.

Here is some points to make more accurate in the future:

- Given sample set is scarce and it is difficult to obtain non-biased statistics for such a little number of samples. It is necessary to do some more tests or to involve some more smart methods then simple statistical tools
- It is necessary to try different distribution laws to find out which one is more suitable for sample set histogram adjusting
- It is necessary to derive performance function distribution to make possible numerical integration for obtaining exact value of probability of failure
- Correlation between random variables should be taken into account

Acknowledgements

I'm indebted to Elena A. Andrianova for her helpful remarks and to Olga I. Belyaeva for her English lessons.

References

[1] Luis Altarejos Garcia (2008). Assessment of the sliding failure probability of a concrete gravity dam.

[2] Alfano, G. and Crisfield, M.A. (2001) Finite Element Interface Models for the Delamination Anaylsis of Laminated Composites: Mechanical and Computational Issues", International Journal for Numerical Methods in Engineering, Vol. 50, pp. 1701-1736

[3] Alfano G., Marfia S., Sacco E. (2004) Influence of water pressure on crack propagation in concrete dams. In: Proceedings of European Congress on Computational Methods in Applied

Sciences and Engineering.
[4] Jimenez-Rodriguez, R., Sitar, N., Chaco´n, J. (2006) System reliability approach to rock slope stability. International Journal of Rock Mechanics & Mining Sciences, vol.43, pp. 847–859
[5] Rosenblueth, E. (1975) Point estimates for probability moments. In: Proceedings of the National Academy of Science, USA, 72 (10)
[6] Iman, R.L.; davenport, J.M.; Zeigler, D.K. (1980) Latin Hypercube Sampling Technical Report SAND79-1473. Sandia Laboratories. Albuquerque
[7] Spaethe, G. (1994) Nadiozhnost' nesushchikh stroitel'nykh konstruktsij (Reliability of load-carrying civil structures), Moscow, Strojizdat (in Russian - translation from german)
[8] Ventsel E. (1999) Theory of probability. Moscow, "Highschool"

XI ICOLD BENCHMARK WORKSHOP ON NUMERICAL ANALYSIS OF DAMS

Valencia, October 20-21, 2011

THEME C

Cabrera Carpio, Miriam Mercedes[1]

Jimenez-Rodriguez, Rafael[1]

CONTACT

Cabrera Carpio Miriam Mercedes, Technical University of Madrid, E.T.S.I. Caminos, Canales y Puertos (Geotecnia), c/Profesor Aranguren s/n (28040, Madrid, Spain), Phone: +(34) 913366772 (ext. 111), mmcc90@gmail.com.

Summary

This article presents the evaluation of different methods of analysis to estimate the conditional probability of sliding failure of a gravity dam, in which we consider the possibility of having the presence of a crack on the dam-foundation contact. The stability of the dam against its sliding failure mode is modeled using limit equilibrium analysis, assuming the dam's behavior as rigid body, and considering the dam-foundation interface as the potential sliding surface. A simple methodology to estimate the characteristic parameters involved in the calculations is presented; and several methods are employed to assess the probability of failure of the dam. Such methods include Level I methods (Estimation of the safety factor); Level II methods (FOSM, Taylor's series); and Level III methods (Simulation, Monte Carlo Method). Results computed with the different methods are compared and briefly discussed.

[1] Technical University of Madrid, E.T.S. Caminos, Canales y Puertos (Geotecnia), Madrid, Spain

1. Introduction

In any risk management strategy, it is necessary to assess and quantify the relevant risks (i.e., probabilities of failure and their consequences) associated to different failure modes so that, based on such analysis, we can decide the actions to implement preventive and protective measures that may decrease their probability of occurrence or their consequences in case of failure.

In the case of dams, each structure has unique conditions and characteristics. Because of such individual character, the task of standardizing risk management practices for dam construction and management has not yet been completely developed. For instance, traditional procedures for quantitative risk analysis in the context of dams have been related to the direct verification of safety factors; more recently, there has been an increasing interest to incorporate risk management techniques from other disciplines, as a way to complement our analytic capabilities, and to help us achieve a better understanding of the behavior of the dam in its environment.

This article aims to compare the results of the analysis of the probability of failure of a specific example dam by some of the more commonly used methods for analysis (level I, II and III). To that end, we study a specific gravity dam, with given loads and boundary conditions, that has been proposed as a benchmark problem.

2. Formulation of the Theme

For the sake of completeness, below we present a brief summary of the main geotechnical characteristics and mechanical properties of the proposed dam and of its foundation.

2.1. Geometry of the dam

The geometry of the dam considered in this Benchmark problem is shown in Figure 1:

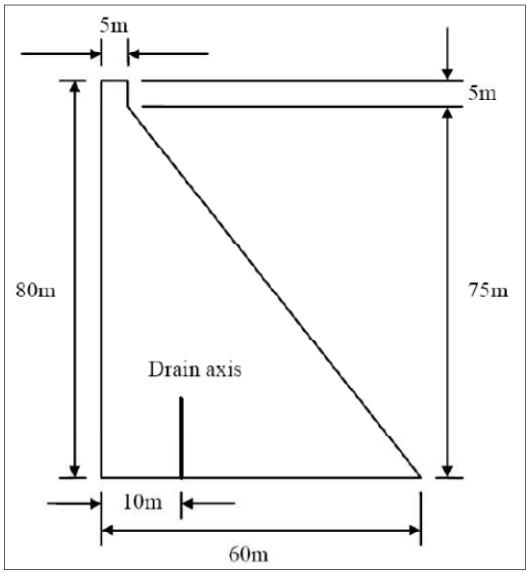

Figure 1. Geometry of the dam

2.2. Materials properties

The material properties of both the dam and its foundation are shown in Tables 1 and 2:

Table 1. Data for dam and foundation materials

Materials Parameters	Dam	Foundation
Mass density (kg/m3)	2400	2700

Friction angle and cohesion at the dam-foundation interface are considered as random variables. Available data in the form of fifteen pairs of values are given in Table 2.

Table 2. Data for friction and cohesion at the interface

Sample	Friction angle (º)	Cohesion (Mpa)	Sample	Friction angle (º)	Cohesion (Mpa)
1	45	0.5	**9**	49	0.1
2	37	0.3	**10**	60	0.2
3	46	0.3	**11**	63	0.2
4	45	0.7	**12**	62	0.4
5	49	0.8	**13**	60	0.7
6	53	0.2	**14**	56	0.1
7	54	0.6	**15**	62	0.4
8	45	0.0			

2.3. Loading

The considered loads are self-weight, hydraulic pressure acting on the upstream face of the dam and uplift acting on the base of the dam. Development of a crack at the interface should be addressed by participants and uplift pressure should be evaluated accordingly.

Two cases of drain effectiveness are considered, with discrete probabilities associated:

- Case A: Drains effective (probability of 0.90)
- Case B: Drains not effective (probability of 0.10)

3. Problem

3.1. Part 1: (Level I)

Participants should generate at least one model of behaviour for the dam and calculate the factor of safety against sliding for the 5 water levels: 75, 78, 80, 82 and 85 meters over dam-foundation contact plane.

3.2. Part 2: (Level II)

Estimate the probability of failure using Level 2 reliability methods for the 5 water levels given above. At least results with the First Order Second Moment (FOSM) Taylor's series approximation should be provided.

3.3. Part 3: (Level III)

Estimate the probability of failure using the Level 3 reliability method Monte Carlo simulation for the 5 water levels given above.

4. Proposed solutions

To solve the Benchmark problem above, we carry out a limit equilibrium analysis of the dam assuming a rigid body behavior and considering the sliding failure through the dam-foundation interface as the only possible failure mode. It is important to emphasize that although plane failure is the only failure mode considered herein, there are other failure modes that could affect a gravity dam there are considered herein.

4.1. Analysis of the random variables involved

We start estimating the statistical distributions to characterize the strength parameters of the foundation rock. To that end, in Figure 2 we plot the values of cohesion (c) and of the tangent of the friction angle (tanϕ), which are derived from laboratory tests (Table 2). Using this graphic representation we can infer if there is some correlation between these variables, and we can also fit the marginal frequency histogram of each variable to a distribution function.

As shown in figure 2, there is not a clear correlation between variables c and tanϕ; therefore they are considered as **independent variables.**

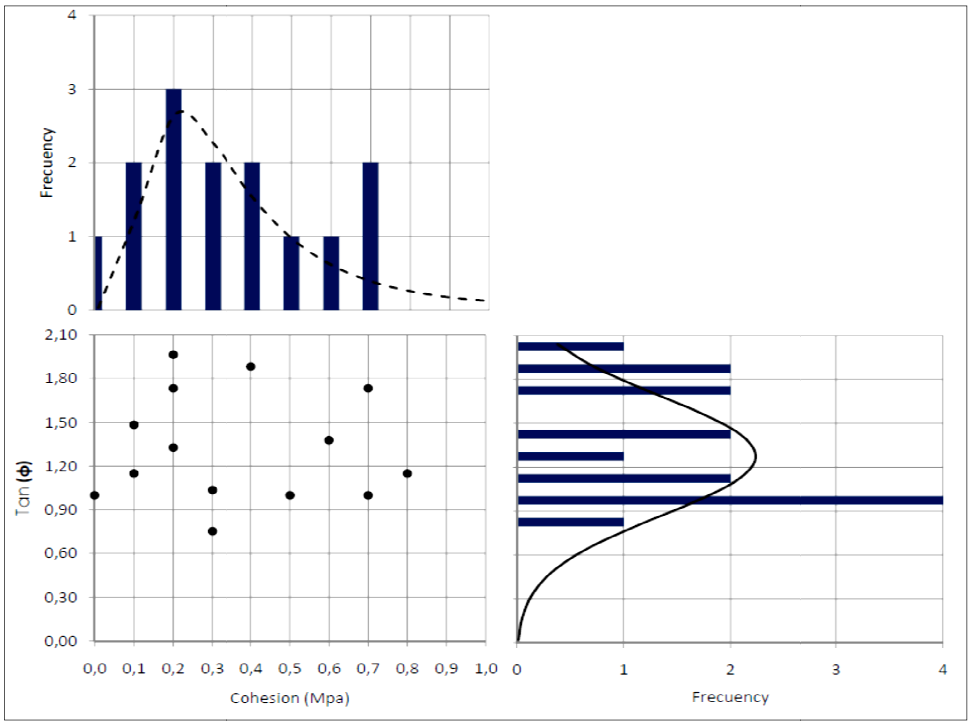

Figure 2. Representation of frequency histogram adjustment to an approximate distribution function. (– – – Lognormal distribution, —— Normal distribution).

Once that the distribution types to be used are defined, we can obtain the probability density functions for each variable (c and tanϕ) which will be subsequently used for the level III analysis. In the case of cohesion, the distribution function used to fit the frequency histogram was a Lognormal, while for tanϕ we used a Normal distribution. The lognormal distribution has

the advantage that it avoids negative values, and for that reason it is commonly employed to model cohesion (see e.g., *Jiménez-Rodríguez et al* [6]); similarly, we model tanϕ (instead of ϕ) as a random variable because it is the value that actually enters into the stability model (see Eq. (17) below). (The beta distribution has been employed in some cases to model friction angle because it is bounded; see *Jiménez-Rodríguez et al* [5, 6] for details. However, for simplicity and to keep our model closer to the assumptions of the FOSM method, we chose to employ the normal distribution for our analysis in this case.)

The lognormal distribution employed to model cohesion is defined by the probability density function given by equation (1). Such probability density function has been plotted in Figure 2 once that the distribution is fitted to the available data. Similarly, the cumulative distribution function of cohesion is presented in Figure 3.

$$f(x;\mu,\sigma) = \frac{1}{x\sigma\sqrt{2\pi}} e^{-\frac{(\ln x-\mu)^2}{2\sigma^2}} \tag{1}$$

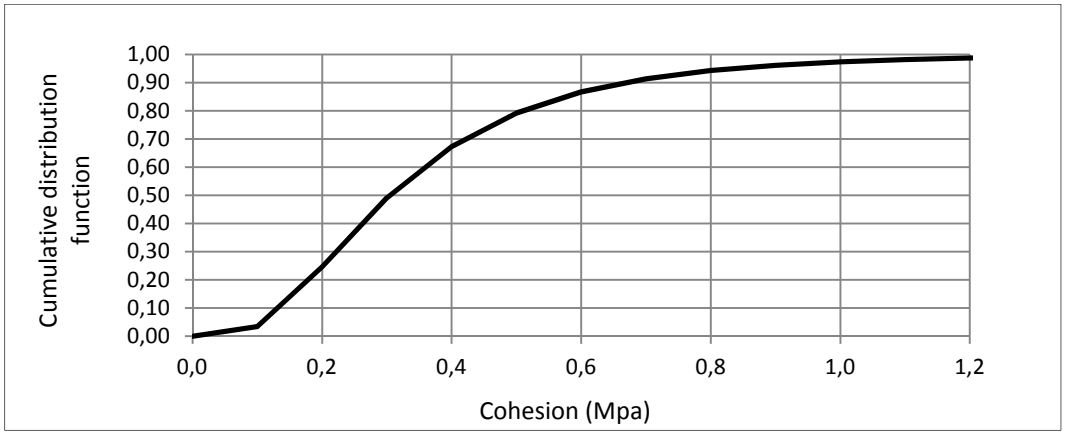

Figure 3. Cumulative distribution function for Cohesion parameter.

The normal distribution used to model the tanϕ parameter has a probability density function given by equation (2). (Once fitted, it has been plotted in Figure 3). The corresponding Cumulative density function of tanϕ values is presented in Figure 4.

$$f(x) = \frac{1}{\sigma\sqrt{2\pi}} e^{-\frac{1}{2}\left(\frac{x-\mu}{\sigma}\right)^2} \tag{2}$$

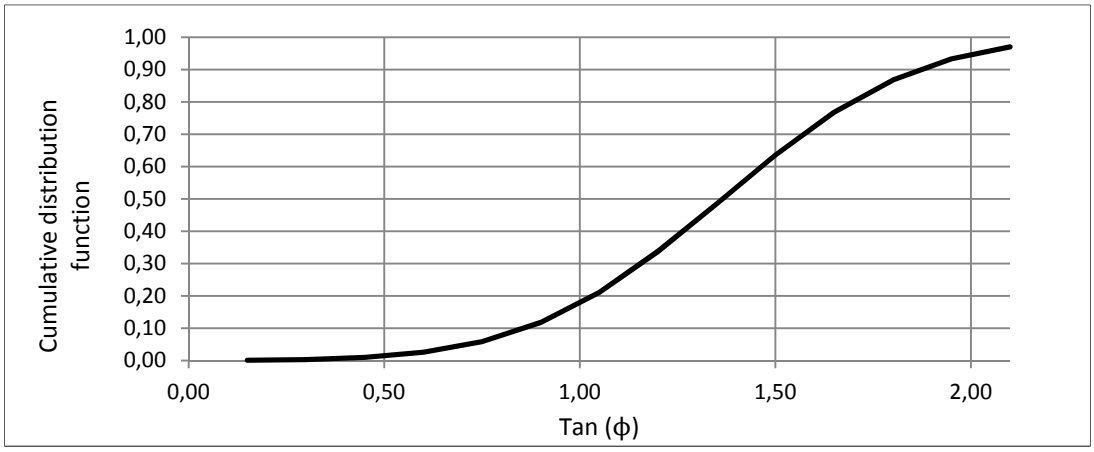

Figure 4. Cumulative distribution function for Tanϕ parameter.

Where:

x, represents the random variable, μ is the statistical mean value, and σ is the standard deviation.

4.2. Estimation of characteristics strength parameters for level II analysis

Based on the available series of fifteen tests which have generated fifteen pairs of values (cohesion and fiction angle), we proceed to estimate the characteristic value for each parameter so that we can late use such values for the analysis required. To do this, three methods have been employed (see below); the final characteristic value will be taken as the average of the three methods employed.

4.2.1. Eurocode Method

The Eurocode 7 defines the characteristic value as "a cautious estimates of the value affecting the occurrence of the limit state". Eurocode 7 also recommends that characteristic values should be selected with 95% confidence, *Eurocode 7* [7].

$$X_{k,sup} = X_m\left(1 + k_n.v_x\right) \tag{3}$$

$$X_{k,inf} = X_m\left(1 - k_n.v_x\right) \tag{4}$$

Where:

X_m: is the parameter's mean value.

K_n: is a statistical coefficient that depends on number of data points available (n) and if the variation coefficient is "known" or "unknown"

Vx: Variation coefficient, obtained by the expression:

$$V_x = \frac{\sigma_x}{X_m} \tag{5}$$

where, σ_x is the standard deviation calculated by the equation:

$$\sigma_x = \sqrt{\frac{\sum_{i=1}^{n}(x_i - x_m)^2}{n-1}} \tag{6}$$

Equations (3) and (4) are employed in cases of using a Normal distribution function. For a Lognormal distribution function the equation becomes, *Eurocode* [8]:

$$X_{k,inf} = e^{(m_y - Kn S_y)} \tag{7}$$

where:

$$m_y = \frac{1}{n}\sum \ln(x_i) \tag{8}$$

$$s_y = \sqrt{\frac{1}{n-1}\sum (\ln x_i - m_y)^2} \tag{9}$$

Figure 5 shows the variation of K_n with the number of samples. Depending on the line selected, the coefficient that can be used to compute characteristic value corresponding to 5% and 50% percentile.

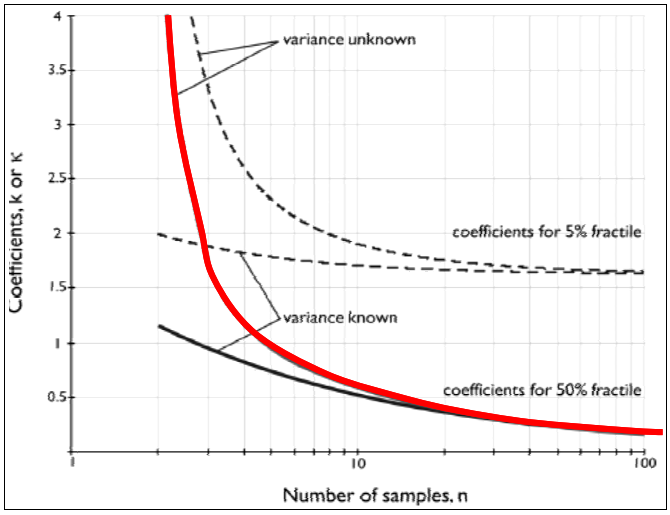

Figure 5. Statistical coefficients for determining the 5 an 50% percentiles with 95% confidence. *Bond* [1].

The expression used to determine the statistical coefficient k_n is given by *Bond* [1]:

$$K_n = t_{n-1}^{95\%}\sqrt{1/n} \tag{10}$$

where $t_{n-1}^{95\%}$ is student's t- value for (n-1) degrees of freedom at a confidence level of 95%.

To estimate the strength along the potential failure surface, we employed the 50% percentile line. This is because for limit states in which the strength of the ground is mobilized over a relatively large scale, the characteristic value can be considered as the mean value of the

strength mobilized along the failure plane. In such cases, it is usual practice to take as characteristics values the average of the parameter, *Bond* [1].

Additionally, the lower limit expression given by Eq. (4) has been used to determine the characteristic strength values to adopt a conservative approach.

4.2.2. Method of "Guía de Cimentaciones de Carreteras":

According to this guide, the characteristic value of a geotechnical parameter is equal to the mean value X_m of all the samples, multiplied or divided by a coefficient ξ, *DGOC* [3]:

$$X_{k,sup} = X_m.\xi \tag{11}$$

$$X_{k,inf} = \frac{X_m}{\xi} \tag{12}$$

The coefficient ξ depends on the type of parameter, on soil heterogeneity and on the number of tests performed to obtain de mean value X_m. Table 3 shows possible values of ξ for some geotechnical parameters in soil with "mean" heterogeneity.

Table 3. Values of coefficient ξ. (*DGOC* [3])

Parameter	**Symbol**	**Number of data used for mean value**			
		n=1	**n=2**	**n=4**	**n=9**
Unit weight	γ	1.05	1.03	1.00	1.00
Tangent of friction angle	Tanϕ'	1.15	1.10	1.05	1.00
Effective Cohesion	c'	1.20	1.15	1.10	1.05
Undrained shear strength	Su	1.25	1.18	1.12	1.07
Unconfined compressive strength, soils	qu	1.30	1.20	1.15	1.10
Unconfined compressive strength, rocks	Rc	1.60	1.40	1.30	1.20

In this case, the equation that generates the lower characteristic value was also used to adopt a conservative approach. Because the values are achieved by fifteen samples of each parameter (c and tan ϕ), the coefficient ξ takes the value 1,05 and 1,00 respectively (see table 3).

4.2.3. Schneider method:

According to Schneider [10], the characteristic value X_k corresponds to the best estimate of the statistical average of the unknown parameter. The simplified expression for estimating the characteristic value is *Schneider* [10]:

$$X_{k,sup} = X_m + K\sigma_x \tag{13}$$

$$X_{k,inf} = X_m - K\sigma_x \tag{14}$$

Where the K coefficient takes the value 0,50. This approximation generates characteristics values with a reasonable precision and is valid for different distributions commonly used in

geotechnical engineering. Table 4 shows the results obtained by the three methods explained above.

Table 4. Results for the estimation of the characteristics values of geotechnical parameters.

Sample	Friction Angle (º)	Cohesion (Mpa)	Tan(ϕ)
1	45	0,5	1,000
2	37	0,3	0,754
3	46	0,3	1,036
4	45	0,7	1,000
5	49	0,8	1,150
6	53	0,2	1,327
7	54	0,6	1,376
8	45	0	1,000
9	49	0,1	1,150
10	60	0,2	1,732
11	63	0,2	1,963
12	62	0,4	1,881
13	60	0,7	1,732
14	56	0,1	1,483
15	62	0,4	1,881
Mean		0,367	1,364
Standard deviation		0,247	0,392
Variation coefficient		0,673	0,287
ξ		1,050	1,000
kn		0,450	0,450
Characteristic Value	**Eurocode M.**	0,231	1,188
	Guía carreteras M.	0,349	1,364
	Shneider M.	0,243	1,168
	Mean Value	**0,274**	**1,240**

4.3. Estimation of crack length: (Cracked base Analysis)

To estimate the length of the crack in the dam interface, we compute the moments about the heel of the dam upstream (point O, see Figure 6).

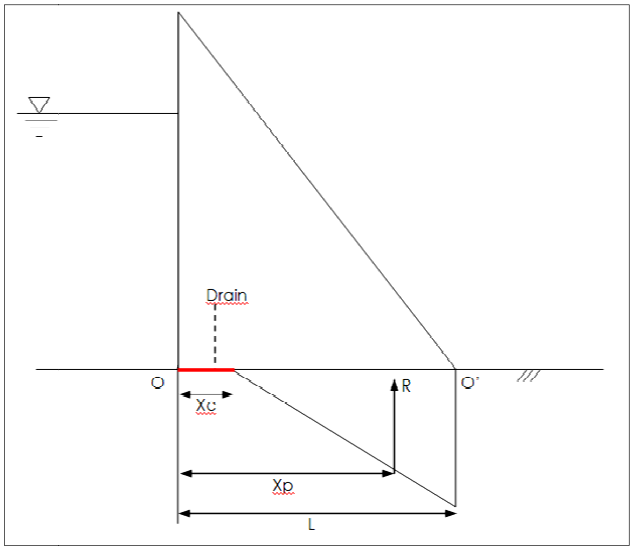

Figure 6. Graphic representation of the general scheme for estimating the length of the crack.

Moments produced by all forces considered are applied to the structure, including weight of the dam, reservoir water level and uplift. The aim of this method is to estimate the location of the line of action of the resultant pressures (R) at the base of the dam. Once this point at the interface is located, and assuming that the variation of effective stress along the base is linear, it can be assumed that the resulting distance from the location of the resultant to the dam foot given by point O', corresponds a third of the total length of contact at the dam-foundation interface (X_p). Therefore the crack length is given by:

$$X_c = L - 3(L - X_p) \tag{15}$$

Where L is the total length of the dam base and Xp is the distance horizontally on the sliding surface, determined by the relation between the resulting from the moments about point O and the sum of vertical forces, as indicated by the expression:

$$X_p = \frac{\sum M_o}{R} \tag{16}$$

The proposed method for estimating the crack length is iterative, assuming for the first calculation the absence of the crack in the base ($X_c = 0$).

Since there are no data on pore pressures in the foundation, or on the failure potential surface, we used certain rules established by the current regulations for estimating uplift. Basically, the uplift depends on the location of the drainage on the vertical with respect to the downstream elevation head, on the efficiency of the drains and on the estimated length of the crack in the concrete-rock interface *FERC* [9].

Figures (7.1) and (7.2) show the uplift diagrams recommended by the Federal Energy Regulatory Commission, applied in estimating the length of the crack to the overall analysis of the stability of the dam:

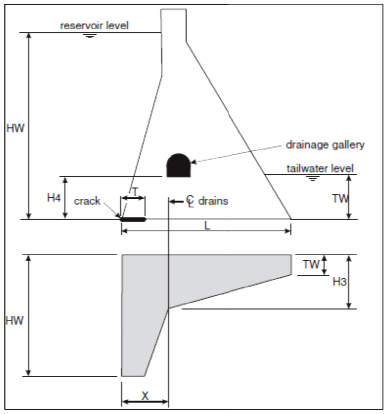

1. For no compression zone not extending to the drain

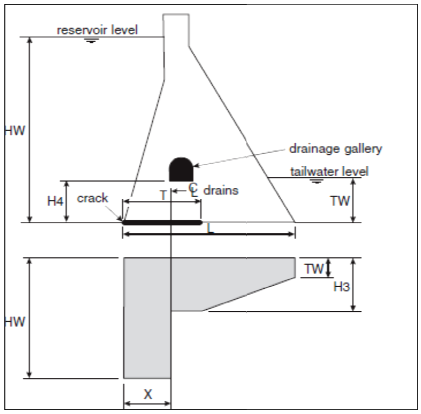

2. No compression zone extending downstream of the drains

Figure 7. Uplift assumptions for concrete gravity dams, *FERC* [9].

Table 5 shows the results of the iteration performed for estimating the length of the crack (Xc) for each level of the reservoir and for the two cases of drainage proposed. In reservoir levels where the length of the crack extends along the entire length of contact, we can infer that failure has occurred, as in fact can be verified by the safety factors that are computed later in section 4.4.

4.4. Part 1 (Level I Analysis): Estimation of safety factor

Once the crack length is obtained for each load case proposed, the safety factor associated to each event, can be obtained by the following equation *DGOC* [3]:

$$Fs = \frac{r}{s} = \frac{N'\left(\tan\varphi\right)_k + B\,c_k}{H_{wi}} \tag{17}$$

Where:

r: is the resistance force, which mainly depends on the conditions and properties of the sliding surface

s: is the de-stabilizing force

N': is the effective force normal to the slip plane, calculated by the difference between the weight of the dam and the estimated uplift;

$$N' = W - U \tag{18}$$

U: is the Uplift pressure under the dam

W: is the dead weight of the dam

B: is the area of application of the cohesive strength on the sliding base, as determined by the area of contact (without crack) given by:

$$B = L - X_c \tag{19}$$

$(\tan\phi)_k$: is the characteristic value of the tangent of the friction angle

c_k: is the characteristic value of the cohesive strength

Hwi: is the upstream water pressure of the reservoir that depends of the water level

Table 5 summarizes the results of Level I analysis for each case-level reservoir and for each drainage condition.

Table 5. Results of the factor of safety estimated.

	Water Level (in m over dam-foundation contact plane)	U (ton/ml)	N' (ton/ml)	Hwi (Ton/ml)	Xc (m)	B (m)	Fs
Efficient Drain	75	825,00	5.085,00	2.812,50	0,00	60,00	**2,83**
	78	858,00	5.052,00	3.042,00	0,00	60,00	**2,60**
	80	880,00	5.030,00	3.200,00	0,00	60,00	**2,46**
	82	902,00	5.008,00	3.360,00	0,00	60,00	**2,34**
	85	1.289,34	4.620,66	3.600,00	11,69	48,31	**1,96**
Inefficient Drain	75	2.250,00	3.660,00	2.812,50	0,00	60,00	**2,20**
	78	3.042,90	2.867,10	3.042,00	18,02	41,98	**1,55**
	80	4.003,59	1.906,41	3.200,00	40,09	19,91	**0,91**
	82	4.920,00	990,00	3.360,00	60,00	0,00	**0,37**
	85	5.100,00	810,00	3.600,00	60,00	0,00	**0,28**

4.5. Part 2 (Level II Analysis): FOSM Taylor's series

Methods for level II reliability analysis employ an approximation, so that instead of considering the complete probability distributions of the variables, we employ only their first two moments.

The result is computed using a Taylor series expansion; where the reliability index (β), is computed as the number of standard deviations that separate the expected value of the function E[g *], from of the limit state surface given by g * (x1, x2, ... xn) = 0. Such β value provides a relative measure of reliability, so that when β value is low, the structure is more insecure (In addition, note that although this method does not provide an exact computation of the probability of failure, such probability of failure can be estimated based on beta using Eq. (25) below.)

From Eq. (17), the limit state function g* is defined in this case as:

$$g^* = FS - 1 = \frac{r}{s} - 1 \tag{20}$$

The expected value of g * is obtained by evaluating the function at a point in n-dimensional space corresponding to the expected values of the random variables:

$$E[g^*] = g^*(E[X_1], E[X_2], E[X_3], \ldots E[X_n]) = \frac{r(E[X_1], E[X_2], E[X_3], \ldots E[X_n])}{s(E[X_1], E[X_2], E[X_3], \ldots E[X_n])} - 1 \quad (21)$$

Considering the independence between random variables involved xi, the variance can be calculated as:

$$Var[g^*] = \sum_i \left(\left(\frac{\partial g^*}{X_i} \right)^2 \sigma_{Xi}{}^2 \right) \quad (22)$$

Where the Taylor series expansion is used to approximate the first order derivatives in cases where the function g * is not linear. To do this, the function g * is evaluated in two points at a distance of one standard deviation from the mean, one on each side, thus:

$$Var[g^*] = \sum_i \left(\left(\frac{g^*(E[X_i + \sigma_{Xi}]) - g^*(E[X_i - \sigma_{Xi}])}{2} \right)^2 \right) \quad (23)$$

Thereby, we can get the reliability index as:

$$\beta = \frac{E[g^*] - (g^*)_{fallo}}{\sigma_{g^*}} = \frac{E[g^*] - 0}{\sigma_{g^*}} = \frac{E[g^*]}{\sigma_{g^*}} \quad (24)$$

Where σ_g^* is the standard deviation of g*, and corresponds to the square root of the variance;

$$Var[g^*] = \sigma_{g^*}{}^2 \quad (25)$$

Table 6 shows the results obtained using this level II analysis approach to the cases proposed in the benchmark problem.

Table 6. Results of reliability analysis, using Level II method.

	Water Level (in m over dam-foundation contact plane)	E [g*]	g* (tanϕ+σ, c)	g* (tanϕ-σ, c)	g* (tanϕ, c+σ)	g* (tanϕ, c-σ)	Var [g*]	β	Φ(-β)
Efficient Drain	75	1,83	2,57	1,08	2,39	1,26	0,8743	1,95	2,530E-02
	78	1,60	2,29	0,92	2,12	1,08	0,7412	1,86	3,147E-02
	80	1,46	2,11	0,82	1,96	0,97	0,6662	1,79	3,642E-02
	82	1,34	1,95	0,72	1,81	0,87	0,6009	1,73	4,209E-02
	85	0,96	1,49	0,43	1,32	0,60	0,4061	1,51	6,594E-02
Inefficient Drain	75	1,20	1,74	0,66	1,76	0,63	0,6066	1,54	6,177E-02
	78	0,55	0,94	0,16	0,91	0,18	0,2843	1,03	1,522E-01
	80	-0,09	0,16	-0,34	0,07	-0,26	0,0874	-0,31	6,200E-01
	82	-0,63	-0,51	-0,76	-0,63	-0,63	0,0148	-5,22	1,000E+00
	85	-0,72	-0,63	-0,81	-0,72	-0,72	0,0086	-7,77	1,000E+00

Table 6 incorporates a column where the probability of failure associated with each event is estimated using the computed reliability indices. To that end we need to assume that:

$$P_{fallo} \equiv P[g^* \leq 0] \approx \Phi(-\beta) \tag{26}$$

Figure 8 shows the variation of the probability of failure associated to each reservoir level and for cases with efficient and inefficient drainage. Predictably, the failure probabilities for case "A" (efficient drainage) are significant lower than for case “B” (inefficient drainage).

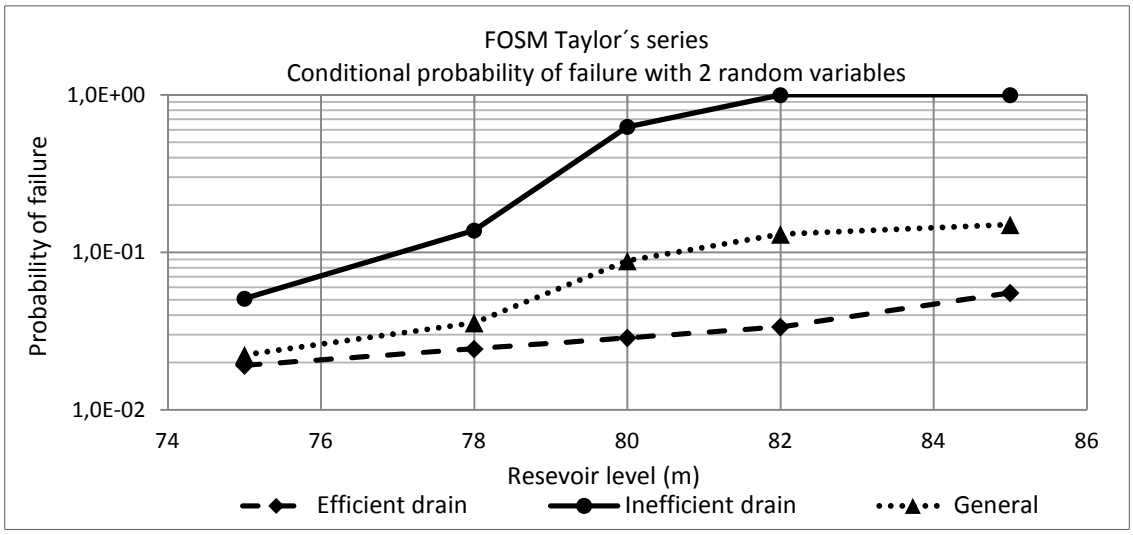

Figure 8. Variation of the probability of failure of the dam, as a function of the reservoir level and drainage condition for application level II, respect to the level of the reservoir. Results computed using Level II analysis.

4.6. Part 3 (Level III Analysis): Monte Carlo simulation method

Monte Carlo simulation is a quantitative technique that uses statistical tools to reproduce, using mathematical models, the random behavior of real systems. The method attempts to assess directly the value of the probability of failure by evaluating the integral.

$$Pf = P[g^*(x_1, x_2, \ldots x_n) \leq 0] = \int_{g^*(x_1, x_2, \ldots x_n) \leq 0} f_{x_1, x_2, \ldots x_n}(x_1, x_2, \ldots x_n)\, dx_1 dx_2 \ldots dx_n \tag{27}$$

where:

$f(x_1, x_2, \ldots X_n)$: is the joint probability density function of the random variables involved (x_1, x_2,.... X_n).

By the Monte Carlo method, we want to obtain the failure probability through the generation of n random variables (or experiments), so that such generated variables follow the (previously known) statistical distribution that characterizes these variables.

The main steps to estimate the probability of failure of the proposed benchmark problem are explained below:

4.6.1. Generation of random variables

After obtaining the statistical distributions for the c and tanϕ random variables, we aim to generate (i.e., to simulate) the values of the n sets of parameters, used to represent the values of the random variables considered.

Such calculations can be easily conducted using common spreadsheet software such as Excel, where the simulation of n "realizations" was performed using the tools for "Random Number Generation" included in this program. With this option, we can easily generate samples from several discrete (Bernoulli, Binomial, Poisson) or continuous distributions variable (Uniform and Normal). We start generating n variables, from as uniform distribution between 0 and 1, (Uc ~ (0.1) and Utanϕ ~ (0 1), see Table 8). The number of experiments for the simulation were n = 100,000.

Following the generation of 100,000 values with uniform distribution between 0 and 1 for each of the random variables considered (c and tanϕ). We used the cumulative distribution function of each parameter to generate the 100,000 final values of (c, tanϕ) pairs required for the simulation (see example in Figure 9).

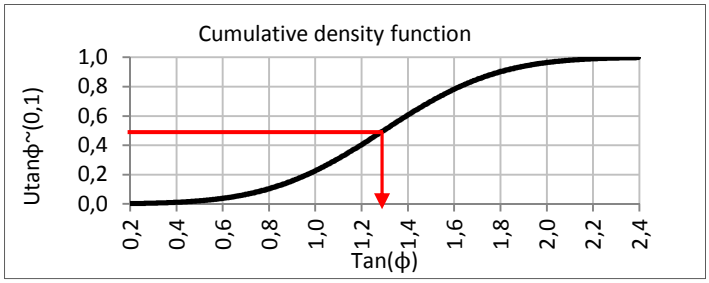

Figure 9. Example of generating of a value tanϕ, based on its cumulative density function.

Once that we have generated the values of c and tanϕ we can use such values for compute the stability conditions for each case, taking into account the different reservoir levels and different drainage conditions. Table 7 shows as example of such computation, note also in Table 7 that if the factor of safety indicates failure (FS<1) then we use an auxiliary variable with value I=1 to indicate it; otherwise, for stable conditions (FS≥1) we use I=0. Such auxiliary "indicator" variables will be late employed for compute the probability of failure.

Table 7. Results of the n experiments for a reservoir level 75 m. Case "B" inefficient drainage.

n	Uc~(0,1)	c (Mpa)	Utanϕ~(0,1)	Tan ϕ	Fs	I
1	0,6854	0,409	0,2152	0,990	2,661	0
2	0,0306	0,097	0,2432	1,026	2,061	0
3	0,8847	0,633	0,4789	1,278	3,661	0
⋮		⋮		⋮		⋮
9.998	0,2948	0,219	0,0049	0,287	0,985	1
99.999	0,4003	0,261	0,5231	1,321	2,945	0
100.000	0,2340	0,195	0,0686	0,716	1,711	0

4.6.2. Estimating of the probability of failure.

A similar table to table 10 can be computed for each reservoir level (Ni) and for each drainage conditions. Then, the conditional probability of failure for a given reservoir level and a specific drainage condition can be computed as:

$$P(F \mid Ni \cap D) = \frac{\sum_{j=1}^{n} I_j}{n} \tag{28}$$

where:

Ni: is the level of the reservoir

D: is the drainage condition (either A or B)

I_j : is the value assigned for each experiment, (0) for FS ≥ 1 and one (1) FS <1

n: is the total number of experiments (n=100.000)

Next, we use the fact that events A and B are mutually exclusive, so that it is possible to obtain the conditional probability of failure of the system for a given reservoir level. Such probability, denoted as P(F|Ni), is given by:

$$P(F \mid Ni) = P(F \mid Ni \cap A)P(A) + P(F \mid Ni \cap B)P(B) \tag{29}$$

Table 8 shows the computed probabilities of failure for the five reservoir levels considered.

Table 8. Results of conditional probabilities of failure (for different reservoir level).

Ni	**Water Level (in m over dam-foundation contact plane)**	**P(F|Ni ∩ A)**	**P(F|Ni ∩ B)**	**P(F|Ni)**
N1	75	2,36E-03	5,66E-03	**2,69E-03**
N2	78	3,25E-03	3,86E-02	**6,78E-03**
N3	80	4,00E-03	4,54E-01	**4,90E-02**
N4	82	5,03E-03	1,00E+00	**1,05E-01**
N5	85	1,32E-02	1,00E+00	**1,12E-01**

Similarly, Figure 10 shows the variation of probability of failure as a function of reservoir level in case of efficient and inefficient drainage. It also shows the conditional probability of failure, for a given reservoir level, computed once that both drainage conditions have been considered over all with their corresponding probability. It can be seen that the curve representing the case with ineffective drains (case B) is more sensitive to the increase of the reservoir level that the curve corresponding to the case with effective drains (case A).

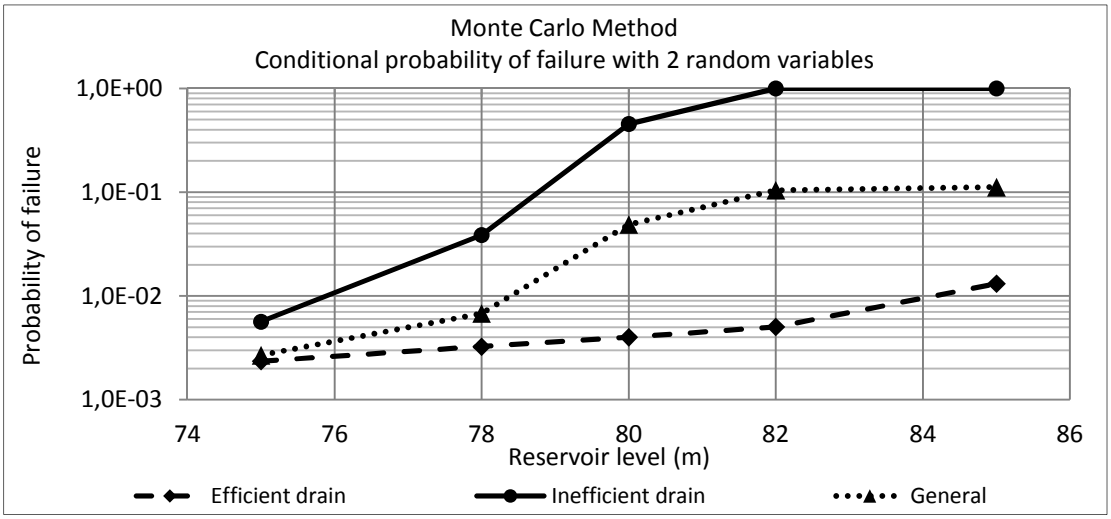

Figure 10. Variation in the probability of failure of the dam, using application-level III, depending on the level of the reservoir, for cases A (efficient drainage) and B (inefficient drainage).

4.7. Discussion of Results

For the deterministic analysis of Level I, we have obtained safety factor values consistent with the estimated crack lengths. For instance for the case "A" (efficient drainage) cracks lengths did not exceed 12 meters and safety factors are always over 1,69. Moreover, in case "B" (inefficient drainage) are obtained for reservoir heights of 80, 82 and 85 meters safety factors of less than 1, so it is clear that the dam is unstable. Note, however, that although the use of characteristic values has allowed as to consider the uncertainty of our strength parameters estimates when we compute safety factors for each drainage condition, it is difficult to incorporate the probabilistic information that performing drains are significantly more likely than non-performing drains.

Previously, we made a comparison of the drainage cases according to the Probability of failure for different reservoir elevations computed with the same level analysis (figures 8 and 10).

To study the influence of the analysis type, next we compare results computed with different methodology of analysis. Figure 11 shows the variation of the probability of failure of the dam, for levels II and III analysis, with respect to reservoir elevation considering efficient drainage (case A). In this figure it is possible compare the accuracy of evaluation methods, where Monte Carlo simulation is expected to be more accurate than FOSM. For this case, it can be observed that there is a large difference (up to one order of magnitude) between the results computed with both methods, and it is also odserved that much difference tend to increase as the probability of failure is lower, (in other words it increases as we enter the “safer” zone where a dam design is expected to be). Note that, studying a similar problem of dam stability against plane failure, *Altarejos et al* [4] also report differences of one order of magnitude – and even larger- between probabilities of failure computed using Level II and Level III method. This emphasizes the importance of using advanced (i.e. Level III) models such as Monte Carlo because, although FOSM is more conservative in this case (it provides higher probabilities of failure) it is not guaranteed that it will be conservative in all cases. In addition, such differences in probabilities of failure computed with different methods can have a significant practical

influence in real projects, as it could affect the acceptability of a dam design. (For recent discussion of design criteria employed by the Us Boureau of Reclamation; see *Scott* [2].

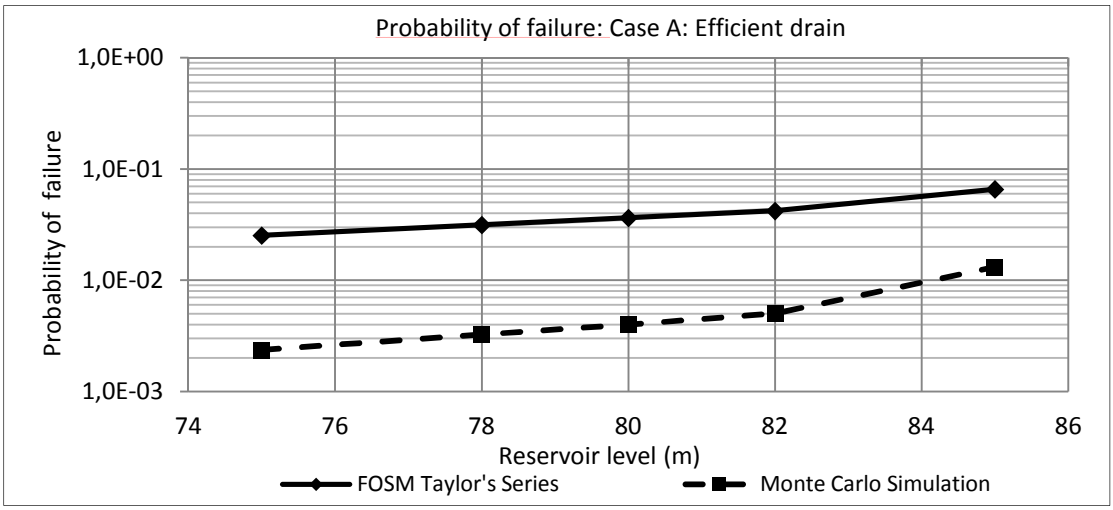

Figure 11. Variation of the probability of failure of the dam with respect to reservoir elevation for case with efficient drainage (case A), using level II and III analysis.

Similarly, Figure 12 shows the variation of the probability of failure of the dam, for levels II and III analysis, with respect to reservoir elevation, but considering inefficient drain this time (case B). We can observe that the probability of failure it is increased dramatically after a reservoir level of 78 meters, indicating very high probability of failure of corresponding to the three last reservoir levels for this case of drainage.

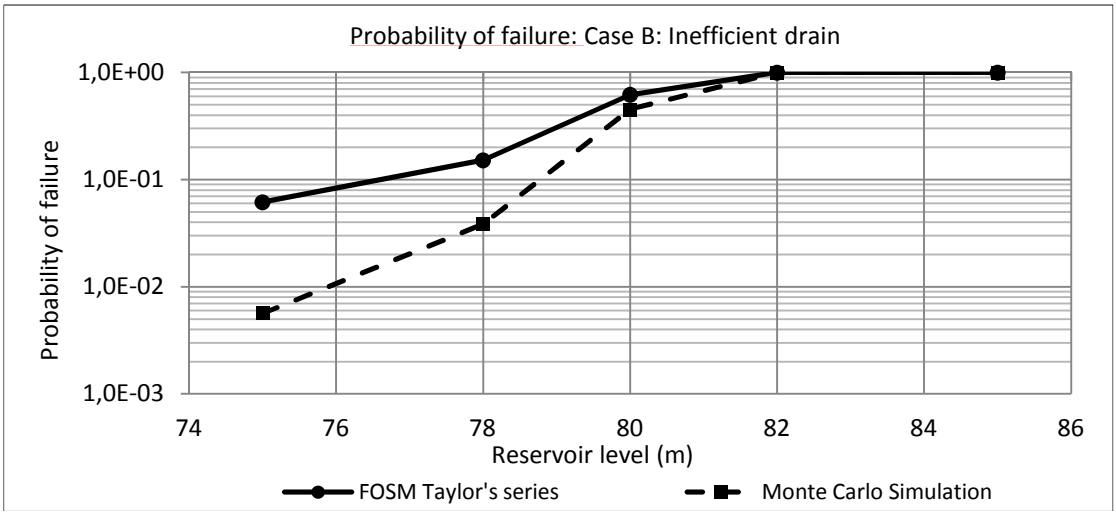

Figure 12. Variation of the probability of failure of the dam with respect to reservoir elevation for case with inefficient drainage (case B), using level II and III analysis.

Additionally, Figure 13 shows the variation of the **general probability** of failure of the dam, for levels II (FOSM) and III analysis (Monte Carlo Simulation), with respect to reservoir elevation. In this case we consider the probability of occurrence in terms of the efficiency of drainage applying Eq. (29), in which is observed the same behavior with respect to the increase of the difference between results when the general probability is lower.

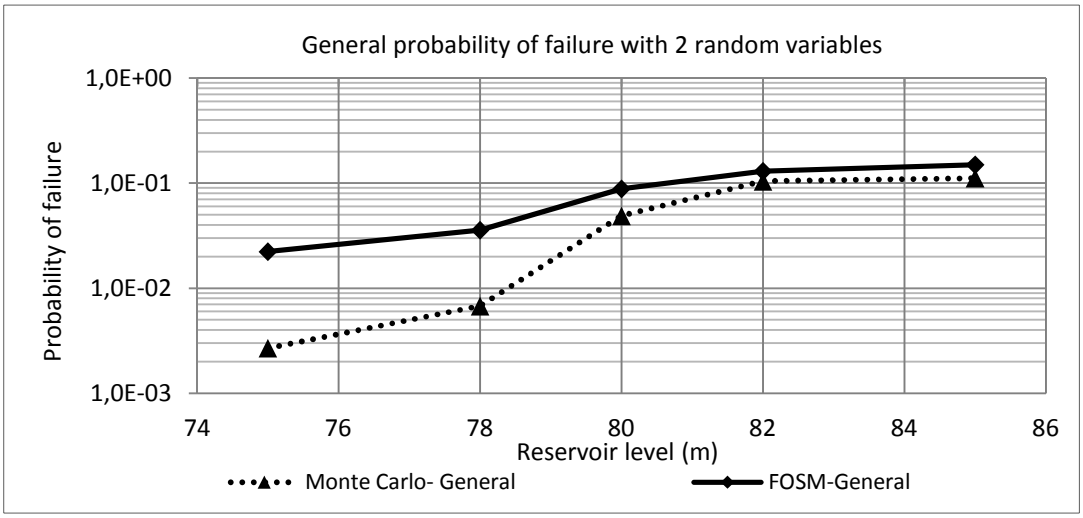

Figure 13. Variation of the general probability of failure of the dam with respect to reservoir elevation, using level II (FOSM) and III analysis (Monte Carlo).

5. Conclusions

This paper presents our computed results of a benchmark problem for analysis of a gravity dam against plane failure due to sliding through the dam-foundation interface. The geometry and material properties of the dam are considered as deterministic, but the strength parameters (cohesion and tangent of friction angle) are considered as random variables to represent the variability reported in a series of shear tests. The possibility of formation of a crack at the base where cohesion is not applied is considered. Several reservoir levels are considered for the analysis, as well as two different drainage conditions (performing and non-performing) with their corresponding probabilities of occurrence.

Three types of analysis are reported: Level I (or deterministic), in which conservative characteristics values of strength parameters are employed to consider parameter variability and to compute the factor of safety of the dam; Level II (FOSM) analysis, in which approximate estimates of the probability of failure are computed employing a first order (linear) approximation of the Limit State Function in conjunction to first and second order statistics (mean and variance only); and Level III (Monte Carlo) analysis, in which "exact" estimates of the probability of failure are computed using simulation methods with full probabilistic information and the real limit state function.

As expected, results indicate that the stability conditions of the dam (as expressed by the safety factor or by the probability of failure) get worse as the reservoir level increases, and they also show that to maintain drains in good conditions is a crucial aspect to increase dam

safety. In addition, they suggest that Level I methods can be employed (with the use of the corresponding characteristic values of the random variables involved) to obtain estimates of dam stability under different combinations of water level and drainage conditions. However, the incorporation of probabilistic information (e.g., the probability of drainage failure) is not natural within this approach, and a full probabilistic approach must be used for such task if we want to use our results into a risk-management framework.

Finally, results show that large differences (of up to one order of magnitude, and probably more in some cases) can be expected between results computed using Level II and Level III methods. Although FOSM results seem to be conservative in this case, this emphasizes the importance of employing "advanced" (i.e., Level III methods) to compute estimates of dam stability under conditions of uncertainty.

References

[1] Bond (2011). A procedure for determining the characteristic value of a geotechnical parameter. 3rd International Symposium on Geotechnical Safety and Risk. Munich, Germany.

[2] Scott G. A. (2011). The practical application of risk assessment to dam safety. Georisk 2011: Risk Assessment and Management (GSP 224) pp. 129-168.

[3] Dirección general de obras de carreteras, DGOC. (2009). Guías de cimentaciones en obras de carreteras. Secretaría de estado de planificación e infraestructuras. Centro de publicaciones del Ministerio de Fomento, Spain.

[4] Altarejos García & Escuder Bueno & Serrano Lombillo & Gómez de Membrillera Ortuño. (2008). Assessment of the conditional probability of failure of concrete gravity dams using probabilistic analysis methods of level II and III (Monte Carlo Simulations). XXXIII Jornadas sudamericanas de ingeniería structural, Santiago, Chile, 2008.

[5] Jiménez-Rodríguez R. & Sitar N. (2007). Rock wedge stability analysis using system reliability methods. Rock Mechanics and Rock Engineering Vol. 40-4, pp. 419-427.

[6] Jiménez-Rodríguez R. & Sitar N. & Chacón J. (2006). System reliability approach to rock slope stability. International Journal of Rock Mechanics and Mining Sciences Vol. 43-6, pp. 847-859.

[7] EN 1997-1 Eurocode 7 : Geotechnical design - Part 1: General rules.

[8] EN 1990 Eurocode: Basis of structural design, Annex D: Design assisted by testing (informative).

[9] Federal Energy Regulatory Commission, FERC. (2000). Engineering guidelines for the evaluation of hydropower projects draft chapter 111, Gravity Dams.

[10] Schneider H.R. (1999). Panel discussion: Definition and determination of characteristic soil properties. Balkema, Vol. 4, pp. 2271-2273.

XI ICOLD BENCHMARK WORKSHOP ON NUMERICAL ANALYSIS OF DAMS

Valencia, October 20-21, 2011

THEME C

ESTIMATION OF THE PROBABILITY OF FAILURE OF A GRAVITY DAM FOR THE SLIDING FAILURE MODE

GASCÓ JIMÉNEZ, MARA

mamgasji@cam.upv.es

Universidad Politécnica de Valencia

Summary

Traditionally, the safety against sliding for gravity dams has been considered by the usage of safety factors. This is always a useful tool for engineering due to its easy calculation and evaluation. Nowadays, the development of dam safety allows calculating the probabilities of failure. This work has been carried out with the aim of establishing relationships between the traditional safety factors and the probabilities of failure. Also, it was studied the most suitable calculation method for this probabilities.

Firstly, the safety factor and the probability of failure for a concrete dam taking into account different water levels in the reservoir are calculated. The mathematical model of analysis used is a two dimensional limit equilibrium.

After that, the results obtained in each case comparing the different methods for establishing the relationships between them and their validity in the safety analysis of a dam are studied. The methods used are the Taylor series, the Point Estimate Method and the Monte Carlo simulation.

Finally, the Monte Carlo method for the calculation of the probability of failure is recommended due to the low failure probability of a dam.

1. Introduction

A gravity dam is analyzed to get relationships between several water levels, factors of safety and probabilities of failure using a limit equilibrium model. The failure mode studied is sliding along the dam-foundation contact.

The traditional way of evaluating dam safety is using safety factors because of its probed good results. Most of the existing dams have been built considering these safety factors. The dam safety approach based on risk analysis has been developed with the aid of the computer's mathematical tools, but its implementation in existing dams is not spread out. For this reason, the results of the different approaches to dam safety are going to be analyzed in this report. These methods are the

safety factor, and the calculation of the probabilities of failure with different methods (Taylor series, Point Estimate Method and the Monte Carlo simulation).

Different water levels and drainage effectiveness situations are considered.

Lastly the different results have been compared in order to obtain conclusions.

2. Case study

The geometry of the dam is shown below:

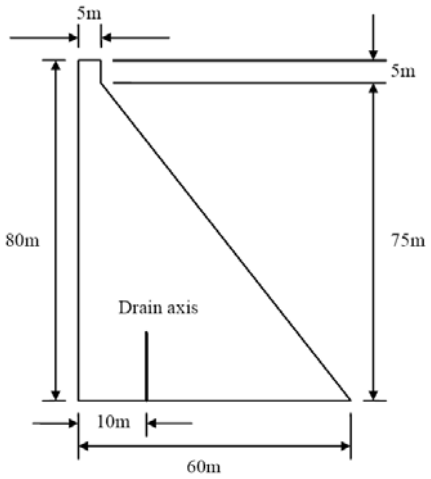

Figure 1: Geometry of the dam

It is necessary to focus on the drain effectiveness because these can be effective and non effective. The probability associated to the first case is 0.9 and 0.1 for the second case. The loading distribution for each case is shown in the following figures:

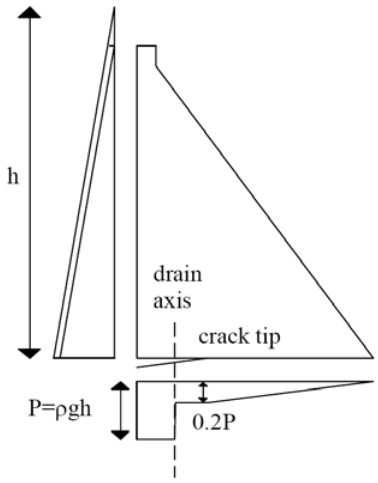

Figure 2: Case drains effective

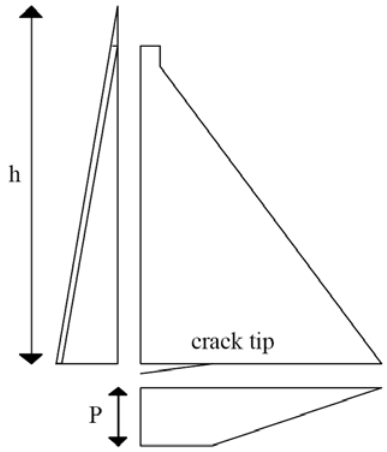

Figure 3: Case drains non effective

It is necessary to focus on the drain effectiveness because these can be effective and non effective. The probability associated to the first case is 0.9 and 0.1 for the second case.

The material properties are given as data. The friction angle and the cohesion are chosen as the mean data taken a normal distribution function.

Table 1: Data for friction angle and cohesion at the interface

Case	Friction angle (˚)	Cohesion (MPa)
1	45	0.5
2	37	0.3
3	46	0.3
4	45	0.7
5	49	0.8
6	53	0.2
7	54	0.6
8	45	0
9	49	0.1
10	60	0.2
11	63	0.4
12	62	0.4
13	60	0.7
14	56	0.1
15	62	0.4
Mean	52.4	0.38
Std. deviation	7.99	0.24

3. Mathematical model of analysis

The mathematical model is a simple two-dimensional limit equilibrium model. The loadings considered have been self-weight, hydraulic pressure acting on the upstream face of the dam and uplift acting on the base of the dam.
Firstly, we have to calculate the forces acting on the dam.
Hydrostatic load, S (N/m), is the driving force and can be evaluated by (Eq.1)

$$S = \frac{1}{2}\rho_w g h^2 \qquad (1)$$

Shear strength, R (N/m), is calculated with (Eq.2)

$$R = (N - U)tg\varphi + B \cdot c \qquad (2)$$

Where,
N (N/m) is the sum of vertical forces acting on the dam-foundation contact surface.
U (N/m) is the uplift.
B (m^2/m) is the area in compression in the dam-foundation contact.
φ (˚) is the friction angle in the contact.
C (Pa) is the cohesion in the contact.

It is assumed that there is not tensile strength in the dam-foundation contact. Therefore, when there are tensile strength in this area a crack is developed.
The model has shown that for several water levels a crack is developed at the interface. This crack produces a variation on uplift pressure that has been considered.
The different crack lengths are shown in the following table:

Table 2: Crack lengths

Water level (m)	Crack length (m)	
	Drain effective	Drain non effective
75	0	0
78	0	18.03
80	0	40.09
82	0	60
85	12.01	60

As we can see in the table above the behavior of the dam is better when drains work correctly. When drains are non effective a crack line is formed even for low water levels and the dam is not stabilized for water level higher than 82m. Therefore drainage system impact on the behavior of the dam is extremely high.

4. Theoretical basis

If our project variables (X_1,X_2,...,X_n) are considered as random variables, it is possible to define the strength function r(x_1,x_2,...,x_n) and the load function s(x_1, x_2,...,x_n) and write the limit state equation as follows:

$$g^*(x_1, x_2, ..., x_n) = g(x_1, x_2, ..., x_n) - 1 = \frac{r(x_1, x_2, ..., x_n)}{s(x_1, x_2, ..., x_n)} - 1 = 0 \quad (3)$$

According to this, the failure domain in the n-dimensional space is defined as all the possible values (x_1,x_2,...,x_n) that verify the condition:

$$g^*(x_1, x_2, ..., x_n) \leq 0 \quad (4)$$

and the safety domain is defined as all possible values (x_1,x_2,...,x_n) that verify the condition:

$$g^*(x_1, x_2, ..., x_n) > 0 \quad (5)$$

Different methods of analysis to estimate the conditional probability of failure on a concrete gravity dam are shown. The failure mode studied is sliding along the dam-foundation contact. These methods can be classified as Level 1, Level 2 and Level 3 methods.

4. 1. Level I: Factor of safety

Consist in the evaluation of the limit state equation for a certain constant value of the variables (X_1,X_2,...,X_n). If the evaluation of the function g* is in the safety domain (according to equation (5)) for these so-called representative values, then the system can be considered safe if is away from the limit n-dimensional hyper surface g*(x_1,x_2,...,x_n)=0 by a safety margin expressed with this factor of safety.

Considering the expression (3) we can obtain:

$$g(x_1, x_2, ..., x_n) = \frac{r(x_1, x_2, ..., x_n)}{s(x_1, x_2, ..., x_n)} \quad (6)$$

We can define the safety factor (GSF) as the one which accomplish the condition:

$$g(x_1, x_2, ..., x_n) - GFS > 0 \quad (7)$$

For the dam considered in the case study:

$$GFS = \frac{R}{S} = \frac{(N - U)tg\varphi + B \cdot c}{1/2\, \rho_w g h^2} \quad (8)$$

This a common tool in civil engineering to check the safety of a dam. Different countries have their own regulatory rules and guidelines for these safety factors in concrete dams.

4.2. Level II

The Level II methods are a first order approximation (linear) of the g* function considering also only the 2 first moments of the joint probability density function. The typical output for these methods is the reliability index β, defined as follows:

$$\beta = \frac{E[g^*] - (g^*)_{fallo}}{\sigma_{g^*}} = \frac{E[g^*] - 0}{\sigma_{g^*}} = \frac{E[g^*]}{\sigma_{g^*}} \quad (9)$$

For obtain the probability of failure there is need to make the assumption of the shape of the g* distribution. One possibility is the assumption of a normal distribution, so the probability of failure ($P_f[g^* \leq 0]$)can be calculated as:

$$P_f[g^* \leq 0] = \Phi(-\beta) \quad (10)$$

The probability of failure has been estimated with two different Level 2 methods. Firstly, the Taylor's series approximation has been applied and later the Rosenblueth's Point Estimate Method (PEM).

Taylor series

The function $g^*(x_1,x_2,...,x_n)$ must be linear to obtain the first two moments of the probability distribution of $g^*(x_1,x_2,...,x_n)$ from the first two moments of the probability distributions of the random variables $X_1,X_2,...,X_n$:

$$g^*(x_1, x_2, ..., x_n) = a_0 + a_1 x_1 + a_2 x_2 + ... a_n x_n \quad (11)$$

The first moment of the probability distribution of g*, assuming that the random variables are correlated and that is a first order approximation, can be calculated as:

$$E[g^*] = g^*(E[X_1], E[X_2], ..., E[X_n]) \quad (12)$$

The variance of the function g*can be calculated assuming independent random variables and approaching the non-linearities by numerical calculation of the partial derivatives by using a very small increment (positive and negative) centered on the expected value, but not so small in order to capture some of these non-linearities. The expression obtained is:

$$Var[g^*] = \sum_i \left(\left(\frac{g^*(E[X_i] + \sigma_{Xi}) - g^*(E[X_i] - \sigma_{Xi})}{2} \right)^2 \right) \quad (13)$$

PEM

The point estimated method determine the first two moments of the performance function g* by the discretization of the probability distributions of the random variables $X_1, X_2, ..., X_n$. This discretization is made in a few points for each random variable (two points in Rosenblueth method), where mass probability is concentrated in such a fashion that the sum of the probabilities assigned to each point is 1 for each random variable.

The method concentrates the mass probability of the random variable X_i in two points, x_{i+} and x_{i-}, each of them with a mass probability of P_{i+} and P_{i-}. Points are centred about the mean value, μ_{Xi}, at a distance of d_{i+} and d_{i-} times the standard deviation σ_{Xi}, respectively.

$$E[g^*] = \sum P_{(\delta 1, \delta 2, ..., \delta n)} g^*_{(\delta 1, \delta 2, ..., \delta n)} \quad (14)$$

And the second moment is:

$$E[g^{*2}] = \sum P_{(\delta 1, \delta 2, ..., \delta n)} g^{*2}{}_{(\delta 1, \delta 2, ..., \delta n)} \quad (15)$$

The variance is calculated with the following expression:

$$Var[g^*] = E[(g^* - \mu_{g^*})^2] = E[g^{*2}] - \mu^2{}_{g^*} \quad (16)$$

4.3. Level III: Monte Carlo Simulation

The level III methods provide a more accurate evaluation of the probability of failure because all the information of the probability density function is considered. Monte Carlo method generates N sets of values for the random variables according to their probability distributions and possible correlations:

$$\hat{x}(i) = \left(x_1, \hat{x}_2, ..., \hat{x}_n \right)_{(i)} ; i = 1, ..., N \quad (17)$$

Generation of these values is accomplished by statistical techniques. The performance function is evaluated for each one of these sets of values, and the number of failures, m, (when $g^* \leq 0$) is calculated. The probability of failure can be then estimated by:

$$P_{failure} \approx \frac{m\left(g^{*}\left(\hat{x}_1, \hat{x}_2, \ldots, \hat{x}_n \right) \leq 0 \right)}{N} = \hat{P}_f \qquad (18)$$

4. Results

4. 1. Factor of safety against sliding

The safety factors obtained are:

Table 3: Factors of safety against sliding

Water level	Level I: Factor of Safety	
	Drains effective	Drains non effective
75	3.16	2.50
78	2.91	1.75
80	2.75	1.01
82	2.61	0.38
85	2.17	0.29

The results are shown in the following figure where it can be observed that the factor value is lower when the water level upstream is rising. Also, it can be seen how the drains effectiveness is very important because when the drains are working, we get a better safety factor. However, the dam is safe in all the studied cases.

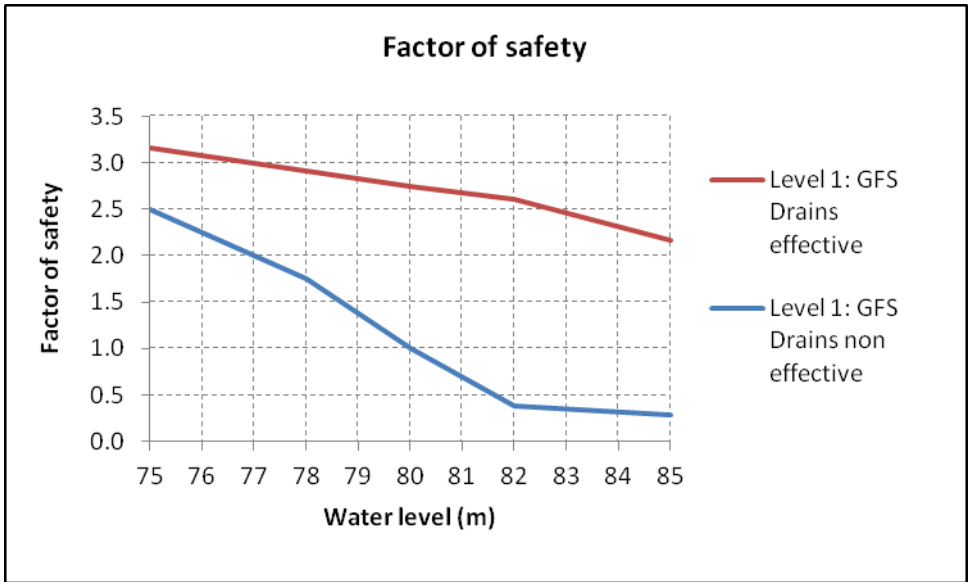

Figure 4: Factor of safety against sliding

4.2. Level 2 reliability model

The next tables show the results obtained for each study case:

Table 4: Level II reliability model: Taylor

Water level (m)	FOSM - Taylor		
	Drains effective	Drains non effective	Total
75	6.80E-03	6.07E-03	6.72E-03
78	8.96E-03	3.04E-02	1.11E-02
80	1.08E-02	4.80E-01	5.77E-02
82	1.30E-02	1.00E+00	1.12E-01
85	2.45E-02	1.00E+00	1.22E-01

Table 5: Level II reliability model: P.E.M.

Water level (m)	P.E.M.		
	Drains effective	Drains non effective	Total
75	4.46E-03	1.40E-02	5.42E-03
78	5.97E-03	5.40E-02	1.08E-02
80	7.27E-03	4.25E-01	4.90E-02
82	8.83E-03	1.00E+00	1.08E-01
85	1.70E-02	1.00E+00	1.15E-01

We can observe that the probability of failure is higher with Taylor's series than with PEM.

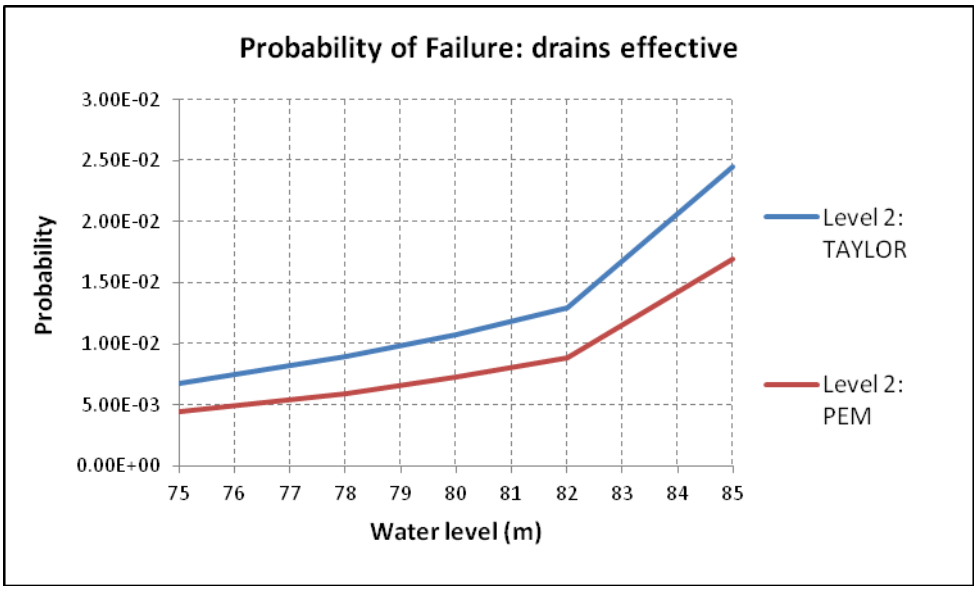

Figure 5: Probability of failure. Level II: drains effective

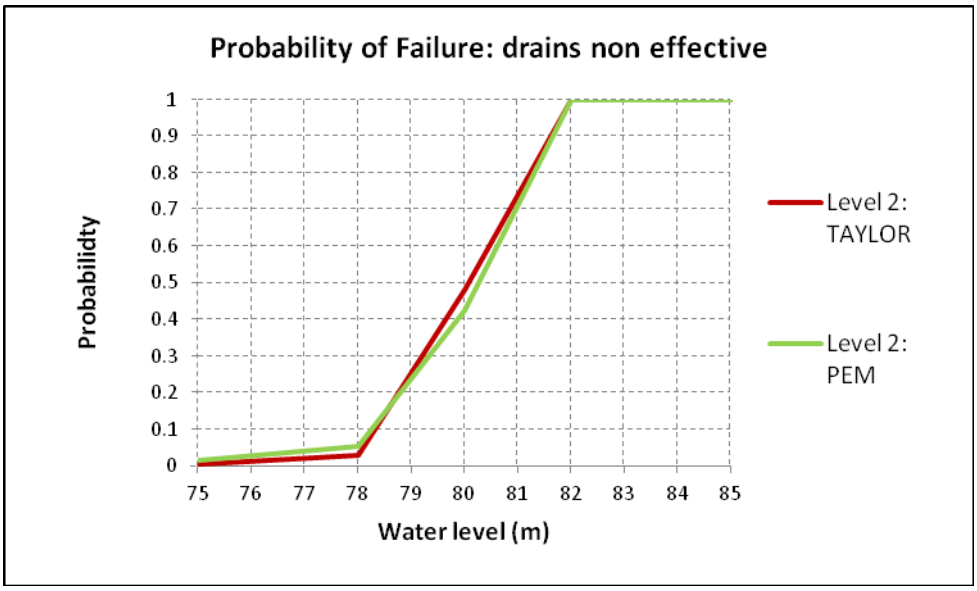

Figure 6: Probability of failure. Level II: drains non effective

As can be appreciated in the above figures, the probability of failure calculated for the lower water levels is higher using the Taylor method in the case of drains effective. In the case of drains non effective, this tendency is the opposite being higher the probability of failure for the PEM method. This behavior can be explained considering that the Point Estimate Method losses precision with the increasing nonlinearity of g*, where g* = (R/S) - 1, that is the problem in the non effective case
Following the g* function is presented for the different combinations considered in the P.E.M. where the lose of linearity in the case of drains effective is more clear.

Table 6: Different combinations to obtain function g* in P.E.M.

Combination in PEM	
1	(- ; -)
2	(- ; +)
3	(+ ; -)
4	(+ ; -)

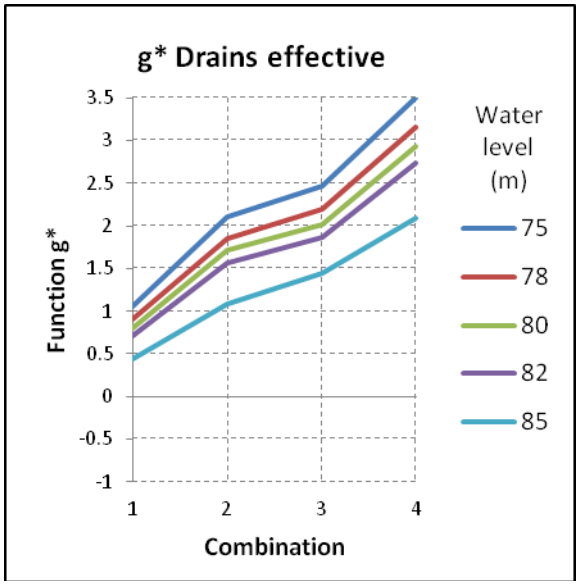

Figure 7: Function g* in P.E.M.: drains effective

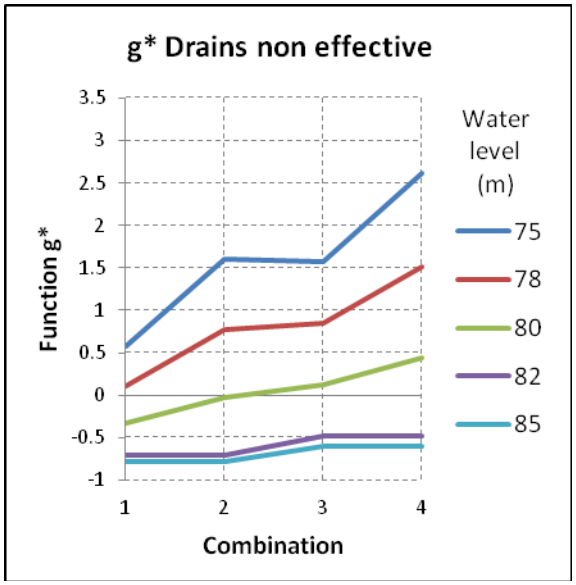

Figure 8: Function g* in P.E.M.: drains non effective

4.3. Level 3 reliability method Monte Carlo simulation

Lastly, it has been calculated the Level 3 method. The sets of values for the random variables have been generated according to the following function distributions:

$$\varphi \sim N(52.4°,8°) \quad [28.4°,76.4°]MPa \tag{19}$$

$$c \sim LN(0.375,0.237) \quad [0,1.5]MPa \tag{20}$$

The probabilities of failure are the followings:

Table 7: Level III: Monte Carlo

Water level (m)	Monte Carlo		
	Drains effective	Drains non effective	Total
75	1.00E-06	1.11E-03	1.12E-04
78	1.10E-04	1.82E-02	1.92E-03
80	1.90E-04	4.88E-01	4.89E-02
82	3.60E-04	1.00E+00	1.00E-01
85	1.24E-03	1.00E+00	1.01E-01

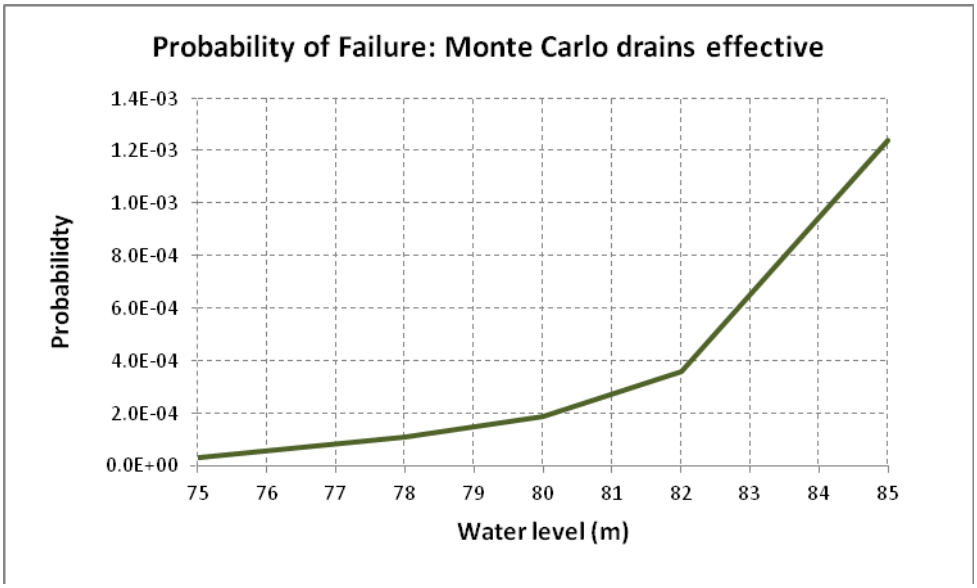

Figure 9: Probability of failure. Level III: drains effective

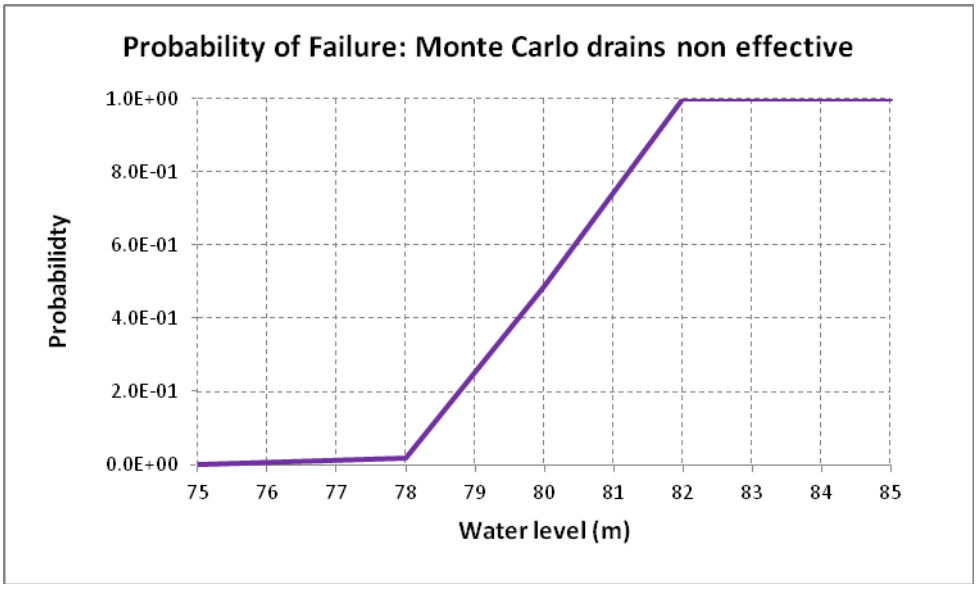

Figure 10: Probability of failure. Level III: drains non effective

4.4. Comparative analyses of probabilities of failure for the different methods

In the next figure are shown the probabilities of failure obtained with the three methods:

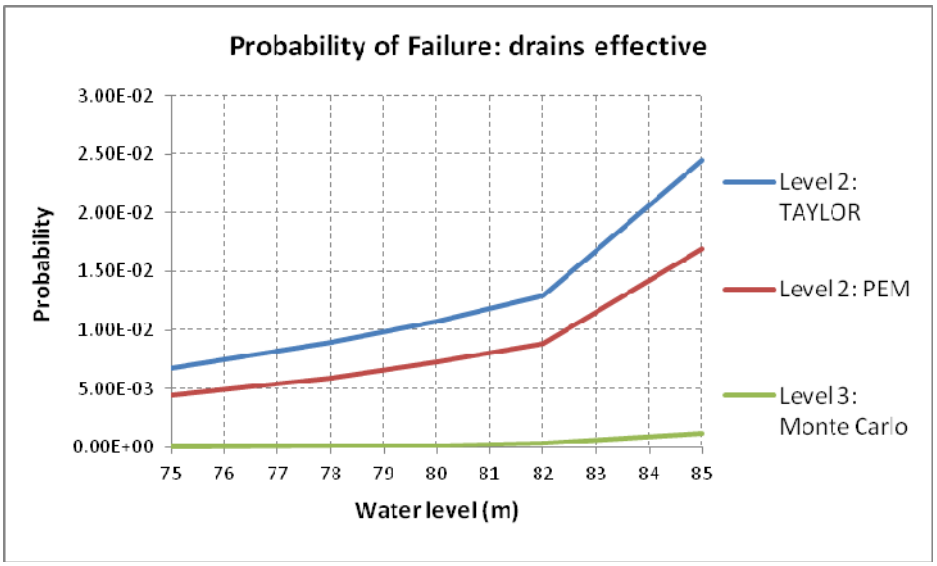

Figure 11: Probability of failure: case drains effective

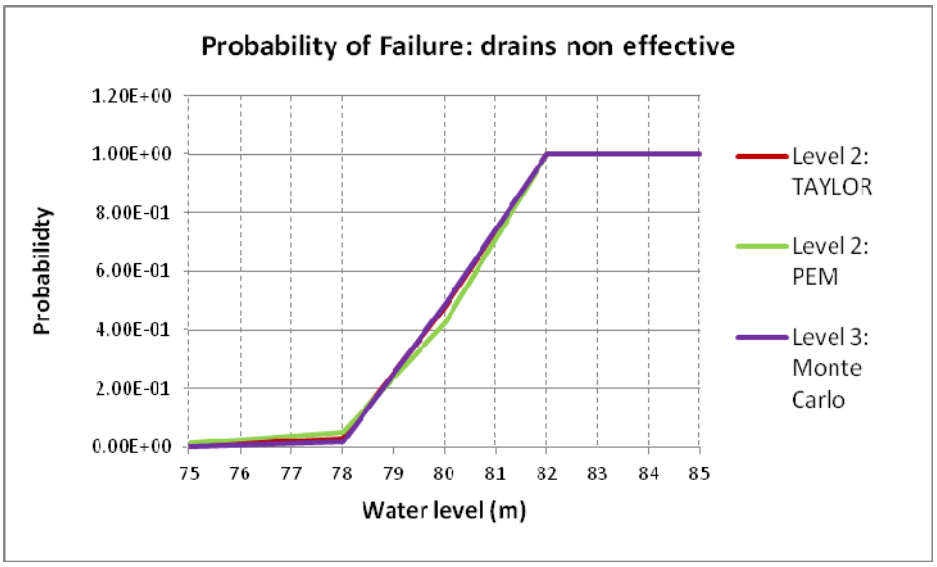

Figure 12: Probability of failure: case drains non effective

It can be observed how the probabilities for levels below the crest seem quite high in level II methods, considering the consequences that the breakage of the dam would have. That is explained because these methods do not calculate properly the lower probabilities. Considering that the most common situation in dams is having very low failure probabilities due to the magnitude of the infrastructure, it is possible to conclude that these methods are not suitable for calculating these probabilities.

Also, it can be seen that the probabilities of failure are closely related to the drains operation, which reveals the importance of a good drain design and its afterwards maintenance in the dam.

4.5. Probability of failure vs factor of safety

In this section is presented the relationship between the safety factor and the probabilities of failure obtained with the different methods studied. The results are shown in next figure:

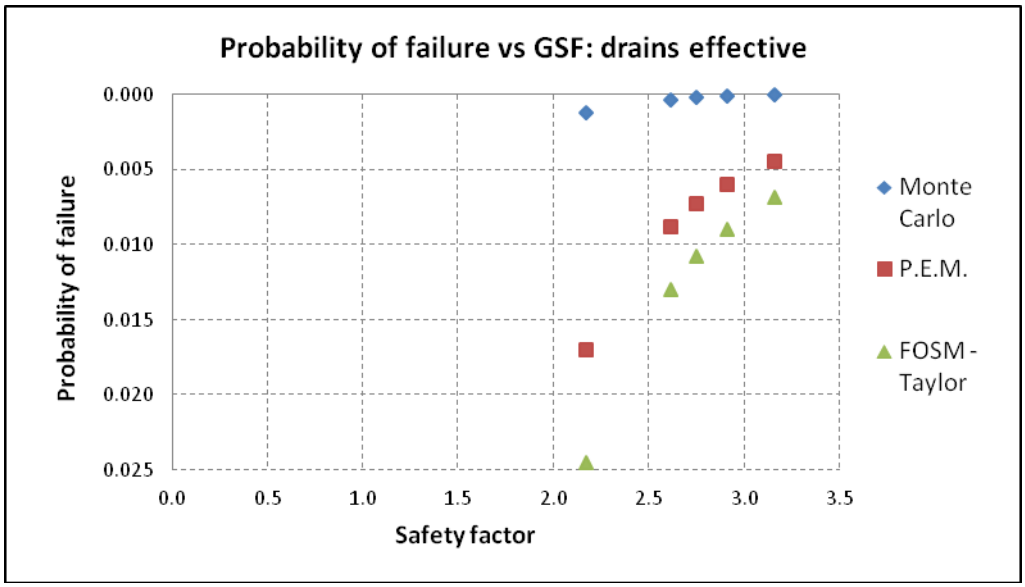

Figure 13: Probability of failure vs Safety Factor: drains effective

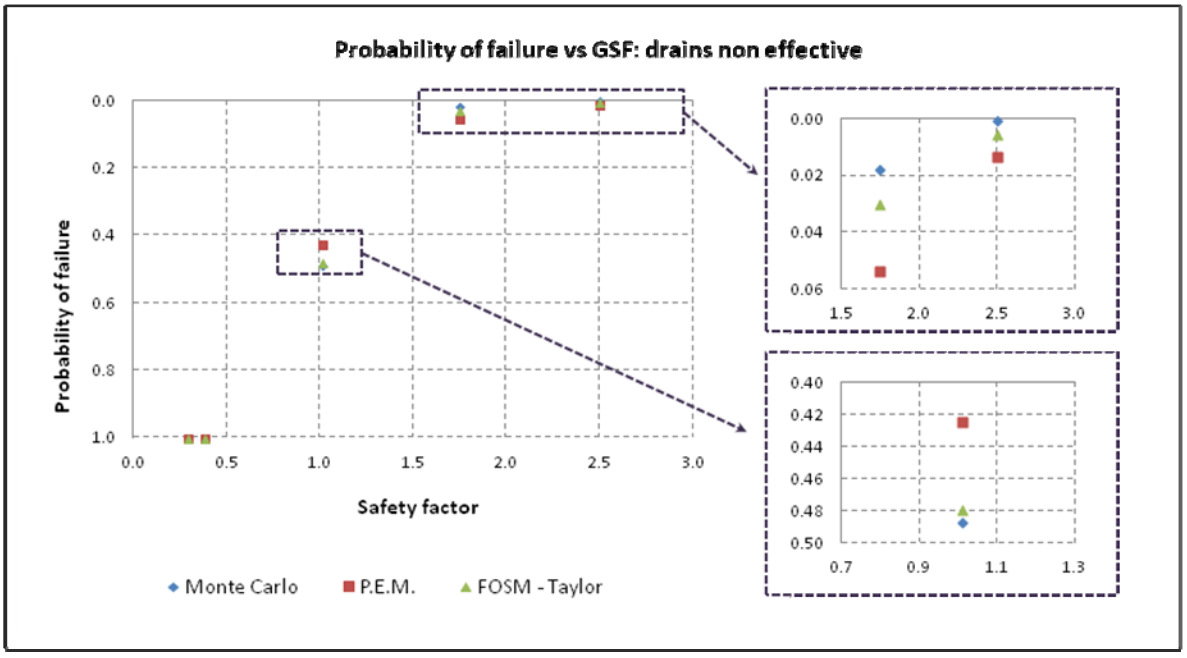

Figure 14: Probability of failure vs Safety Factor: drains effective

It can be observed how a certain value of the safety factor has obtained different probabilities of failure depending on the method selected. The results of probability of failure for the different methods obtained for each safety factor reveal that the Monte Carlo provides suitable probability of failure according the meaning of the safety factor.

5. CONCLUSIONS

Method of safety factors does not provide probability of failure. It is a traditional method which minimum required values are different depending on the guideline considered.

Considering the results obtained in the different methods, it can be observed how the probabilities obtained are in general too high, considering the consequences that the breakage of the dam would

have. Mainly, it can be observed that in the case of level 2 methods, the probabilities obtained are too high because these methods do not calculate properly the lower probabilities. Considering that the most common situation in dams is having very low failure probabilities due to the magnitude of the infrastructure, it is possible to conclude that these methods are not suitable for calculating these probabilities.

In conclusion, the most accurate model to estimate the probability of failure in this case is the Monte Carlo one due to the low failure probability of a dam.

Lastly, it is important to remark that the probabilities of failure are closely related to the drains operation, which reveals the importance of a good drainage design and its later maintenance in the dam.

6. REFERENCES

[1] Altarejos García, L. & Escuder Bueno, I. (2011). Slides in the subject "Evaluation of security in dams". Master "Hydraulic engineering and the environment" UPV.

[2] Altarejos García, L. (2008). Assessment of the sliding failure probability of a concrete gravity dam. 2nd International Week on Risk Analysis as applied to Dam Safety and Dam Security.

[3] Altarejos-García, L.; Escuder-Bueno, I.; Serrano-Lombillo, A. & Morales-Torres, A. (2011). Factor of safety and probability of failure in concrete dams. 3rd International Week on Risk Analysis as applied to Dam Safety and Dam Security.

XI ICOLD BENCHMARK WORKSHOP ON NUMERICAL ANALYSIS OF DAMS

Valencia, October 20-21, 2011

THEME C: ESTIMATION OF THE PROBABILITY OF FAILURE OF A GRAVITY DAM FOR THE SLIDING FAILURE MODE

Altarejos-Garcia, Luis[1]

Escuder-Bueno, Ignacio[2]

Serrano-Lombillo, Armando[3]

CONTACT

Luis Altarejos-Garcia, Polytechnic University of Valencia, Environment and Hydraulic Engineering Department. Building 4E - Camino de Vera s/n, 46022 Valencia, Spain. +34963877007 (ext 76142); luis.ag@hma.upv.es.

Summary

The objective of Theme C is to obtain relationships between water levels, factors of safety and probabilities of failure for a gravity dam considering the failure mode of sliding along the dam-foundation contact. The dam proposed is taken from the Theme 2 of the 1999 ICOLD Benchmark. This is done using two models of analysis for the dam-foundation system together with reliability techniques. The models that have been tested are a limit equilibrium model and an elastic deformable body model. The factor of safety against sliding is then calculated for several water levels.

Following this step, the probability of failure for the sliding failure mode is estimated using two different Level 2 reliability methods: FOSM Taylor Method and Point Estimate Method. Also a Level 3 Monte Carlo simulation method is used.

The results show that factors influencing the probability of failure rely not only on parameter uncertainty, as uncertainties of several sources are present throughout the process. The main sources of uncertainty identified are the type of model of analysis for stability, the crack opening and propagation criteria, the factor of safety definition (it is not unique), the statistical fitting of probability distributions to sample data, the selection of characteristic values of parameters to evaluate the factor of safety, and the type of reliability analysis model chosen to estimate the probabilities of failure.

Despite this overall picture, some useful information can be gained regarding the safety of the dam if a probability approach is carried out together with the classical factor of safety evaluation.

[1] Associate Professor, Polytechnic University of Valencia & CTO Projects, iPresas. Valencia, Spain
[2] Professor, Polytechnic University of Valencia, Spain.
[3] CTO Research & Development, iPresas. Valencia, Spain.

1. Formulation of the problem

In this section the problem to be solved is summarized.

1.1. Geometry of the dam

The geometry of the dam is depicted in Fig. 1. The full geometry including the foundation is shown in Fig. 2. The foundation has a rectangular shape with height of 80 m and a total length of 300 m (120 m upstream, 60 m under de dam, 120 m downstream).

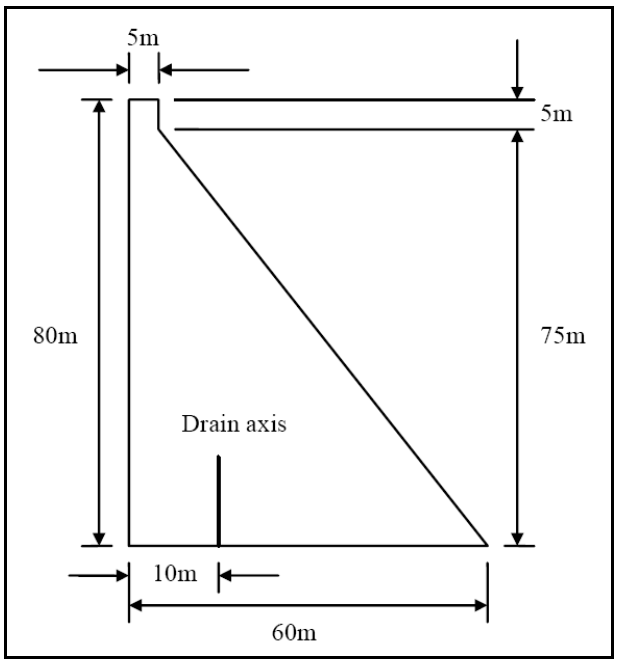

Figure 1: Dam geometry

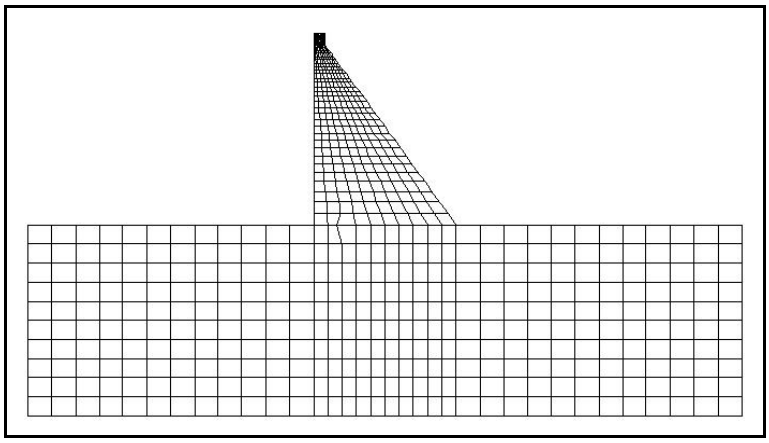

Figure 2: Dam and foundation geometry

1.2. Material properties

Data on material properties for dam and foundation are given in Table 1. Data for material properties for dam-foundation interface are given in Table 2. Friction angle and cohesion at the dam-foundation interface are considered as random variables. Available data in the form of fifteen pairs of values are given in Table 3.

Table 1: Data for dam and foundation materials

MATERIAL PARAMETERS	DAM	FOUNDATION
Young's modulus (MPa)	24000	41000
Poisson's ratio	0,15	0,10
Mass density (kg/m3)	2400	2700
Compressive strength (MPa)	24	40
Tensile strength (MPa)	1,5	2,6
Strain at peak compressive strength	0,0022	0,0025
Strain at end of compressive softening curve	0,10	0,15
Fracture energy (N/m)	150	200

Table 2: Data for dam-foundation interface

MATERIAL PARAMETERS	VALUE
Shear stiffness (MPa/mm)	20
Tensile strength (MPa)	0,0
Friction angle (°)	See Table 3
Cohesion (MPa)	See Table 3
Dilatancy angle (°)	0
Softening modulus (MPa/mm)	-0,7

Table 3: Data for friction and cohesion at the interface

SAMPLE	FRICTION ANGLE (°)	COHESION (MPa)
1	45	0,5
2	37	0,3
3	46	0,3
4	45	0,7
5	49	0,8
6	53	0,2
7	54	0,6
8	45	0,0
9	49	0,1
10	60	0,2
11	63	0,2
12	62	0,4
13	60	0,7
14	56	0,1
15	62	0,4

1.3. Loading

The considered loadings are self-weight, hydraulic pressure acting on the upstream face of the dam and uplift acting on the base of the dam. Five water levels are considered: 75, 78, 80 (crest level), 82 and 85 m. Development of a crack at the interface is considered and uplift pressure is updated accordingly, as it is shown in Fig. 3. Two cases of drain effectiveness are considered, with discrete probabilities associated:

- Case A: Drains effective (probability of 0,90)
- Case B: Drains not effective (probability of 0,10)

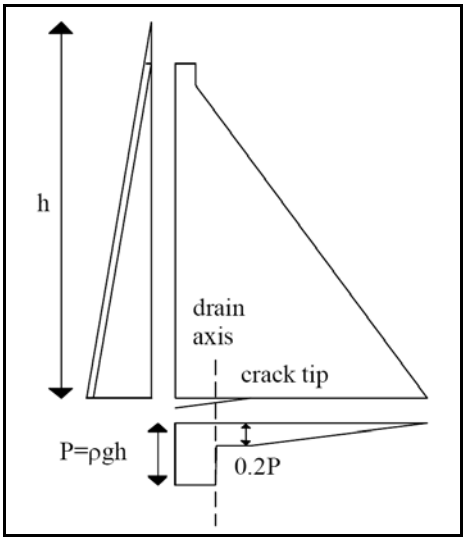

Case A. Drains effective

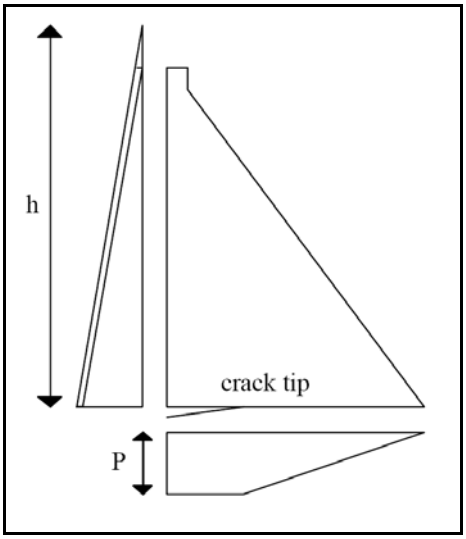

Case B. Drains ineffective

Figure 3: Dam and foundation geometry

1.4. Results to be provided

Considering the failure mode of sliding along the dam foundation contact, the results are divided in three parts.

Part 1: Relationship between water levels and factor of safety.

The factor of safety is evaluated using two 2D models of analysis: a rigid body Limit Equilibrium Model (LEM) and an elastic deformable body model implemented in the finite difference code FLAC 2D (Itasca) for the 5 water levels considered.

Part 2: Relationship between water level and probability of failure with Level 2 methods.

The probability of failure has been estimated using the LEM model together with two Level 2 reliability methods: the First Order Second Moment Taylor Approximation (FOSM) and the Point Estimate Method (PEM), for the 5 water levels considered.

Part 3: Relationship between water level and probability of failure with Level 3 methods.

The probability of failure has been estimated using both LEM and FLAC models together with Level 3 Monte Carlo simulation method for the 5 water levels considered.

2. Models of analysis

In this section the models of analysis for the sliding failure mode are described.

2.1. Rigid body Limit Equilibrium Model (LEM)

Sliding stability can be analyzed with a rigid body 2D Limit Equilibrium Model. The hydrostatic load, S (N/m), is the driving force and can be evaluated for a water height, h(m), by Equation (1).

$$S = \frac{1}{2}\rho_w g h^2 \tag{1}$$

The shear strength, R(N/m) is calculated with Equation (2).

$$R = (N - U)tg\varphi + B \times c \tag{2}$$

N (N/m) is the sum of vertical forces acting on the dam-foundation contact surface.

U (N/m) is the uplift.

B (m^2/m) is the area in compression in the dam-foundation contact.

φ (°) is the friction angle in the contact.

c (Pa) is the cohesion in the contact.

The resisting force is defined according to the Mohr-Coulomb model, considering zero dilatancy and zero tensile strength to be developed at the contact. The two parameters governing its behaviour are thus the friction angle, φ, the cohesion, c. Uplift is thus considered as an active force acting along the dam-foundation contact.

One of the aspects that control the response of the dam is the possibility of crack initiation and propagation along the contact plane. The model used presents an initiation and propagation criteria based on a comparison between the tensile strength and the tensile stress, see *USACE* [1]. If tensile stress exceeds the tensile strength crack initiation happens. Crack opening causes a change in uplift pressure distribution under the dam. It also causes a reduction of the zone under compressive stress, resulting in a decrease of the resisting force together with a redistribution of stresses at the base. This process continues and the crack propagates downstream until the tensile stress evaluated at the tip of the crack is lower than the tensile strength. It may happen that this condition is not met and the crack propagates throughout the base causing dam failure by instability or excessive compressive stresses at the toe. Simulation of the process is carried out by an iterative process, where once initiation criteria is verified, a small crack increment is assumed, uplift is re-evaluated and stress distribution is calculated.

The factor of safety is defined according to Equation (3).

$$FS = \frac{R}{S} \tag{3}$$

2.2. Elastic deformable body model (FLAC)

In this model, both the dam and the foundation are considered as elastic deformable bodies. The model has been implemented in the code FLAC 2D (Itasca, 1994). This code uses a lagrangian explicit scheme to solve the equation of motion, with references to the deformed shape. Plane strain is hypothesized. Each zone of the model is subjected to its stress-strain law.

One of FLAC features is its programming language embedded called FISH, that enables to define variables and functions to capture loading sequences, non linear behaviour on discontinuities and so on.

The model solve the full equations of motion in Equation (4) using an explicit time-marching scheme of calculation by time-steps.

$$\rho \frac{\partial \dot{u}_i}{\partial t} = \frac{\partial \sigma_{ij}}{\partial x_j} + \rho g_i \tag{4}$$

where:

ρ: mass density
$\dot{u}_i$: components of velocity vector
t: time
σ_{ij}: components of stress tensor
x_j: components of coordinate vector
g_i: components of gravitational acceleration (body forces)

Using the equations of motion to solve static problems leads to larger times of calculation but provides numerical stability even when physical instability is reached.

The mesh geometry is shown in Fig. 2. The boundary conditions are prescribed displacements in part of the boundary of the numerical grid of the foundation. The X-displacements are zero at the grid points along the bottom of the foundation and the Y-displacements are zero at the grid points along the right and left lateral sides of the foundation.

The constitutive model adopted for dam and foundation is linear elastic, as it is an acceptable first approach due to the low level of stress expected in gravity dams.

The interface between dam and foundation is characterized by Coulomb sliding and tensile separation. An interface is represented in FLAC as a normal and shear stiffness between two planes which may contact one another, as depicted in Fig. 4. The Coulomb shear-strength criterion limits the shear force to the maximum value controlled by the friction angle and the cohesion. If the magnitude of the tensile normal stress exceeds the bond strength (which is zero in this case) at any point the bond breaks for that point and it behaves thereafter as unbounded (separation and slip allowed). If a crack is formed, uplift is updated using a FISH function, according to Fig. 3.

The factor of safety in this case is defined according to Equation (5) as the ratio between the value of the parameter controlling the stability, φ, (or c), and the value of the parameter when failure occurs, φ_{FAIL}, (or c_{FAIL}). In (6) a linear degradation from values (φ, c) to (0,0) is assumed.

$$FS = \frac{\varphi}{\varphi_{FAIL}} = \frac{c}{c_{FAIL}} \tag{5}$$

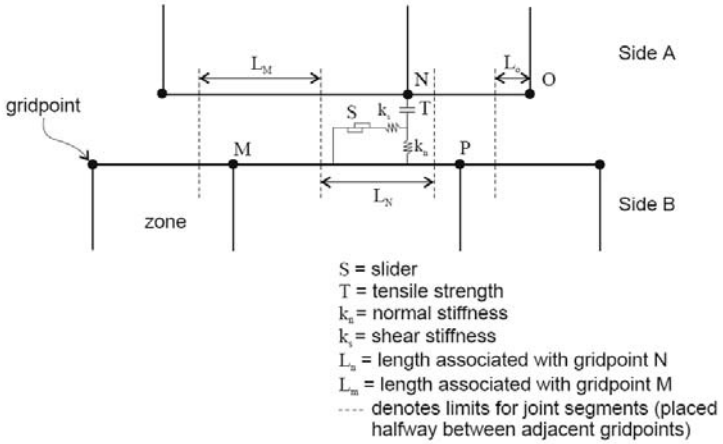

Figure 4: Interface model in FLAC

3. Variables

All the variables of the problem are deterministic, each of them having a single value with a probability of one, except for the drain effectiveness, with two possible values, and for the friction angle and the cohesion at the interface, where a sample of 15 different values is provided. This variability is the reason for doing probability-based safety estimations. The drain effectiveness is considered in the evaluation of the uplift value at the drain line. This uplift value has a discrete probability distribution with only two possible values. Let P be the value of the uplift pressure under the heel of the dam, which varies linearly with the water level, h. Then, the uplift pressure under the drain line can be taken as 0,2P with a probability of 0,9 or as P with a probability of 0,1.

Fifteen pairs of values are given for friction angle and cohesion, as shown in Table 3. These two parameters are considered as random values. To apply Level 2 reliability methods only the first two moments of the distributions of the parameters are needed, while for Level 3 methods the full probability density distributions should be known.

3.1. Friction angle

Several distributions have been test to fit the given data of friction angle values. The Normal distribution fits very well to the data, although it is an unbounded distribution whereas the friction angle is certainly a bonded parameter. In Table 4 and in Fig. 5 the results of the adaptation are summarized.

Table 4: Probability distribution for friction angle

(°)	SAMPLE	ADAPTATION TO NORMAL DISTRIBUTION
Mean, μ	52,4	52,4
Standard deviation, σ	7,99	7,99
Minimum value	37	-∞
Maximum value	63	+∞

The Normal distribution is an upper and lower unbounded distribution, so a truncation is needed to give the adaptation a physical meaning and so avoiding sampling unrealistic very low or even negative values of the friction angle with Level 3 methods.

Sample values are in the (-2σ; +2σ) interval. Truncation of the function between [-3σ; +3σ] is adopted, which means that all values will be in the range [28,4°; 76,4°]. The standard deviation of the truncated function is now σ = 7,86° as it can be seen in Table 5.

Table 5: Probability distribution for friction angle

(°)	ADAPTATION TO NORMAL DISTRIBUTION	TRUNCATION OF ADAPTED NORMAL DISTRIBUTION
Mean, μ	52,4	52,4
Standard deviation, σ	7,99	7,86
Minimum value	-∞	28,4
Maximum value	+∞	76,4

The calculations with Level 2 methods will be done with values (μ, σ) from the sample and the calculations with Level 3 methods will be done with the truncated adapted distribution.

3.2. Cohesion

Several distributions have been test to fit the given data of cohesion values. As cohesion is a bonded parameter with a minimum value of zero, it is usual to check for lower bonded distributions. A problem arises as one of the given data values is exactly zero, which makes it impossible to fit lower bonded distributions that assign a null probability to that value of zero. To avoid this problem, that single value can be omitted in the adaptation. Another possibility is to change the single zero value by a non-zero value, still lower than the rest, for example by an order of magnitude. This second option has been selected, changing the c=0 value for c=0,01. The sample and adaptation values are shown in Tables 6 and 7. In Fig. 5 the results of the adaptation are summarized.

Table 6: Probability distribution for cohesion, including the single zero value.

(MPa)	SAMPLE (with c=0)	ADAPTATION TO LOGNORMAL DISTRIBUTION
Mean, μ	0,367	Not possible
Standard deviation, σ	0,247	
Minimum value	0	
Maximum value	0,80	

Table 7: Probability distribution for cohesion, changing the single zero value.

(MPa)	SAMPLE (with c=0,01)	ADAPTATION TO LOGNORMAL DISTRIBUTION
Mean, μ	0,367	0,458
Standard deviation, σ	0,246	0,678
Minimum value	0,01	0
Maximum value	0,80	+∞

The Lognormal distribution is an upper unbounded distribution, so a truncation is needed to give the adaptation a physical meaning and so avoiding sampling unrealistic very high values of the cohesion with Level 3 methods. The probability function is truncated for a value of 2 MPa, which is reasonable upper physical limit for the cohesion at the interface. The truncation of the distribution changes the mean and the standard deviation of the truncated function, as it can be seen in Table 8.

Table 8: Probability distribution for cohesion, changing the single zero value.

(MPa)	ADAPTATION TO LOGNORMAL DISTRIBUTION	TRUNCATION TO LOGNORMAL DISTRIBUTION
Mean, μ	0,458	0,375
Standard deviation, σ	0,678	0,368
Minimum value	0	0
Maximum value	$+\infty$	2

The calculations with Level 2 methods will be done with values (μ, σ) from the sample and the calculations with Level 3 methods will be done with the truncated adapted distribution.

3.3. Correlation between variables

The correlation coefficient for the sample values of φ and c is ρ = -0,014 so the variables are considered as not correlated.

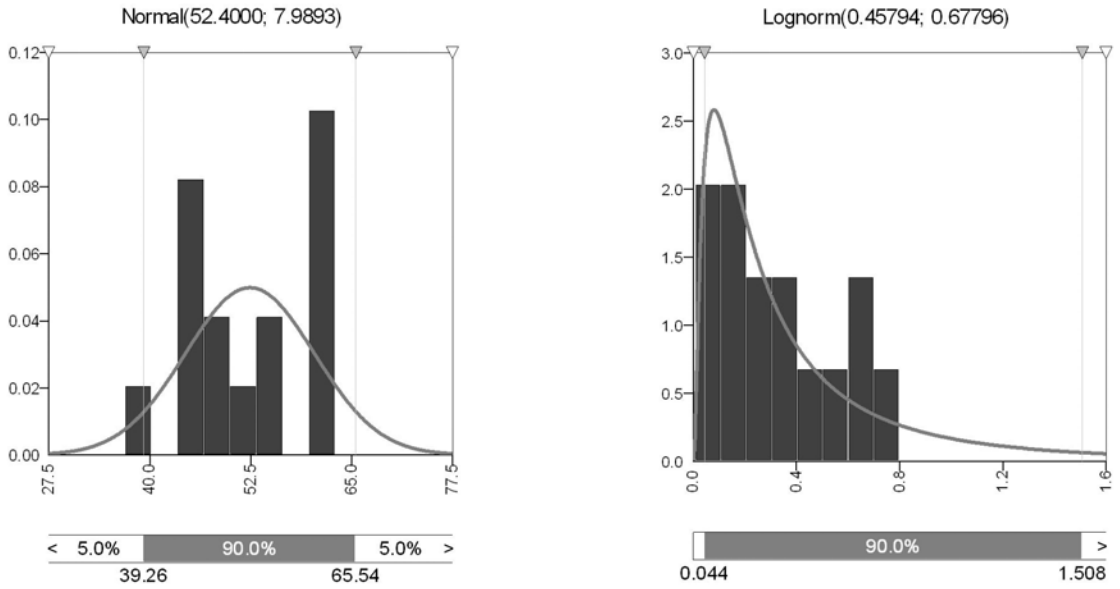

Figure 5: Probability distributions adapted to sample values. Normal distribution for friction angle (left) and Lognormal distribution for cohesion (right).

4. Reliability methods

In this section the reliability methods used to assess the probability of failure are briefly described.

4.1. Level 2 methods

A performance function $g^*(x_1,x_2,\ldots,x_n)$ is defined according to Equation (6).

$$g^* = FS - 1 \tag{6}$$

The typical output of these methods is the reliability index, β, which is defined as the number of standard deviations between the expected value of the function $g^*(x_1,x_2,\ldots,x_n)$ and the limit state value defined as $g^*(x_1,x_2,\ldots,x_n)=0$, as it is shown in Equation (7). This value gives us a relative measure of reliability (distance between the most probable value and the failure domain), in the sense that the larger the value of β, the safer the structure will be, but it does not tells us anything about the probability of failure by itself.

$$\beta = \frac{\mathrm{E}[g^*] - (g^*)_{\text{fallo}}}{\sigma_{g^*}} = \frac{\mathrm{E}[g^*] - 0}{\sigma_{g^*}} = \frac{\mathrm{E}[g^*]}{\sigma_{g^*}} \tag{7}$$

As $X_1,X_2,\ldots,X_n$ are random variables, $g^*(x_1,x_2,\ldots,x_n)$ is a random variable with a certain probability distribution, usually unknown. To get an estimate of the probability of failure, and hypothesis on the shape of this distribution is to be done. With the shape of the probability distribution and its first two moments, both the reliability index and the probability of failure can be obtained.

4.1.1. First Order Second Moment (FOSM) Taylor Approximation

The function $g^*(x_1,x_2,\ldots,x_n)$ must be linear to obtain the first two moments of the probability distribution of $g^*(x_1,x_2,\ldots,x_n)$ from the first two moments of the probability distributions of the random variables $X_1,X_2,\ldots,X_n$. The first moment of the probability distribution of g*, assuming that the random variables are uncorrelated can be calculated with Equation (8).

$$\mathrm{E}[g^*] = g^*\left(\mathrm{E}[X_1], \mathrm{E}[X_2], \ldots, \mathrm{E}[X_n]\right) \tag{8}$$

So the expected value of g* is obtained evaluating the function in the n-dimensional point corresponding to the expected values of the random variables. If the random variables are independent, the variance of g* is calculated with Equation (9).

$$\mathrm{Var}[g^*] = \sum_i \left(\left(\frac{\partial g^*}{\partial X_i} \right)^2 \sigma_{X_i}^2 \right) \tag{9}$$

First order derivatives can be obtained straightforward if g* is a linear function. If it is not, first order derivatives are approximated by the first order elements of the Taylor's series expansion of g* about the expected values. The partial derivatives are calculated numerically using a very small increment (positive and negative) centred on the expected value. Following the USACE practice, a large increment of one standard deviation will be used, in order to capture some of the behaviour of the nonlinear functions, as in Equation (10).

$$\frac{\partial g^*}{\partial X_i} \approx \frac{g^*\left(E[X_i]+\sigma_{X_i}\right)-g^*\left(E[X_i]-\sigma_{X_i}\right)}{\left(X_i+\sigma_{X_i}\right)-\left(X_i+\sigma_{X_i}\right)} = \frac{g^*\left(E[X_i]+\sigma_{X_i}\right)-g^*\left(E[X_i]-\sigma_{X_i}\right)}{2\sigma_{X_i}} \tag{10}$$

And the square of the first order derivative can be estimated by Equation (11).

$$\left(\frac{\partial g^*}{\partial X_i}\right)^2 \approx \frac{1}{\sigma_{X_i}^2}\left(\frac{g^*\left(E[X_i]+\sigma_{X_i}\right)-g^*\left(E[X_i]-\sigma_{X_i}\right)}{2}\right)^2 \tag{11}$$

Substituting Equation (11) in Equation (9) the variance has the expression of Equation (12).

$$\mathrm{Var}[g^*] = \sum_i \left(\left(\frac{g^*\left(E[X_i]+\sigma_{X_i}\right)-g^*\left(E[X_i]-\sigma_{X_i}\right)}{2}\right)^2\right) \tag{12}$$

With this method a number of 2n+1 evaluations of the performance function g* is needed, being n the number of random variables considered.

4.1.2. Point Estimate Method

The point estimated method determine the first two moments of the performance function g* by the discretization of the probability distributions of the random variables $X_1,X_2,...,X_n$. This discretization is made in a few points for each random variable (two or three points), where mass probability is concentrated in such a fashion that the sum of the probabilities assigned to each point is 1 for each random variable, see *Rosenblueth* [2] and *Harr* [3]. With this method there is no need to evaluate partial derivatives of the performance function g*. A disadvantage of the method is that the performance function has to be evaluated 2n times, being n the number of random variables. If n is large, the method requires a considerable computational effort, above all if g* evaluation is not straightforward.

The method concentrates the mass probability of the random variable Xi in two points, xi+ y xi-, each of them with a mass probability of P_{i+} and P_{i-}. Points are centred about the mean value, μ_{Xi}, at a distance of d_{i+} and d_{i-} times the standard deviation, σ_{Xi} , respectively, as it is shown in Equation (13).

$$\begin{aligned} P_{i+} + P_{i-} &= 1 \\ x_{i+} &= \mu_{X_i} + d_{i+}\cdot\sigma_{X_i} \\ x_{i-} &= \mu_{X_i} + d_{i-}\cdot\sigma_{X_i} \end{aligned} \tag{13}$$

Coefficients d_{i+} y d_{i-} are determined using the skew coefficient, γ_i, of the random variable X_i , with Equation (14).

$$\begin{aligned} d_{i+} &= \frac{\gamma_i}{2} + \sqrt{1+\left(\frac{\gamma_i}{2}\right)^2} \\ d_{i-} &= d_{i+} - \gamma_i \end{aligned} \tag{14}$$

Probabilities are assigned to each point according to Equation (15).

$$P_{i+} = \frac{d_{i-}}{d_{i+} + d_{i-}}$$
$$P_{i-} = 1 - P_{i+} \tag{15}$$

A number of 2n values of discrete probabilities should be obtained by combination of the point probabilities of each random variable with the other random variable's probabilities. These probabilities are $P(\delta_1,\delta_2,...,\delta_n)$, where δ_i is the sign (+ or -). Values of these probabilities are calculated with Equation (16).

$$P_{(\delta 1,\delta 2,...,\delta n)} = \prod_{i=1}^{n} P_{i,\delta i} + \sum_{i=1}^{n-1}\left(\sum_{j=i+1}^{n} \delta_i \delta_j a_{ij} \right) \tag{16}$$

Where the coefficients a_{ij} are calculated with Equation (17).

$$a_{ij} = \frac{\frac{\rho_{ij}}{2^n}}{\sqrt{\prod_{i=1}^{n}\left(1+\left(\frac{\gamma_i}{2}\right)^2\right)}} \tag{17}$$

Being ρ_{ij} the correlation coefficient between random variables X_i y X_j.

The performance function g* has to be evaluated 2n times, corresponding to the 2n possible combinations of discrete probability points $P(\delta_1,\delta_2,...,\delta_n)$, obtaining $g^*(\delta_1,\delta_2,...,\delta_n)$. Once this is accomplished, the moment of m order of the probability distribution of g* is determined by Equation (18).

$$E\left[g^{*m}\right] \approx \sum P_{(\delta 1,\delta 2,...,\delta n)} g^{*m}_{(\delta 1,\delta 2,...,\delta n)} \tag{18}$$

So for the first moment is calculated with Equation (19).

$$E[g^*] = \sum P_{(\delta 1,\delta 2,...,\delta n)} g^*_{(\delta 1,\delta 2,...,\delta n)} \tag{19}$$

And for the second moment with Equation (20).

$$E\left[g^{*2}\right] = \sum P_{(\delta 1,\delta 2,...,\delta n)} g^{*2}_{(\delta 1,\delta 2,...,\delta n)} \tag{20}$$

The variance of g* can be calculated by Equation (21).

$$Var[g^*] = E\left[\left(g^* - \mu_{g^*}\right)^2\right] = E\left[g^{*2}\right] - \mu^2_{g^*} \tag{21}$$

So it is possible to determine the mean and the variance of the probability distribution of g* but the shape of the distribution is not known. If what we want is a probability of failure, again a hypothesis of how g* is distributed is to be done. The method loses precision with the increasing nonlinearity of g* and if moments over the second are to be obtained. It does not provide a measure of the contribution of each random variable to the overall variance, so it is not an adequate method to filter the most relevant random variables.

4.2. Level 3 methods

Level 3 methods provide a more accurate evaluation of the probability of failure, as they consider all the information of the probability density function and not only the first two moments. The formulation of the problem is given in Equation (22).

$$P_f\left[g^*(x_1, x_2, ..., x_n) \le 0\right] = \int_{g^*(x_1,x_2,...,x_n)\le 0} f_{X_1,X_2,...,X_n}(x_1, x_2, ..., x_n)\,dx_1 dx_2 ... dx_n \tag{22}$$

The integral can be evaluated with simulation methods (Monte Carlo Methods). With the simulation methods we generate N sets of values for the random variables according to their probability distributions and possible correlations, see Equation (23).

$$\hat{x}_{(i)} = \left(\hat{x}_1, \hat{x}_2, ..., \hat{x}_n\right)_{(i)} ; \mathbf{i = 1, ..., N} \tag{23}$$

Generation of these values can be accomplished with several statistical techniques. The performance function is evaluated for each one of these sets of values, and the number of failures, m, (when $g^* \le 0$) is calculated. The probability of failure can be then estimated by Equation (24).

$$P_{fallo} \approx \frac{m\left(g^*\left(\hat{x}_1, \hat{x}_2, ..., \hat{x}_n\right) \le 0\right)}{N} = \hat{P}_f \tag{24}$$

This method of simulation is the normal Monte Carlo method ("Hit or Miss Monte Carlo Method"). These simulation methods are deemed "exact methods" in the sense that they provide the exact value of the probability of failure when $N \to \infty$. For lower values of N, what we get is an approximation of the value of the integral in Equation (22). The estimator of the probability of failure shows a mean and a variance given by Equation (25).

$$\begin{aligned} E\left[\hat{P}_f\right] &= P_f \\ \sigma^2_{\hat{P}_f} &= \frac{1}{N} P_f\left(1 - P_f\right) \end{aligned} \tag{25}$$

The accuracy of the estimation is measured by the inverse of the standard deviation of the estimator, which is proportional to $N^{0,5}$. The N evaluations of the performance function form a sample of a random variable, so it is possible to fit probability distributions to this sample. Once the probability distribution function F_{g^*}, of the performance function is derived, the probability of failure is straightforward calculated with Equation (26).

$$P_f = P\left[g^* \le 0\right] = F_{g^*}(0) \tag{26}$$

The problem is that in the tails of the distribution it is difficult to get an accurate fitting, and these are usually the key areas to estimate the probability of failure.

To avoid the usual large number of calculations needed as the equilibrium problem (either with the LEM or the FLAC models) has to be solved for each sample to evaluate g*, there are techniques such as the response surface, *Altarejos et al* [4].

If it is possible to define this surface analytically for each water level, calculations are deeply simplified, as it is only needed to evaluate if a sampled value falls in the safe domain or in the failure domain, which are defined by the response surface for each water level. In the problem of sliding along the dam-foundation contact, the response surface can be obtained when only two random variables are considered in the analysis. In this 2D domain of the random variables, the limit surface becomes a limit curve. With the LEM model it is possible to derive the analytical expression of the limit curve. Let the two random variables be the friction angle, φ, and the cohesion, c, and let L be the driving force, N the normal force acting on the contact plane, U the uplift force and B* the area under compression in the base of the dam. Then, the limit curve is given by Equation (27).

$$c = a_0 + a_1 \cdot tg\varphi \tag{27}$$

where the coefficients a_0 and a_1 are calculated with Equation (28).

$$\begin{aligned} a_0 &= \frac{L}{B^*} = \tau_m \\ a_1 &= -\frac{N-U}{B^*} = -\sigma_m \end{aligned} \tag{28}$$

The coefficient a_0 is the mean shear stress acting on the surface, τ_m, and the coefficient a_1 is the mean compressive stress acting on the surface. When the limit curve is known the probability of failure can be calculated as it is depicted in Fig. 6.

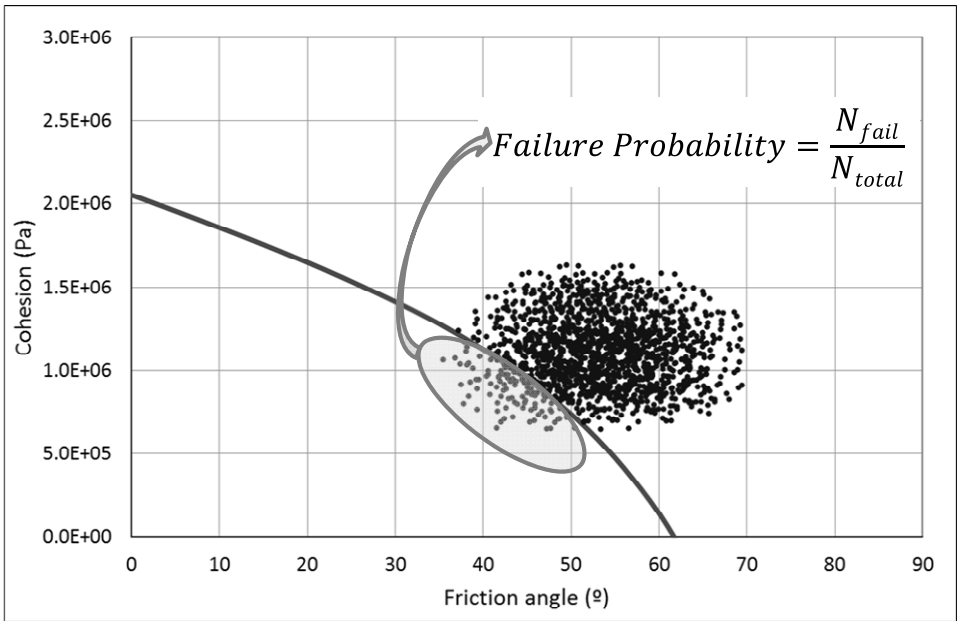

Figure 6: Calculation of the probability of failure with the limit curve.

The limit curve for the limit equilibrium model in the space (tgφ, c) is a straight line. If pairs of values (tgφ, c) obtained with the elastic deformable body model follow a straight line as well, the problem is reduced to a linear regression. Points on the limit surface are estimated by a radial sweep with joint degradation paths for friction angle and cohesion with initial points in the boundaries of the feasible region and final point the origin of coordinates. For each water level considered, points are obtained on the limit surface and a line is fitted to them.

5. Results

5.1. Part 1: Relationship between water levels and factor of safety

To allow consistent comparison between the factors of safety computed with different models of analysis, the factor of safety using the LEM model has been calculated with Equation (3) based on the ratio between strength force and driving force and also with Equation (5), based on the ratio between the characteristic value of the parameter and the value that leads to failure.
In any case, a decision has to be made about what characteristic values of the strength parameters (φ, c) should be used to evaluate the factor of safety. In this case, the characteristic values selected have been the mean values estimated from the sample. The results in terms of the water level – factor of safety relationship is shown in Table 9 and in Fig. 7.

Table 9: Relationship between water levels and Factor of safety

WATER LEVEL (m)	DRAINS EFFECTIVE			DRAINS INEFFECTIVE		
	LEM model		FLAC model	LEM model		FLAC model
	FS = R/T	FS = $\varphi/\varphi_{\_fail}$	FS = $\varphi/\varphi_{\_fail}$	FS = R/T	FS = $\varphi/\varphi_{\_fail}$	FS = $\varphi/\varphi_{\_fail}$
75	3,15	2,53	2,51	2,49	2,07	1,91
78	2,90	2,34	2,33	1,74	1,50	1,62
80	2,75	2,22	2,10	1,01	1,00	1,27
82	2,61	2,12	1,00	0,44	0,73	0,90
85	2,17	1,79	0,87	0,41	0,72	0,87

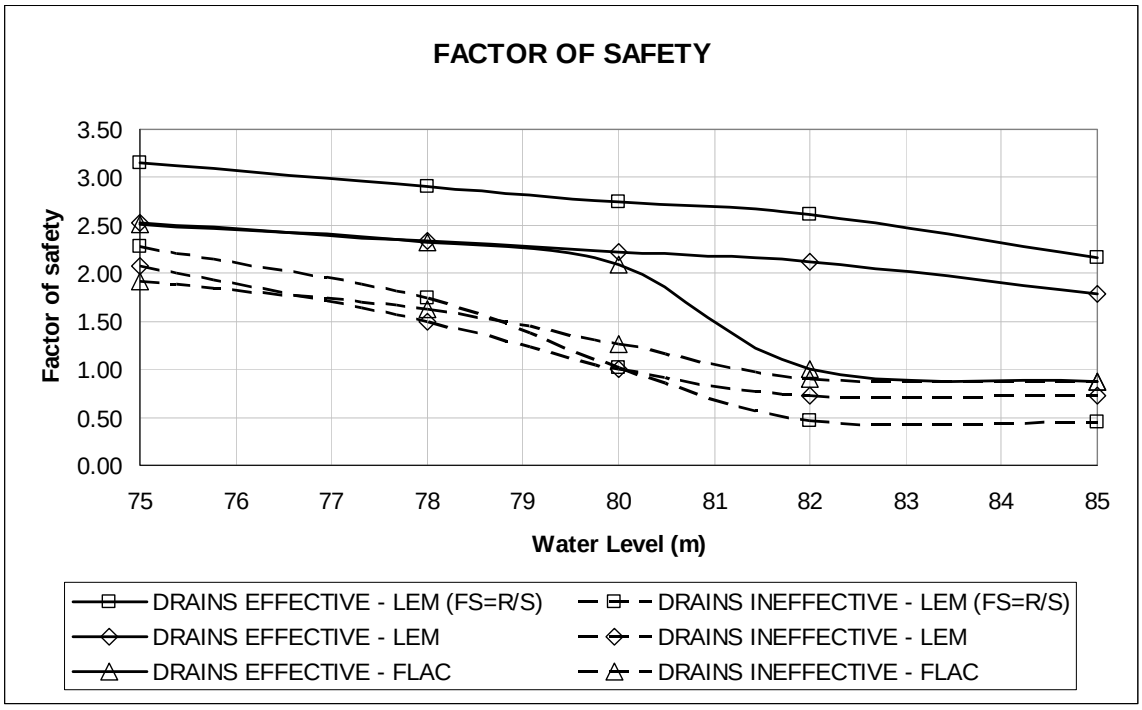

Figure 7: Water level – factor of safety

5.2. Part 2: Relationship between water level and probability of failure with Level 2 methods

The probability of failure has been estimated using the LEM model together with two Level 2 reliability methods: the First Order Second Moment Taylor Approximation (FOSM) and the Point Estimate Method (PEM), for the 5 water levels considered. Probabilities have been calculated for each case of drain performance. The total probability of failure, $P_{FAILURE}$, for each water level, can be obtained with Equation (22) combining the two discrete probabilities of drain performance, P_D, for drains effective (P_D = 0,9) and for drains ineffective (P_D=0,1).

$$P_{FAILURE} = P_D \times P\left(fail \middle| P_D = 0{,}9\right) + P_D \times P\left(fail \middle| P_D = 0{,}1\right) = \\ = 0{,}9P\left(fail \middle| P_D = 0{,}9\right) + 0{,}1P\left(fail \middle| P_D = 0{,}1\right) \quad (22)$$

The results are shown in Table 10 and in Fig. 8 to 10.

Table 10: Relationship between water level and probability of failure with Level 2 methods

WATER LEVEL (m)	DRAINS EFFECTIVE		DRAINS INEFFECTIVE		TOTAL PROBABILITY	
	P(fail | PD=0,9)		P(fail | PD=0,1)		$P_{FAILURE}$	
	FOSM	PEM	FOSM	PEM	FOSM	PEM
75	$7{,}56\times10^{-3}$	$5{,}12\times10^{-3}$	$2{,}24\times10^{-2}$	$1{,}64\times10^{-2}$	$9{,}05\times10^{-3}$	$6{,}25\times10^{-3}$
78	$1{,}04\times10^{-2}$	$6{,}80\times10^{-3}$	$1{,}58\times10^{-1}$	$5{,}53\times10^{-2}$	$2{,}51\times10^{-2}$	$1{,}17\times10^{-2}$
80	$1{,}23\times10^{-2}$	$8{,}14\times10^{-3}$	$4{,}86\times10^{-1}$	$4{,}34\times10^{-1}$	$5{,}96\times10^{-2}$	$5{,}07\times10^{-2}$
82	$1{,}46\times10^{-2}$	$9{,}97\times10^{-3}$	$1{,}00\times10^{0}$	$1{,}00\times10^{0}$	$1{,}13\times10^{-1}$	$1{,}09\times10^{-1}$
85	$2{,}70\times10^{-2}$	$1{,}88\times10^{-2}$	$1{,}00\times10^{0}$	$1{,}00\times10^{0}$	$1{,}24\times10^{-1}$	$1{,}17\times10^{-1}$

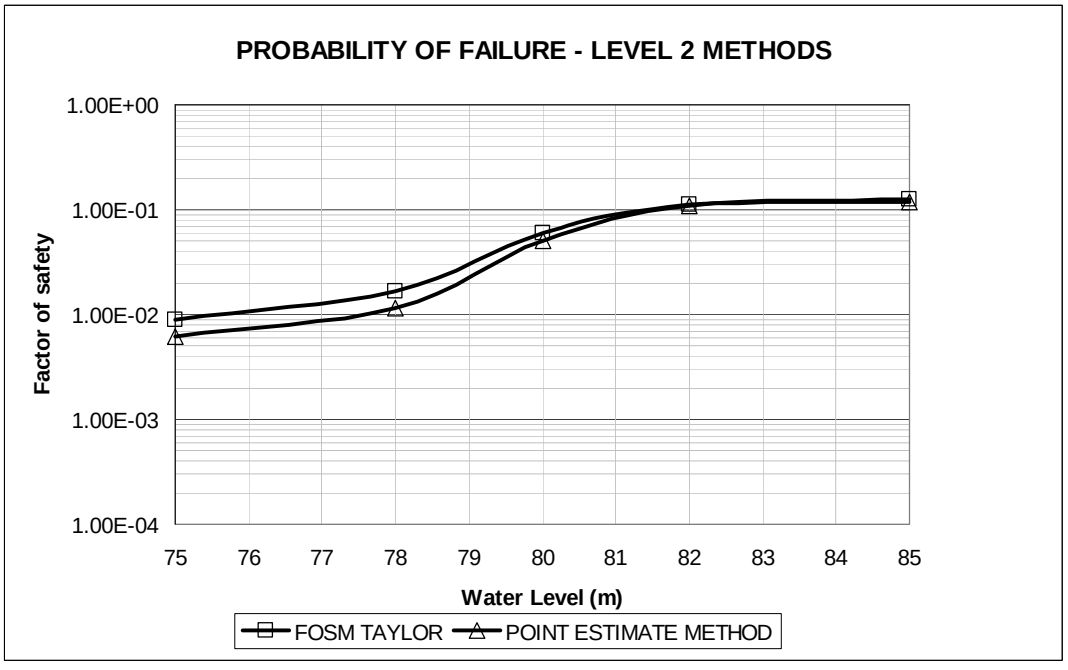

Figure 8: Water level – probability of failure with Level 2 methods. Total probability.

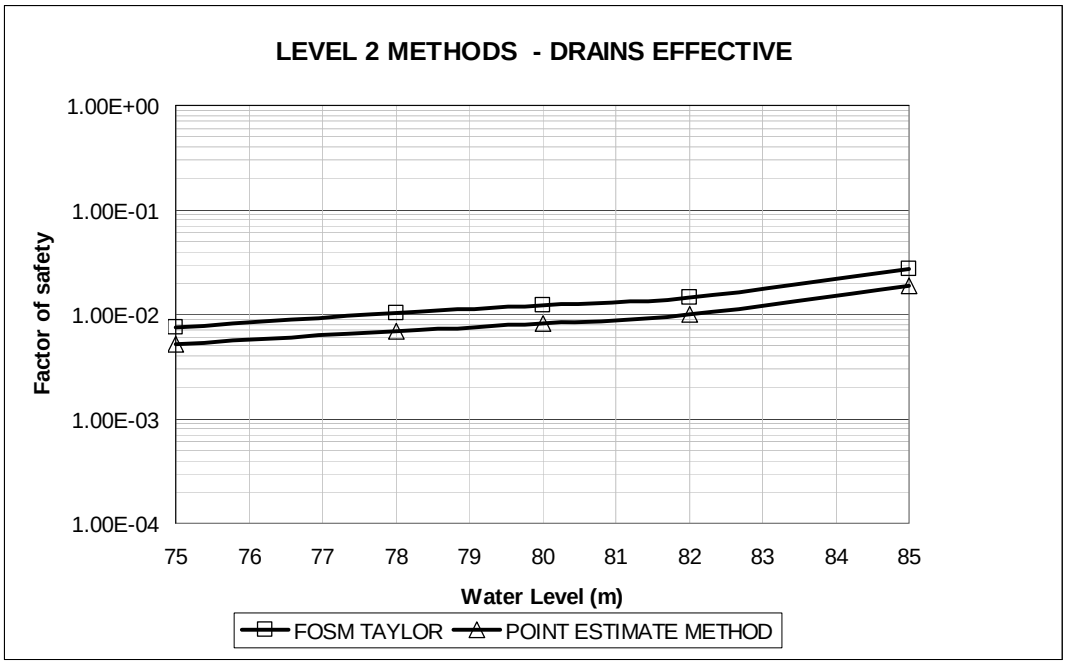

Figure 9: Water level – probability of failure. LEM model and Level 2 methods. Drains effective

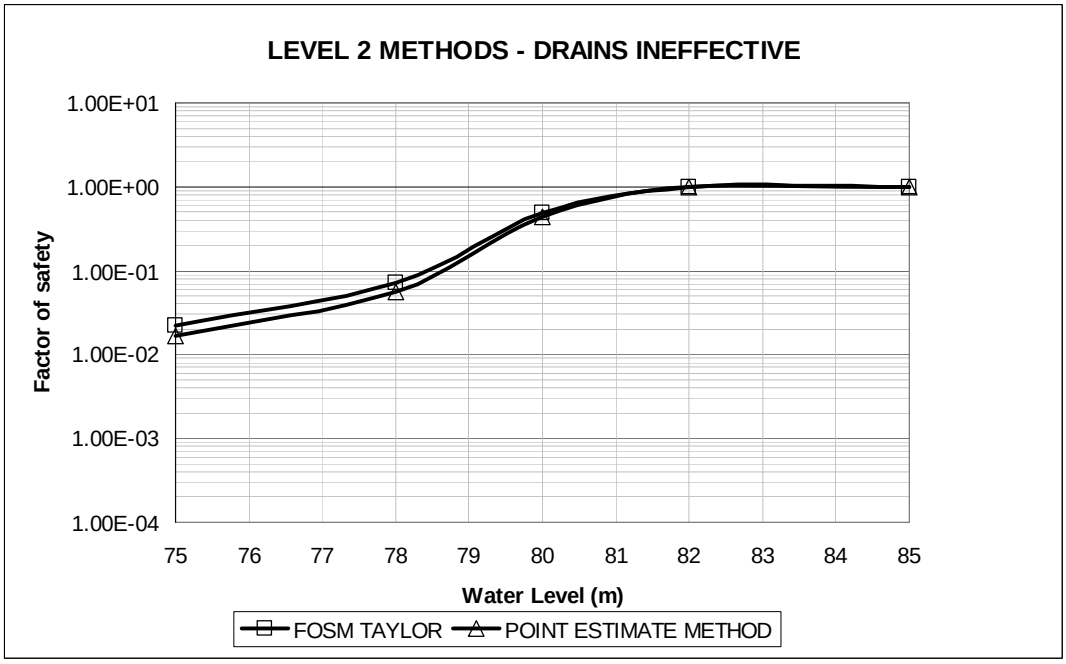

Figure 10: Water level – probability of failure. LEM model and Level 2 methods. Drains ineffective

5.3. Part 3: Relationship between water level and probability of failure with Level 3 methods

The probability of failure has been estimated using both LEM and FLAC models together with Level 3 Monte Carlo simulation method for the 5 water levels considered. Probabilities have been calculated for each case of drain performance. The total probability of failure, $P_{FAILURE}$, for each water level, can be obtained with Equation (22). The results are shown in Table 11 and in Fig. 11 to 13.

Table 11: Relationship between water level and probability of failure with Level 3 method

WATER LEVEL (m)	DRAINS EFFECTIVE		DRAINS INEFFECTIVE		TOTAL PROBABILITY	
	$P(fail \mid P_D=0,9)$		$P(fail \mid P_D=0,1)$		$P_{FAILURE}$	
	LEM	FLAC	LEM	FLAC	LEM	FLAC
75	$2,00\times10^{-7}$	$5,00\times10^{-7}$	$5,96\times10^{-3}$	$5,00\times10^{-5}$	$5,96\times10^{-4}$	$5,45\times10^{-6}$
78	$5,30\times10^{-5}$	$1,00\times10^{-4}$	$1,92\times10^{-2}$	$2,49\times10^{-2}$	$1,97\times10^{-3}$	$2,58\times10^{-3}$
80	$1,60\times10^{-4}$	$3,90\times10^{-4}$	$5,11\times10^{-1}$	$9,31\times10^{-2}$	$5,12\times10^{-2}$	$9,66\times10^{-3}$
82	$4,00\times10^{-4}$	$9,85\times10^{-1}$	$9,91\times10^{-1}$	$9,85\times10^{-1}$	$9,94\times10^{-2}$	$9,85\times10^{-1}$
85	$4,40\times10^{-3}$	$9,85\times10^{-1}$	$9,94\times10^{-1}$	$9,85\times10^{-1}$	$1,03\times10^{-1}$	$9,85\times10^{-1}$

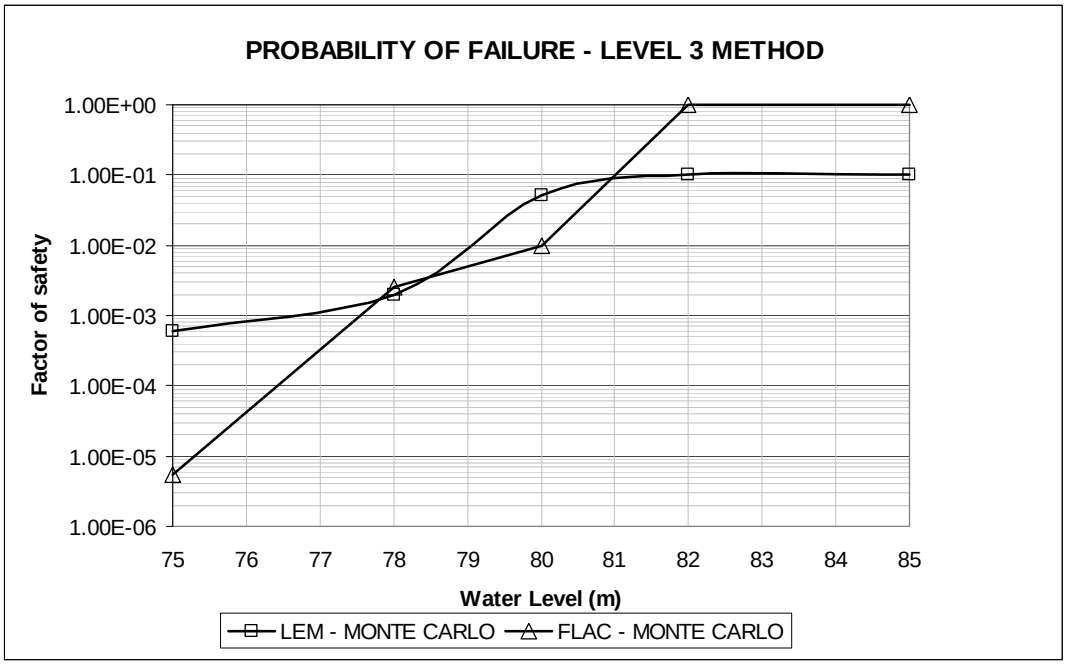

Figure 11: Water level – probability of failure. LEM and FLAC models with Level 3. Total probability

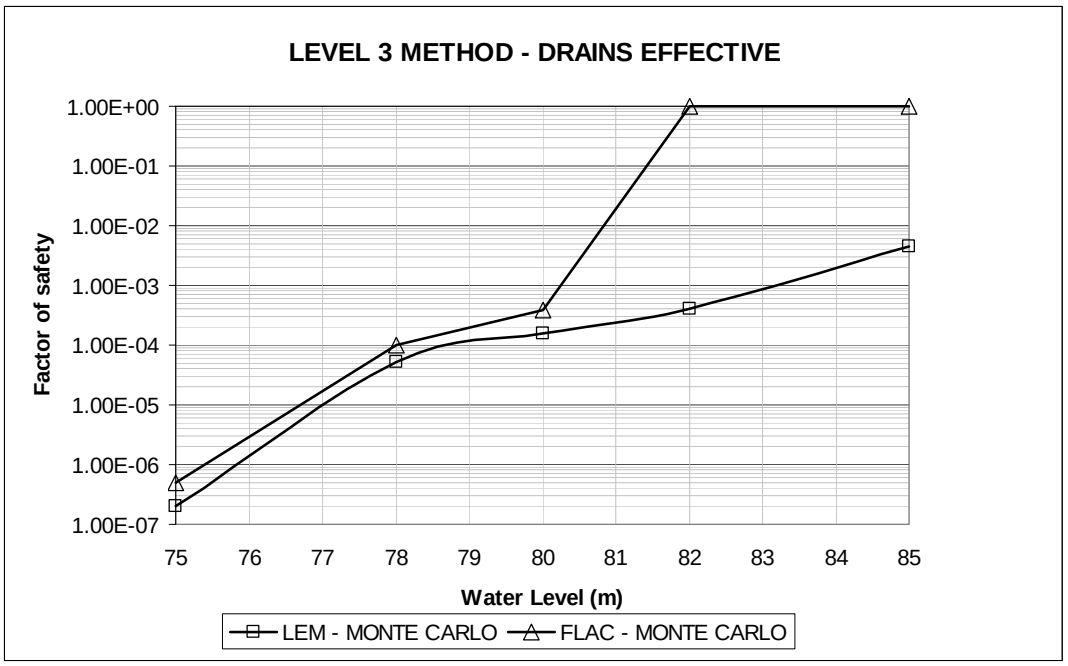

Figure 12: Water level – probability of failure. LEM and FLAC models with Level 3. Drains effective

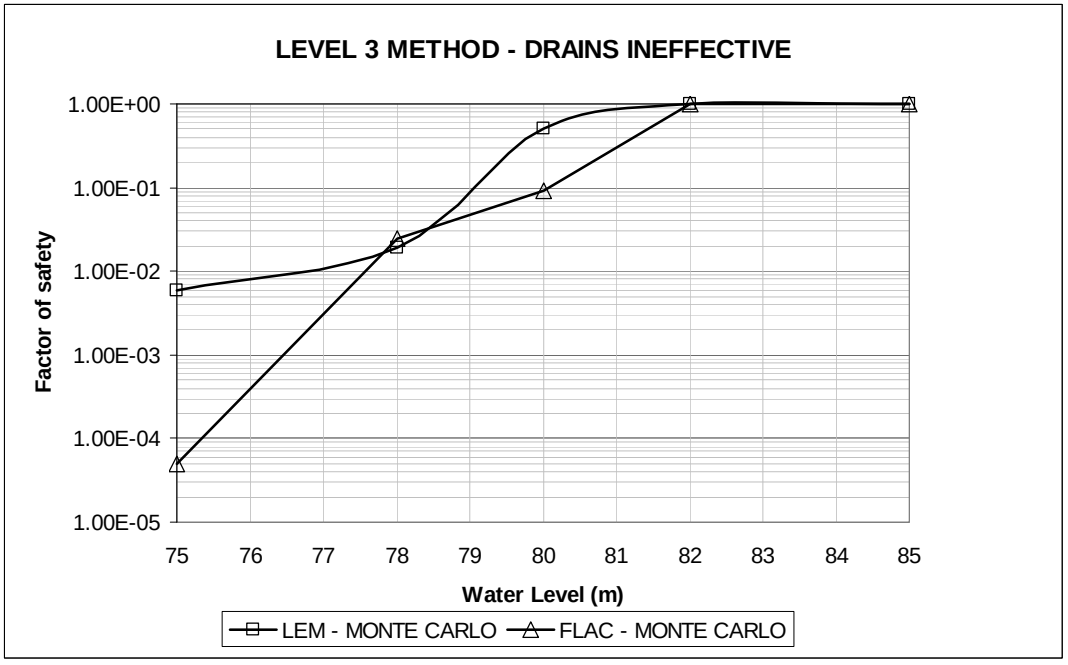

Figure 13: Water level – probability of failure. LEM and FLAC models with Level 3. Drains ineffective

6. Discussion

From the results obtained, it is shown that with LEM method, when drains are effective, the safety factors are relatively high, even for water levels above the dam crest. This situation seems somehow unrealistic. On the other hand, with the FLAC model the safety factor is reduced for water levels higher than the dam crest, which seems to be a more likely situation. The impact of the drain effectiveness is very strong, as factors of safety are highly influenced by the uplift. The results in terms of factor of safety show a common trend for different models if drains are ineffective.

When a set of data for strength parameters is available, the question of what values should be selected as characteristic values to evaluate the factor of safety is very important. Usually mean values are used, but it is a decision subjected to engineering judgement. Another important thing is how the factor of safety is defined. As it can be seen in Fig. 7, using the same LEM model of analysis and the same set of data of strength parameters, the values of the factor of safety can differ depending upon its definition (as a ratio of forces or as a ratio of strength parameters). So comparisons of results obtained from distinct models with different definitions of the factor of safety are not straightforward and should be carefully analyzed.

Regarding the results obtained with Level 2 reliability methods together with the LEM mode, it is the author's opinion that the values of the conditional probabilities of failure obtained for the case of drain effectiveness are unrealistically high for normal water levels under the dam crest, and may be low for water levels above the dam crest. This is due to the inherent limitations of the methods. In particular FOSM method seems unable to capture correctly the probabilities of failure. In the case of drain effectiveness FOSM method gives values of probability with an order of magnitude of 10^{-2}, whereas PEM method gives values of 10^{-3} and Level 3 Monte Carlo method produces values of 10^{-4} and lowers for water levels below the dam crest. When drains are ineffective all the methods lead to similar values for water levels above the crest.

Comparing the results obtained with LEM and FLAC models using Level 3 Monte Carlo method, when drains are effective it is shown that both models give similar values for normal water levels, below the dam crest. As water levels exceed the dam crest, the probability of failure estimated with FLAC model approaches a value of 1 while LEM model predicts values below 10^{-2}, thus showing a very different behaviour, based on the different stress distribution along the dam foundation-contact considered in the models. This stress distribution is controlling the opening and propagation of a crack under the dam. The linear stress distribution assumption embedded in the LEM model seems to be on the 'unsafe' side. A consequence of this is that if overtopping can occur, a more detailed model of analysis should be prepared to evaluate the dam stability.

7. Conclusions

In this paper a probabilistic stability assessment has been carried out for an 80 m high gravity. Two different 2D models of analysis have been considered: a Limit Equilibrium Model and an elastic deformable body model implemented in the code FLAC. Factors of safety have been calculated for 5 different water levels and for two conditions of the drainage system effectiveness, thus showing the strong impact of this on the dam stability. How the factor of safety is defined and what characteristic values are used in its evaluations are key issues of the problem.

The probability of failure has been estimated as the strength parameters of friction angle and cohesion have been considered as random variables. The adaptation of probability distributions to parameters in dam engineering should be done carefully and it should be examined in the light of engineering judgement, so the physical meaning of the parameters is not lost in the mathematical process of fitting distributions.

Two different Level 2 methods, based on the first two moments of the probability distributions of the random variables have been tested. FOSM method seems inadequate to handle successfully the non linearities present in the problem as the probabilities estimated with this method are unrealistically high. The Point Estimate Method provides a better approximation but the probabilities still seem to be too high to be reliable.

Level 3 Monte Carlo simulation method has been used with both LEM and FLAC models of analysis. For water levels below the dam crest both models show similar results and the probabilities of failure are much lower than with Level 2 methods. For water levels above the crest, the LEM model seems to be on the 'unsafe' side, as it predicts lower probabilities of failure than FLAC model. In any case, the Level 3 Method is preferable and should be used whenever possible.

More research is needed to handle uncertainties, as parameter uncertainty is just a part of the problem, but other sources of uncertainty have become present explicitly throughout the process.

References

[1] USACE – US Army Corps of Engineers (2000). Evaluation and comparison of stability analysis and uplift criteria for concrete gravity dams by three federal agencies. ERDC/ITL TR-00-1. Washington DC.

[2] Rosenblueth, E. (1975). Point estimates for probability moments. Proceedings of the National Academy of Science, USA, 72 (10)

[3] Harr, M.E. (1987). Reliability-based design in civil engineering. John Wiley & Sons.

[4] Altarejos García, L.; Escuder Bueno, I.; Serrano Lombillo, A. & Membrillera Ortuño, M. (2008). Assessment of the conditional probability of failure of concrete gravity dams using probabilistic analysis methods of level II and III (Monte Carlo Simulations). XXXIII Jornadas sudamericanas de ingeniería estructural, Santiago, Chile, 2008.

XI ICOLD BENCHMARK WORKSHOP ON NUMERICAL ANALYSIS OF DAMS

Valencia, October 20-21, 2011

THEME C - SYNTHESIS

ESTIMATION OF THE PROBABILITY OF FAILURE OF A GRAVITY DAM FOR THE SLIDING FAILURE MODE

Altarejos-Garcia, Luis[1]

Escuder-Bueno, Ignacio[2]

Serrano-Lombillo, Armando[3]

CONTACT

Luis Altarejos-Garcia, Polytechnic University of Valencia, Environment and Hydraulic Engineering Department. Building 4E - Camino de Vera s/n, 46022 Valencia, Spain. +34963877007 (ext 76142); luis.ag@hma.upv.es.

Summary

This document summarizes the contributions to Theme C of the 11th Benchmark Workshop on Numerical Analysis of Dams held in Valencia (Spain) on October 20-21, 2011.

The objective of Theme C has been to obtain relationships between water levels, factors of safety and probabilities of failure for a gravity dam considering the failure mode of sliding along the dam-foundation contact. The dam proposed is taken from the Theme 2 of the 1999 ICOLD Benchmark. This is done using different models of analysis for the dam-foundation system together with reliability techniques.

Contributions from 8 teams have been reported, which comes to show the interest of the dam engineering community for this topic.

Results presented by contributors open a field of discussion on the main sources of uncertainties, which include models of analysis, factor of safety definition and statistical analysis of random variables.

[1] Associate Professor, Polytechnic University of Valencia & CTO Projects, iPresas. Valencia, Spain
[2] Professor, Polytechnic University of Valencia, Spain.
[3] CTO Research & Development, iPresas. Valencia, Spain.

1. Foreword

In this context of dam safety engineering, risk-based analysis techniques are being developed, offering not only a complementary view to the classical approach to dam safety, but also an entire new tool that can help robust management of dam safety, including some useful criteria to rationalize dam investments and a better understanding of the risk posed by dams, see *Escuder et al [1]*.

Risk analysis methodologies need risk quantification. For an initial state of the dam-reservoir system, and for a certain failure mode, this risk quantification requires the estimation of both the probability of the loading scenarios and the conditional probability of the associated response of the dam-reservoir system, together with the estimation of the consequences.

In dam engineering, the main loading scenarios are those of hydrological and seismic nature, so the estimation of the probability of floods and earthquakes has been on the focus of researchers and engineers for a long time. The estimation of the conditional probability of the response of a system for a certain loading scenario can be done with the help of reliability theory, which is based on a powerful mathematical framework that has been used successfully on the field of structural analysis. The estimation of consequences (in terms of loss of lives and impacts on economy), for a certain response of the dam-reservoir system represents a much more recent landmark in dam safety engineering. However, the development of this issue during the last decades of the past century has been remarkable.

Following the distinction between the three components of risk aforementioned, the problem proposed herein deals with the second of them: conditional probability of the response of a dam-reservoir system for a certain loading scenario. The conditional probability can be assessed by means of three different methods, namely historical references, probability elicitation, and reliability analysis. Probability estimation of the response of complex systems such as dams is an issue subjected to much controversy and discussion by dam engineering community.

2. Aim of Theme C

The objective of Theme C is to obtain relationships between water levels, factors of safety and probabilities of failure for an 80 m high gravity dam considering the failure mode of sliding along the dam foundation contact. This can be done using models of analysis for the dam-foundation system together with reliability techniques that allow for uncertainties in the parameters, using random variables.

For the purpose of comparison and evaluation of advances in this field, the dam proposed is taken from the Theme 2 of the 1999 ICOLD Benchmark.

The proposed exercise is to analyse the dam with a 2D model. The model should be chosen by participants and it can be a limit equilibrium model or a deformable body model. The factor of safety against sliding is then calculated for several water levels.

Following this step, participants should estimate the probability of failure for the sliding failure mode using at least one Level 2 reliability method and a Level 3 Monte Carlo simulation method.

The charts provided by different teams are compared and analysed by formulators.

3. Formulation of the problem

In this section the problem to be solved is summarized.

3.1. Geometry of the dam

The geometry of the dam is depicted in Fig. 1. The full geometry including the foundation is shown in Fig. 2. The foundation has a rectangular shape with height of 80 m and a total length of 300 m (120 m upstream, 60 m under de dam, 120 m downstream).

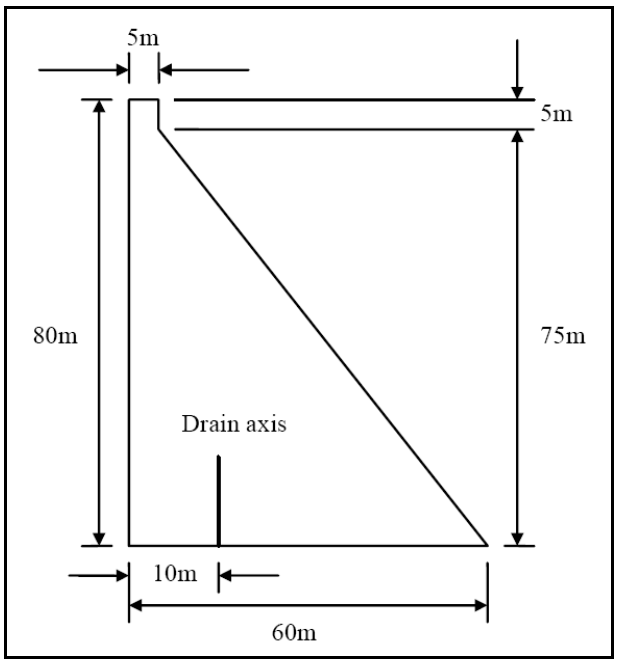

Figure 1: Dam geometry.

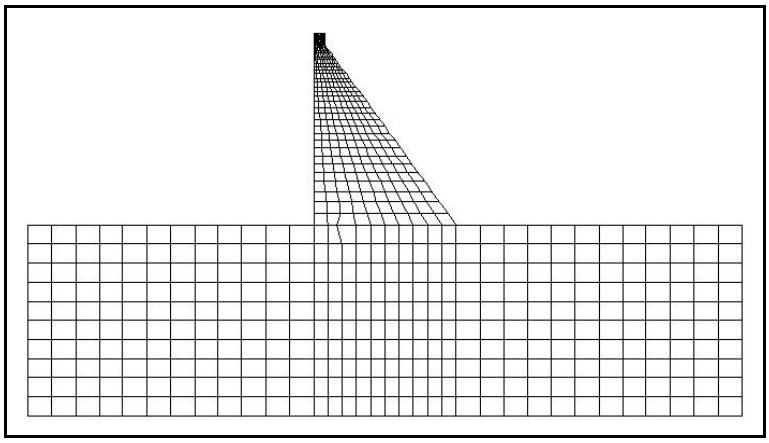

Figure 2: Dam and foundation geometry.

3.2. Material properties

Data on material properties for dam and foundation are given in Table 1. Data for material properties for dam-foundation interface are given in Table 2. Friction angle and cohesion at the dam-foundation interface are considered as random variables. Available data in the form of fifteen pairs of values are given in Table 3.

Table 1: Data for dam and foundation materials.

MATERIAL PARAMETERS	DAM	FOUNDATION
Young's modulus (MPa)	24000	41000
Poisson's ratio	0,15	0,10
Mass density (kg/m3)	2400	2700
Compressive strength (MPa)	24	40
Tensile strength (MPa)	1,5	2,6
Strain at peak compressive strength	0,0022	0,0025
Strain at end of compressive softening curve	0,10	0,15
Fracture energy (N/m)	150	200

Table 2: Data for dam-foundation interface.

MATERIAL PARAMETERS	VALUE
Shear stiffness (MPa/mm)	20
Tensile strength (MPa)	0,0
Friction angle (°)	See Table 3
Cohesion (MPa)	See Table 3
Dilatancy angle (°)	0
Softening modulus (MPa/mm)	-0,7

Table 3: Data for friction and cohesion at the interface.

SAMPLE	FRICTION ANGLE (°)	COHESION (MPa)
1	45	0,5
2	37	0,3
3	46	0,3
4	45	0,7
5	49	0,8
6	53	0,2
7	54	0,6
8	45	0,0
9	49	0,1
10	60	0,2
11	63	0,2
12	62	0,4
13	60	0,7
14	56	0,1
15	62	0,4

3.3. Loading

The considered loadings are self-weight, hydraulic pressure acting on the upstream face of the dam and uplift acting on the base of the dam. Five water levels are considered: 75, 78, 80 (crest level), 82 and 85 m. Development of a crack at the interface is considered and uplift pressure is updated accordingly, as it is shown in Fig. 3. Two cases of drain effectiveness are considered, with discrete probabilities associated:

- Case A: Drains effective (probability of 0,90)
- Case B: Drains not effective (probability of 0,10)

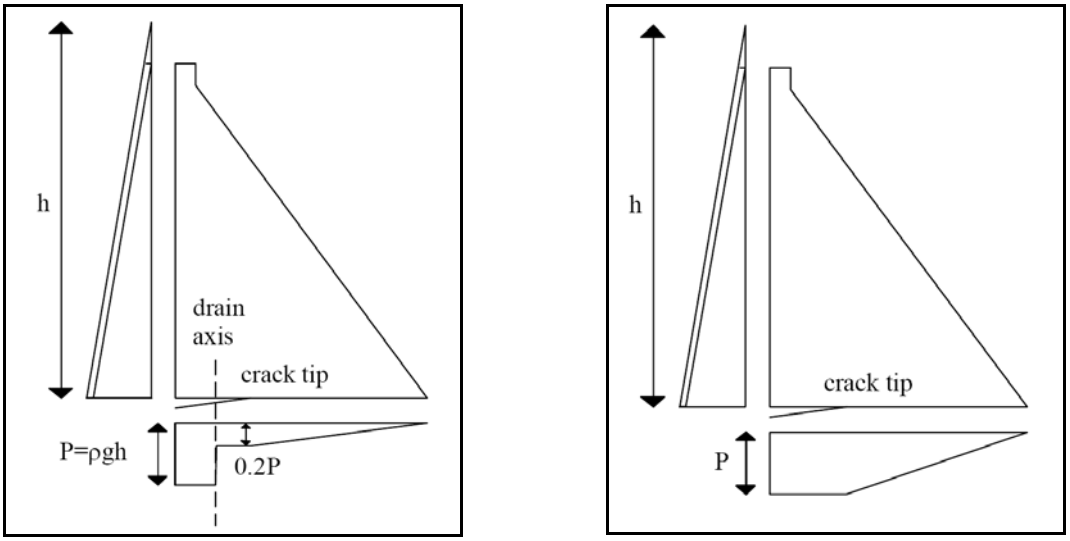

Case A. Drains effective

Case B. Drains ineffective

Figure 3: Loading cases.

3.4. Results to be provided

Considering the failure mode of sliding along the dam foundation contact, the results are divided in three parts.

- Part 1: Relationship between water levels and factor of safety.
- Part 2: Relationship between water level and probability of failure calculated with Level 2 methods.
- Part 3: Relationship between water level and probability of failure calculated with Level 3 methods.

4. Participants

Theme C has had 8 contributions which are listed in Table X. They come from research centres (3), universities (3), a consultant company (1), and a mixed team formed by a consultant company and a university (1).

Table 4: Contributors to Theme C.

ID	AUTHORS	INSTITUTION	COUNTRY
RSE	Faggiani, G; Frigerio, A.; Masarati, P.; Meghella, M.	Ricerca Sistema Energetico	ITALY
UTCB	Popovici, A.; Ilinca, C.	Tech. University of Bucharest	ROMANIA
SC-AG	Touileb, B.	Sogreah Consultants	FRANCE
RIT	Krounis, A.; Johansson, F.	Royal Institute of Technology	SWEDEN
VNIIG	Shcherba, D.	JSC "VEDENEEV VNIIG"	RUSSIA
UPM	Cabrera, M.; Jiménez, R.	Polytechnic University of Madrid	SPAIN
UPV	Gascó, M.	Polytechnic University of Valencia	SPAIN
iPresas	Escuder, I.; Altarejos, L.; Serrano, A.	iPresas Risk Analysis & Polytechnic University of Valencia	SPAIN

The relatively high number of participants on Theme C shows the interest of the engineering community in the field of the reliability-based approach to dam safety.

5. Models of analysis

The models of analysis for the sliding failure mode used by contributors are listed in Table X. They have been characterized by their main features:

- Type of model of analysis
- Crack opening and propagation criteria at the dam-foundation contact
- Type of model for the dam-foundation shear strength
- Factor of safety definition

5.1. Type of model of analysis

All contributors have considered at least a 2D rigid body limit equilibrium model (LEM). Despite the strong evolutions developed in more sophisticated, finite element-based models, LEM is still recognized by contributors as the most popular and accepted method to evaluate the safety against sliding, see *Krounis & Johansson* [X]. In this model the dam is idealized as a beam with variable section. The normal stress along horizontal planes is assumed to vary linearly, see *Frigerio et al* [X]. Two teams have considered deformable body models to evaluate the crack length, implemented in Finite Element Model codes (FEM).

In particular, UTCB team has used an elastic FEM model implemented in code SAP2000 to compare the crack length with that estimated with LEM. VNIIG team has used a FEM model implemented in code ANSYS to calculate the crack length, and then the sliding stability is evaluated using LEM equations.

One team, iPresas, has considered a 2D elastic Finite Difference Model (FDM) model implemented in code FLAC 2D in addition to the LEM model.

5.2. Crack opening and propagation criteria at the dam-foundation contact

In LEM models the evolution of the horizontal crack is simulated reducing accordingly the effective area at the dam-foundation contact that provides resistance to overturning moment. The uplift is updated along the cracked length according to Fig. X. According to given data, tensile strength is zero at the interface.

In FEM model used by UTCB no crack opening and propagation is simulated, as the interface model seems to be of 'glued' type, where grid points between dam and foundation are kept together, and tensile stresses are allowed to develop.

In the FEM model used by VNIIG a bilinear cohesive zone model (the Alfano & Criesfeld traction-separation model) is adopted for the interface, with a maximum tensile strength of 0,3 MPa.

In the FDM model used by iPresas, the crack opening and propagation is simulated. If the magnitude of the tensile normal stress exceeds the bond strength (which is zero in this case) at any point the bond breaks for that point and it behaves thereafter as unbounded (separation and slip between contact surfaces allowed).

5.3. Type of model for the dam-foundation shear strength contact

When using LEM model, the failure envelope defined by the Mohr-Coulomb model has been adopted by all contributors. The shear strength is defined by friction coefficient, tan(φ), and cohesion, c, acting along the effective contact area, which is the part under compressive stresses.

The same model has been used by iPresas in the FLAC 2D model.

5.4. Factor of safety definition

The factor of safety definition used by all contributors using LEM models is that of the ratio between shear strength force and driving force along the dam-foundation contact, as shown in Equation (1).

$$FS = \frac{R}{S} \tag{1}$$

The driving force is the water pressure acting on the upstream slope of the dam. The shear strength, R(N/m), is calculated with Equation (2).

$$R = (N - U)tg\varphi + B \times c \tag{2}$$

where:

N (N/m) is the sum of vertical forces acting on the dam-foundation contact surface.

U (N/m) is the uplift.

B (m^2/m) is the area in compression in the dam-foundation contact.

φ (°) is the friction angle in the contact.

c (Pa) is the cohesion in the contact.

This definition of shear strength has strong assumptions implicit, as it is assumed that the ultimate capacity is achieved at every point of the sliding surface and that the cohesion acts along the surface without any variation, see *Krounis and Johansson* [X].

When stability is analyzed with a finite difference or finite element numerical model, it is common to adopt an alternative definition, where the factor of safety is , the ratio between the value of the parameter controlling the stability, φ, (or c), and the value of the parameter when failure occurs, φ_{FAIL}, (or c_{FAIL}). In Equation (3) a linear degradation from values (φ, c) to (0,0) is assumed.

$$FS = \frac{\varphi}{\varphi_{FAIL}} = \frac{c}{c_{FAIL}} \tag{3}$$

This is the definition adopted by iPresas team for the FLAC model. To allow consistent comparison between FS values calculated with LEM and FLAC, two values of FS have been computed with the LEM model for each water level, according to Equations (1) and (3).

A key point related to the factor of safety evaluation is the decision on what values of friction angle and cohesion should go into the calculations.

Table 5: Models of analysis.

ID	MODEL	CRACK OPENING AND PROPAGATION	SLIDING MODEL AT THE INTERFACE	FS DEFINITION
RSE	2D LEM	If σ_t<0 (tensile) a crack develops (σ_n=0 along crack)	Mohr-Coulomb	FS = R/S
UTCB	2D LEM	If σ_t<0 (tensile) a crack develops (σ_n=0 along crack)	Mohr-Coulomb	FS = R/S
	2D FEM Linear elastic (SAP2000)	Crack is assumed to have the length of the area with tensile stresses	Not considered ('glued' interface)	FS not calculated. The model is used to evaluate crack length
SC-AG	2D LEM (CADAM)	If σ_t<0 (tensile) a crack develops (σ_n=0 along crack)	Mohr-Coulomb	FS = R/S
RIT	2D LEM	Crack opening seems to affect only uplift values	Mohr-Coulomb	FS = R/S
VNIIG	2D LEM	Calculated with FEM model	Mohr-Coulomb	FS = R/S
	2D FEM (ANSYS)	Bilinear cohesive, zone model (Alfano&Criesfeld), with σ_{max} = 0,3 MPa		FS not calculated. The model is used to evaluate crack length
UPM	2D LEM	If σ_t<0 (tensile) a crack develops (σ_n=0 along crack)	Mohr-Coulomb	FS = R/S
UPV	2D LEM	If σ_t<0 (tensile) a crack develops (σ_n=0 along crack)	Mohr-Coulomb	FS = R/S
iPresas	2D LEM	If σ_t<0 (tensile) a crack develops (σ_n=0 along crack)	Mohr-Coulomb	FS = R/S & FS = φ/φ_{FAIL}
	2D FDM (FLAC)	If σ_t<0 (tensile) a crack develops (σ_n=0 along crack)	Mohr-Coulomb	FS = φ/φ_{FAIL}

6. Variables

6.1. Friction angle

The statistical analysis of given data for friction angle proposed by contributors is shown in Table X.

Five teams (UTCB, SC-AG, VNIIG, UPV and iPresas) have considered the friction angle, φ, as a random variable. Two teams (RIT and UPM) have considered the friction coefficient, $\tan\varphi$, as the random variable. Another team (RSE) has considered both cases.

All contributors have considered that the friction angle, or the friction coefficient, is normally distributed. One contributor (VNIIG) has considered the Beta distribution for the friction angle.

Although in some cases the values have not been explicitly given, seems that all contributors have considered the mean and standard deviation values from the sample given.

Four teams (UTCB, VNIIG, UPV and iPresas) have considered a truncation in the normal probability density distribution, with a minimum and a maximum value.

Most of the teams have considered the mean value as the characteristic value that goes into the evaluation of the factor of safety. One team (SC-AG) has considered in addition a lower and an upper value. One team (UPM) has done an in-depth analysis of possible characteristic values according to several approaches, including Eurocode 7.

Table 6: Statistical analysis of data for friction angle.

ID	VAR.	PROB. DIST	MEAN	S.D.	MIN	MAX	CHAR. VALUE
RSE	φ	Normal	N/S	N/S	$-\infty$	$+\infty$	N/S
	$tg\varphi$	Normal	N/S	N/S	$-\infty$	$+\infty$	N/S
UTCB	φ	Normal	52,4°	N/S	25°	80°	52,4°
SC-AG	φ	Normal	52,4°	N/S	$-\infty$	$+\infty$	48,36° lower 52,40° aver. 56,44° upper
RIT	$tg\varphi$	Normal	1,36	0,39	$-\infty$	$+\infty$	1,36
VNIIG	φ	Normal Beta	52,4°	7,99°	10°	70°	N/S
UPM	$tg\varphi$	Normal	1,36	0,39	$-\infty$	$+\infty$	1,24
UPV	φ	Normal	52,4°	8°	28,4°	76,4°	52,4°
iPresas	φ	Normal	52,4°	7,99°	28,4°	76,4°	52,4°

N/S: Not specified

6.2. Cohesion

The statistical analysis of given data for cohesion proposed by contributors is shown in Table X. Four teams (RIT, UPM, UPV and iPresas) have considered that the cohesion, c, is lognormally distributed. Two teams (UTCB and SC-AG) have considered that the cohesion is normally distributed. One contributor (VNIIG) has considered both distributions, normal and lognormal. One contributor (RSE) has considered three possible distributions for the cohesion: normal, lognormal and Rayleigh.

Seems that all contributors have considered the mean and standard deviation values from the sample given. The UTCB team has considered an asymmetrical truncation in the normal distribution. Two teams (UPV and iPresas) have considered an upper truncation for the lognormal distribution.

Most of the teams have considered the mean value as the characteristic value that goes into the evaluation of the factor of safety. Again, team from SC-AG has considered in addition a lower and an upper value, and UPM team has done an analysis of possible characteristic values, as with friction.

Table 7: Statistical analysis of data for cohesion.

ID	VAR.	PROB. DIST	MEAN (MPa)	S.D. (MPa)	MIN (MPa)	MAX (MPa)	CHAR. VALUE (MPa)
RSE	c	Normal	N/S	N/S	-∞	+∞	N/S
	c	Rayleigh	N/S	N/S	0	+∞	N/S
	c	Lognormal	N/S	N/S	0	+∞	N/S
UTCB	c	Normal	0,367	N/S	0	0,8	0,367
SC-AG	c	Normal	0,367	N/S	-∞	+∞	0,242 lower 0,367 average 0,492 upper
RIT	c	Lognormal	0,48	0,40	0	+∞	0,37
VNIIG	c	Normal	0,367	0,246	N/S	+∞	N/S
		Lognormal	0,367	0,246	0	+∞	N/S
UPM	c	Lognormal	0,367	0,247	0	+∞	0,274
UPV	c	Lognormal	0,375	0,237	0	1,5	0,375
iPresas	c	Lognormal	0,367	0,247			0,367
	c	Lognormal	0,375	0,368	0	2,0	

N/S: Not specified

6.3. Correlation between variables

All participants considered the random variables as independent, without any correlation between them.

7. Reliability methods

7.1. Level 2 methods

Level 2 methods of analysis considered by contributors are summarized in Table X. In all cases, these methods have been applied together with Limit Equilibrium Models. All contributors have considered the FOSM Taylor method. In two cases (SC-AG and UPM) this has been the only Level 2 method used. Two teams (UPV and iPresas) have considered in addition to FOSM the Point Estimate Method. Two teams (RSE and RIT) have considered in addition to FOSM the Hasofer-Lind Method. Finally, two teams (UTCB and VNIIG) have considered all three methods (FOSM, PEM and Hasofer-Lind).

Table 8: Level 2 reliability methods used by contributors.

ID	FOSM TAYLOR	POINT ESTIMATE METHOD	HASOFER & LIND METHOD
RSE	YES	NO	YES
UTCB	YES	YES	YES
SC-AG	YES	NO	NO
RIT	YES	NO	YES
VNIIG	YES	YES	YES
UPM	YES	NO	NO
UPV	YES	YES	NO
iPresas	YES	YES	NO

7.2. Level 3 methods

All contributors have conducted Level 3 analyses with Monte Carlo simulation method. In one case (VNIIG) sampling has been done with Latin Hypercube as well as with pure Monte Carlo sampling.

Table 9: Level 3 reliability methods used by contributors.

ID	LEVEL 3 METHOD	TOOL	NUMBER OF SIMULATIONS
RSE	Monte Carlo	MATLAB	1.000.000
UTCB	Monte Carlo	MATHCAD	Not specified
SC-AG	Monte Carlo	CADAM	250.000
RIT	Monte Carlo	MATLAB	Not specified
VNIIG	Monte Carlo		1.000.000
	Latin Hypercube		1.000.000
UPM	Monte Carlo		100.000
UPV	Monte Carlo	@RISK	Variable [10.000 - 1.000.000]
iPresas	Monte Carlo	@RISK	Variable [10.000 - 10.000.000]

8. Results

8.1. Part 1: Relationship between water levels and factor of safety

Results of relationships obtained by contributors between water levels and factors of safety are plotted in Fig. 4 (drains effective) and Fig. 5 (drains ineffective). In these figures, results from six teams are plotted (SC-AG, RIT, VNIIG, UPM, UPV and iPresas). Results from the other two teams (RSE and UTCB) have been represented in a different figure, as they follow a different approach.

The iPresas team has provided three results. One corresponds to LEM with the classical FS definition as the ratio between resistant and driving forces. The other two results correspond with an alternative definition of the factor of safety as the ratio between the characteristic value of a strength parameter and the degraded value of the parameter that leads to failure. One is for LEM model and the other is for FLAC model.

8.1.1. Factor of safety. Drains effective

From Fig. 4 it can be seen that very close values of the factor of safety have been obtained as long as similar models and assumptions are made (SC-AG, RIT, UPV, iPresas).

The UPM calculates a slightly less factor of safety as the characteristic values used for (φ,c) or (tanφ,c) are not mean values but lower values.

The VNIIG team provides values much lower than the rest. Maybe this is due to the fact that computed crack length is zero with LEM models while some cracking is predicted with the cohesive zone model used by VNIIG, even for water level of 75 m. With this model the stress distribution at the contact is not linear, so some stress concentration at the tip of the crack is modelled.

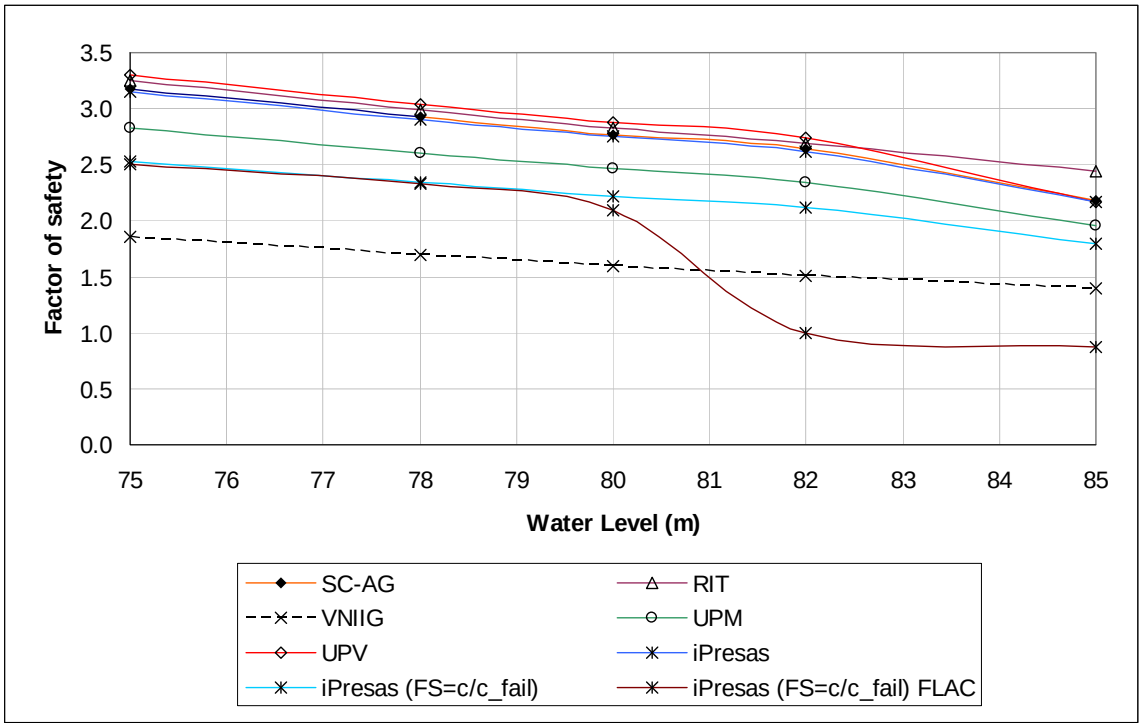

Figure 4: WL – FS. Drains effective.

When the alternative definition of FS is considered, values are slightly less but the shape of the curve is the same, showing similar behaviour. When a deformable body model like FLAC is used, stresses at the contact are not linear, showing stress concentrations at the heel and at the toe. With this model, as long as a crack is not developed, the calculated values of the factor of safety match very well with those of LEM model.

While LEM models do not predict cracking even for severe overtopping (water levels 5 m over the dam crest), the FLAC model predicts starting of cracking for water levels close to the dam crest, and strong cracking propagation for 2 m overtopping (water level at 82 m).

8.1.2. Factor of safety. Drains ineffective

From Fig. 5 it can be seen that very close values of the factor of safety have been obtained as long as similar models and assumptions are made (SC-AG, UPV and iPresas predicts almost the same values, with failure taking place for water levels close to the dam crest). The results from RIT team differ in this case, showing higher factors of safety than the rest. This is considered to be from some assumption in the calculation of the factor of safety under cracking condition, maybe regarding the effective contact area where shear strength is mobilized.

The alternative definition of the factor of safety leads to lower values than the classical definition when FS>1 and to higher values when FS<1. It can be seen in Fig. X that the curves for both definitions of the factor of safety cross each other at FS=1, as it was expected, so the failure condition is well captured regardless which definition of FS is used, when the LEM model is considered.

It also very interesting to notice that when cracking occurs, the LEM model leads to lower safety factors than the FLAC model.

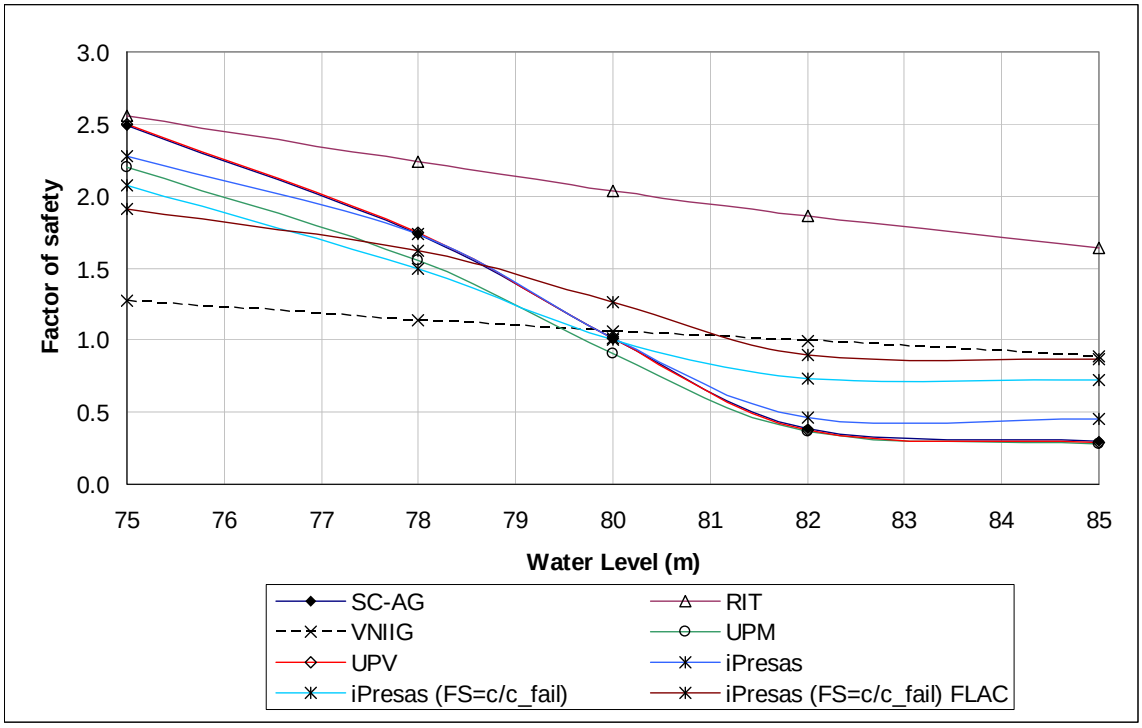

Figure 5: WL – FS. Drains ineffective.

The results from VNIIG team show lower safety factors than the rest for water levels under the dam crest.

8.1.3. Factor of safety. Other cases

In Fig. 6 results from RSE and UTCB teams are presented.

RSE team has provided averaged values of the factor of safety: FS = 0,9×FS(drains effective) + 0,1×FS(drains ineffective).

Team from UTCB has performed calculations of the factor of safety with a single weighted uplift distribution where the value of uplift at the drain line is 0,9×value with drains effective + 0,1×value with drains ineffective.

These results are shown separately as they cannot be compared in a homogeneous way with the results provided by other teams.

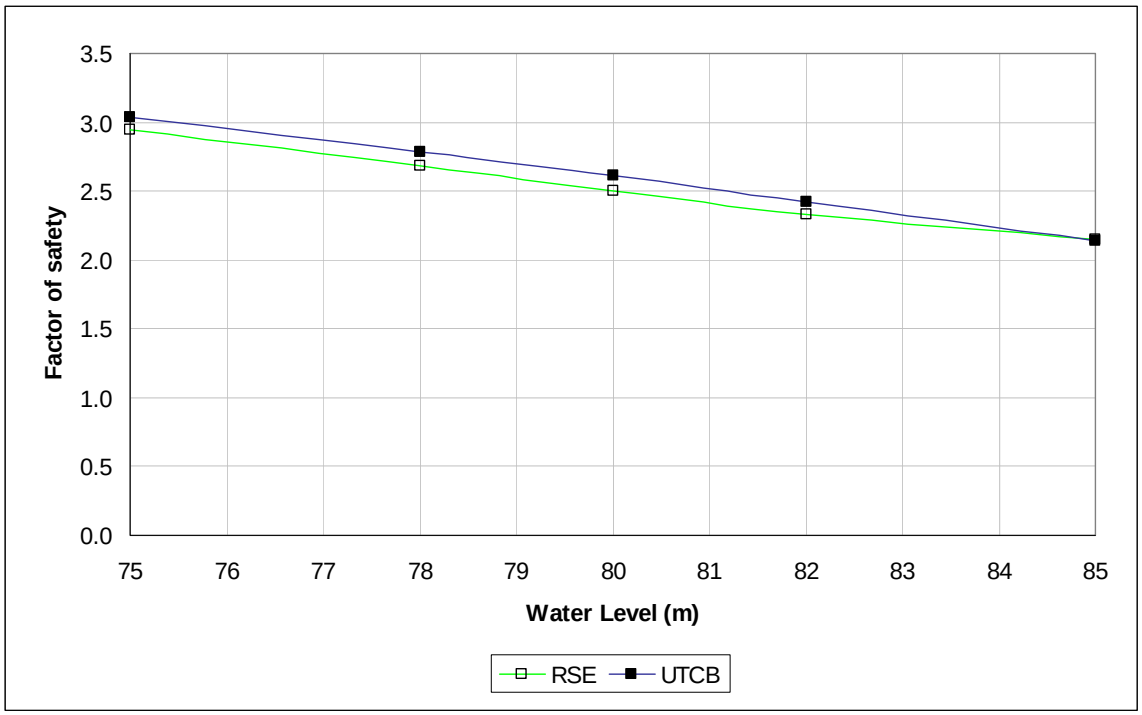

Figure 6: WL – FS. Combined values with drain performance probabilities.

8.2. Part 2: Relationship between water level and probability of failure with Level 2 methods: FOSM Taylor Method

Results of relationships obtained by contributors between water levels and probabilities of failure are plotted in Fig. 7 (drains effective) and Fig. 8 (drains ineffective).

In all cases, the model of analysis used has been the LEM model.

Five teams have provided the results explicitly for both drain performance cases (RIT, VNIIG, UPM, UPV and iPresas) and also for the total probability taking into account probabilities of drain performance, while the other three (RSE, UTCB and SC-AG) have provided the only the total value of probability.

8.2.1. FOSM Taylor. Drains effective

From Fig. 7 it can be seen that very close values of the probability of failure have been obtained by three teams (RIT, UPV and iPresas). UPM provides lower values while probabilities estimated by VNIIG are slightly higher.

In any case the shape of the curves shows a very smooth increase of probabilities with water levels.

A key point to consider is the value of the probabilities itself, with values close to 10-2 for most water levels, which seem unrealistically high.

It is a surprising thing that RIT and UPM values differ despite the fact that both of them have considered (tanφ,c) as random values instead of (φ,c),as the rest of the teams have done.

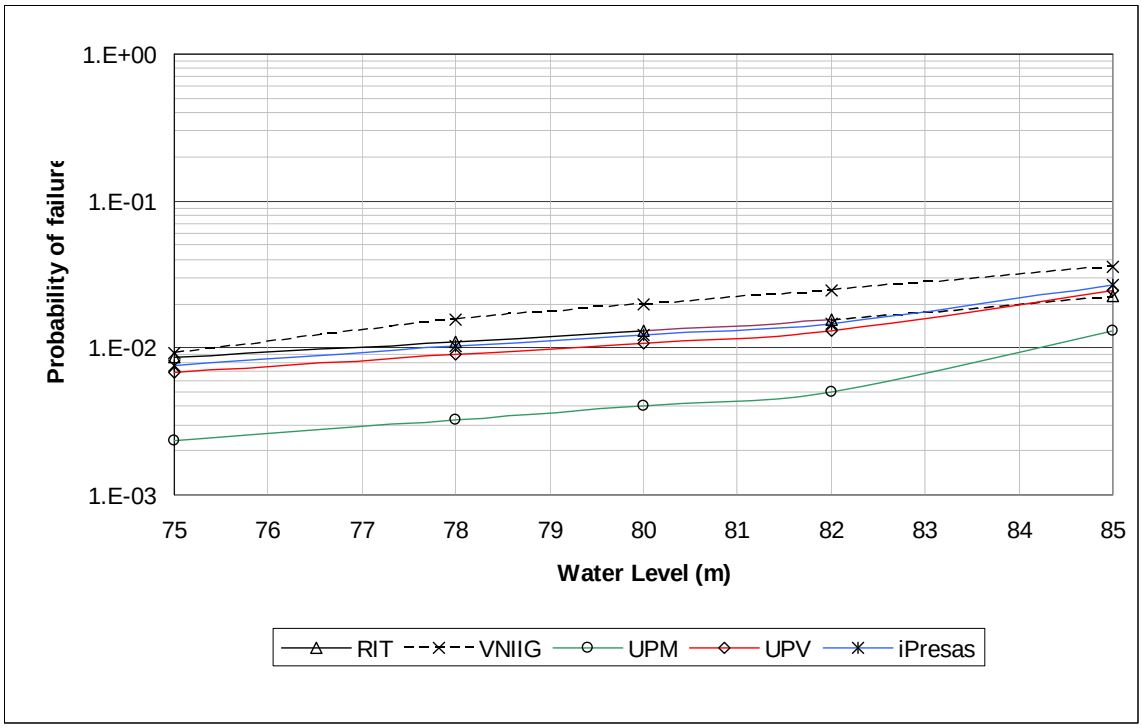

Figure 7: WL – Pf (FOSM). Drains effective.

8.2.2. FOSM Taylor. Drains ineffective

The curves in Fig. 8 show clearly a difference between models used by RIT and VNIIG and the rest under cracked conditions.

Under drain system failure probabilities predicted are extremely high, in the range 10-2 to 1.

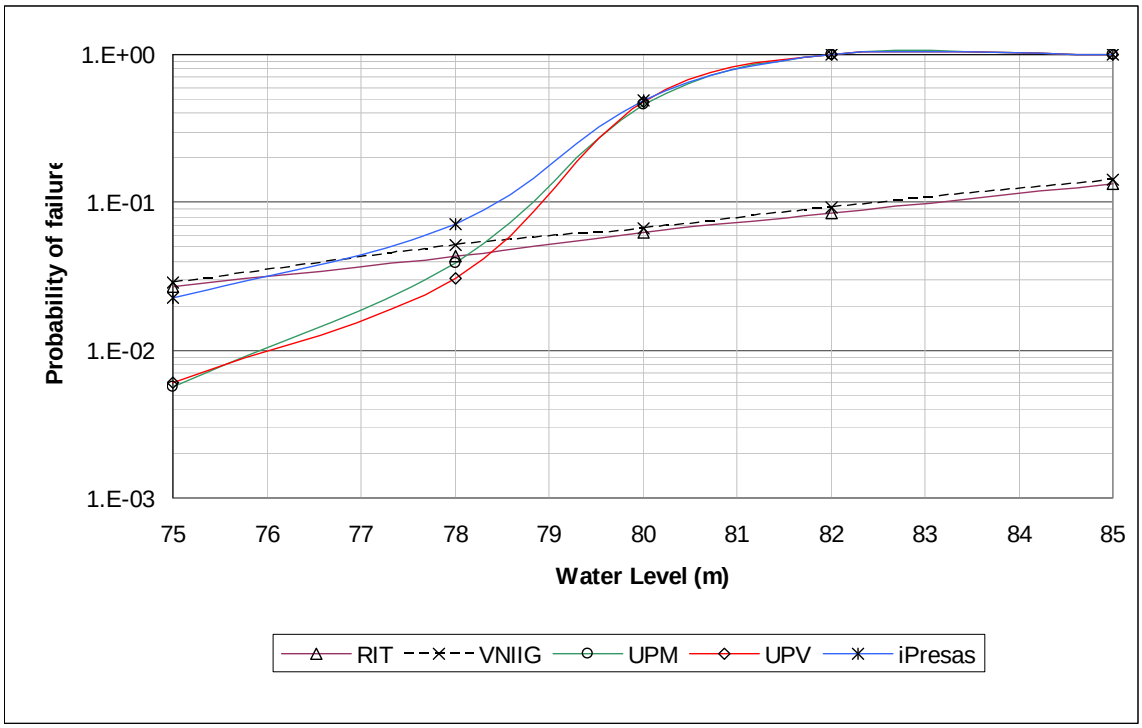

Figure 8: WL – Pf (FOSM). Drains ineffective.

8.2.3. FOSM Taylor. Total probability

The curves in Fig. 9 show the results of total probability from the 8 contributors.

Good agreement is found between all teams for water levels of 75 and 78 m. For higher water levels the results differ, but by less than an order of magnitude.

It is very interesting to check the effect of considering (tanφ,c) or (φ,c) as random variables, as it has been shown by RSE team, which provides both curves. As it can be seen, at least for the dam under study, the effect is negligible.

It can also be seen that SC-AG and iPresas have obtained almost exactly the same results.

The total probability moves in the range 10-3 to 10-1.

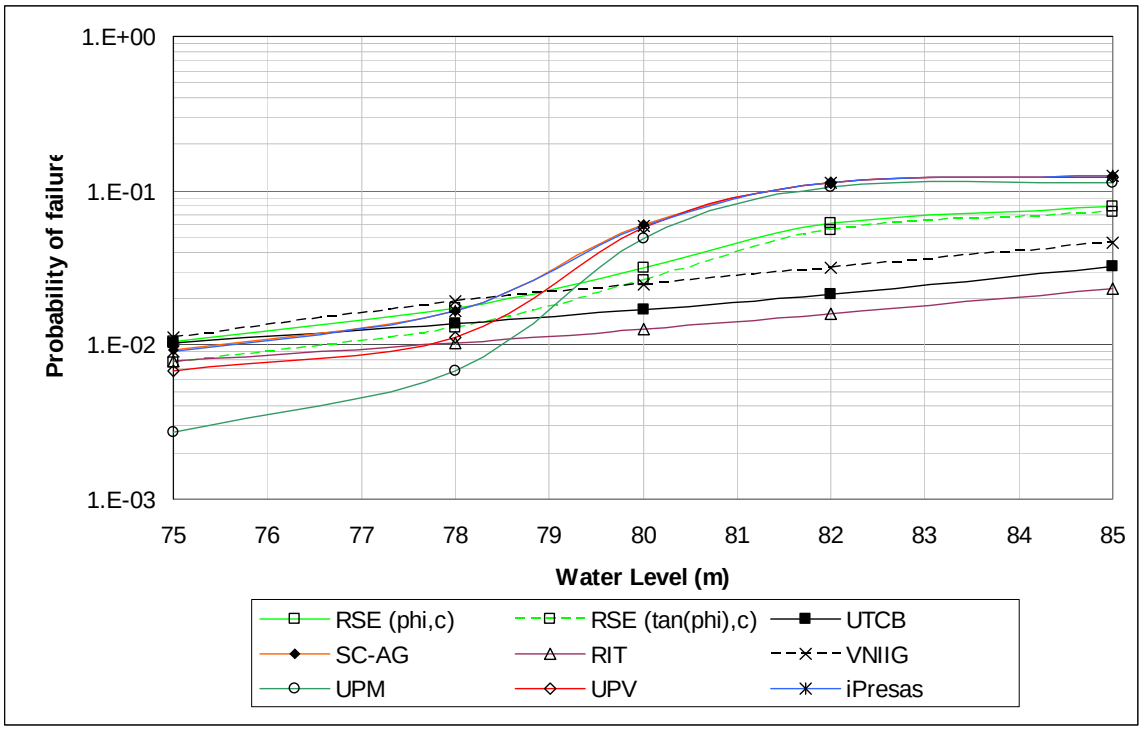

Figure 9: WL – Pf (FOSM). Total probability.

8.3. Part 2: Relationship between water level and probability of failure with Level 2 methods: Point Estimate Method

Four teams have done calculations of probabilities of failure with the Point Estimate Method (UTCB, VNIIG, UPV and iPresas). Three of them (VNIIG, UPV and iPresas) have provided the results explicitly for both drain performance cases and also for the total probability taking into account probabilities of drain performance.

As it has been mention before, team from UTCB has performed calculations using a single weighted uplift distribution where the value of uplift at the drain line is 0,9×value with drains effective + 0,1×value with drains ineffective. According to this, results of probability have been provided.

Results of relationships obtained by contributors between water levels and probabilities of failure are plotted in Fig. 10 (drains effective) and Fig. 11 (drains ineffective).

In all cases, the model of analysis used has been the LEM model.

8.3.1. Point Estimate Method. Drains effective

From Fig. 10 it can be seen that very close values of the probability of failure have been obtained by three teams (VNIIG, UPV and iPresas).

Comparing Fig. 10 with Fig. 7 it can be seen that probabilities estimated with the Point Estimate Method are slightly lower than those estimated with FOSM. The difference is roughly by half an order of magnitude.

In any case, the probabilities for water levels under the dam crest seem unrealistically high.

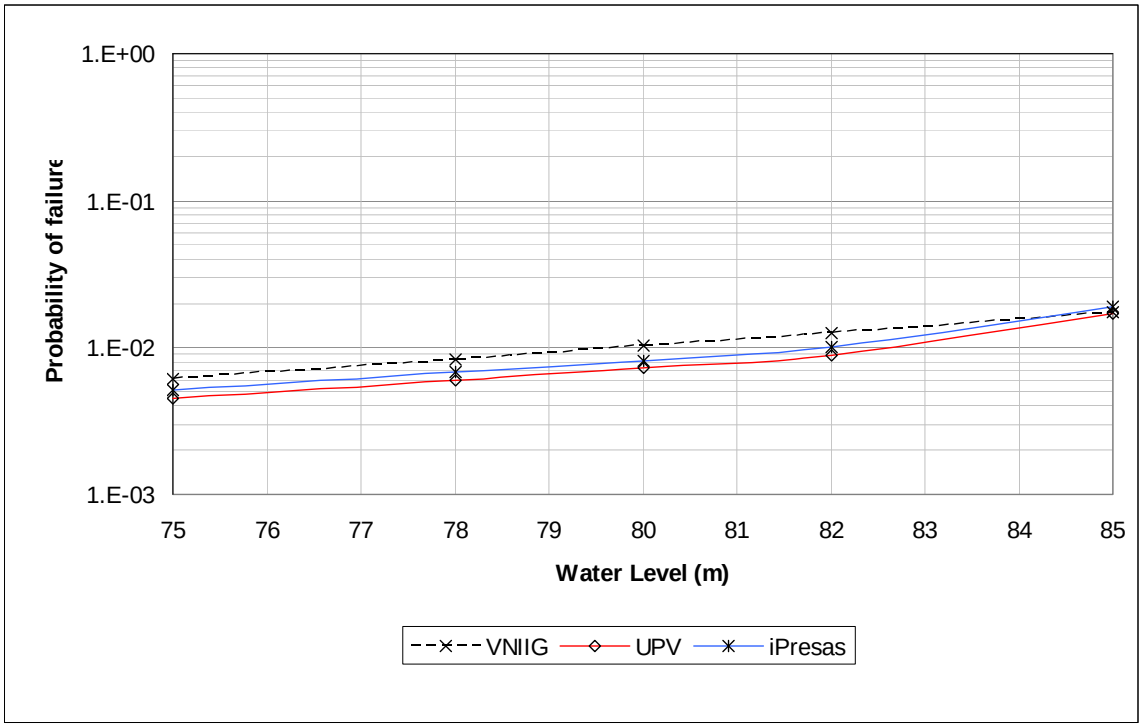

Figure 10: WL – Pf (PEM). Drains effective.

8.3.2. Point Estimate Method. Drains ineffective

The curves in Fig. 11 show again the difference between models of analysis used by VNIIG and the rest under cracked conditions. Under drain system failure probabilities predicted are extremely high, in the range 10-2 to 1. Results are very similar to those obtained with FOSM.

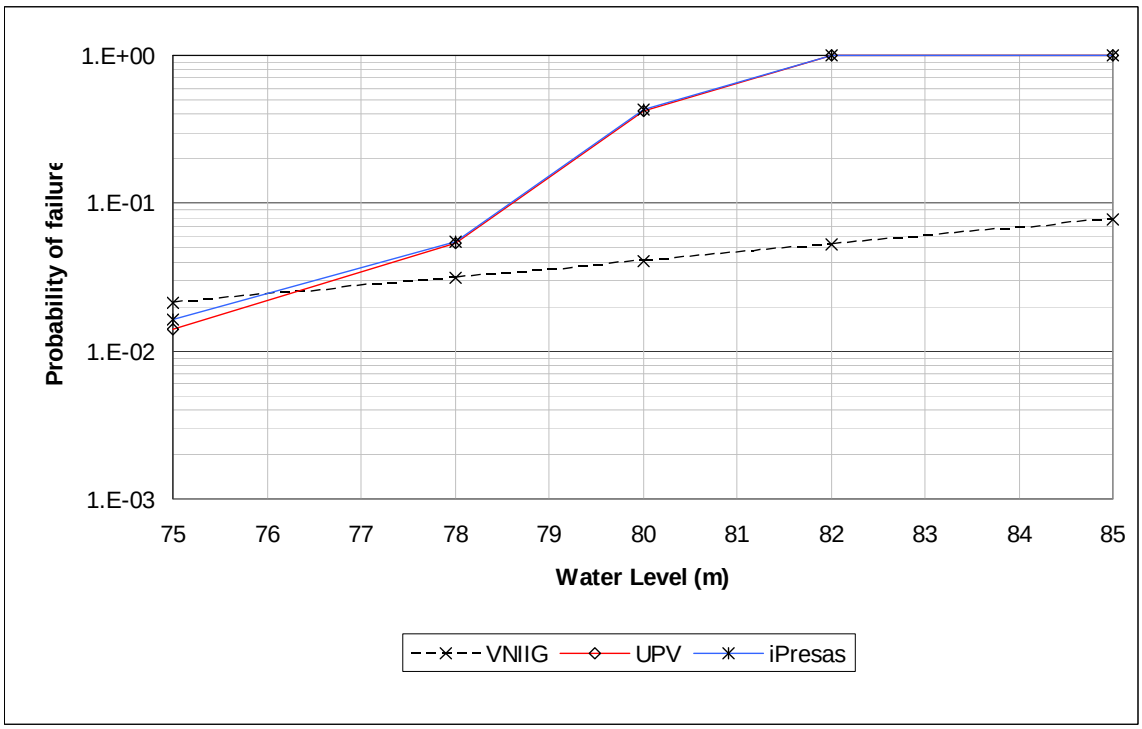

Figure 11: WL – Pf (PEM). Drains ineffective.

8.3.3. Point Estimate Method. Total probability

The curves in Fig. 12 show the results of total probability from all 4 contributors.

The same pattern identified before for FOSM method appears here, as good agreement is found between all teams for water levels of 75 and 78 m. For higher water levels the results differ, but by less than an order of magnitude.

The total probability moves in the range 5×10-3 to 10-1.

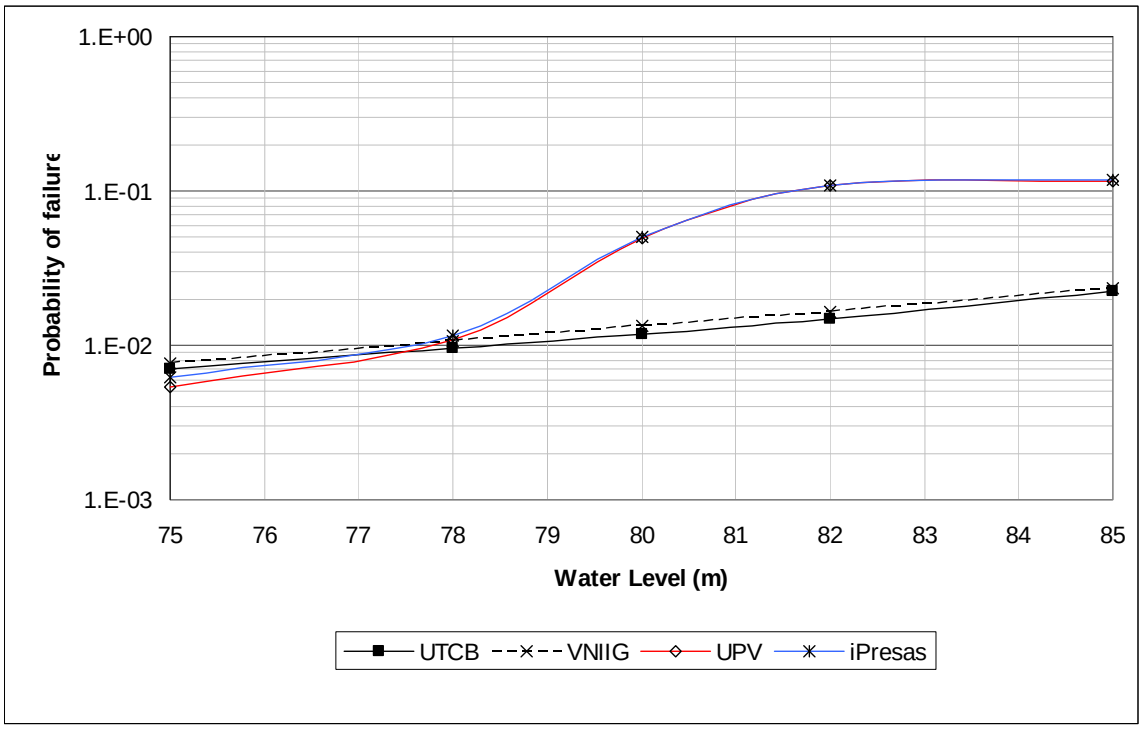

Figure 12: WL – Pf (PEM). Total probability.

8.4. Part 2: Relationship between water level and probability of failure with Level 2 methods: Hasofer-Lind Method

Four teams have done calculations of probabilities of failure with the Hasofer-Lind Method (RSE, UTCB, RIT and VNIIG). Two of them (RIT and VNIIG) have provided the results explicitly for both drain performance cases and also for the total probability taking into account probabilities of drain performance.

Again, UTCB has performed calculations using a single weighted uplift distribution where the value of uplift at the drain line is: (0,9×value with drains effective) + (0,1×value with drains ineffective).

Results of relationships obtained by contributors between water levels and probabilities of failure are plotted in Fig. 13 (drains effective) and Fig. 14 (drains ineffective).

In all cases, the model of analysis used has been the LEM model.

8.4.1. Hasofer-Lind Method. Drains effective

From Fig. 13 it can be seen that similar values of the probability of failure have been obtained by both teams (RIT and VNIIG).

In any case the shape of the curves shows again a very smooth increase of probabilities with water levels.

As it happens with previous Level 2 methods, the values of the probabilities are in the range 10-3 to 10-2 for most water levels, which seem unrealistically high for the lower water levels.

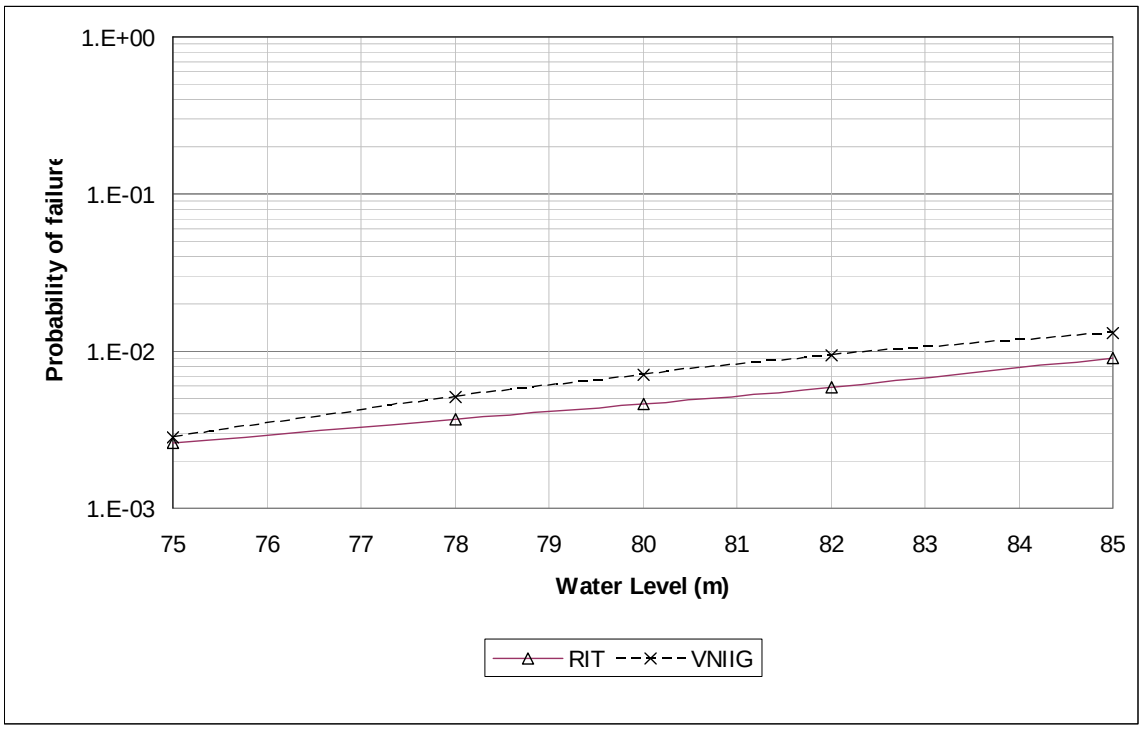

Figure 13: WL – Pf (Hasofer-Lind). Drains effective.

8.4.2. FOSM Taylor. Drains ineffective

The curves in Fig. 14 show a similar pattern in the results provided by RIT and VNIIG.

As it was the case with other Level 2 methods, under drain system failure probabilities predicted are extremely high, but not reaching a value of 1. They keep in the range from 10-2 to 10-1. In the case of VNIIG this is due to the crack opening and simulation model, with provides a limited crack length

8.4.3. FOSM Taylor. Total probability

The curves in Fig. 15 show the results of total probability from all 4 contributors.

Results from all teams have a remarkable dispersion as no team has obtained the same results and the maximum and minimum values for each water level vary by an order of magnitude.

As it has been shown with FOSM Taylor, again it is very interesting to check the effect of considering ($\tan\varphi$,c) or (φ,c) as random variables, according to results provided by RSE team. As it can be seen, at least for the dam under study, the effect is negligible, above all for the higher water levels.

The total probability moves in the range 10-3 to 10-1.

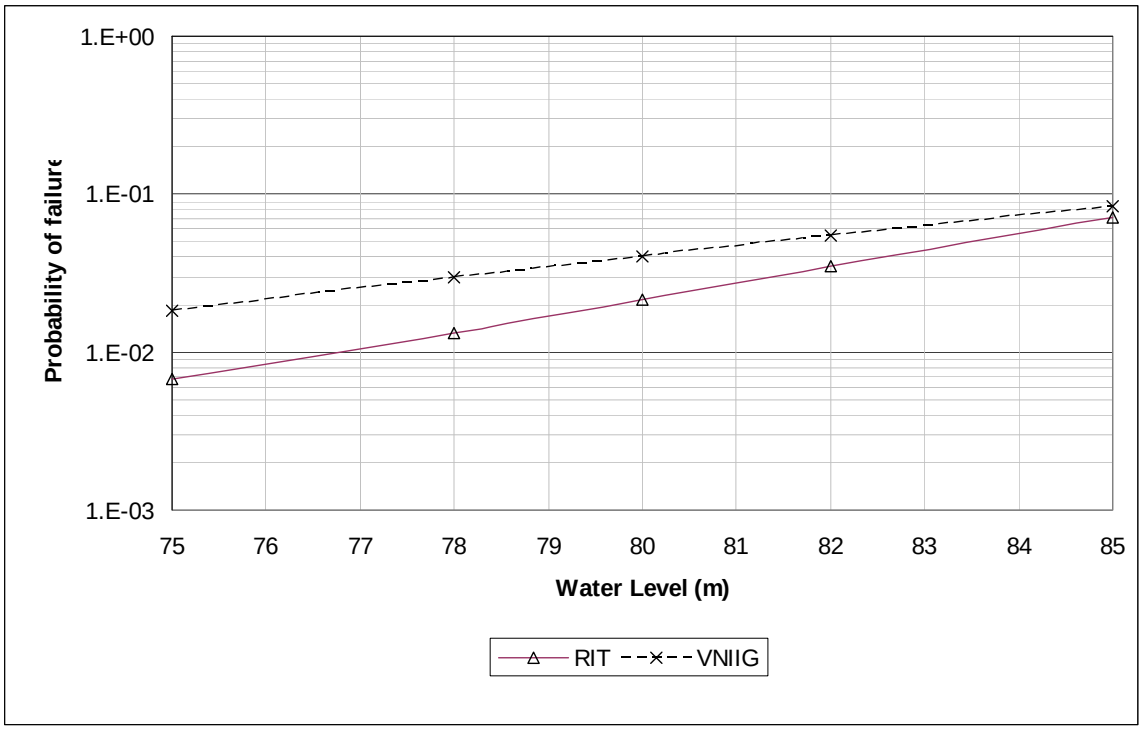

Figure 14: WL – Pf (Hasofer-Lind). Drains ineffective.

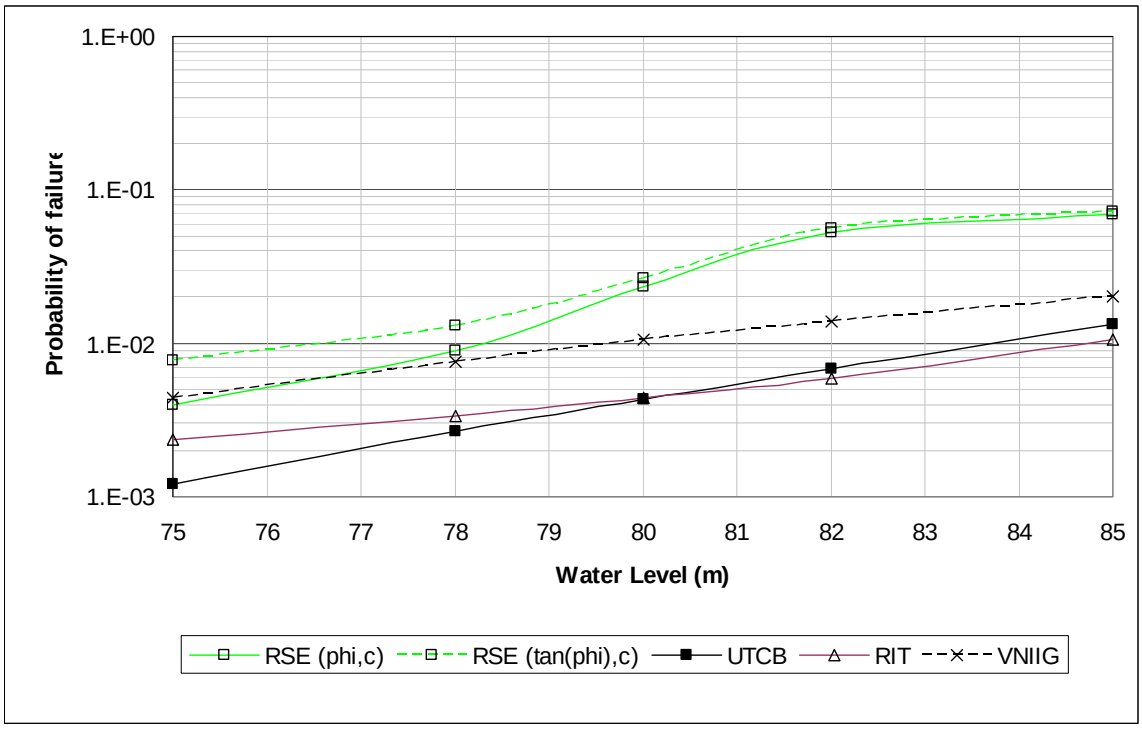

Figure 15: WL – Pf (Hasofer-Lind). Total probability.

8.5. Part 3: Relationship between water level and probability of failure with Level 3 methods

All 8 teams have provided results of probability of failure with Level 3 methods. As with this method all the information of the Probability Distribution Functions (PDF) of the random variables is transferred into the performance function, to allow consistent comparison between the results provided, the results have been grouped according to the PDFs used by contributors.

Six teams (RSE, RIT, VNIIG, UPM, UPV and iPresas) have considered a Normal PDF for friction angle (or friction coefficient) and a Lognormal PDF for cohesion. Five of them (RIT, VNIIG, UPM, UPV and iPresas) have provided the results explicitly for both drain performance cases and also for the total probability taking into account probabilities of drain performance.

Four teams (RSE, UTCB, SC-AG and VNIIG) have considered a Normal PDF for friction angle (or friction coefficient) and a Normal PDF for cohesion as well. All of them have provided the results for the total probability taking into account probabilities of drain performance. Again, UTCB has performed calculations using a single weighted uplift distribution where the value of uplift at the drain line is: (0,9×value with drains effective) + (0,1×value with drains ineffective).

All teams have used the LEM model, and the iPresas team has used in addition a deformable body model implemented in finite difference code FLAC 2D.

8.5.1. Level 3. Friction Normal and cohesion Lognormal. Drains effective

From Fig. 16 it can be seen that when tanφ is used as a random variable instead of φ, higher values of probability are obtained systematically, as shown by results from RIT and UPM teams. The rest of the curves in Fig. 16 have been obtained considering φ as a random variable ,showing similar values of the probability of failure, except for water level 75 m, where results from UPV and iPresas teams are much lower than the rest by several orders of magnitude. The reason for this may rely in the truncation of the PDF of the friction angle considered by UPV and iPresas teams, which prevents sampling from lower values of friction angle.

With FLAC model the results are similar to those with LEM model for water levels below the dam crest. For higher water levels, when FLAC model is used, higher probabilities of failure are obtained, as unstable crack propagation is predicted for water level of 82 m and higher. So FLAC model predicts a brittle behaviour of the dam for water levels over the crest.

8.5.2. Level 3. Friction Normal and cohesion Lognormal. Drains ineffective

With drains ineffective the probabilities of failure are much higher. Results from UPM, which calculates with tanφ as a random variable instead of φ, give higher probabilities of failure, but the effect is less pronounced that in the case of drains effective.

Results from RIT, which correspond to the lower probability of failure, though based on tanφ hypothesis, are somehow distorted due to the treatment on the cracked zone in the stability calculations.

Results from VNIIG model, which predicts stable crack development with relatively short lengths for any water level under the hypothesis of drains ineffective, give, in general, lower values of probability. Among the other results, FLAC model predicts the lower probabilities of failure for water levels under the crest of the dam.

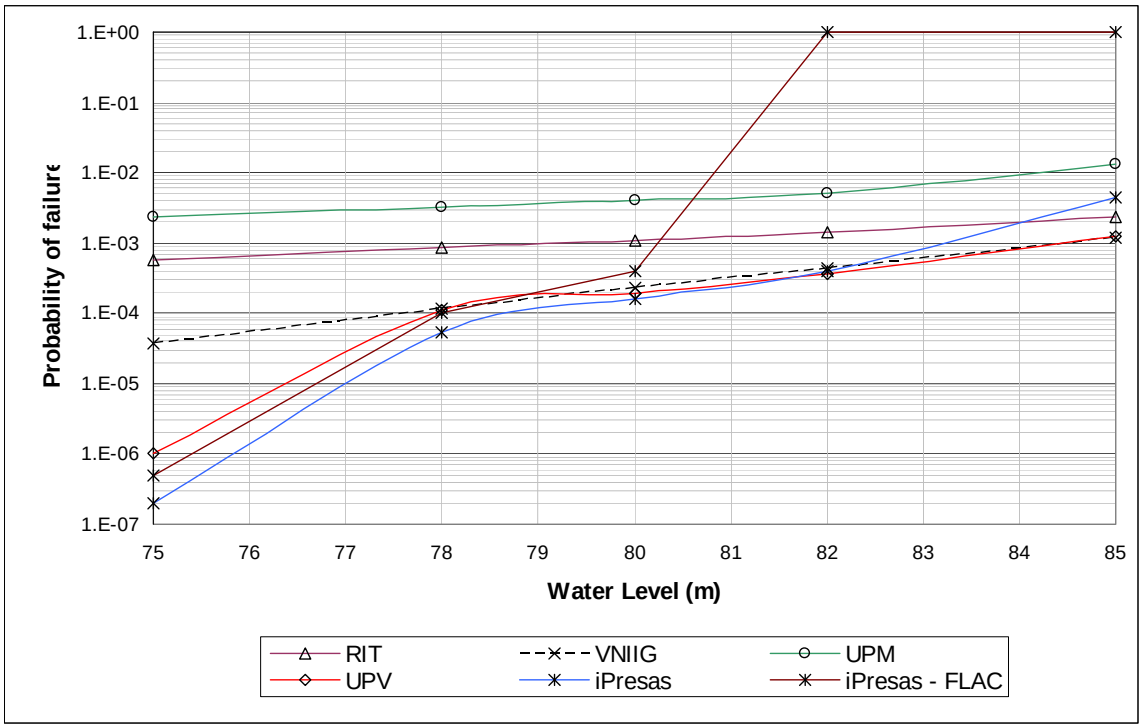

Figure 16: WL – Pf (Monte Carlo). Friction Normal and cohesion Lognormal. Drains effective.

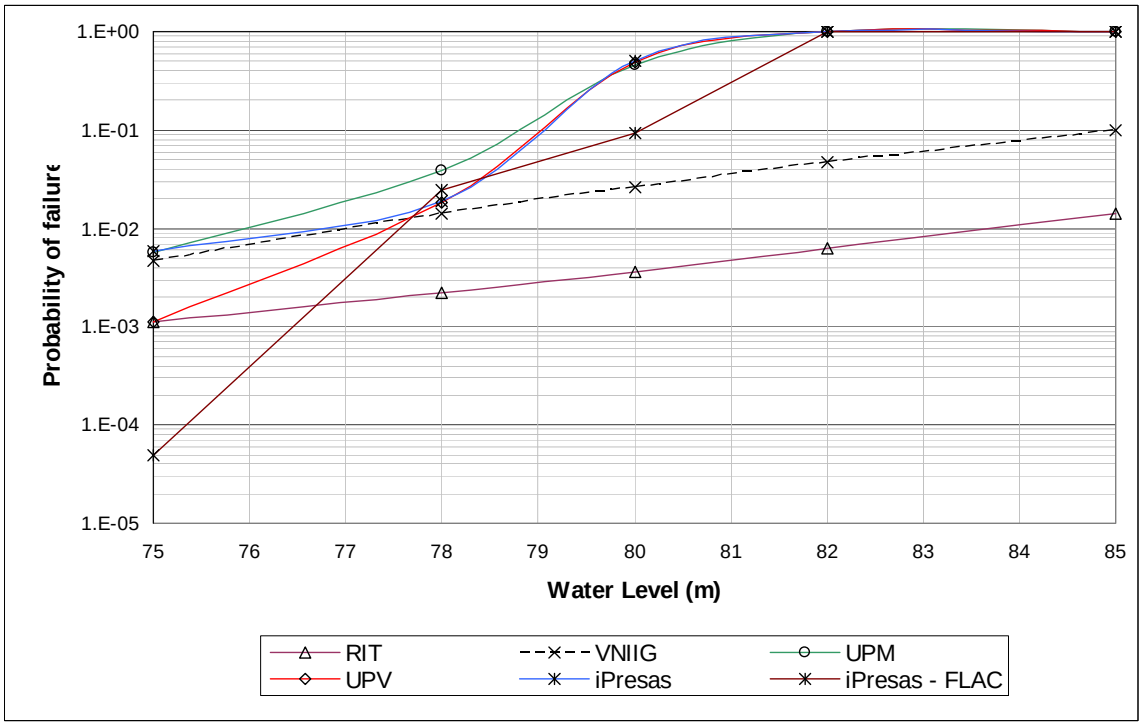

Figure 17: WL – Pf (Monte Carlo). Friction Normal and cohesion Lognormal. Drains ineffective.

8.5.3. Level 3. Friction Normal and cohesion Lognormal. Total probability

The curves in Fig. 18 show the results of total probability from the 6 contributors.

Stronger differences are found for the lower water levels.

The increase in values of probability derived from considering (tanφ,c) instead of (φ,c) as random variables, is confirmed with the results provided by RSE team.

The total probability for water level 75 m moves in the range 5×10-6 to 2×10-3.

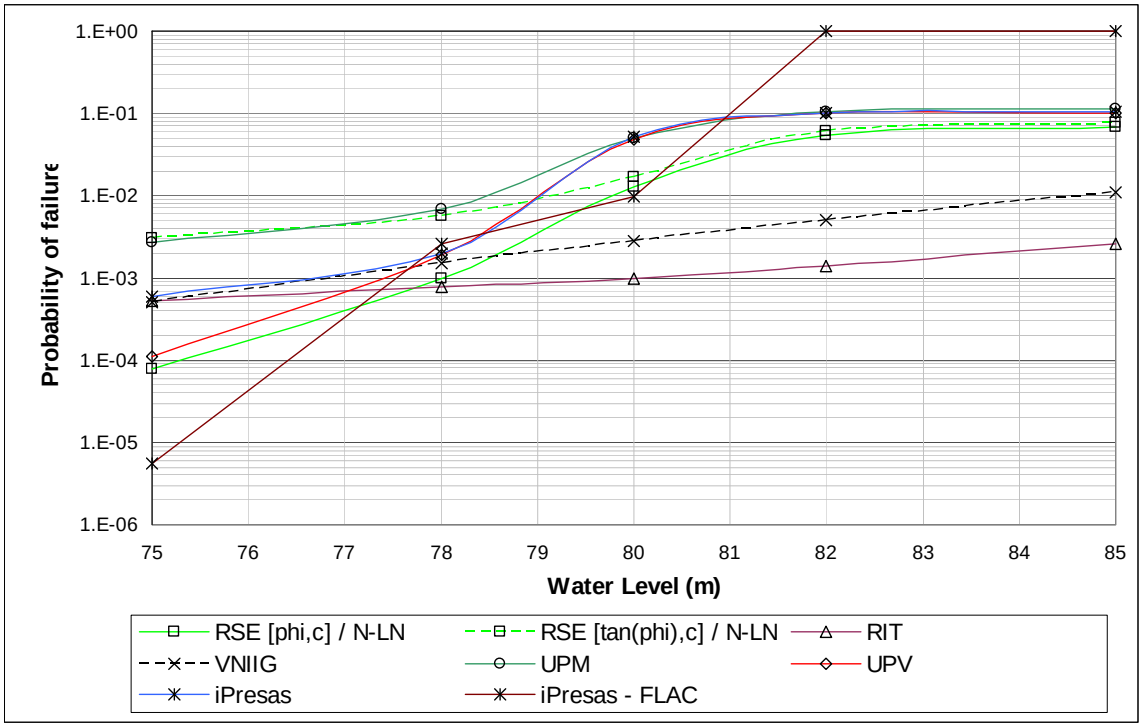

Figure 18: WL – Pf (Monte Carlo). Friction Normal and cohesion Lognormal. Total probability.

8.5.4 Level 3. Friction Normal and cohesion Normal. Total probability

Results from the four teams (RSE, UTCB, SC-AG and VNIIG) that have considered a Normal PDF for friction angle (or friction coefficient) and a Normal PDF for cohesion are shown in Fig. 19. The results correspond to total probability, considering the drain performance probabilities.

The probabilities tend to be higher than in previous hypothesis. As an exception, the curve from SC-AG team show low probability for water levels of 75 m (null, and so not shown in the graph) and of 78 m.

RSE team has made a very interesting exercise of comparing different PDF for cohesion (Normal, Rayleigh and Lognormal), in combination with two possibilities for friction treatment as a random variable (tanφ or φ). The results are shown in Fig. 20. Previous results are confirmed as higher probabilities are obtained when tanφ is used instead of φ.

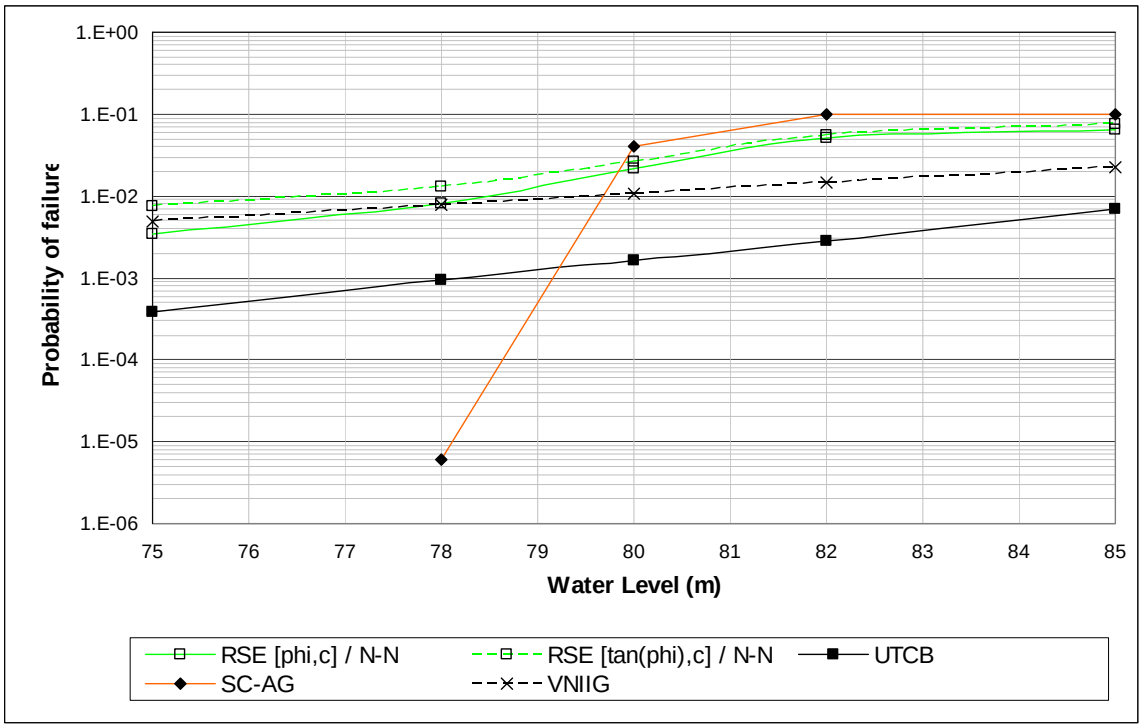

Figure 19: WL – Pf (Monte Carlo). Friction Normal and cohesion Normal. Total probability.

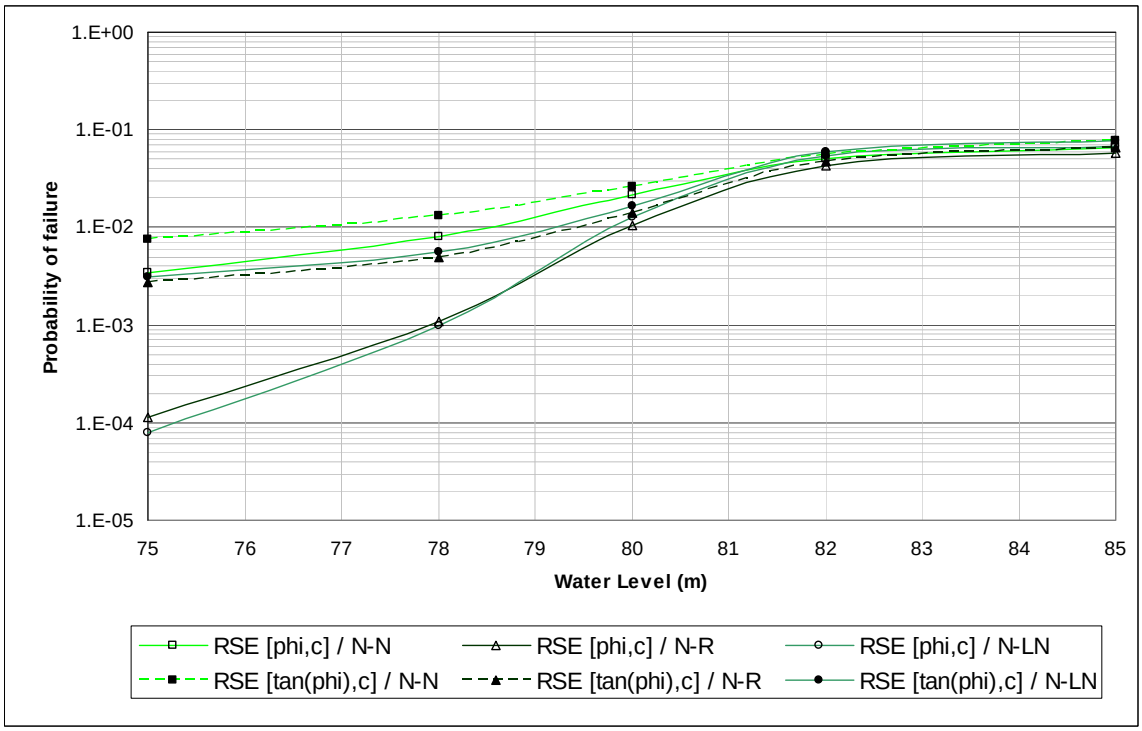

Figure 20: WL – Pf (Monte Carlo). Total probability. Results for different combinations of probability distributions for friction angle (φ) and cohesion (Normal-Normal; Normal-Rayleigh; Normal-Lognormal) and friction coefficient (tgφ) and cohesion (Normal-Normal; Normal-Rayleigh; Normal-Lognormal). RSE.

9. Discussion

All contributors have made very interesting approaches to the problem posed as Theme C of the XI Benchmark Workshop.

The first conclusion that can be derived from the Benchmark is that participants have made different decisions on every step of the process, and those decisions have had its reflections in the dispersion of the results. This comes to show that when an engineering problem, even a relatively simple, straight, and well-known one, is combined with reliability techniques, the results should be analyzed in the light of sound engineering judgement to get meaningful and useful information to assess the dam safety.

The discussion has been structured according to:

- Decisions on models of analysis
- Decisions on random variables
- Decisions on reliability methods
- Results obtained

9.1. Decisions on models of analysis

All 8 teams have used at least a Limit Equilibrium Model of analysis, and most participants have chosen the same approach to evaluate the crack opening and propagation.

Team from VNIIG has used a fracture mechanics approach to evaluate the crack length which is different from the rest. It has been shown that this model produces results which are different from the rest. Cracking is predicted even for the lowest water level of 75 m with drains effective, which is not the case in any other model. On the other hand, the cohesive zone model used predicts cracking stabilization even for the highest water level of 85 m under the condition of drains ineffective, while the other models predict crack propagation from heel to toe, without stabilization.

iPresas team has used two models, the classical LEM and a deformable body model implemented in FLAC 2D code. The crack opening and propagation criteria has been the same as for LEM models, being the only difference that tensile stresses are computed on a non-linear basis, allowing for stress concentrations at the heel and at the toe. This model matches very well with LEM model as long as tensile stresses are not present (this is to say, for lower water levels). When tensile stress appears, FLAC model predicts more severe crack propagation that LEM model and so higher probabilities of failure.

Another important thing is how the factor of safety is defined. As it can be seen in Fig. 4 and in Fig. 5, using the same LEM model of analysis and the same set of data of strength parameters, the values of the factor of safety obtained by iPresas tam differ depending upon its definition (as a ratio of forces or as a ratio of strength parameters). So comparisons of results obtained from distinct models with different definitions of the factor of safety are not straightforward and should be carefully analyzed.

9.2. Decisions on random variables

The decision on how friction is treated (if the random variable is the friction angle, φ, or the friction coefficient, $\tan\varphi$), has some impact on the results obtained. Different teams have done different approaches. According to the results obtained, seems that when $\tan\varphi$ is selected, and a Normal PDF is assumed, the probabilities are higher than when φ is selected and considered normally distributed.

Another decision is what PDF may be reasonable to use. In Theme C an unusually high number of data were provided to make the fitting of distributions process easier, but it is not always the case in real world problems, where few data are available (if any). Even with this number of data, several distributions have been suggested or considered by contributors (Normal, Lognormal, Rayleigh and Beta distributions).

Decisions related to PDFs are not only linked to what distributions are selected but also to the physical meaning of the adaptation. When an unbounded PDF as the Normal is used, a decision on its truncation becomes a key point of the process, as it has been shown by the results obtained. Again, lot of engineering judgement comes into play when assessing the minimum values to be adopted for truncation of a PDF.

Another decision that has been put into question is how to treat the probabilities of the drainage system condition. One team has proposed to use a probability-weighted uplift distribution in the dam-foundation contact, while the rest have solve the problem considering two drainage system conditions, and the total probability has been obtained combining the individual probabilities in an event tree fashion, which is considered a preferable approach.

When calculating the factor of safety, another key point is the characteristic value that should go into the formula. A discussion on this point has been included in UPM paper, see *Cabrera-Carpio & Jiménez-Rodríguez* [7]. This decision has again a strong impact on the numerical value of the factor of safety and so with dam safety decision that may be based on it.

9.3. Decisions on reliability methods

The decision on what reliability method is used is another important issue. Analysis with Level 2 methods is relatively easy to perform and, as long as the number of variables is low, it is not much time-consuming. Level 3 Monte Carlo simulation methods give more precise results but when the models of analysis are complex the computing effort is much higher.

Level 2 and Level 3 methods have been used in combination with LEM model of analysis. The iPresas team has presented a solution using Level 3 Monte Carlo simulation together with a FLAC 2D. Probabilities have been computed using the limit curve concept (as a 2D degeneration of the more general n-dimensional Limit Hyper-Surface concept when only two random variables are present).

The shape of the water level-probability curve obtained with FLAC model seems more realistic in principle than those obtained with LEM.

9.4. Results obtained

The factors of safety obtained with LEM model in the hypothesis of drains effective do not show much sensitivity to water level, even for water levels above the dam crest. Good agreement is found between different teams, with values in the range of 3,5 to 1,5. With FLAC model the factor of safety reaches unity for 2 m overtopping, while LEM models predict stability.

When drains are not effective, factors of safety reach a value of 1 near the dam crest level. FLAC and LEM models lead to similar results.

The impact of the choice of the characteristic value is very strong, as it can be seen from UPM results in Fig. 4.

The impact of the definition of the factor of safety is also very important, as it can be seen from iPresas curves in Fig. 4.

In general, good agreement between results obtained and engineering practice values for safety factors is found.

In terms of the probabilities of failure obtained with Level 2 methods, good agreement is found between different teams. It can be observed that the different decisions made have produced a spread of the results in a bandwidth of an order of magnitude, see Fig. 7 to 15.

A major aspect to be highlighted is the disproportionately high values of probabilities obtained with Level 2 methods for water levels below the dam crest with these reliability methods, with values systematically higher than 10-3.

Another result is that probabilities obtained with the different Level 2 methods do not differ significantly, even for the case when drains are effective.

Level 3 methods provide lower probabilities of failure, with values below 10-3, when drains are effective. When drains are ineffective results show that probabilities are higher than 10-3.

Comparing the results obtained with LEM and FLAC models using Level 3 Monte Carlo method, when drains are effective it is shown that both models give similar values for normal water levels, below the dam crest. As water levels exceed the dam crest, the probability of failure estimated with FLAC model approaches a value of 1 while LEM model predicts values below 10^{-2}, thus showing a very different behaviour, based on the different stress distribution along the dam foundation-contact considered in the models. This stress distribution is controlling the opening and propagation of a crack under the dam. The linear stress distribution assumption embedded in the LEM model seems to be on the 'unsafe' side. A consequence of this is that if overtopping can occur, a more detailed model of analysis should be prepared to evaluate the dam stability.

10. Conclusion

This paper is the synthesis of the results presented by contributors to Theme C "Estimation of the probability of failure of a gravity dam for the sliding failure mode", of the 11th ICOLD Benchmark Workshop on Numerical Analysis of Dams. The high number of participants has shown the growing interest of the dam engineering community in the topic of reliability-based safety assessment.

The problem solved has been the probabilistic stability assessment of 80 m high gravity. Two different 2D models of analysis have been considered: a Limit Equilibrium Model and an elastic deformable body model implemented in the code FLAC. The probability of failure has been estimated as the strength parameters of friction angle and cohesion have been considered as random variables.

More realistic results of probability of failure for lower water levels, which are the more frequent ones, seem to be obtained with deformable body models.

Results presented by contributors open a field of discussion on the main sources of uncertainties, which include models of analysis, factor of safety definition and statistical analysis of random variables.

Future benchmark problems in this topic may be addressed to go deeper into any or several of these questions, to fill the gap between everyday engineering practice and reliability based dam safety assessment.

More research is needed to handle uncertainties, as parameter uncertainty is just a part of the problem, but other sources of uncertainty have become present explicitly throughout the process.

References

[1] Escuder-Bueno, I.; Altarejos-García, L. & Serrano-Lombillo, A. (2011). Formulation of Theme C. Estimation of the probability of failure of a gravity dam for the sliding failure mode. Polytechnic University of Valencia, Spain.

[2] Faggiani, G.; Frigerio, A.; Masarati, P. & Meghella, M. (2011). Solution to Theme C. Sliding failure probability estimation of a concrete gravity dam. RSE S.p.A., Environment and Sustainable Development Department, Milan, Italy.

[3] Popovici, A. & Ilinca, C. (2011). Solution to Theme C. Analysis of the sliding failure probability of a gravity dam profile based on limit equilibrium method. Technical University of Civil Engineering. Bucharest, Romania.

[4] Touileb, B. (2011). Solution to Theme C. Gravity dam probability of sliding failure with overtopping and conditional drainage. Sogreah Consultants, ARTELIA Group. Echirolles, France.

[5] Krounis, A. & Johansson, F. (2011). Solution to Theme C. Estimation of the probability of failure of a gravity dam for the sliding failure mode. Royal Institute of Technology. Stockholm, Sweden.

[6] Shcherba, D. (2011). Solution to Theme C. Estimation of the probability of failure of a gravity dam for the sliding failure mode. JSC "VEDENEEV VNIIG". Saint-Petersburg, Russia.

[7] Cabrera-Carpio, M.M. & Jiménez-Rodríguez, R. (2011). Solution to Theme C. Polytechnic University of Madrid, Spain.

[8] Gascó-Jiménez, M. (2011). Solution to Theme C. Estimation of the probability of failure of a gravity dam for the sliding failure mode. Polytechnic University of Valencia, Spain.

[9] Altarejos García, L.; Escuder Bueno, I. & Serrano Lombillo, A. (2011). Solution to Theme C. Estimation of the probability of failure of a gravity dam for the sliding failure mode. iPresas and Polytechnic University of Valencia, Spain.